DISSERTATION

THE USE OF HUMAN KERATINOCYTES FOR ASSESSING THE CYTOTOXICITY AND CARCINOGENIC POTENTIAL OF CHEMICALS AND CHEMICAL MIXTURES

Submitted by

Dong-Soon Bae

Department of Environmental and Radiological Health Sciences

In partial fulfillment of the requirements

for the Degree of Doctor of Philosophy

Colorado State University

Fort Collins, Colorado

Fall 2002

COLORADO STATE UNIVERSITY

August 16, 2002

WE HEREBY RECOMMEND THAT THE DISSERTATION PREPARED UNDER OUR SUPERVISION BY DONG-SOON BAE ENTITLED **THE USE OF HUMAN KERATINOCYTES FOR ASSESSING THE CYTOTOXICITY AND CARCINOGENIC POTENTIAL OF CHEMICALS AND CHEMICAL MIXTURES** BE ACCEPTED AS FULFILLING IN PART THE REQUIREMENTS FOR THE DEGREE OF DOCTOR OF PHILOSOPHY.

Committee on Graduate Work

Advisor

Department Head

ABSTRACT OF DISSERTATION

THE USE OF HUMAN KERATINOCYTES FOR ASSESSING THE CYTOTOXICITY AND CARCINOGENIC POTENTIAL OF CHEMICALS AND CHEMICAL MIXTURES

From a public health perspective, exposure to single chemicals is seldom relevant. The problem of mixtures is extremely important because the rules governing their interactions and the consequent alterations of biological systems are directly related to toxic endpoints and public health. The mechanisms for chemical interactions are not well studied. To better understand the nature and biological significance of interactions in mixtures, we studied the acute cytotoxic and chronic carcinogenic effects of arsenic (As^{3+}) alone or in a metal mixture that also included cadmium (Cd^{2+}), chromium ($Cr^{3+ \text{ and } 6+}$), and lead (Pb^{2+}) in human keratinocytes.

The underlying goal of these studies is to determine the cytotoxic and potential carcinogenic effects of As alone and in an environmentally relevant metal mixture on human keratinocytes and to identify molecular markers for chemical carcinogenesis. Application of these biomarkers to assess the potential carcinogenicity of untested chemicals will be very useful and important to improve a current paradigm, the chronic animal bioassay, for chemical carcinogenicity testing. This objective is being met through meticulous cytotoxicity analyses of the metal mixture in four human keratinocyte strains

utilizing a statistical additivity model, determination of the transforming potential of As and an As-containing metal mixture by the use of the immortal human epidermal keratinocyte (RHEK-1) transformation assay, and identification of a common suite of genes altered in 4 chemically-transformed malignant RHEK-1 cell lines utilizing DNA microarray and Real Time Reverse Transcription-Polymerase Chain Reaction (RT-PCR) technologies.

The significant results of this research were: (1) As, Cr, Cd, and Pb in a mixture interact with each other to alter cytotoxicity in human keratinocytes in a dose- and cell strain-dependent manner; (2) these cytotoxic interactions may involve cellular defense mechanisms, as levels of glutathione and metallothioneins were substantially enhanced in mixture groups associated with antagonistic cytotoxic interactions; (3) chronic low level exposure of RHEK-1 cells to As alone or to a mixture containing As, Cr, Cd, and Pb inhibited spontaneous malignant conversion of this cell type. In contrast, a single treatment with 1-methyl-3-nitro-1-nitrosoguanidine (MNNG) enhanced neoplastic transformation; (4) utilization of cDNA microarray and Real Time RT-PCR methodologies demonstrated unique patterns of gene expression among 3 RHEK-1 cell populations treated with As, the metal mixture, or MNNG; (5) DNA microarray analyses on 4 chemically transformed RHEK-1 cell lines following exposure to 2 doses of MNNG, 4-nitroquinoline-1-oxide (NQO), or 2,3,7,8-tetrachlorodibenzo-*p*-dioxin (TCDD) identified a common battery of genes for potential molecular markers of the carcinogenic process, as well as chemical-specific alterations of gene expression.

The utilization of human keratinocytes in this study highlights the potential for advancing alternative methods for assessing chemical cytotoxicity and carcinogenicity.

Further gene expression analyses on phenotypically distinct stages (i.e., anchorage-dependent, anchorage-independent, morphologically transformed, tumorigenic) of RHEK-1 cells after chemical treatment will help us to correlate alterations in their expression with these stages and may identify early stage biomarkers for chemical carcinogenesis. The characterization of a causal relationship between chemical exposure and cancer may aid in the hazard identification step for risk assessment of other untested xenobiotics.

Dong-Soon Bae

Department of Environmental and Radiological Health Sciences

Colorado State University

Fort Collins, CO 80523

Fall, 2002

ACKNOWLEDGMENTS

I would like to express my appreciation to my PhD graduate committee for all their advice and encouragement. When I was frustrated and in need of a new advisor in 1997, Dr. Raymond Yang gave me a chance to pursue my graduate study here at CETT. I thank him with all my heart for giving me the direction to be an independent and thinking researcher and for cultivating my ability to express and present my ideas. I would like to thank Dr. Julie Campain for her guidance in writing scientific journal articles and research proposals and her enthusiasm in helping me improve my capability to stand up for myself. She is the only person I can call "Julie" rather than "Dr. Campain." She has been one of the best mentors I have had in my academic life. For Dr. Michael Fox, thank you for all the discussions on cytotoxicity assays and for your encouragement through an impressive writing on CMB newsletters. For Dr. William Hanneman, thank you for your initiative in setting up tools for genomics study in your lab and for encouraging me to explore a cutting edge DNA microarray technology two years ago. For Dr. Moiz Mumtaz, thank you for your encouragement and professional comments on my research proposal.

I would also like to thank Dr. Stephen Benjamin for diagnosing tumor cells and for valuable discussions. For Dr. Ruth Billings, thank you for your guidance during the first year of my PhD study at CSU. Thanks to everyone at CETT who helped in many ways with my research project. Special appreciation is expressed to Micaela Reddy,

Wendy Pott, Maxine Henessey, Laura Chubb, Linda Monum, Damon Perez, Christine Battaglia, and Ken Liao.

I would like to thank Dr. Yong-Tae Lee at Yeungnam University in Korea for starting me on the path to a scientific career in the Biochemistry field and for encouraging me to pursue a graduate degree in USA. I extend my appreciation to all members in Chinju Rotary Club, South Korea. They sponsored me to be an ambassadorial scholar and financially supported me during the first year of my graduate study in 1997.

Special recognition and appreciation are expressed to my parents, brothers, and a sister who have sent love and encouragement across the Pacific Ocean. Finally, I would like to thank my husband and my daughter Soo, who have provided love, faith, understanding, and patience. I love both of you very much and could not have done this without both of you.

DEDICATION

This dissertation is dedicated to the most supportive husband of mine.

TABLE OF CONTENTS

CHAPTER 1

General Introduction

I. Heavy Metals: Utilization, Environmental Contamination, and Human Exposure

There is an accumulating contamination of water sources and the food chain with toxic and carcinogenic metals. Exposure to metals is of significant concern to people who live near hazardous waste sites, as well as to people who work in certain industrial settings. Metals differ from other toxic substances in that they are neither created nor destroyed by humans. Nevertheless, their utilization by humans influences the potential for health effects. Human industrial activity may greatly shorten the residence time of metals in ore, may form new compounds, and may greatly enhance worldwide distribution (Nriagu *et al.*, 1988; Nriagu, 1989).

People are exposed to metal mixtures rather than to individual metals. For accurate analysis of the adverse effects of metal mixtures on both humans and the environment, mixture studies need to be carried out and must be taken into consideration during the process of risk assessment. The information from mixture studies would lead to more accurate risk assessments that are tailored to specific metal mixtures encountered in environmental settings. The second rationale for the importance of studies on metal mixtures is that several experimental lines of evidence suggest that various metals interact toxicologically (Diaz-Barriga *et al*, 1990; Mahaffey *et al.*, 1981; Shimada *et al.*,

1998). In other words, exposure to one metal will affect the toxicological potency or properties of another metal. The large number of possible combinations of metals in mixtures, and the limited resources available for such studies require innovative approaches to detect and predict potential toxicological interactions. Thus, we were interested in developing a tool to accurately and efficiently assess possible cytotoxic interactions and cell transformation potential (as a method for carcinogen identification) following exposure to either an individual metal or a metal mixture. Ultimately, the current studies will help us to understand the biological processes that drive metal-mediated cytotoxicity and tumorigenesis, particularly with respect to metals in environmentally relevant metal mixtures.

The metal mixture studied in this thesis is composed of arsenic (As), cadmium (Cd), chromium (Cr), and lead (Pb), which are the top four metals in site frequency count by the Agency for Toxic Substances and Disease Registry (ATSDR) Completed Exposure Pathway Site Count Report (ATSDR, 2001). A completed exposure pathway is an exposure pathway that links a contaminant source to a receptor population. These metals most often occur together; they are present in 8 of 10 and 5 of 10 of the Top 10 Binary Combinations of Contaminants in soil and water, respectively (Fay and Mumtaz, 1996).

II. Background review on As, Cr, Cd, and Pb individually or in combination

Arsenic

Source and Exposure

Arsenic (As) is widely distributed in the environment and exposure to inorganic arsenic is a major health concern. Inorganic As exists in two valence status, arsenite [As(III)] and arsenate [(As(V)]. Humans are exposed to As in environmental and occupational settings. In some areas of the world rich in geologic deposits, such as the southwest coast of Taiwan and areas of Mexico, Argentina, Chile, India, Thailand, China, and Bangladesh, naturally-occurring high levels of As in groundwater have been reported (Cebrian *et al.*, 1994; Choprapawon and Rodcline, 1997; Das *et al.*, 1994; Hopenhayn-Rich *et al.*, 1998; Luo *et al.*, 1997; Rahman *et al.*, 1999; Rivara *et al.*, 1997; Tseng *et al.*, 1968). As has been identified as one of the most common groundwater contaminants near hazardous waste disposal sites in the United States (Faroon *et al.*, 1994), likely the result of its widespread use and production in agriculture and industry. As is utilized in various ways: in pesticides, during smelting of many metals, in silicon water technology such as computer microchips, in chemical weapons, and in traditional forms of medicine.

Absorption, Distribution, Metabolism, Excretion

As enters the human body through ingestion, inhalation, or skin absorption. Gastrointestinal and pulmonary absorption of As correlates closely with compound solubility: in general, the more soluble the compound, the greater its absorption (Vahter, 1983). As(III) is taken into cells by passive diffusion and is more toxic than As(V), which competes with phosphate for uptake. In the bloodstream, As is distributed between the

erythrocytes and the plasma, and the relative amounts in each compartment depend on a variety of factors, including the valence and dose of As administered, as well as the species of animal (Vahter and Norin, 1980). The extent of biotransformation of As varies considerably among species. In most mammals, the metabolic pathway of As involves a series of methylation steps, resulting in the formation of monomethylarsonic acid (MMA) and dimethylarsinic acid (DMA) (Vahter, 1983). The methylated metabolites of As are less reactive with tissue macromolecules and are eliminated more rapidly than As itself. The methylation process has classically been considered a detoxification pathway (Buchet *et al.*, 1981). Some recent data, however, indicate that the methylated metabolites of As, particularly DMA, may be at least partially responsible for its carcinogenic effects (Yamamoto *et al.*, 1995 and 1997). The major route of excretion of most As compounds is via the urine, although small amounts of As are removed via skin, sweat, hair, and breast milk.

Acute and Chronic Toxicity

There are a large number of studies in humans and animals on the acute toxic effects of ingested As. In nearly all cases, the most immediate effects are vomiting, diarrhea, and gastrointestinal hemorrhage, and death may ensue from fluid loss and circulatory collapse. Some accounts of fatal As poisoning describe both gastrointestinal effects soon after ingestion and extensive damage to multiple organ systems prior to death (ATSDR, 2000)

Epidemiologic studies demonstrated a strong correlation between levels of As in the drinking water and increased incidence of peripheral vascular diseases (Tseng *et al.*,

1997), cerebrovascular disease (Chiou *et al.*, 1997), and cancers of skin, lung, kidney, liver, colon, prostate, and bladder (Engel *et al.*, 1994; Penn, 1990). The largest epidemiologic database of a population environmentally exposed to As consists of residents in villages located along the southwest coast of Taiwan. Water in the artesian wells in these regions contains very high levels of arsenic, ranging in concentration from 0.01 to 1.82 mg/L (Tseng *et al.*, 1968). A clear dose-response relationship between well water As concentration and the development of skin cancer has been demonstrated in this population (Chen *et al.*, 1985). Epidemiologic studies of US populations exposed to As-contaminated drinking water have yielded equivocal results. A positive association between As exposure and prostate cancer was reported from a cohort of 2,023 residents in Millard County, Utah exposed to median drinking water As concentrations ranging from 14-166 μg/L. Among 3,237 residents of Lane County, Oregon exposed to As-contaminated drinking water at concentrations of up to 2,150 μg/L (mean of 8.6 μg/L), no association between As concentration and the incidence of skin cancer was detected (Morton *et al.*, 1976).

Despite overwhelming evidence of the carcinogenicity of As in humans (Chen *et al.*, 1985; Engel *et al.*, 1994; Morton *et al.*, 1976; Penn, 1990; Tseng *et al.*, 1968), its transforming effects have not been definitively demonstrated in laboratory animal models. In chronic cancer bioassays with As(III) or As(V) in several species of animals (i.e., Wistar, Osborne-Mendel, Long-Evans rats, Swiss mice, beagle dogs, Cynomolgus monkeys), an observable increase in tumor development was not observed (Byron *et al.*, 1967; Kanisawa and Schroeder, 1967 and 1969; Kroes *et al.*, 1974; Thorgeirsson *et al.*, 1994). Interestingly, several studies in mice suggest that As may actually decrease the

formation of a variety of spontaneous tumors (i.e., skin, lung, and breast) (Kanisawa and Schroeder, 1967; Milner and Seattle, 1969; Schrauzer *et al.*, 1978). In Swiss mice, lifetime administration of 5 mg/L As(III) via the drinking water led to a significant decrease in the development of spontaneous lung tumors compared to controls (Kanisawa and Schroeder, 1967). Administration of 0.01% As(III) to C x C_3H hybrid mice via the drinking water during the initiation and promotion stages resulted in a decrease in the development of skin papillomas compared to controls (Milner and Seattle, 1969). Although inbred female C_3H/St mice chronically exposed to drinking water containing 2 mg/L As(III) demonstrated no significant difference in mammary adenocarcinoma incidence compared to controls, an increase in tumor onset age (latency) in treated mice compared to controls was observed (Schrauzer *et al.*, 1978).

Much laboratory animal evidence suggests that As does not act as an initiator in the process of multistage carcinogenesis, but rather as a promoter, progressor, or cocarcinogen. In male Wistar-King rats intratracheally administered a mixture of 0.26 mg arsenic trioxide and 0.4 mg benzo-*a*-pyrene (BaP), a higher incidence of pulmonary carcinoma was observed compared to controls receiving only 0.4 mg BaP (Ishinishi *et al.*, 1977). Male Wistar rats administered 160 mg/L sodium arsenite in the drinking water following intraperitoneal injection of diethylnitrosamine (DEN) developed significantly more renal adenocarcinomas compared to control rats treated with either sodium arsenite alone or DEN alone (Shirachi *et al.*, 1983).

Putative Mechanisms for Carcinogenesis

Despite a wealth of epidemiologic data, the mechanism by which As causes human cancers are unclear. Even though no single hypothesis for the mechanism of As carcinogenicity has widespread support, so far 7 plausible hypotheses regarding As's carcinogenic mode of action have been generated. These are (1) mutagenicity; (2) promotion; (3) progression; (4) cocarcinogenicity; (5) alterations in DNA methylation; (6) production of reactive oxygen species; and (7) inducible tolerance to As. The detailed information about putative mechanisms for As carcinogenesis can be found in Pott *et al.* (2001). In this dissertation research, we attempted to test the hypothesis that As is involved in a promotional (or progressional) step during carcinogenesis; in these studies, the initiated human keratinocytes, RHEK-1, were chronically exposed to a low level of As(III). Figure 1.1 illustrates schematically where the immortal keratinocytes such as RHEK-1 cells would fit into the heavy metal-mediated transformation/carcinogenic process. The promotional effects of As have been demonstrated in a variety of *in vivo* and *in vitro* models. Using Tg.AC transgenic mice that carry the v-Ha-*ras* oncogene, Germolec *et al.* demonstrated the co-promotional effect of As on the development of skin papillomas (Germolec *et al.*, 1998). In an investigation of the effect of As on hepatocellular proliferation, Sprague-Dawley rats were orally administered As(III) (1.6, 8.2, or 24.6 mg/kg) 21 and 4 hours prior to sacrifice (Brown and Kitchin, 1996). A marker of cell proliferation, hepatic ornithine decarboxylase, was increased in activity in treated rats compared to controls. In cultured human keratinocytes, low micromolar concentrations of As(III) have been shown to induce overexpression of the growth factors granulocyte macrophage-colony stimulating factor (GM-CSF) and transforming growth

factor α (TGF α) (Germolec *et al.*, 1996 and 1997). Proliferation of keratinocytes as assessed by an increase in cell numbers, expression of the c-*myc* oncogene, and incorporation of [^{3}H]thymidine into DNA was also observed. These data support a promotional role for As in a known human target tissue (Germolec *et al.*, 1996 and 1997). Similar alterations in growth factor expression were noted in samples of skin lesions obtained from residents of the Blackfoot disease-endemic region in Taiwan (Germolec *et al.*, 1998).

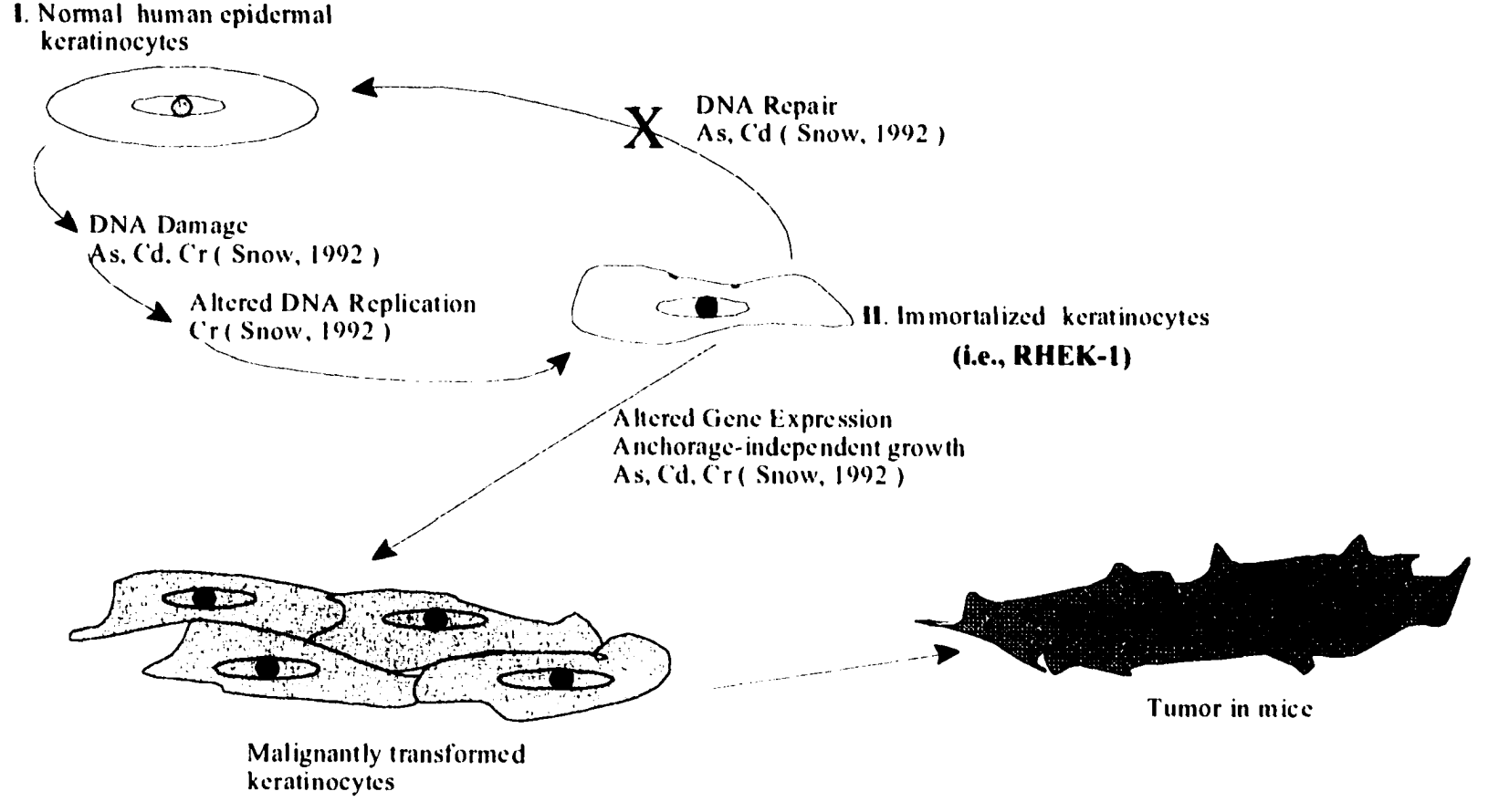

Fig. 1.1 Roles of individual metals in multistage cell transformation

Chromium

Source and Exposure

On a worldwide basis, about 80% of the Cr mined goes into metallurgical applications. In 1985, chromium trioxide produced was used for metal plating and treatment, wood treatment, and preservatives (NIH, 2001). The primary routes of potential human exposure to Cr and certain Cr compounds are inhalation, ingestion, and dermal contact. In occupational and environmental settings, Cr exists primarily in 2 valence states: hexavalent [Cr(VI)] and trivalent [Cr(III)] chromium. The chemical properties of Cr (i.e., solubility and speciation) are integral to its effectiveness. Cr(VI) is up to 1000 times more toxic than Cr(III) (Katz and Salem, 1993). Exposure to environmental Cr is an emerging concern. Cr is widely distributed in air, water, soils, and food, through which the general population can be exposed. For example, in Hudson County, New Jersey, Cr-containing industrial waste was deposited in landfills and also used in construction material for several decades. This resulted in more than 160 residential and commercial areas having excessive levels of insoluble Cr compounds in the soil and indoor dust (Freeman *et al.*, 1997)

Absorption, Distribution, Metabolism, Excretion

Cr(III) can cross cell and other membranes when the ligand environment is favorable (Bianchi and Levis, 1988). It has been suggested that Cr(III) may be toxic even though only very small amounts are able to penetrate into cells (Debetto and Luciani, 1988). The question concerning whether small amounts of Cr(III) might be toxic is complicated by the fact that Cr(III) is considered essential in mammals for maintenance

of glucose, lipid, and protein metabolism (Anderson, 1986; Sperling *et al.*, 1992). The essentiality of Cr(III) and the kinetic behavior of Cr(VI) and Cr(III) are important considerations in the development of a global understanding of Cr kinetics and toxicity.

Cr(VI) enters cells through membrane anionic transporters. Particulate Cr(VI) is uptaken by phagocytosis. Intracellular Cr(VI) is metabolically reduced to the ultimate Cr(III). Both Cr(III) and the reductional intermediate Cr(V), not Cr(VI), are capable of interactions with cellular macromolecules (i.e., DNA, RNA, proteins, and lipids). Cr(VI) that is systematically absorbed is reduced to Cr(III) *in vivo* by components of the blood and tissue prior to excretion (Lewalter *et al.*, 1985). Cr is excreted primarily in the urine. Elevated urine Cr concentrations can be used as a general marker of exposure to Cr.

Acute and Chronic Toxicity

Cr(VI) compounds: calcium chromate, chromium trioxide, lead chromate, strontium chromate, and zinc chromate are *known to be human carcinogens* based on sufficient evidence of carcinogenicity in humans (IARC, 1987). Cr(VI) is classified as Group A-*known human carcinogen* by the inhalation, but not by the oral route of exposure. Industrial exposure to certain Cr compounds has been associated with increased risk of respiratory tract cancers via inhalation exposure (Cohen *et al.*, 1993; French *et al.*, 1997; Hayes, 1997) and can cause allergic contact dermatitis in the workplace following skin contact (Lammintausta and Maibach, 1990). Cr(VI) is known to damage mucous membranes and cause renal damage (Dobney and Greenway, 1994). For Cr(VI), animal data are consistent with the findings of human epidemiological studies (Glaser *et al.*, 1986; Steinhoff *et al.*, 1983).

Several animal carcinogenicity studies using Cr(III) exposure by the ingestion or inhalation route have reported negative results between exposure and tumor incidence for rats and mice (Ivankovic and Preussman, 1975; Levy and Venitt, 1975). The International Agency for Research on Cancer (IARC, 1990) concluded that the animal data are inadequate for the evaluation of the carcinogenicity of Cr(III) compounds. Cr(III) is, therefore, classified as a Group D-*not classified as to its human carcinogenicity*.

Putative Mechanisms for Carcinogenesis

Due to the diversity in its solubility, speciation, and cellular/molecular effects, the study of Cr carcinogenesis is very complex. In the past 10 years there has been a considerable research effort directed toward understanding the mechanisms by which the known mutagen and human carcinogen chromate can cause DNA impairment. Cr-induced DNA-DNA interstrand crosslinks, intracellular reduction, oxidative processes and the tumor suppressor gene p53 are some of the major factors that may play a significant role in determining the cellular outcome in response to Cr exposure (Singh *et al.*, 1998). A number of DNA lesions including DNA-protein crosslinks (Tsapakos *et al.*, 1983; Wedrychowski *et al.*, 1985), DNA-interstrand crosslinks, single-strand breaks (Hamilton and Wetterhahn, 1986), and DNA-amino acid crosslinks (Zhitkovich *et al.*, 1995) have been observed after treatment of cultured mammalian cells with chromate. These lesions result in various types of functional damage such as: (1) DNA polymerase arrest and inhibition of DNA replication; (2) RNA polymerase arrest and inhibition of transcription; (3) inhibition of DNA topoisomerase; and (4) mutagenesis (Bridgewater *et al.*, 1994a and 1994b; Manning *et al.*, 1992; Xu *et al.*, 1992 and 1996). The intracellular

reduction of chromate is crucial for the formation of DNA lesions (Bianchi and Levis, 1988). *In vitro* studies have shown that glutathione (GSH), ascorbic acid, and cysteine have the ability to reduce Cr(VI). The metabolic reduction of Cr(VI) generates oxidative stress (probably in the form of reactive oxygen species), as well as the transient intermediate pentavalent and tetravalent oxidation states of Cr (Snow, 1992). These reduction products elicit a broad spectrum of genotoxic effects on DNA. DNA damage subsequently up regulates p53 and may initiate DNA repair, cell cycle arrest or apoptosis in Cr-treated cells.

Cadmium

Source and Exposure

The main use of cadmium is in electroplating or galvanizing because of its noncorrosive properties. Cd is a by-product of zinc and lead mining, refining, and smelting, which are important sources of environmental pollution (Friberg *et al.*, 1986; WHO, 1992). Factors contributing to the presence of Cd in soil are fallout from the air, Cd-containing water used for irrigation, and Cd added to fertilizers. The major route of environmental exposure to Cd for the general population is via consumption of contaminated food. In general, industrialized regions provide areas of greatest exposure to Cd, whereas rural areas can be quite low. Workplace exposure is particularly hazardous where there are Cd fumes or airborne Cd particulates (Waalkes *et al.*, 1992).

Absorption, Distribution, Metabolism, Excretion

Cd absorption is highly route dependent. In acute and chronic animal experiments, 5-20% of inhaled Cd has been recovered in the lungs (Nordberg *et al.*, 1985). The majority of particles deposited in the alveoli will be absorbed sooner or later depending on their solubility. Cd absorbed from the lungs or the gastrointestinal tract is mainly stored in the liver and kidneys, where more than half of the body burden will be deposited (Friberg *et al.*, 1974). The small, cysteine-rich protein known as metallothioneins (MT) is the main storage and transport protein for Cd (Nordberg, 1978; Nordberg *et al.*, 1992). It is estimated that the biological half-time of Cd in humans and laboratory animals can vary a great deal (between 93 days and 50 years) depending on the different study methods used (i.e., using radioactive Cd or kinetic compartment models). Most studies suggested, however, a half-time of 15-20 years in humans (Kjellstrom and Nordberg, 1978; Shaikh and Smith, 1980). When Cd-thionein is present in the plasma, it is quickly cleared by glomerular filtration and reabsorbed in the renal tubules or excreted in the urine (Cherian and Shaikh, 1975). When reabsorbed in the tubular cells, Cd-thionein is catabolized in the lysosome, releasing Cd ions. Most ingested Cd is excreted in the feces (Waalkes *et al.*, 1992).

Acute and Chronic Toxicity

In general, the route and duration of exposure ultimately determines which organs become targets of Cd toxicity. Acute exposures have been associated with damage to the testis, liver, and lungs. Inhalation of Cd fumes or other heated Cd-containing materials may produce an acute chemical pneumonitis and pulmonary edema. The principal long-

term effects of low-level exposure to Cd are chronic obstructive pulmonary disease and emphysema and chronic renal tubular disease (Friberg *et al.*, 1986).

Cd is a carcinogenic in both humans and animals by all routes of exposure tested (IARC, 1993). However, at particular target sites, sensitivity to the carcinogenic and toxic effects of Cd often depends on the species, strain, age, and sex of the animal (IARC, 1993). There have been a number of epidemiological studies intended to determine a relationship between occupational (respiratory) exposure to Cd and cancers in lung, prostate, and hematopoietic system (Kjellstrom *et al.*, 1979; Sorahan and Waterhouse, 1983; Waalkes *et al.*, 1992). Cd has been accepted by IARC as a Category 1 (human) carcinogen based primarily on its relationship to pulmonary tumors (IARC, 1993). In experimental animals, testes are the common target sites for Cd carcinogenesis (Waalkes *et al.*, 1992). Leydig cell tumors or hyperplasias are the most common testicular proliferative lesions found after Cd exposure in rodents.

Putative Mechanisms for Carcinogenesis

Although the mechanisms underlying Cd carcinogenesis have not been determined, experimental evidences suggest several theories for tumor induction by Cd as follows: (1) MTs play important roles in both mitigating and mediating Cd carcinogenicity. MT sequesters Cd in the cells and thereby acts as a detoxifying agent. At the same time, MT serves as a carrier of Cd between tissues, mainly from the liver to kidney where Cd, which has been released from degraded MT, exerts toxic effects (Jin *et al.*, 1998). Most evidence available at present indicates that toxicity to the kidney is related to the balance between toxic "free" Cd and Cd-MT in renal cells. MT may

mediate species-specific susceptibility to Cd-induced pulmonary carcinogenesis (Oberdorster *et al.*, 1994), and deficiencies in MT may leave mammalian testes and the rat ventral prostate particularly susceptible to the carcinogenic effects of the metal (Coogan *et al.*, 1994; Shiraishi *et al.*,1995); (2) Sarkar (1995) postulated that Cd replacement in DNA-binding zinc finger proteins may enhance cellular redox processing by Fenton reaction and generate free radicals to cause DNA damage; (3) The involvement of oxidative stress as a mechanism of chronic Cd-induced hepatotoxicity and renal toxicity was supported by Shaikh *et al* (1999). Inhibition of components of the antioxidant defense system accelerated and administration of antioxidants protected against Cd toxicity; and (4) Misra *et al* (1998) supported the hypothesis that direct modification of DNA is not the basis for Cd-induced transformation and suggested that Cd acts indirectly by interacting with the cells' DNA replication machinery or with factors involved in the transcription of cellular damage response genes.

Lead

Source and Exposure

Lead (Pb) is a common element in the earth's crust; its ubiquitous presence in bioavailable forms in the environment is due largely to human activities (Needleman, 1992). Pb is used in metalworking and in ceramics manufacture in Mexico and other countries (Rojas-Lopez, 1994) and thus, continues to be of concern to public health. Pb can be found in the air, in rivers and lakes, and in plants and animals, including those ingested by humans (U.S. Department of Health and Human Services, 1993). Studies carried out on toxicity mechanisms indicated that the most toxic Pb compounds are the

organic divalent cation such as lead acetate and lead phosphate (Nilsson, 1989). The primary routes of potential human exposure to lead acetate and lead phosphate are ingestion, inhalation, and dermal contact.

Absorption, Distribution, Metabolism, Excretion

Inhaled or ingested Pb is absorbed throughout the body systemically like Ca (O'Flaherty, 1998). Pb in plasma is distributed to primarily bone and soft tissues. Some portion of Pb is partitioned to a variety of low-molecular weight proteins in addition to hemoglobin (Lolin and O'Gorman, 1988). The age- and physiological state-dependent redistribution of Pb in bone to blood plasma is a unique phenomenon of Pb metabolism. Thus, plasma Pb is designated the pool from which both distribution and excretion occur. The rate of Pb excretion into urine and feces is dependent on plasma concentration of Pb.

Acute and Chronic Toxicity

Animal carcinogenicity data after exposure to soluble Pb salts are sufficient to classify Pb as a *probable human carcinogen* (IRIS, 1993). More than 10 rodent bioassays have shown statistically significant increases in renal tumors and cerebral gliomas with dietary and subcutaneous exposure to several Pb salts (Azar *et al.*, 1972; Kasprzak *et al.*, 1985; Koller *et al.*, 1985). Pb compounds are capable of inducing chromosomal aberrations *in vivo* (Grandjean *et al.*, 1983) and in tissue cultures (U.S. EPA, 1986). *In vitro* neoplastic transformation of Syrian hamster embryo (SHE) cells by Pb acetate was reported by DiPaolo *et al.* (1978).

Exposure to environmental Pb may affect numerous organ systems, of particular importance is the central nervous system (CNS) (Goyer, 1993; Munoz *et al.*, 1993). The resulting adverse effects of Pb include mental retardation, impaired cognitive functions, and behavioral abnormalities, particularly in children (ATSDR, 1992). At least 3 million children in the United States suffer the behavioral and cognitive effects of Pb exposure. The CNS undergoes development during the first few years of life. During this time, infants and children are especially sensitive to Pb poisoning. The mechanism leading to these manifestations are mostly unknown (Angle, 1993). Pb also affects the peripheral nervous system, induces an inflammatory response, and modulates immune functions.

Putative Mechanism for Carcinogenesis

Pb induction of renal adenocarcinoma in rats and mice is dose related and has not been reported at levels below that which produces nephrotoxicity. Pb-induced tumors maybe a consequence of increased cellular proliferation (Calabrese and Baldwin, 1992). Pb compounds have been shown to stimulate the proliferation of renal tubular epithelial cells (Choie and Richter, 1980). As of today, there is no putative mechanism for Pb-mediated cerebral gliomas in experimental rats.

Metal Mixtures

Source and Exposure

Humans are rarely exposed to only one toxic element, and manifestations from other metals may also be present. In fact, 100 or more different chemicals can be found at a single hazardous waste site in varying combinations in water, soil, and air (De Rosa *et*

al., 1996). Human exposure to As, Cr, Cd, and Pb can occur after both occupational and environmental exposure to high levels of these elements. For example, children who develop Pb intoxication from ingestion of paint may be exposed to Cd as well; Cd is used as a pigment in yellow and some red paints. In industrial situations exposure to a number of elements may occur simultaneously, such as in primary and secondary metal smelters. These metals rank particularly high on the ATSDR Completed Exposure Pathway Site Count Report and pose the some of the highest risk to public health (ATSDR, 1997). Their priority rankings are Pb, 2; As, 4; Cd, 6; and Cr, 7.

Challenges in Mixture Studies

Because of the infinite number of potential combinations of chemicals in mixtures and the limited resources available, it would be impossible to test all of them using empirical approaches (Yang, 1992). In fact, the actual mixture effect for a given set of constituents might strongly depend on the actual composition of the mixture (i.e., the ratios of constituent), as well as their nature (Verhaar *et al.*, 1997). Numerous laboratories have carried out detailed studies on the toxic effects of As, Cd, Cr, and Pb individually as discussed above. The specific studies on individual metals are helpful in that knowledge of the molecular effects of individual metals may provide insight into which metal in a mixture may be responsible for an observed toxicological endpoint. One approach to the assessment of chemical mixtures is the toxic equivalency factor approach, which normalizes the dose of each component of the mixture against that of the most potent compound, the relative potencies are then summed to estimate the toxic potency of the mixture (Safe, 1998). However, definition of the toxicity of combinations

of metals strictly on the basis of individual metal toxicity has been shown to be unreliable and certainly appears imprudent (Mahaffey *et al.*, 1981). A more realistic approach has to be taken in evaluation of potential human health risks of exposure to metal mixtures.

Given the complexity of mixture issues, it is not surprising that research approaches in mixtures toxicology have varied. The use of standard safety factor approaches and response surface analyses have applied to multicomponent mixtures (Groten *et al.*, 1997; Nesnow *et al.*, 1998). More recently, analyses of xenoestrogen and metal mixtures using the concepts of response and concentration addition have demonstrated the combination effects of chemical interactions in mixtures (Kortenkamp and Altenburger, 1998; Tully *et al.*, 2000). Particularly, the reevaluation on previously published data with mixtures of xenoestrogens using the method of isoboles have shown that much published work suffers from an undue focus on measuring effects of mixtures at only one dose level. Assessments of combination effects were frequently complicated by a lack of information on dose-response relationships. Some studies that purportedly showed absence of synergy had in fact overlooked synergisms (Ashby *et al.*, 1997; Kortenkamp and Altenburger, 1998). And authors emphasized that reliable determinations of the type of combination effect are based on a dose-response analysis of individual agents and the mixture (Kortenkamp and Altenburger, 1998). Integrated quantitative structure-activity relationships and physiologically based pharmacokinetic-pharmacodynamic modeling have been proposed to better understand the pharmacokinetics and dynamics of complex mixtures of petroleum products (Verhaar *et al.*, 1997). The studies described here have stimulated research in the toxicology community regarding this complex, and yet very important, area of research.

Carcinogenicity of Metal Mixtures

There have been a few studies assessing the toxicity of carcinogenic metal mixtures that have been carried out to identify and characterize metal-metal interactions. For instance, Diaz-Barriga *et al.* (1990) has found that when Cd and As were co-administered, they are more toxic than when given alone. Concurrent exposure to Pb (200 ppm), Cd (50 ppm), and As(V) (50 ppm), as well as individual metal treatment was studied in the rat to characterize effects on toxicity and tissue metal concentrations (Mahaffey *et al.*, 1981). These studies indicated that interactions between common toxic elements do occur and are characterized by alterations in both tissue trace metal levels and toxicity (Mahaffey *et al.*, 1981). Recently, one study indicated that Cd can block apoptosis induced by Cr and the suppression of apoptosis by Cd may be a significant aspect of its carcinogenic mechanism (Shimada *et al.*, 1998). Hochadel and Waalkes (1997) reported that the sequence of exposure to Cd and As determined the extent of toxic effects in male Fisher rats. As pretreatment markedly reduced hepatotoxicity and mortality in rats due to Cd exposure. However, Cd pretreatment did not alter the lethality of the high dose of As and had no effect on As-induced hepatotoxicity. The aspect of sequence of exposure clearly should be included as an important element in assessment of the combination toxicity of metals. Tully *et al.* (2000) studied metal-metal interactions through use of metal-responsive promoters linked to the luciferase reporter gene. Surprisingly, no evidence of synergistic toxicity with regard to gene expression by a battery of 13 different promoters was seen with a mixture of 7.5 μM Cd(II), 750 μM Cr(III) and 100 μM Pb(II) in recombinant HepG2 cells (Tully *et al.*, 2000).

Interactions between Essential Metals and Nonessential Metals

There are several essential metals that can, under the appropriate exposure scenarios, act in a toxic manner, either alone or in combination with other metals. Interactions between the physiologically essential metals calcium (Ca), magnesium (Mg), and zinc (Zn) and the carcinogenic metals nickel (Ni) and Cd were investigated to help elucidate the mechanisms of action of the carcinogenic metals by several investigators (Kasprzak and Poirier, 1985; Kasprzak *et al.*, 1987; Poirier *et al.*, 1983). Numerous experiments indicate that the acutely toxic and carcinogenic activity of metal can be either enhanced or inhibited by concurrent administration of other essential metals such as Mg (Durlach *et al.*, 1986, Kasprzak *et al.*, 1987; Nordberg *et al.*, 1985). Durlach and colleagues demonstrated that Mg acts as a competitive antagonist of Pb and Cd. For example, Cd competes with Ca for absorption from the gut and the excess Zn decreases the carcinogenicity of Cd (Lucis *et al.*, 1972; Washko and Cousins, 1975).

III. Use of *in vitro* cell culture systems for screening potential carcinogens

To supplement the conventional two-year bioassays for carcinogenesis, *in vitro* cell transformation assays have been extensively used for a rapid screening tool for potential carcinogens and tumorigenesis promoters as well as for mechanistic studies with chemical carcinogens (Boone *et al.*, 1995). Following the report by Berwald and Sachs on the induction of morphological transformation in Syrian hamster embryo cells by the carcinogen BaP, a host of *in vitro* oncogenic transformation systems have been developed based on a variety of rodent and human cells (Berwald and Sachs, 1963, 1965; Kakunaga, 1973; Milo *et al.*, 1978; Reznikoff *et al.*, 1973). These *in vitro* model systems

represent a powerful research tool in addressing two diverse aspects of cancer research. First, *in vitro* systems, free of host-mediated homeostatic influences, afford the opportunity to evaluate both qualitative and quantitative aspects of oncogenic transformation. Second, *in vitro* systems make it possible to study the cellular and molecular mechanisms involved in chemically, physically, or virally induced carcinogenesis (Hall and Hei, 1990). The human cell systems (i.e., human fibroblasts, keratinocytes, and uroepithelial cells) are complex, but are most relevant to the assessment of cancer risk in the human. While assays involving the established fibroblast cell lines are highly repeatable and quantitative, systems involving the human epithelial cells are less quantitative (Hall and Hei, 1986; Hall *et al.*, 1989).

Cellular transformation is characterized in part by altered cell growth, anchorage-independent proliferation, loss of contact inhibition, and immortality. Transformation *in vitro* is an experimental endpoint associated with changes in gene expression, oncogene activation, or signal transduction. These changes lead to mutant oncogene protein products and/or to increased expression of normal protooncogene protein products. These multiple changes may, in the aggregate, be responsible for the cumulative morphologically transformed, anchorage-independent, tumorigenic phenotype (Billings *et al.*, 1987; Land *et al.*, 1983a and 1983b; Shuin *et al.*, 1986).

All known carcinogenic metals have been shown to induce morphological transformation of cells in culture in one or more assay system (Landolph, 1990). Pb-mediated cellular transformation is discussed above in the literature review on Pb. Malignant transformation after exposure to As is addressed in detail in Chapter 6.

Cr(VI), as lead chromate, induced morphological transformation in cultured SHE cells, C3H/10T1/2 murine cell line, Balb/3T3 A31 mouse embryo fibroblasts, and human diploid foreskin fibroblasts (Biedermann and Landolph, 1987; Dipaolo and Casto, 1979; Patierno *et al.*, 1988; Saffiotti and Bertolero, 1988). Morphological transformation was reported following exposure to Cd as cadmium salts in SHE cells and Balb/3T3 A31 mouse embryo fibroblasts (Dipaolo and Casto, 1979; Rivedal and Sanner, 1981; Saffiotti and Bertolero, 1989).

IV. General keratinocyte transformation system

Human epidermal cells have been chosen for cancer research for the last two decades as they can be obtained relatively easily during plastic surgery and techniques for epidermal cell culture have been well established (Kuroki *et al.*, 1989). An attempt to transform primary human epidermal cells by BaP and TPA was made by Kuroki *et al.* (1989), but they did not succeeded in obtaining chemically-induced transformants. As of today, it has not been possible to generate a transformed human cell line by treatment with chemicals alone. In contrast, studies with immortalized human cells have demonstrated that the later stages of transformation can be readily induced by carcinogenic chemicals. For example, three chemicals (MNNG, NQO, and TCDD) have been shown to malignantly transform a virally (adenovirus12-simian virus 40; Ad12-SV40) immortalized human keratinocyte cell line, RHEK-1 (Rhim *et al.*, 1986; Yang *et al.*, 1992). This cell line contained the SV40 tumor antigen, but was not tumorigenic in nude mice (Rhim *et al.*, 1986). RHEK-1 cells were also utilized for studying neoplastic conversion by a variety of virus/viral oncogenes (i.e., Kirsten murine sarcoma virus, c-H-

ras, *ras*, *bas*, *fes*, *fms*, *erb*B, *src*) and X-ray (Rhim *et al.*, 1988; Rhim, 1989). This *in vitro* system has been very useful when employed to study the multistep nature of human epithelial cell carcinogenesis.

For over 60 years, studies of multi-stage skin carcinogenesis have been extensively carried out using both isolated primary and immortalized keratinocytes *in vitro* and murine *in vivo* model systems and have defined several genotypic and phenotypic alterations occurring during the transformation process (Choi *et al.*, 1991; Gaido *et al.*, 1992; Glick *et al.*, 1991, 1994; Pietenpol *et al.*, 1990; Punnonen *et al.*, 1994; Yuspa, 1994). For example, multiple benign squamous papillomas precede the development of an occasional squamous cell carcinoma. The incidence of carcinomas can be substantially enhanced by treating papilloma-bearing mice with mutagens such as urethane, NQO, or cisplatinum suggesting that a distinct genetic event is responsible for malignant conversion (Yuspa and Greenhalgh, 1989). Scientific discoveries derived from studies in mouse skin have proven to be landmarks in cancer research include: the binding of carcinogens to DNA; the monoclonal origin of benign and malignant tumors; the powerful tumor-promoting action of phorbol esters; the antipromoting potency of retinoids and steroids; the modifying role of age, caloric intake, and specific dietary constituents on cancer induction; the variable risk for benign tumors to progress to cancer; the separation of mechanistically distinct stages in cancer pathogenesis (initiation, promotion, premalignant progression, malignant conversion); and the requirement for multiple genetic changes in malignant conversion (Yuspa, 1994).

V. Effects of metals on keratinocytes

Studies on the acute effects of the As on such critical cellular and molecular events as differential expression of growth factors, oncogene activation, and cell proliferation and differentiation were carried out in two consecutive studies (Germolec *et al.*, 1996 and 1997). As has substantial effects on epidermal keratinocytes *in vitro*, altering expression of important growth regulatory factors (TGFα and TGF β2) and growth-promoting cytokines (tumor necrosis factor α, GM-CSF) (Germolec *et al.*, 1996 and 1997). Total cell numbers, as well as *c-myc* expression and incorporation of [^{3}H]thymidine, both indicators of cell proliferation, were also elevated in keratinocyte cultures treated with sodium arsenite. These studies demonstrated that growth factors and growth-promoting cytokines could play a significant role in As-induced skin cancer. As has also shown to increase expression of cytokine interleukin-8 in cultured keratinocytes (Yen *et al.*, 1996). A recent study with the HaCaT human keratinocytes by Hamadeh *et al.* (1999) proposed disruption of the p53-mdm2 loop regulating cell cycle arrest as a model for As-related skin carcinogenesis. Interestingly, one study has shown that As(V) suppresses involucrin, one of the suprabasal differentiation markers, expression and keratinocyte programming by altering the transcription factors AP1 and AP2 (Kachinskas *et al.*, 1994 and 1997).

The cytotoxic effects of Cr(VI) and Cr(III) on normal human keratinocytes and the HaCaT keratinocyte cell line were characterized by a previous study (Little *et al.*, 1996). Normal human keratinocytes showed a much greater variability in their response to Cr(VI) than HaCaT cells and were generally more resistant to Cr(VI)-induced cytotoxicity. The potassium chromate suppresses expression of differentiation markers in

human keratinocyte line SCC-9 as As(V) does (Kachinskas *et al.*, 1997). Chromate is the most common cause of allergic contact dermatitis among men (Fregert *et al.*, 1969). Previous studies by Gueniche *et al.* (1994) indicated that Cr mediates an aggressive cellular effect during allergic contact dermatitis by inducing cytokine TNFα and nuclear stress protein Hsp72 in normal human keratinocytes (Gueniche *et al.*, 1994).

Cd induced a low expression level of TNFα detectable by immunocytochemistry correlating with the induction of nuclear protein Hsp72 which is closely linked genetically with the TNFα locus in normal human keratinocytes (Gueniche *et al.*, 1994).

VI. Utilization of DNA microarray technology to understand gene expression changes in toxicological problems

During the past two decades, genome-scale sequencing efforts directed toward the Human Genome Project (Collins *et al.*, 1998), as well as several model organisms, generated large-scale databases. As a result, numerous new genes were discovered, some of them encoding proteins with a function that is still unknown. New technologies, such as DNA microarray, incorporating this information are radically altering biological research in many scientific disciplines including cancer biology, toxicology, and the applied areas of disease diagnostics and drug development (Afshari, 2002). Today, in the scientific literature, the number and diversity of data generated from microarray experiments are impressive. Tracking the numbers of publications in PubMed reveals that, since 1995, over 2,000 papers have included the microarray technology (Afshari, 2002). In 1999 and 2000, there was the biggest increase in the number of microarray literature papers. Scientists in the arena of cancer biology have been some of the most industrious at incorporating this technology into their studies. The comparison of gene

expression in various stages of tumor development (Alizadeh *et al.*, 1999; DeRish *et al.*, 1996; Hedenfalk *et al.*, 2001; Khan *et al.*, 1999; Ramaswamy *et al.*, 2001; Sorlie *et al.*, 2001) and monitoring expression of premalignant and tumorigenic cells following exposure to anticancer agents or tumor promoters (Golub *et al.*, 1999; Scherf *et al.*, 2000; Shipp *et al.*, 2002; van't Veer *et al.*, 2002) utilized the microarray technique. Several laboratories (Alizadeh *et al.*, 2000; Golub *et al.*, 1999) demonstrated that gene expression profiling of patient lymphoma samples improved distinction of tumor classification and provided insight on clinical outcome. These and other data indicate that one important benefit of this technology might be to inform clinicians of better, specific markers for cancer diagnosis, prognosis and treatment (Dhanasekaran *et al.*, 2001).

Toxicogenomics is a new scientific subdiscipline that combines the emerging technologies of genomics and bioinformatics to identify and characterize mechanisms of action of known and suspected toxicants. Currently, the premier toxicogenomic tools are the DNA microarray and the DNA chip. Although toxicologists are sure to find more uses for microarrays than can be predicted, microarrays will likely be used in the immediate future to better address a number of key toxicological issues, including mode of action, dose-response relationships, chemical interactions and hazard identification in chemical mixtures, and human exposure assessment (CIIT, 2001). Each issue is separately addressed. (1) Microarrays will be useful in gaining a better understanding of how particular chemicals interact with genes that are associated with a mode of action to produce a particular kind of toxic response. To advance this concept, an analysis of gene expression patterns for different chemicals after different doses or times of exposure or in genetically altered experimental animals will allow a clearer understanding of the genes

that are mechanistically linked to a toxicological response. (2) Microarrays can be used to characterize the changes in expression of thousands of genes at a wide range of doses to characterize the linearity or nonlinearity of dose-response curves that work through both receptor and nonreceptor systems. Pitot (Pitot, 1993) and McClellan (McClellan, 1995) have previously suggested a conceptual framework for such studies. (3) Microarrays have two immediate uses in better understanding the health risks of exposure to chemical mixtures. First, in defined animal systems where toxic effects are well characterized, interactions between two or more chemicals could be evaluated by comparing changes in gene expression of the mixture with the sum of the changes for each individual chemical. Gene expression levels that are not additive (i.e., the expression of each gene is more or less than that predicted by the addition of each chemical) would indicate interaction of the chemicals. With this type of analysis, the rules for interaction between chemicals having similar or different modes of action could be determined. Second, mixtures consisting of unknown chemicals or known chemicals with unknown toxic properties could be evaluated in laboratory animals or primary human cells for changes in gene expression. The composite fingerprint produced by the mixture could be compared to a database of profiles of different mode-of-action classes to determine the types of chemicals in the mixture and their potential for adverse human effects. (4) A challenge for toxicologists is to determine the level and adverse effects of chemical exposure in humans. Assessment of exposure is usually based on chemical levels in blood or tissues or on measurement of biomarkers of toxicity such as increases in DNA adducts. Another useful biomarker may be changes in gene expression as measured by microarrays. Promising new technologies would allow assessment of gene expression in circulating

blood lymphocytes or tissue biopsies. In studies where human volunteers are exposed to defined levels of chemicals, gene expression fingerprints of an individual could be compared before and after exposure to identify genes whose expression levels are altered after chemical exposure. These studies in humans could be compared to similar studies in rodents in which correlations between toxicity and alterations in specific genes are made. Based on the fingerprinting technique discussed above, these comparisons may lead to the identification of the mode-of-action class and an estimate of the tissue dose.

Dissertation Objective

This thesis project focused on studies of the cytotoxic and carcinogenic effects of As or an As-containing metal mixture on human keratinocytes; their long-term goal is to contribute to the development of an alternative and efficient approach to test the cytotoxic and carcinogenic potentials of environmentally relevant chemicals/chemical mixtures. **Five specific aims** to meet the dissertation objective were designated as follows: **(1)** To determine the cytotoxicity of As, Cd, Cr, and Pb, and to characterize cytotoxic interactions among these metals in a mixture, in human epidermal keratinocytes; **(2)** To assess the transforming potential of As and the As-containing 4 metal mixture as compared to a known carcinogen, MNNG, in the immortal keratinocyte cell line, RHEK-1; **(3)** To identify alterations in gene expression that correlate with enhancement or inhibition of spontaneous malignant conversion in cell lines established from specific aim 2 using cDNA microarray and Real Time RT-PCR methodologies; **(4)** To correlate alterations in a defined subset of genes with sequential stages in the RHEK-1 transformation process by MNNG using Real Time RT-PCR approach; and **(5)** To

identify genes commonly affected in RHEK-1 cells transformed by multiple chemical agents, MNNG, NQO, and TCDD, by the use of DNA microarray analysis.

The first step toward achieving these specific aims was to obtain individual metal (As, Cr, Cd, and Pb) cytotoxicity curves which would be utilized for identifying metal-metal interactions and characterizing the types of interactions in a metal mixture in 4 human keratinocyte strains (Chapter 2). Acute cytotoxicity data served as a basis for designing the long-term exposure dose level for As and the metal mixture in RHEK-1 cell transformation studies in Chapter 3. In Chapters 3 and 4, the gene expression changes accompanying enhancement or inhibition of spontaneous transformation by MNNG or As/mixture, respectively, were (semi)quantitatively measured by cDNA microarray and Real Time RT-PCR technologies. A common battery of genes altered during transformation of RHEK-1 by MNNG, NQO, and TCDD, as well as chemical-specific gene changes was detected by the use of oligo DNA microarrays in Chapter 5.

References

Afshari, C. A. Perspective: microarray technology, seeing more than spots. Endocrinology, *143*: 1983-1989, 2002.

Alizadeh, A. A., Eisen, M. B., Davis, R. E., Ma, C., Lossos, I. S., Rosenwald, A., Boldrick, J. C., Sabet, H., Tran, T., Yu, X., Powell, J. I., Yang, L., Marti, G. E., Moore, T., Hudson, J., Jr., Lu, L., Lewis, D. B., Tibshirani, R., Sherlock, G., Chan, W. C., Greiner, T. C., Weisenburger, D. D., Armitage, J. O., Warnke, R., Staudt, L. M., and . Distinct types of diffuse large B-cell lymphoma identified by gene expression profiling. Nature, *403*: 503-511, 2000.

Alizadeh, A., Eisen, M., Davis, R. E., Ma, C., Sabet, H., Tran, T., Powell, J. I., Yang, L., Marti, G. E., Moore, D. T., Hudson, J. R., Jr., Chan, W. C., Greiner, T., Weisenburger, D., Armitage, J. O., Lossos, I., Levy, R., Botstein, D., Brown, P. O., and Staudt, L. M. The lymphochip: a specialized cDNA microarray for the genomic-scale analysis of gene expression in normal and malignant lymphocytes. Cold Spring Harb.Symp.Quant.Biol, *64*: 71-78, 1999.

Anderson, R. A. Chromium metabolism and its role in disease processes in man. Clin.Physiol Biochem., *4*: 31-41, 1986.

Angle, C. R. Childhood lead poisoning and its treatment. Annu.Rev.Pharmacol Toxicol, *33*: 409-434, 1993.

Ashby, J., Lefevre, P. A., Odum, J., Harris, C. A., Routledge, E. J., and Sumpter, J. P. Synergy between synthetic oestrogens? Nature, *385*: 494, 1997.

ATSDR. Toxicological Profiles for Arsenic. 2000. Atlanta, Georgia, Department of Health and Human Services, Public Health Service.

ATSDR. Toxicological Profiles for Lead. 1992. Atlanta, Georgia, Department of Health and Human Services, Public Health Service.

ATSDR. 1997 CERCLA priority list of hazardous substances that will be the subject of toxicological profiles & support document. Atlanta, Georgia, Department of Health and Human Services, Public Health Service. 1997.

ATSDR. 2001 CERCLA priority list of hazardous substances. Atlanta, Georgia, Department of Health and Human Services, Public Health Service. 2001.

Azar, A., Trochimowicz, H. J., and Maxfield, M. E. Review of lead studies in animals carried out at Haskell Laboratory-Two year feeding study and response to hemorrhage study. Barth, D., Berlin, A., Engel, R., Recht, P., and Smeets, J. 199-208. 1973. Amsterdam, The Netherlands, Commission of the European Communities, Luxemberg. Environmental health aspects of lead: Proceedings International Symposium; October 1972.

Berwald, Y. and Sachs, L. In vitro transformation with chemical carcinogens. Nature, *200*: 1182-1184, 1963.

Berwald, Y. and Sachs, L. In vitro transformation of normal cells to tumor cells by carcinogenic hydrocarbons. J Natl.Cancer Inst., *35*: 641-661, 1965.

Bianchi, V. and Levis, A. G. Review of genetic effects and mechanisms of action of chromium compounds. Sci Total Environ., *71*: 351-355, 1988.

Biedermann, K. A. and Landolph, J. R. Induction of anchorage independence in human diploid foreskin fibroblasts by carcinogenic metal salts. Cancer Res, *47*: 3815-3823, 1987.

Billings, P. C., Shuin, T., Lillehaug, J., Miura, T., Roy-Burman, P., and Landolph, J. R. Enhanced expression and state of the c-myc oncogene in chemically and X- ray-transformed C3H/10T1/2 Cl 8 mouse embryo fibroblasts. Cancer Res, *47*: 3643-3649, 1987.

Boone, L. R., Moore, K. G., Phelps, W. C., and Woo, Y. Molecular biology of virally-induced cell transformation and tumorigenesis. *In* J. C. Arcos, M. F. Argus, and Y. Woo (eds.), Chemical induction of cancer; Modulation and combination effects: An inventory of the many factors which influence carcinogenesis, pp. 541-609. Boston: Birkhauser, 1995.

Bridgewater, L. C., Manning, F. C., and Patierno, S. R. Base-specific arrest of in vitro DNA replication by carcinogenic chromium: relationship to DNA interstrand crosslinking. Carcinogenesis, *15*: 2421-2427, 1994a.

Bridgewater, L. C., Manning, F. C., Woo, E. S., and Patierno, S. R. DNA polymerase arrest by adducted trivalent chromium. Mol.Carcinog., *9*: 122-133, 1994b.

Brown, J. L. and Kitchin, K. T. Arsenite, but not cadmium, induces ornithine decarboxylase and heme oxygenase activity in rat liver: relevance to arsenic carcinogenesis. Cancer Lett., *98*: 227-231, 1996.

Buchet, J. P., Lauwerys, R., and Roels, H. Urinary excretion of inorganic arsenic and its metabolites after repeated ingestion of sodium metaarseite by volunteers. International Archives of Occupational & Environmental Health, *48*: 111-118, 1981.

Byron, W. R., Bierbower, G. W., Brouwer, J. B., and Hansen, W. H. Pathologic changes in rats and dogs from two-year feeding of sodium arsenite or sodium arsenate. Toxicology & Applied Pharmacology, *10*: 132-147, 1967.

Calabrese, E. J. and Baldwin, L. A. Lead-induced cell proliferation and organ-specific tumorigenicity. Drug Metab Rev., *24*: 409-416, 1992.

Cebrian, M. E., Albores, A., Garcia-Vargas, G., Del Razo, L. M., and Ostrosky-Wegman, P. Chronic Arsenic Poisoning in Humans: The Case of Mexico. *In* J. O. Nriagu (ed.), Arsenic in the Environment; Part II: Human Health and Ecosystem Effects, vol. 27, 1 ed, pp. 93-107. New York: John Wiley and Sons, Inc., 1994.

Chen, C.-J., Chuang, Y.-C., Lin, T.-M., and Wu, H.-Y. Malignant neoplasms among residents of a blackfoot disease-endemic area in Taiwan: high-arsenic artesian well water and cancer. Cancer Res., *45*: 5895-5899, 1985.

Cherian, M. G. and Shaikh, Z. A. Metabolism of intravenously injected cadmium-binding protein. Biochem.Biophys.Res Commun., *65*: 863-869, 1975.

Choi, E. J., Toscano, D. G., Ryan, J. A., Riedel, N., and Toscano, W. A. Dioxin induces transforming growth factor-α in human keratinocytes. J Biol Chem *266*: 9591-9597. 1991.

Chiou, H. Y., Hsueh, Y. M., Hsieh, L. L., Hsu, L. I., Hsu, Y. H., Hsieh, F. I., Wei, M. L., Chen, HC, Yang, H. T., Leu, L. C., Chu, T. H., Chen-Wu, C., Yang, M. H., and Chen, C. J. Arsenic methylation capacity, body retention, and null genotypes of glutathione S-transferase M1 and T1 among current arsenic-exposed residents in Taiwan. Mutat.Res., *386* : 197-207, 1997.

Choie, D. D. and Richter, G. W. Effects of lead on the kidney. *In* R. L. Singhall and J. A. Thomas (eds.), Lead Toxicity, pp. 187-212. Baltimore: Urban and Schwarzenberg, 1980.

Choprapawon, C. and Rodcline, A. Chronic arsenic poisoning in Ronpibool Nakhon Sri Thammarat, the southern province of Thailand. *In* C. O. Abernathy, R. L. Calderon, and W. R. Chappell (eds.), Arsenic. Exposure and Health Effects, pp. 69-77. New York, NY: Chapman & Hall, 1997.

CIIT. Toxicogenomics. www.ciit.org 2001.

Cohen, M. D., Kargacin, B., Klein, C. B., and Costa, M. Mechanisms of chromium carcinogenicity and toxicity. Crit Rev.Toxicol., *23*: 255-281, 1993.

Collins, F. S., Patrinos, A., Jordan, E., Chakravarti, A., Gesteland, R., and Walters, L. New goals for the U.S. Human Genome Project: 1998-2003. Science, *282*: 682-689, 1998.

Coogan, T. P., Shiraishi, N., and Waalkes, M. P. Apparent quiescence of the metallothionein gene in the rat ventral prostate: association with cadmium-induced prostate tumors in rats. Environ.Health Perspect., *102 Suppl 3*: 137-139, 1994.

Das, D., Chatterjee, A., Samanta, G., Mandal, B., Chowdhury, T. R., Chowdhury, P. P., Chanda, C., Basu, G., and Lodh, D. Arsenic contamination in groundwater in six districts of West Bengal, India: the biggest arsenic calamity in the world. Analyst, *119*: 168N-170N, 1994.

Debetto, P. and Luciani, S. Toxic effect of chromium on cellular metabolism. Sci Total Environ., *71*: 365-377, 1988.

DeRisi, J., Penland, L., Brown, P. O., Bittner, M. L., Meltzer, P. S., Ray, M., Chen, Y., Su, Y. A., and Trent, J. M. Use of a cDNA microarray to analyse gene expression patterns in human cancer [see comments]. Nature Genetics, *14*: 457-460, 1996.

De Rosa, C. T., Johnson, B. L., Fay, M., Hansen, H., and Mumtaz, M. M. Public health implications of hazardous waste sites: findings, assessment and research. Food Chem.Toxicol, *34*: 1131-1138, 1996.

Dhanasekaran, S. M., Barrette, T. R., Ghosh, D., Shah, R., Varambally, S., Kurachi, K., Pienta, K. J., Rubin, M. A., and Chinnaiyan, A. M. Delineation of prognostic biomarkers in prostate cancer. Nature, *412*: 822-826, 2001.

Diaz-Barriga, F., Llamas, E., Mejia, J. J., Carrizales, L., Santoyo, M. E., Vega-Vega, L., and Yanez, L. Arsenic-cadmium interaction in rats. Toxicology, *64*: 191-203, 1990.

DiPaolo, J. A. and Casto, B. C. Quantitative studies of in vitro morphological transformation of Syrian hamster cells by inorganic metal salts. Cancer Res, *39*: 1008-1013, 1979.

DiPaolo, J. A., Nelson, R. L., and Casto, B. C. In vitro neoplastic transformation of Syrian hamster cells by lead acetate and its relevance to environmental carcinogenesis. Br.J Cancer, *38*: 452-455, 1978.

Dobney, A. M. and Greenway, G. M. Online determination of chromium by adsorptive cathodic stripping voltammetry. Analyst, *119*: 293-297, 1994.

Durlach, J., Bara, M., Guiet-Bara, A., and Collery, P. Relationship between magnesium, cancer and carcinogenic or anticancer metals. Anticancer Res, *6*: 1353-1361, 1986.

Engel, R. R., Hopenhayn-Rich, C., Receveur, O., and Smith, A. H. Vascular Effects of Chronic Arsenic Exposure: A Review. Epidemiologic Reviews, *16*: 184-209, 1994.

Faroon, O. M., Williams, M., and O'Connor, R. A Review of the Carcinogenicity of Chemicals Most Frequently Found at National Priorities List Sites. Toxicology and Industrial Health, *10*: 203-230, 1994.

Fay, M. and Mumtaz, M. M. Development of a priority list of chemical mixtures occurring at 1188 hazardous waste sites using the HazDat database. Food Chem.Toxicol., *34*: 1163-1165, 1996.

Freeman, N. C., Stern, A. H., and Lioy, P. J. Exposure to chromium dust from homes in a Chromium Surveillance Project. Arch.Environ.Health, *52*: 213-219, 1997.

Fregert, S., Hjorth, N., Magnusson, B., Bandmann, H. J., Calnan, C. D., Cronin, E., Malten, K., Meneghini, C. L., Pirila, V., and Wilkinson, D. S. Epidemiology of contact dermatitis. Trans.St.Johns.Hosp.Dermatol.Soc., *55*: 17-35, 1969.

French, C., Peters, W., Maxwell, B., Rice, G., Colli, A., Bullock, R., Cole, J., Heath, E., Turner, J., Hetes, B., Brown, D. C., Goldin, D., Behling, H., Loomis, D., and Nelson, C. Assessment of health risks due to hazardous air pollutant emissions from electric utilities. Drug Chem.Toxicol., *20*: 375-386, 1997.

Friberg, L., Elinder, C. G., Kjellstrom, T., and Nordberg, G. F. Cadmium and health, a toxicological and epidemiological appraisal. Vol. II. Effects and Response.Cleveland, Ohio: CRC Press, 1986.

Gaido, K. W., Maness, S. C., Leonard, L. S., and Greenlee, W. F. 2,3,7,8-Tetrachlorodibenzo-p-dioxin-dependent regulation of transforming growth factors-α and β2 expression in a human keratinocyte cell line involves both transcriptional and post-transcriptional control. J Biol Chem, *267*: 24591-24595, 1992.

Germolec, D. R., Spalding, J., Boorman, G. A., Wilmer, J. L., Yoshida, T., Simeonova, P. P., Bruccoleri, A., Kayama, F., Gaido, K., Tennant, R., Burleson, F., Dong, W., Lang, R. W., and Luster, M. I. Arsenic can mediate skin neoplasia by chronic stimulation of keratinocyte-derived growth factors. Mut Res, *386*: 209-218, 1997.

Germolec, D. R., Spalding, J., Yu, H.-S., Chen, G. S., Simeonova, P. P., Humble, M. C., Bruccoleri, A., Boorman, G. A., Foley, J. F., Yoshida, T., and Luster, M. I. Arsenic enhancement of skin neoplasia by chronic stimulation of growth factors. Am.J.Pathol., *153*: 1775-1785, 1998.

Germolec, D. R., Yoshida, T., Gaido, K., Wilmer, J. L., Simeonova, P. P., Kayama, F., Burleson, F., Dong, W., Lang, R. W., and Luster, M. I. Arsenic induces overexpression of growth factors in human keratinocytes. Toxicol Appl Pharmacol, *141*: 308-318, 1996.

Glaser, U., Hochrainer, D., Kloppel, H., and Oldiges, H. Carcinogenicity of sodium dichromate and chromium (VI/III) oxide aerosols inhaled by male Wistar rats. Toxicology, *42*: 219-232, 1986.

Glick, A. B., Lee, M. M., Darwiche, N., Kulkarni, A. B., Karlsson, S., and Yuspa, S. H. Targeted deletion of the TGF-beta 1 gene causes rapid progression to squamous cell carcinoma. Genes Dev., *8*: 2429-2440, 1994.

Glick, A. B., Sporn, M. B., and Yuspa, S. H. Altered regulation of TGF-beta 1 and TGF-alpha in primary keratinocytes and papillomas expressing v-Ha-ras. Mol.Carcinog., *4*: 210-219, 1991.

Golub, T. R., Slonim, D. K., Tamayo, P., Huard, C., Gaasenbeek, M., Mesirov, J. P., Coller, H., Loh, M. L., Downing, J. R., Caligiuri, M. A., Bloomfield, C. D., and

Lander, E. S. Molecular classification of cancer: class discovery and class prediction by gene expression monitoring. Science, *286*: 531-537, 1999.

Goyer, R. A. Lead toxicity: current concerns. Environ.Health Perspect., *100*: 177-187, 1993.

Grandjean, P., Wulf, H. C., and Niebuhr, E. Sister chromatid exchange in response to variations in occupational lead exposure. Environ.Res, *32*: 199-204, 1983.

Groten, J. P., Schoen, E. D., van Bladeren, P. J., Kuper, C. F., van Zorge, J. A., and Feron, V. J. Subacute toxicity of a mixture of nine chemicals in rats: detecting interactive effects with a fractionated two-level factorial design. Fundam.Appl Toxicol, *36*: 15-29, 1997.

Gueniche, A., Viac, J., Lizard, G., Charveron, M., and Schmitt, D. Effect of various metals on intercellular adhesion molecule-1 expression and tumour necrosis factor alpha production by normal human keratinocytes. Arch.Dermatol.Res, *286*: 466-470, 1994.

Hall, E. J. and Hei, T. K. Oncogenic transformation of cells in culture: pragmatic comparisons of oncogenicity, cellular and molecular mechanisms. Int J Radiat.Oncol.Biol Phys., *12*: 1909-1921, 1986.

Hall, E. J. and Hei, T. K. Modulating factors in the expression of radiation-induced oncogenic transformation. Environ.Health Perspect., *88*: 149-155, 1990.

Hall, E. J., Hei, T. K., and Miller, R. C. Modulation of the oncogenic potential of various anticancer modalities. Front Radiat.Ther.Oncol., *23*: 131-139, 1989.

Hamadeh, H. K., Vargas, M., Lee, E., and Menzel, D. B. Arsenic disrupts cellular levels of p53 and mdm2:A potential mechanism of carcinogenesis. Biochem.Biophys.Res.Commun., *263*: 446-449, 1999.

Hamilton, J. W. and Wetterhahn, K. E. Chromium (VI)-induced DNA damage in chick embryo liver and blood cells in vivo. Carcinogenesis, *7*: 2085-2088, 1986.

Hayes, R. B. The carcinogenicity of metals in humans. Cancer Causes Control, *8*: 371-385, 1997.

Hedenfalk, I., Duggan, D., Chen, Y., Radmacher, M., Bittner, M., Simon, R., Meltzer, P., Gusterson, B., Esteller, M., Kallioniemi, O. P., Wilfond, B., Borg, A., and Trent, J. Gene-expression profiles in hereditary breast cancer. N.Engl.J Med., *344*: 539-548, 2001.

Hochadel, J. F. and Waalkes, M. P. Sequence of exposure to cadmium and arsenic determines the extent of toxic effects in male Fischer rats. Toxicology *116*: 89-98, 1997.

Hopenhayn-Rich, C., Biggs, M. L., and Smith, A. H. Lung and kidney cancer mortality associated with arsenic in drinking water in Cordoba, Argentina. International Journal of Epidemiology, *27*: 561-569, 1998.

IARC. Hexavalent chromium. 1987. Lyon, France, IARC Press. IARC Monographs on the evaluation of carcinogenic risks to humans.

IARC. Chromium, Nickel and Welding. 1990. Lyon, France, IARC Press. IARC Monographs on the evaluation of carcinogenic risks to humans.

IARC. Beryllium, cadmium, mercury, and exposure in the glass manufacturing industry. (58), 119-238. 1993. Lyon, France, IARC Press. IARC Monographs on the evaluation of carcinogenic risks to humans.

IRIS Lead and compounds (inorganic), Integrated Risk Information System http://www.epa.gov/iriswebp/iris/subst/0277.htm1993

Ishinishi, N., Kodama, Y., Nobutomo, K., Inamasu, T., Kunitake, and Suenaga, Y. Outbreak of chronic arsenic poisoning among retired workers from an arsenic mine in Japan. Environmental Health Perspectives, *19*: 121-125, 1977.

Ivankovic, S. and Preussman, R. Absence of toxic and carcinogenic effects after administration of high doses of chromic oxide pigment in subacute and long-term feeding experiments in rats. Food Cosmet.Toxicol., *13*: 347-351, 1975.

Jin, T., Lu, J., and Nordberg, M. Toxicokinetics and biochemistry of cadmium with special emphasis on the role of metallothionein. Neurotoxicology, *19*: 529-535, 1998.

Kachinskas, D. J., Phillips, M. A., Qin, Q., Stokes, J. D., and Rice, R. H. Arsenate perturbation of human keratinocyte differentiation. Cell Growth Differ., *5*: 1235-1241, 1994.

Kachinskas, D. J., Qin, Q., Phillips, M. A., and Rice, R. A. Arsenate suppression of human keratinocyte programming. Mut Res, *386*: 253-261, 1997.

Kakunaga, T. A quantitative system for assay of malignant transformation by chemical carcinogens using a clone derived from BALB-3T3. Int J Cancer, *12*: 463-473, 1973.

Kanisawa, M. and Schoreder, H. A. Life Term Studies on the Effects of Arsenic, Germanium, Tin, and Vanadium on Spontaneous Tumors in Mice. Cancer Research, *27*: 1192-1195, 1967.

Kanisawa, M. and Schroeder, H. A. Life term studies on the effect of trace elements on spontaneous tumors in mice and rats. Cancer Research, *29*: 892-895, 1969.

Kasprzak, K. S., Hoover, K. L., and Poirier, L. A. Effects of dietary calcium acetate on lead subacetate carcinogenicity in kidneys of male Sprague-Dawley rats. Carcinogenesis, *6*: 279-282, 1985a.

Kasprzak, K. S. and Poirier, L. A. Effects of calcium and magnesium acetates on tissue distribution of carcinogenic doses of cadmium chloride in Wistar rats. Toxicology, *34*: 221-230, 1985b.

Kasprzak, K. S., Waalkes, M. P., and Poirier, L. A. Effects of essential divalent metals on carcinogenicity and metabolism of nickel and cadmium. Biol Trace Elem Res, *13*: 253-273, 1987.

Katz, S. A. and Salem, H. The toxicology of chromium with respect to its chemical speciation: a review. J Appl.Toxicol., *13*: 217-224, 1993.

Khan, J., Saal, L. H., Bittner, M. L., Chen, Y., Trent, J. M., and Meltzer, P. S. Expression profiling in cancer using cDNA microarrays. Electrophoresis, *20*: 223-229, 1999.

Kjellstrom, T., Friberg, L., and Rahnster, B. Mortality and cancer morbidity among cadmium-exposed workers. Environ.Health Perspect., *28*: 199-204, 1979.

Kjellstrom, T. and Nordberg, G. F. A kinetic model of cadmium metabolism in the human being. Environ.Res, *16*: 248-269, 1978.

Koller, L. D., Kerkvliet, N. I., and Exon, J. H. Neoplasia induced in male rats fed lead acetate, ethyl urea, and sodium nitrite. Toxicol Pathol., *13*: 50-57, 1985.

Kortenkamp, A. and Altenburger, R. Synergisms with mixtures of xenoestrogens: a reevaluation using the method of isoboles. Sci Total Environ., *221*: 59-73, 1998.

Kroes, R., van Logten, M. J., Berkvens, J. M., de Vries, T., and van Esch, G. J. Study on the carcinogenicity of lead arsenate and sodium arsenate and on the possible synergistic effect of diethylnitrosamine. Food & Cosmetics Toxicology, *12*: 671-679, 1974.

Kuroki, T., Chida, K., Hosomi, J., and Kondo, S. Use of human epidermal cells in the study of carcinogenesis. J Invest Dermatol., *92*: 271S-274S, 1989.

Lammintausta, K. H. and Maibach, H. F. Contact dermatitis due to irritation. *In* R. M. Adams (ed.), Occupational Skin Disease, 2nd ed, pp. 1-3. Philadelphia: W.B. Saunders, 1990.

Land, H., Parada, L. F., and Weinberg, R. A. Cellular oncogenes and multistep carcinogenesis. Science, *222*: 771-778, 1983a.

Land, H., Parada, L. F., and Weinberg, R. A. Tumorigenic conversion of primary embryo fibroblasts requires at least two cooperating oncogenes. Nature, *304*: 596-602, 1983b.

Landolph, J. R. Neoplastic transformation of mammalian cells by carcinogenic metal compounds: cellular and molecular mechanisms. Biological Effects of Heavy Metals, pp. 1-18. 1990.

Levy, L. S. and Venitt, S. Proceedings: Carcinogenic and mutagenic activity of chromium containing materials. Br.J Cancer, *32*: 254-255, 1975.

Lewalter, J., Korallus, U., Harzdorf, C., and Weidemann, H. Chromium bond detection in isolated erythrocytes: a new principle of biological monitoring of exposure to hexavalent chromium. Int.Arch.Occup.Environ.Health, *55*: 305-318, 1985.

Little, M. C., Gawkrodger, D. J., and MacNeil, S. Chromium- and nickel-induced cytotoxicity in normal and transformed human keratinocytes: an investigation of pharmacological approaches to the prevention of Cr(VI)-induced cytotoxicity. Br.J Dermatol., *134*: 199-207, 1996.

Lolin, Y. and O'Gorman, P. An intra-erythrocytic low molecular weight lead-binding protein in acute and chronic lead exposure and its possible protective role in lead toxicity. Annals of Clinical Biochemistry, *25*: 688-697, 1988.

Lucis, O. J., Lucis, R., and Aterman, K. Tumorigenesis by cadmium. Oncology, *26*: 53-67, 1972.

Luo, Z. D., Zhang, Y. M., Ma, L., Zhang, G. Y., He, X., Wilson, R., Byrd, D. M., Griffiths, J. F., Lai, S., He, L., Grumski, K., and Lamm, S. H. Chronic arsenicism and cancer in Inner Mongolia-Consequences of well-water arsenic levels greater than 50 μg/l. *In* C. O. Abernathy, R. L. Calderon, and W. R. Chappell (eds.), Arsenic. Exposure and Health Effects, pp. 55-68. New York, NY: Chapman & Hall, 1997.

Mahaffey, K. R., Capar, S. G., Gladen, B. C., and Fusenig, N. E. Concurrent exposure to lead, cadmium, and arsenic. Effects on toxicity and tissue metal concentrations in the rat. J Lab Clin Med, *98*: 463-481, 1981.

Manning, F. C., Xu, J., and Patierno, S. R. Transcriptional inhibition by carcinogenic chromate: relationship to DNA damage. Mol.Carcinog., *6*: 270-279, 1992.

McClellan, R. O. Risk assessment and biological mechanisms: lessons learned, future opportunities. Toxicology, *102*: 239-258, 1995.

Milner, J. E. and Seattle, M. D. The effect of ingested arsenic on methylcholanthrene-induced skin tumors in mice. Archives of Environmental Health, *18*: 7-11, 1969.

Milo, G. E., Jr. and DiPaolo, J. A. Neoplastic transformation of human diploid cells in vitro after chemical carcinogen treatment. Nature, *275*: 130-132, 1978.

Misra, R. R., Smith, G. T., and Waalkes, M. P. Evaluation of the direct genotoxic potential of cadmium in four different rodent cell lines. Toxicology, *126*: 103-114, 1998.

Morton, W., Starr, G., Pohl, D., Stoner, J., Wagner, S., and Weswig Skin cancer and water arsenic in Lane County, Oregon. Cancer, *37*: 2523-2532, 1976.

Munoz, H., Romiew, I., Palazuelos, E., Mancilla-Sanchez, T., Meneses-Gonzalez, F., and Hernandez-Avila, M. Blood lead level and neurobehavioral development among children living in Mexico City. Arch.Environ.Health, *48*: 132-139, 1993.

Needleman, H. L. Human Lead Exposure.Boca Raton, FL: CRC Press, 1992.

Nesnow, S., Mass, M. J., Ross, J. A., Galati, A. J., Lambert, G. R., Gennings, C., Carter, W. H., Jr., and Stoner, G. D. Lung tumorigenic interactions in strain A/J mice of five environmental polycyclic aromatic hydrocarbons. Environ.Health Perspect., *106 Suppl 6*: 1337-1346, 1998.

NIH. Chromium Hexavalent Compounds, 9th Report on Carcinogens. http://ehp.niehs.hih.gov/roc/toc9.html. 2001.

Nilsson, J. R. *Tetrahymena* in Cytotoxicology: With special reference to effects of heavy metals and selected drugs. Eur.J.Protistol., *25*: 2-25, 1989.

Nordberg, M. Studies on metallothionein and cadmium. Environ.Res, *15*: 381-404, 1978.

Nordberg, M., Jin, T., and Nordberg, G. F. Cadmium, metallothionein and renal tubular toxicity. *In* G. F. Nordberg, R. F. M. Herber, and L. Alessio (eds.), Cadmium in the Human Environment: Toxicity and Carcinogenicity, pp. 293-297. Lyon: IARC Scientific Publications no118, 1992.

Nordberg, G. F., Kjellstrom, T., and Nordberg, M. Metabolism and Kinetics. *In* L. Friberg, C. G. Elinder, T. Kjellstrom, and G. F. Nordberg (eds.), Cadmium and Health Vol I, pp. 103-197. Boca Raton, FL: CRC Press, 1985.

Nriagu, J. O. A global assessment of natural sources of atmospheric trace-metals. Nature, *338*: 47-49, 1989.

Nriagu, J. O. and Pacyna, J. M. Quantitative assessment of worldwide contamination of air, water and soils by trace metals. Nature, *333*: 134-139, 1988.

Oberdorster, G., Cherian, M. G., and Baggs, R. B. Correlation between cadmium-induced pulmonary carcinogenicity, metallothionein expression, and inflammatory processes: a species comparison. Environ.Health Perspect., *102 Suppl 3*: 257-263, 1994.

O'Flaherty, E. J. Physiologically based models of metal kinetics. Crit Rev.Toxicol, *28*: 271-317, 1998.

Patierno, S. R., Banh, D., and Landolph, J. R. Transformation of C3H/10T1/2 mouse embryo cells to focus formation and anchorage independence by insoluble lead chromate but not soluble calcium chromate: relationship to mutagenesis and internalization of lead chromate particles. Cancer Res, *48*: 5280-5288, 1988.

Penn, A. International Commission for Protection Against Environmental Mutagens and Carcinogens. ICPEMC Working Paper 7/1/1. Mutational events in the etiology of arteriosclerotic plaques. Mutation Research, *239*: 149-162, 1990.

Pietenpol, J. A., Holt, J. T., Stein, R. W., and Moses, H. L. Transforming growth factor beta 1 suppression of c-myc gene transcription: role in inhibition of keratinocyte proliferation. Proc.Natl.Acad Sci U.S.A, *87*: 3758-3762, 1990.

Pitot, H. C. The molecular biology of carcinogenesis. Cancer, *72*: 962-970, 1993.

Poirier, L. A., Kasprzak, K. S., Hoover, K. L., and Wenk, M. L. Effects of calcium and magnesium acetates on the carcinogenicity of cadmium chloride in Wistar rats. Cancer Res, *43*: 4575-4581, 1983.

Pott, W. A., Benjamin, S. A., and Yang, R. S. Pharmacokinetics, metabolism, and carcinogenicity of arsenic. Rev.Environ.Contam Toxicol., *169*: 165-214, 2001.

Punnonen, K., Denning, M. F., Rhee, S. G., and Yuspa, S. H. Differences in the regulation of phosphatidylinositol-specific phospholipase C in normal and neoplastic keratinocytes. Mol.Carcinog., *10*: 216-225, 1994.

Rahman, M., Tondel, M., Ahmad, S. A., Chowdhury, I. A., Faruquee, M. H., and Axelson, O. Hypertension and arsenic exposure in Bangladesh. Hypertension, *33*: 74-78, 1999.

Ramaswamy, S., Tamayo, P., Rifkin, R., Mukherjee, S., Yeang, C. H., Angelo, M., Ladd, C., Reich, M., Latulippe, E., Mesirov, J. P., Poggio, T., Gerald, W., Loda, M., Lander, E. S., and Golub, T. R. Multiclass cancer diagnosis using tumor gene expression signatures. Proc.Natl.Acad Sci U.S.A, *98*: 15149-15154, 2001.

Reznikoff, C. A., Bertram, J. S., Brankow, D. W., and Heidelberger, C. Quantitative and qualitative studies of chemical transformation of cloned C3H mouse embryo cells sensitive to postconfluence inhibition of cell division. Cancer Res, *33*: 3239-3249, 1973.

Rhim, J. S. Neoplastic transformation of human epithelial cells in vitro. Anticancer Res., *9*: 1345-1365, 1989.

Rhim, J. S., Fujita, J., Arnstein, P., and Aaronson, S. A. Neoplastic conversion of human keratinocytes by adenovirus 12-SV40 virus and chemical carcinogens. Science, *232*: 385-388, 1986.

Rhim, J. S., Kawakami, T., Pierce, J., Sanford, K., and Arnstein, P. Cooperation of V-oncogenes in human epithelial cell transformation. Leukemia, *2*: 151S-159S, 1988.

Rivara, M. I., Cebrian, M., Corey, G., Hernandez, M., and Romieu, I. Cancer risk in an arsenic-contaminated area of Chile. Toxicology & Industrial Health, *13*: 321-338, 1997.

Rivedal, E. and Sanner, T. Metal salts as promoters of in vitro morphological transformation of hamster embryo cells initiated by benzo(a)pyrene. Cancer Res, *41*: 2950-2953, 1981.

Rojas-Lopez, M., Santos-Burgoa, C., Rios, C., Hernandez-Avila, M., and Romieu, I. Use of lead-glazed ceramics is the main factor associated to high lead in blood levels in two Mexican rural communities. J Toxicol Environ.Health, *42*: 45-52, 1994.

Safe, S. H. Hazard and risk assessment of chemical mixtures using the toxic equivalency factor approach. Environ.Health Perspect., *106 Suppl 4*: 1051-1058, 1998.

Saffiotti, U. and Bertolero, F. Neoplastic transformation of Balb/3T3 cells by metals: is a multistep molecular mechanism required for the further induction of a metastatic phenotype? 1988. Collegio Universitario, Urbino, Italy, 1st Int. Meet. Mol. Mech. Metal Toxic. Carcinogen.

Saffiotti, U. and Bertolero, F. Neoplastic transformation of BALB/3T3 cells by metals and the quest for induction of a metastatic phenotype. Biol Trace Elem Res, *21*: 475-482, 1989.

Sarkar, B. Metal replacement in DNA-binding zinc finger proteins and its relevance to mutagenicity and carcinogenicity through free radical generation. Nutrition, *11*: 646-649, 1995.

Scherf, U., Ross, D. T., Waltham, M., Smith, L. H., Lee, J. K., Tanabe, L., Kohn, K. W., Reinhold, W. C., Myers, T. G., Andrews, D. T., Scudiero, D. A., Eisen, M. B., Sausville, E. A., Pommier, Y., Botstein, D., Brown, P. O., and Weinstein, J. N. A gene expression database for the molecular pharmacology of cancer. Nat.Genet., *24*: 236-244, 2000.

Schrauzer, G. N., White, D. A., McGinness, J. E., Schneider, C. J., and Bell, L. J. Arsenic and Cancer: Effects of Joint Administration of Arsenite and Selenite on the Genesis of Mammary Adenocarcinoma in Inbred Female C_3H/St Mice. Bioinroganic Chemistry, *9*: 245-253, 1978.

Shaikh, Z. A. and Smith, J. C. Metabolism of orally ingested cadmium in humans. Dev.Toxicol Environ.Sci, *8*: 569-574, 1980.

Shaikh, Z. A., Vu, T. T., and Zaman, K. Oxidative stress as a mechanism of chronic cadmium-induced hepatotoxicity and renal toxicity and protection by antioxidants. Toxicol Appl Pharmacol, *154*: 256-263, 1999.

Shimada, H., Shiao, Y. H., Shibata, M., and Waalkes, M. P. Cadmium suppresses apoptosis induced by chromium. Journal of Toxicology & Environmental Health, *54*: 159-168, 1998.

Shipp, M. A., Ross, K. N., Tamayo, P., Weng, A. P., Kutok, J. L., Aguiar, R. C., Gaasenbeek, M., Angelo, M., Reich, M., Pinkus, G. S., Ray, T. S., Koval, M. A., Last, K. W., Norton, A., Lister, T. A., Mesirov, J., Neuberg, D. S., Lander, E. S., Aster, J. C., and Golub, T. R. Diffuse large B-cell lymphoma outcome prediction by gene-expression profiling and supervised machine learning. Nat.Med., *8*: 68-74, 2002.

Shirachi, D. Y., Johansen, M. G., McGowan, J. P., and Tu, S.-H. Tumorigenic Effect of Sodium Arsenite in Rat Kidney. Proceedings of the Western Pharmacology Society, *26*: 413-415, 1983.

Shiraishi, N., Hochadel, J. F., Coogan, T. P., Koropatnick, J., and Waalkes, M. P. Sensitivity to cadmium-induced genotoxicity in rat testicular cells is associated with minimal expression of the metallothionein gene. Toxicol Appl Pharmacol, *130*: 229-236, 1995.

Shuin, T., Billings, P. C., Lillehaug, J. R., Patierno, S. R., Roy-Burman, P., and Landolph, J. R. Enhanced expression of c-myc and decreased expression of c-fos protooncogenes in chemically and radiation-transformed C3H/10T1/2 Cl 8 mouse embryo cell lines. Cancer Res, *46*: 5302-5311, 1986.

Singh, J., Carlisle, D. L., Pritchard, D. E., and Patierno, S. R. Chromium-induced genotoxicity and apoptosis: relationship to chromium carcinogenesis. Oncol.Rep., *5*: 1307-1318, 1998.

Snow, E. T. Metal carcinogenesis: mechanistic implications. Pharmacol.Ther., *53*: 31-65, 1992.

Sorahan, T. and Waterhouse, J. A. Mortality study of nickel-cadmium battery workers by the method of regression models in life tables. Br.J Ind.Med., *40*: 293-300, 1983.

Sorlie, T., Perou, C. M., Tibshirani, R., Aas, T., Geisler, S., Johnsen, H., Hastie, T., Eisen, M. B., van de, R. M., Jeffrey, S. S., Thorsen, T., Quist, H., Matese, J. C., Brown, P. O., Botstein, D., Eystein, L. P., and Borresen-Dale, A. L. Gene expression patterns of breast carcinomas distinguish tumor subclasses with clinical implications. Proc.Natl.Acad Sci U.S.A, *98*: 10869-10874, 2001.

Sperling, M., Yin, X., and Welz, B. Differential determination of chromium(VI) and total chromium in natural waters using flow injection on-line separation and preconcentration electrothermal atomic absorption spectrometry. Analyst, *117*: 629-635, 1992.

Steinhoff, S., Gad, S. C., Hatfield, G. K., and et al. Listing sodium dichromate and soluble calcium chromate for carcinogenicity in rats. Bayer AG Institute of Toxicology. 1983. Unpublished Work

Thorgeirsson, U. P., Dalgard, D. W., Reeves, J., and Adamson, R. H. Tumor incidence in a chemical carcinogenesis study of nonhuman primates. Regulatory Toxicology & Pharmacology, *19*: 130-151, 1994.

Tsapakos, M. J., Hampton, T. H., and Wetterhahn, K. E. Chromium(VI)-induced DNA lesions and chromium distribution in rat kidney, liver, and lung. Cancer Res, *43*: 5662-5667, 1983.

Tseng, C.-H., Chong, C.-K., Chen, C.-J., and Tai, T.-Y. Lipid Profile and Peripheral Vascular Disease in Arseniasis-Hyperendemic Villages in Taiwan. Angiology, *48*: 321-335, 1997.

Tseng, W. P., Chu, H. M., How, S. W., Fong, J. M., Lin, C. S., and Yeh, S. Prevalence of skin cancer in an endemic area of chronic arsenicism in Taiwan. Journal of the National Cancer Institute, *40*: 453-463, 1968.

Tully, D. B., Collins, B. J., Overstreet, J. D., Smith, C. S., Dinse, G. E., Mumtaz, M. M., and Chapin, R. E. Effects of arsenic, cadmium, chromium, and lead on gene expression regulated by a battery of 13 different promoters in recombinant HepG2 cells. Toxicol Appl Pharmacol, *168*: 79-90, 2000.

U.S.Department of Health and Human Services. Toxicological profile for lead. 1993. ATSDR/TP-92/12.

U.S.EPA. Air Quality Criteria Document for Lead. Volumes III, IV. 1986. Prepared by the Office of Health and Environmental Assessment, Environmental Criteria and Assessment Office, Research Triangle Park, NC, for the Office of Air Quality Planning and Standards. EPA-600/8-83/028dF.

Vahter, M. Metabolism of Arsenic. *In* B. A. Fowler (ed.), Biological and Enviromental Effects of Arsenic, vol. 6, pp. 171-298. Amsterdam: Elsevier Science Publishers B.V., 1983.

Vahter, M. and Norin, H. Metabolism of 74As-labeled trivalent and pentavalent inorganic arsenic in mice. Environ.Res., *21*: 446-457, 1980.

van't Veer, L. J., Dai, H., van de Vijver, M. J., He, Y. D., Hart, A. A., Mao, M., Peterse, H. L., van der, K. K., Marton, M. J., Witteveen, A. T., Schreiber, G. J., Kerkhoven, R. M., Roberts, C., Linsley, P. S., Bernards, R., and Friend, S. H. Gene expression profiling predicts clinical outcome of breast cancer. Nature, *415*: 530-536, 2002.

Verhaar, H. J., Morroni, J. R., Reardon, K. F., Hays, S. M., Gaver, D. P., Jr., Carpenter, R. L., and Yang, R. S. A proposed approach to study the toxicology of complex

mixtures of petroleum products: the integrated use of QSAR, lumping analysis and PBPK/PD modeling. Environ.Health Perspect., *105 Suppl 1*: 179-195, 1997.

Waalkes, M. P., Coogan, T. P., and Barter, R. A. Toxicological principles of metal carcinogenesis with special emphasis on cadmium. Crit Rev.Toxicol, *22*: 175-201, 1992.

Washko, P. W. and Cousins, R. J. Nutr Rep Int, *11*: 113-127, 1975.

Wedrychowski, A., Ward, W. S., Schmidt, W. N., and Hnilica, L. S. Chromium-induced cross-linking of nuclear proteins and DNA. J Biol.Chem., *260*: 7150-7155, 1985.

WHO. Cadmium, Environmental Health Criteria 134. 87-89. 1992. Geneva, WHO.

Xu, J., Bubley, G. J., Detrick, B., Blankenship, L. J., and Patierno, S. R. Chromium(VI) treatment of normal human lung cells results in guanine- specific DNA polymerase arrest, DNA-DNA cross-links and S-phase blockade of cell cycle. Carcinogenesis, *17*: 1511-1517, 1996.

Xu, J., Wise, J. P., and Patierno, S. R. DNA damage induced by carcinogenic lead chromate particles in cultured mammalian cells. Mutat.Res, *280*: 129-136, 1992.

Yamamoto, S., Konishi, Y., Matsuda, T., Murai, T., Shibata, M.-A., Matsui-Yuasa, I., Otani, S., Kuroda, K., Endo, G., and Fukushima, S. Cancer Induction by an Organic Arsenic Compound, Dimethylarsinic Acid (Cacodylic Acid), in F344/DuCrj Rats after Pretreatment with Five Carcinogens. Cancer Research, *55*: 1271-1276, 1995.

Yamamoto, S., Wanibuchi, H., Hori, T.-A., Yano, Y., Matsui-Yuasa, I., Otani, S., Chen, H., Yoshida, K., Kuroda, K., Endo, G., and Fukushima, S. Possible carcinogenic potential of dimethylarsinic acid as assessed in rat *in vivo* models: a review. Mutat.Res., *386*: 353-361, 1997.

Yang, R. S. Strategy for studying health effects of pesticides/fertilizer mixtures in groundwater. Rev.Environ.Contam Toxicol, *127*: 1-22, 1992.

Yang, J. H., Thraves, P., Dritschilo, A., and Rhim, J. S. Neoplastic transformation of immortalized human keratinocytes by 2,3,7,8-tetrachlorodibenzo-p-dioxin. Cancer Res., *52*: 3478-3482, 1992.

Yen, H. T., Chiang, L. C., Wen, K. H., Chang, S. F., Tsai, C. C., Yu, C. L., and Yu, H. S. Arsenic induces interleukin-8 expression in cultured keratinocytes. Archives of Dermatological Research, *288*: 716-717, 1996.

Yuspa, S. H. The pathogenesis of squamous cell cancer: lessons learned from studies of skin carcinogenesis--thirty-third G. H. A. Clowes Memorial Award Lecture. Cancer Res, *54*: 1178-1189, 1994.

Yuspa, S. H. and Greenhalgh, D. A. Molecular mechanisms of malignant conversion in skin carcinogenesis. Princess Takamatsu Symp., *20*: 281-288, 1989.

Zhitkovich, A., Voitkun, V., and Costa, M. Glutathione and free amino acids form stable complexes with DNA following exposure of intact mammalian cells to chromate. Carcinogenesis, *16*: 907-913, 1995.

CHAPTER 2

Toxicological Interactions among Arsenic, Cadmium, Chromium, and Lead in Human Keratinocytes

Dong-Soon Bae, Chris Gennings, Walter H. Carter, Jr., Raymond S.H. Yang, and Julie A. Campain

ABSTRACT

To evaluate health effects of chemical mixtures, such as multiple heavy metals in drinking water, we have been developing efficient and accurate hazard identification strategies. Thus, in this study, we determine the cytotoxicity of arsenic, cadmium, chromium, and lead, and characterize interactions among these metals in human epidermal keratinocytes. Three immortal keratinocyte cell lines (RHEK-1, HaCaT, and NM1) and primary keratinocytes (NHEK) were used. A statistical approach applying an additivity response surface methodology was used to test the validity of the additivity concept for a four metal mixture. Responses of the four keratinocyte strains to the metal mixture were highly dose-dependent. A growth stimulatory effect (hormesis) was observed in RHEK-1, NM1, and NHEK cells with the metal mixture at low concentrations (low ppb range). This hormesis effect was not significant in HaCaT. As the mixture concentration increased, a trend of additivity changed to synergistic cytotoxicity in all four cell strains. However, in NHEK, RHEK-1, and HaCaT, at the highest mixture concentrations tested, the responses to the metal mixtures were

antagonistic. In NM1, no significant antagonistic interaction among the metals was observed. To explore a mechanistic basis for these differential sensitivities, levels of glutathione and metallothioneins I and II were determined in the keratinocyte cell strains. Initial data are consistent with the suggestion that synergistic cytotoxicity turned to antagonistic effects because at highest mixture exposure concentrations cellular defense mechanisms were enhanced.

INTRODUCTION

Both occupational and environmental exposures to hazardous metals, such as arsenic (As), cadmium (Cd), chromium (Cr), and lead (Pb), are significant toxicological concerns. Not only do these metals lead to acute toxicity at higher concentrations, but they may also mediate development of additional pathologic conditions in individuals exposed chronically to low levels. Environmentally relevant metals seldom occur alone. Rather, they most often occur in hazardous waste sites or ground water supplies in combination with other contaminants; this substantially complicates the risk assessment process for these chemicals. In general, within the scientific community, the concept of "additivity" is assumed for low level exposures to the component chemicals in a mixture (Svendsgaard and Hertzberg, 1994). The definition of additivity used here is that described by Berenbaum (1985, 1989). Whether this is a valid assumption for metal mixtures needs to be tested. This project is, therefore, an attempt to test such an additivity concept at low exposure levels. The metals chosen for our studies are highly relevant to human exposure. As, Cd, Cr, and Pb, are the top four metals in site frequency count by the ATSDR Completed Exposure Pathway Site Count Report (ATSDR, 1997); three of

these, As, Pb, and Cd are among the Superfund Top 10 Priority Hazardous Substances (DeRosa *et al.*, 1996), i.e. those considered to pose the greatest hazard to human health. In addition, as confirmed by ATSDR using the HazDat database, these metals most often occur together; they are present in 8 of 10 and 5 of 10 of the Top 10 Binary Combinations of Contaminants in soil and water, respectively (Fay and Mumtaz, 1996).

As part of a larger study, we describe here an evaluation of the acute cytotoxicity of As, Cd, Cr, and Pb alone and together in a mixture in human epidermal keratinocytes, a highly relevant cell type. The skin is a critical target organ for As-mediated pathological effects, including proliferative disorders such as hyperkeratosis and, in many cases, carcinogenesis. Due to high As (and other metal) concentrations in many drinking water supplies, acute toxicity and development of neoplastic skin lesions have become health problems of global proportions. Both As and Cr, a well known skin sensitizer, have substantial effects on epidermal keratinocytes *in vitro*, altering expression of several growth regulatory factors and inhibiting the normal process of differentiation (Cohen *et al.*, 1993; Germolec *et al.*, 1996, 1997; Kachinskas *et al.*, 1997; Ye *et al.*, 1995;Yen *et al.*, 1996). Little is known, however, about the exact mechanism of toxicity *in vivo* of either metal alone or the effects of the two metals when they are present together or in complex mixtures with other metals on this cell type. To address this issue, an additivity response surface methodology was utilized to permit detailed statistical analysis of the cytotoxic interactions among As, Cd, Cr, and Pb when present together in a mixture. In addition, mechanistic studies are described in which the roles of glutathione (GSH) and metallothionein-I and -II (hMT) in the observed metal-metal interactions are explored.

MATERIALS AND METHODS

Chemicals

Sodium metaarsenite ($NaAsO_2$), cadmium chloride ($CdCl_2$), chromium oxide (CrO_3), chromium chloride ($CrCl_3$), lead acetate ($(C_2H_3O_2)_2Pb\cdot 3H_2O$), dimethyl sulphoxide (DMSO), 3-[4,5-Dimethylthiazol-2-yl]-2,5-diphenyltetrazolium bromide (MTT), aprotinin, Nonidet P-40, and phenylmethanesulfonyl flouride (PMSF) were purchased from Sigma Chemical Co. (St. Louis, MO).

Cell lines and culture reagents

Cryopreserved normal human epidermal keratinocytes (NHEK) were purchased from the Clonetics Corp. (San Diego, CA). NHEK cells were grown in defined Keratinocyte Growth Medium-KGM™ containing bovine pituitary extract (BPE), human epidermal growth factor (hEGF), insulin, hydrocortisone, transferrin, epinephrine, and an antibiotic, GA-1000 (Clonetics Corp). Spontaneously immortalized HaCaT and NM1 keratinocyte cell lines were obtained from Dr. N. Fusenig, German Cancer Research Center (Heidelberg, Germany) (Boukamp *et al.*, 1988) and Dr. J. Kubilus, Mattek Corp. (Ashland, MA) (Baden *et al.*, 1987), respectively. The AD12/SV40 immortalized keratinocyte cell line (RHEK-1) was obtained from Dr. J. Rhim (Center for Prostate Disease Research, Rockville, MD) (Rhim *et al.*, 1985; Yang *et al.*, 1992). Each of the keratinocyte cell strains used in our studies was isolated from different individuals; NHEK is, in fact, a pooled population of cells from multiple individuals. Early passage NIH3T3 cells were obtained from American Type Culture Collection (Manassas, VA). RHEK-1 and HaCaT were cultured in Dulbecco's Modified Eagle's medium (DMEM) supplemented with 100 U/ml penicillin, 0.1 mg/ml streptomycin, 10 mM *L*-glutamine,

and 10 % fetal bovine serum (FBS) (Summit Biotechnology, Ft. Collins, CO). The NM1 cell line was cultivated in DMEM supplemented with 0.4 g/ml hydrocortisone, 10 ng/ml EGF, 1 nM cholera toxin, 20 % FBS, 100 U/ml penicillin, 0.1 mg/ml streptomycin, 10 mM *L*-glutamine, and 0.2 mM $CaCl_2$ on an NIH3T3 feeder layer as described by Rheinwald and Green (1975, 1977). NIH3T3 cells for feeder layers were lethally irradiated with an MK-1-68A Mark 1 Cs-137 sealed source cabinet irradiator at 1466 rad/min (J.L. Shepard and Associates, Glendale, CA) and replated 24 hr prior to use. For co-cultures, irradiated feeder cells were plated at a 1:3 ratio with NM1 cells. Feeder layers were removed from co-cultures prior to trypsinization of NM1 with a vigorous rinse of the flasks with 0.02 % EDTA. All keratinocyte strains were grown at 37°C in a humidified atmosphere of 5 % CO_2. Hydrocortisone and epidermal growth factor (EGF) were purchased from Sigma Chemical Co. (St. Louis, MO). Cholera toxin was purchased from Gibco BRL (Grand Island, NY).

Killing curves with individual metals or the metal mixture

For toxicity studies, NHEK was plated at 2.4 x 10^4 cells/well in 6-well plastic tissue culture plates and grown for 24 hr before metal treatment. RHEK-1 and HaCaT cell lines were plated at 1 x 10^4 cells/well. NM1 was plated at a density of 1 x 10^4 cells/well with 3 x 10^3 irradiated NIH3T3 feeder cells. Triplicate wells of cells were treated with increasing concentrations of As, Cr, Cd, Pb, or a mixture of the four metals for 24 hr. Metal stock solutions were prepared in deionized distilled water and sterilized by filtration through 0.2 μm filters. Concentrations used for As and Cr were 0.3, 1, 3, 10, and 100 μM. The Cr stock solution was made by mixing a 1:1 ratio of trivalent and

hexavalent chromium. Cd and Pb were administered at 3, 10, 30, 100, and 300 μM. To prepare the four metal mixtures, 50X stock solutions were made for the four individual cell lines which, when diluted to their final 1X concentrations in cell cultures, contained the levels of each As, Cr, and Cd giving 50 % cell killing in individual cytotoxicity assays (LD_{50}). The concentrations of these three metals in the 1X mixture solutions for the four cell types were: RHEK-1 [6.1 μM As, 7.1 μM Cr, 14 μM Cd]; HaCaT [4.8 μM As, 6.8 μM Cr, 56 μM Cd]; NM1 [9.0 μM As, 5.3 μM Cr, 55 μM Cd]; NHEK [7.7 μM As, 4.9 μM Cr, 6.1 μM Cd]. Lead acetate concentration in these 1X solutions was 100 μM, as we were unable to get complete killing at any dose in HaCaT, NM1, and NHEK. Lead acetate concentration in 1X solution for RHEK-1 was 120 μM, the estimated LD_{50}. To generate dose-response data, the mixture stock solutions were serially diluted 1:3 to get 0.333, 0.111, 0.037, 0.0123, 0.004, and 0.0014X dilution groups as a final concentration in cell cultures. Deionized distilled water was used as the vehicle control in all cases. After 24 hr exposure to the individual metals or the four-metal mixture, cells were refed with fresh metal-free medium and incubated for 3 d prior to viability analysis by the MTT assay (Mossman, 1983). At least three independent experiments were conducted in each of the four cell strains for individual metal and the metal mixture cytotoxicity curves.

MTT assay

The MTT assay was carried out using a modification of the method of Mossman (1983). MTT was dissolved at 5 mg/ml in phosphate-buffered saline. This stock solution was filtered through a 0.2 μm filter and stored at 4°C for up to 2 wk. Immediately before use,

the stock solution was diluted to 0.5 mg/ml with serum-free culture medium to make a working solution. Medium was aspirated from cells to be analyzed and MTT working solution (1 ml) was added to each well. Cells were incubated at 37°C for 3 hr, after which time, the MTT was removed by aspiration. Cells were subsequently lysed by addition of 0.5 ml of DMSO. The absorbence at 550 nm of samples as well as a DMSO control was read on a Microplate Autoreader (Bio-Tek Instruments, Inc., Winooski, VT). The absorbance of the DMSO blank was subtracted from all values. All absorbance values were expressed as a percent of water vehicle control. Absorbance measured in the MTT assay was converted to percent cell viability and analyzed by Minitab 11 (State College, PA) and SigmaPlot 4.0 (Chicago, IL) for determination of LD_{50} values.

Statistical analyses on mixture interaction

The fundamental definition of additivity used in the construction of the nonlinear additivity model ($f_{add}(x)$) is that chemicals that combine additively do not change the slope of other chemicals in the mixture. That is, if the slope of Chemical A changes in the presence of Chemical B then the chemicals are said to interact. If the slope of Chemical A does NOT change in the presence of Chemical B then the chemicals are said to combine additively. Further, the nonlinear additivity model can be algebraically expressed in terms of Berenbaum's interaction index conditioning on the maximum and minimum responses (parameterized with γ and α). It can thus be claimed that the nonlinear additivity model is consistent with dose addition as defined by Berenbaum's interaction index (Berenbaum, 1985, 1989). On the other hand, one can manipulate the response to a metameter that changes the nonlinear model to a linear model (here, -log(-

$\log((y-\alpha)/\gamma))$ which is called the complementary log-log transformation). On this response metameter, one can think of the model as being associated with response addition since the added effect of the i^{th} chemical is $\beta_i x_i$. So, the additivity model used in the analysis is consistent with several concepts of additivity or zero interaction. The claim that 'greater than additivity' implies synergism and 'less than additivity' implies antagonism is based on the demonstration that the additivity model is (conditionally) related to Berenbaum's interaction index which makes the claim of synergism/antagonism depending on whether the index is less/greater than one.

Single chemical data were experimentally observed to support the estimation of an additivity surface (Berenbaum, 1985, 1989; Gennings and Carter, 1995; Gennings *et al.*, 1997, 2002) to the single metal data. Separate analyses were conducted on the data for each cell line. At least three independent experiments were conducted and analyzed for each of the four cell lines. The endpoint of interest was percent viability. For the analyses considered here, the data from the individual experiments were grouped together and an experiment effect was not considered.

Seven mixture (M=7) points were observed with a specified mixing ratio (here, based on the LD_{50}s) with n_m observations at each and $M^* = \sum_{m=1}^{M} n_m$ total mixture observations. Let μ_m be the mean at the m^{th} mixture point, and $\mu_{add.m}$ be the mean under additivity. The hypothesis of no interaction is equivalent to $\delta_m = \mu_m - \mu_{add.m} = 0$, m=1,…, M. Assume $\mu_{add.m} = f_{add}(x_m; \theta)$ where $Var(Y)=\sigma^2$. Gennings *et al.* (2002) develop a test of the hypothesis $\Delta=[\delta_1,\ldots, \delta_M]' = 0'$ based on a Wald-type test

$$W_M(\Delta) = \frac{\hat{\Delta}'[Var(\hat{\Delta})]^{-1}\hat{\Delta}}{MSE}$$

which follows an $F_{M,N-p}$. Let $f_{add}(x; \theta_1)$ be the additivity model with unknown parameter vector θ_1; let $f_m(x; \theta_2)$ be the model along the fixed ratio ray using total dose for x and unknown parameters θ_2. Suppose it is possible to express the parameter vector θ_2 as a function of parameters in θ_1 under the hypothesis of additivity, i.e., $\lambda=a(\theta_1)-\theta_2=0$. Then for large samples,

$$\frac{\hat{\lambda}[Var(\hat{\lambda})]^{-1}\hat{\lambda}}{MSE}$$

which follows an $F_{p-q,\ N-p-q}$ in a test comparing the two curves. Gennings *et al.* (2002) also use a $100(1-\alpha)\%$ simultaneous confidence band on the difference between the curves. These methods are illustrated in the analysis of four metals (As, Cd, Cr, and Pb) where the endpoint of interest is percent viability of treated NHEK. The mixing ratio is the LD_{50} ratio of the four metals. Seven dilutions along this ray were experimentally observed. The additivity model was

$$f_{add}(x) = \alpha + \gamma[\exp(-\exp(-(\beta_0 + \beta_1 x_1 + \beta_2 x_2 + \beta_3 x_3 + \beta_4 x_4)))]$$

and the model for the mixture data along the fixed-ratio ray was

$$f_M(x) = \alpha^* + \gamma^*[\exp(-\exp(-(\beta_0^* + \beta_1^* t + \beta_2^* t^2)))].$$

So, $\theta_1 = [\alpha, \gamma, \beta_0, \beta_1, \beta_2, \beta_3, \beta_4]'$ and $\theta_2=[\alpha^*, \gamma^*, \beta_0^*, \beta_1^*, \beta_2^*]'$

where x_1, x_2, x_3, x_4 are the concentrations of As, Cd, Cr, and Pb, respectively,

t is the total dose = $\sum_{i=1}^{4} x_i$

α is an unknown parameter associated with the minimum response,

γ is an unknown parameter associated with the maximum response,

β_0 is an unknown parameter associated with the intercept on the complementary log log scale,

β_1 is an unknown parameter associated with the slope of arsenic,

β_2 is an unknown parameter associated with the slope of cadmium,

β_3 is an unknown parameter associated with the slope of chromium,

β_4 is an unknown parameter associated with the slope of lead

α^* is an unknown parameter associated with the minimum response,

γ^* is an unknown parameter associated with the maximum response,

β_0^* is an unknown parameter associated with the intercept on the complementary log log scale,

β_1^* is an unknown parameter associated with the slope of the mixture data,

β_2^* is an unknown parameter associated with the quadratic effect of the mixture data,

Under additivity, $\lambda = [\alpha-\alpha^*, \gamma-\gamma^*, \beta_0-\beta_0^*, \Sigma\beta_i-\beta_1^*, \beta_2^*]' = 0'$. Unknown parameters were estimated using PROC NLIN in SAS (Cary, NC). Single chemical data were used to estimate $f_{add}(x)$ and mixture data were used to estimate $f_M(x)$. Details of the methods are provided in Gennings *et al.* (2002).

Western blot for MT protein

Cell homogenates were prepared by sonication of cells in 600 µl of ice-cold 50 mM Tris-HCl (pH 8.0), 150 mM NaCl, 0.02% sodium azide, 100 µg/ml PMSF, 1 µg/ml aprotinin, and 1% NP-40. Homogenates were clarified by centrifugation at 20,000 x *g* for 45 min at 4°C. Total protein concentration was determined using the BCA (Bio-Rad, Hercules, CA) assay. Samples (50 µg of total protein) from the four keratinocyte strains treated for 24 hr

with increasing concentrations of the four metal mixture were analyzed for human MT proteins using sodium dodecyl sulfate polyacrylamide gel electrophoresis (SDS-PAGE) (Laemmli, 1970) in 10 – 20% gradient gels. Proteins were transferred electrophoretically to nitrocellulose membranes. The resulting membranes were incubated in 2.5% glutaraldehyde for 1 h and then washed 3 times for 5 min in phosphate buffer (8.1 mM Na_2HPO_4, 1.2 mM KH_2PO_4, 2.7 mM KCl, pH 7.4). Monoethanolamine (50 mM) was added to the third wash solution to quench residual glutaraldehyde reactivity. MT proteins were detected by Immun-Star Chemiluminescent Protein Detection Systems (Bio-Rad, Hercules, CA). A monoclonal antibody to polymerized equine renal MT-1 and MT-2 (Dako, Corp., Carpinteria, CA) was used for immunodetection. The chemiluminescent images were quantified using a Nikon AF camera and the NIH Image 1.55 b20 software (NIH, Bethesda, MD). In NM1, where we were unable to detect significant levels of MT expression, overall protein content and quality in cell lysates were confirmed by probing for cyclin G1 (Horne *et al.*, 1996) expression using a rabbit polyclonal antibody from Santa Cruz Biotechnology (Santa Cruz, CA). Data are expressed as mean ± SEM. Statistical comparisons were performed using one-way ANOVA (Dunnett's multiple comparison test) (Tamhane and Dunlop, 2000). Values were considered to be significant when $p < 0.05$ (Minitab, Inc., State College, PA).

GSH Assay

A colorimetric assay was carried out to quantify intracellular levels of GSH (Anderson, 1989). Cell homogenates were prepared as described above except that the cell suspension was centrifuged at 3,000 x *g*. The resulting cleared lysates were used for

analysis. GSH concentrations in 100 μg samples from the four keratinocyte strains treated with increasing concentrations of the metal mixture were measured by BIOXYTECH GSH-400 as per the manufacturer's directions (OXIS International, Inc., Portland, OR). The concentration range of exposure in the four metal mixtures were: 0.08-6.1 μM As, 0.17-14 μM Cd, 0.09-7.1 μM Cr, and 1.48-120 μM Pb for RHEK-1; 0.06-4.8 μM As, 0.69-56 μM Cd, 0.08-6.8 μM Cr, and 1.23-100 μM Pb for HaCaT; 0.11-9.0 μM As, 0.67-55 μM Cd, 0.065-5.3 μM Cr, and 1.23-100 μM Pb for NM1; and 0.095-7.7 μM As, 0.075-6.1 μM Cd, 0.060-4.9 μM Cr, and 1.23-100 μM Pb for NHEK, corresponding to 0.0123X to 1X mixture dilutions in all cell lines. Data are expressed as mean ± SEM. Statistical comparisons were performed using one-way ANOVA (Dunnett's multiple comparison test) (Tamhane and Dunlop, 2000). Values were considered to be significant when $p < 0.05$ (Minitab, Inc., State College, PA).

RESULTS

Human keratinocytes are differentially sensitive to As, Cr, Cd, and Pb.

To characterize the effects of As, Cr, Cd, and Pb individually on human keratinocytes, we performed cytotoxicity studies in primary human epidermal keratinocytes (NHEK) and three immortalized human keratinocyte cell lines (RHEK-1, HaCaT, and NM1) using the MTT assay as a measure of cell viability. As would be expected, all four metals showed a dose-dependent cytotoxic effect, as expressed by decreased absorbance values of treated cells. The mean LD_{50} values for As, Cr, and Cd were 6.1, 7.1, 14 μM for RHEK-1; 4.8, 6.8, 56 μM for HaCaT; 9.0, 5.3, 55 μM for NM1; and 7.7, 4.9, 6.1 μM for NHEK, respectively. It can be seen from this data that the four keratinocyte strains showed similar sensitivities to As and Cr. In contrast, substantial differences in sensitivity to Cd were observed among the four cell strains. The LD_{50} value for Pb in RHEK-1 was determined to be 120 μM. However, Pb toxicity in NHEK, HaCaT, and NM1 was so low, we were unable to accurately determine the LD_{50} concentrations. In NM1, we were unable to get 50 % lethality in cultures treated with Pb concentrations as high as 300 μM.

Toxicological interactions among As, Cr, Cd, and Pb are present in human keratinocytes

To characterize potential cytotoxic interactions among As, Cd, Cr, and Pb in human keratinocytes, cell killing curves were generated for mixtures of the four metals. The approximate concentrations of As, Cr, Cd, and Pb in the mixture at the LD_{50} in each of the four keratinocyte strains were respectively, as follows: RHEK-1 [2.1, 2.4, 4.7, 40

μM]; HaCaT [2.7, 3.8, 31, 56 μM]; NM1 [2.2, 1.3, 14, 25 μM]; and NHEK [4.8, 3.0, 3.8, 62 μM]. Subsequently, thorough statistical analyses were carried out on the data from these cytotoxicity assays for individual metals as compared to the four metal mixture. An approach, developed by Carter and Gennings (Gennings and Carter, 1995; Gennings *et al.*, 1997), using an additivity model permits testing the hypothesis that chemicals in a mixture act in an additive fashion. This model is described in detail in Gennings *et al.* (2002). Separate statistical analyses were conducted on the data from each keratinocyte strain.

Overall, the fit of the data seems adequate for the models associated with the four cell strains. The estimated model parameters as described in Materials and Methods and their associated sample standard errors and p values in four keratinocyte strains are provided in Table 2.1. All of the model parameters were significantly different from zero. The slope parameters associated with each of the four metals were negative and significant in all four models. This indicates that, as expected, as the concentration of the metal increases, the % viability decreases significantly regardless of the cell strain.

The additivity model was fit to the single metal data to generate prediction intervals for each metal mixture group. Even though we are dealing with single chemical dose response curves, the purpose for using the additivity model was to generate proper α, β, γ parameter values to be used in the statistical modeling of the chemical mixtures. A representative plot of the observed and predicted responses under additivity to the individual metals in RHEK-1 is shown in Fig. 2.1. It can be seen from this figure that the individual chemical data points cluster in a band along the identity line, indicating an adequate fit of the single chemical data using the additivity model. The data from each of

TABLE 2.1

Estimated cell-specific parameters for the additivity model

Cell	Parameter [a]	Estimate	Asymptotic standard error	P value
RHEK-1	α	28.3	1.08	<0.001
	γ	79.8	8.36	<0.001
	β_0	1.58	0.429	<0.001
	β_1	-0.240	0.0437	<0.001
	β_2	-0.215	0.0401	<0.001
	β_3	-0.171	0.0357	<0.001
	β_4	-0.019	0.0038	<0.001
HaCaT	α	5.6969	2.4001	0.0177
	γ	114.5	12.6018	<0.001
	β_0	1.2907	0.3409	<0.001
	β_1	-0.220	0.0391	<0.001
	β_2	-0.1623	0.0295	<0.001
	β_3	-0.0215	0.0038	<0.001
	β_4	-0.00411	0.0009	<0.001
NM1	α	13.028	2.4165	<0.001
	γ	116.3	19.7721	<0.001
	β_0	1.114	0.4654	0.0167
	β_1	-0.1349	0.0366	<0.001
	β_2	-0.1761	0.0433	<0.001
	β_3	-0.0233	0.00636	<0.001
	β_4	-0.00408	0.00116	<0.001
NHEK	α	8.762	2.5778	<0.001
	γ	107.7	13.0091	<0.001
	β_0	1.8656	0.6579	0.0046
	β_1	-0.1971	0.0582	<0.001
	β_2	-0.2588	0.0669	<0.001
	β_3	-0.1771	0.0558	0.0015
	β_4	-0.00776	0.0021	<0.001

[a] The parameters utilized in the model are described in Materials and Methods and in detail in Gennings *et al.* (2002). Also shown are the standard errors and p values associated with the different parameters. All parameters, derived from the individual metal data for the four cell strains, were significantly different from zero with p values < 0.02.

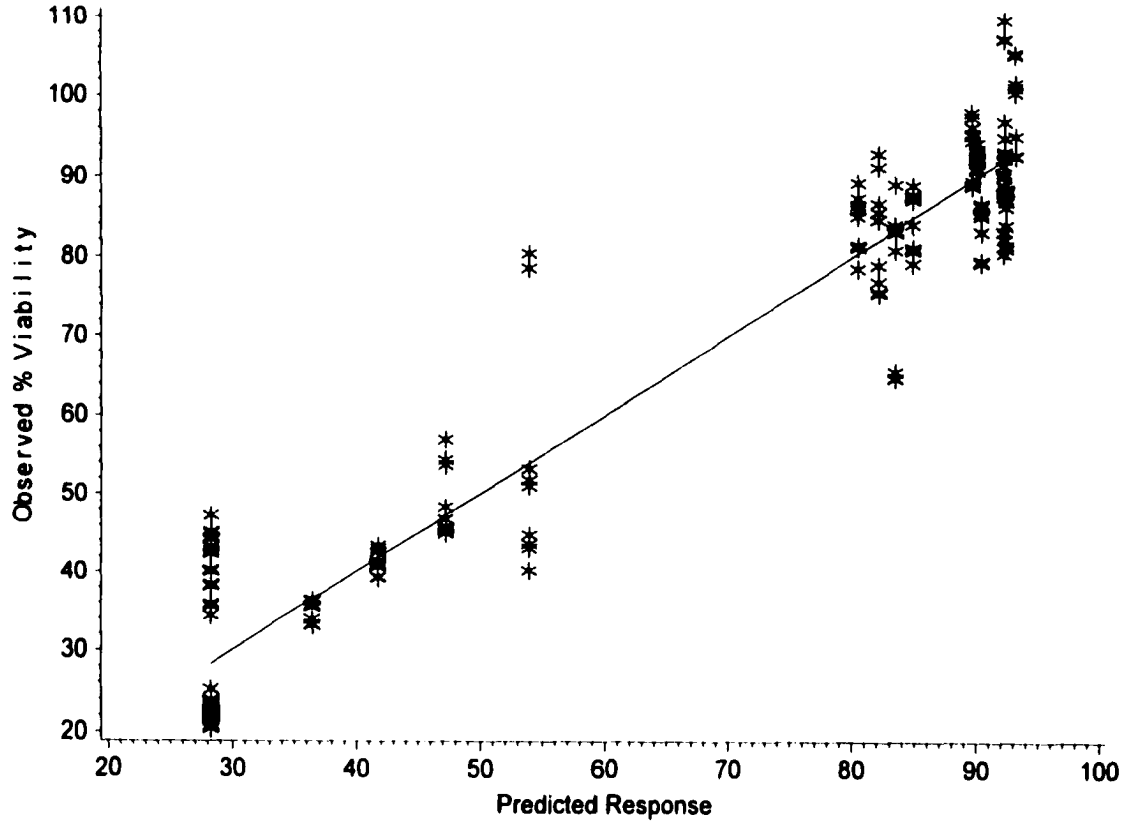

FIG. 2.1 Observed versus predicted responses for the fit of the single metal data in RHEK-1. The asterisks (*) represent the individual data points plotted in a graph of the observed versus model predicted responses. The line is the identity line (y = x) so that a cluster of points in a band along this line indicates a reasonable fit of the data.

the other three keratinocyte cell lines, although not shown, also showed adequate fit. More variability was associated with the responses in NHEK as compared to the other three cell lines (Gennings *et al.*, 2002); this may well be a function of the fact that NHEK are pooled populations of primary cells isolated from different individuals with intrinsic variations in sensitivity to toxic insult. Representative dose-response curves for the individual metals in RHEK-1 are graphically shown in Fig. 2.2. The best-fit lines determined for the single chemical data in each cell strain were used to derive parameters α, β and γ for the additivity model as described in Materials and Methods and in Gennings *et al.* (2002). The single chemical data demonstrated that the responses associated with exposure to lead have more variability than the other three metals, with levels of lead at 300 μM and percent viability between 30 and 60 % for the four cell strains (data not shown).

The observed responses in the keratinocyte strains at the seven mixture dilution points are provided in Tables 2.2A-D. These tables also provided the predicted responses under the hypothesis of additivity. Based on the comparison of the observed responses and the prediction intervals under additivity, there appears to be interactions among the four metals with regard to cytotoxicity for all four cell strains. The corresponding prediction intervals (Table 2.2) can be used to determine the direction of the interaction. In the RHEK-1, NM1, and NHEK cell strains the lowest concentration of the metal mixture was associated with growth stimulation (Tables 2.2A, C, and D). This may be due to hormesis (Calabrese, 1997; Stebbing, 1982). The quadratic terms were initially included in the additivity model for NHEK to see if the single chemical data also demonstrated this "hormesis-like" effect. However, in this case, the quadratic terms were

Exposure of RHEK-1 to increasing concentrations of As, Cr, Cd, and Pb and analysis of cell viability by the MTT assay were carried out as described in Materials and Methods. Three independent experiments with triplicate data points were run for RHEK-1. Individual data points measuring cell viability are plotted as a function of metal concentration (*). The line is the best-fit line. Single metal data was used to estimate the α, β, and γ parameters. These parameters were subsequently used in the model to predict responses to serial dilutions of a four metal mixture under the assumption of additivity.

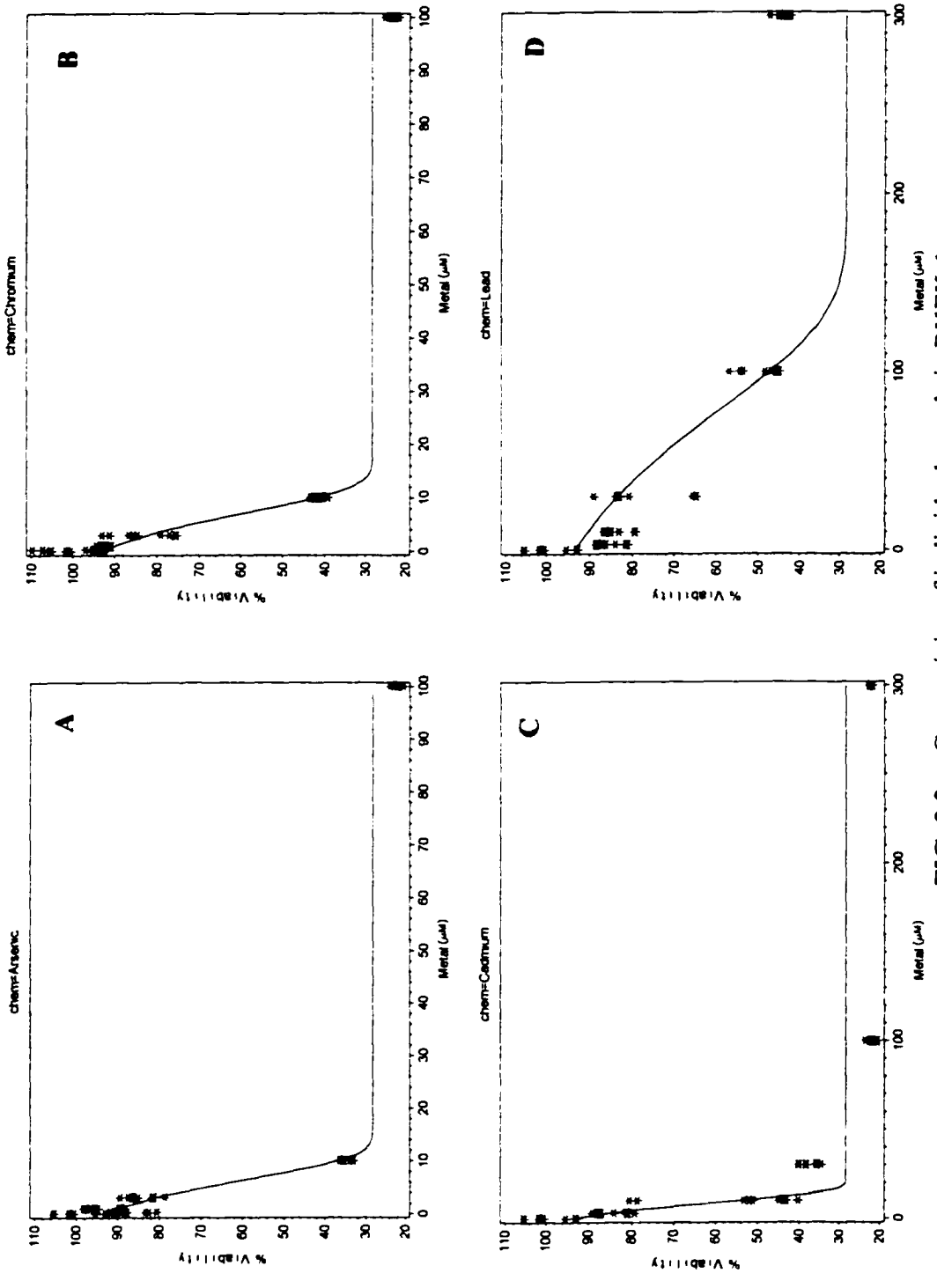

FIG. 2.2 Cytotoxicity of individual metals in RHEK-1.

TABLE 2.2

Observed mean % viability and predicted responses under the hypothesis of additivity in keratinocytes

A. RHEK-1

Mixture Dilution	Observed Mean Response	Variance Of Observed Mean	Predicted Response Under Additivity	P value	95% Prediction Intervals Under Additivity
0.0014X	104.5	3.1	93.1	<0.001*	[88.9, 97.3]¥
0.004X	96.0	1.4	92.8	0.059	[89.5, 96.1]
0.0123X	95.1	2.1	91.9	0.075	[88.4, 95.4]
0.037X	85.1	4.1	89.0	0.081	[84.7, 93.3]
0.111X	63.3	1.6	77.4	<0.001*	[73.4, 81.4]**
0.333X	50.5	0.4	33.7	<0.001*	[30.1, 37.3]#
1X	30.0	0.9	28.3	0.243	[25.4, 31.1]

B. HaCaT

Mixture Dilution	Observed Mean Response	Variance Of Observed Mean	Predicted Response Under Additivity	P value	95% Prediction Intervals Under Additivity
0.0014X	96.7	4.3	92.5	0.080	[87.9, 97.2]
0.004X	94.4	2.3	92.3	0.261	[88.6, 96.0]
0.0123X	85.1	5.3	91.5	0.011*	[86.6, 96.5]**
0.037X	79.3	4.7	89.2	<0.001*	[84.5, 93.8]**
0.111X	76.2	1.9	81.1	0.009*	[77.4, 84.7]**
0.333X	66.0	4.4	49.2	<0.001*	[43.5, 54.9]#
1X	30.6	1.6	5.7	<0.001*	[0.34, 11.1]#

(continued)

TABLE 2.2 continued

C. NM1

Mixture Dilution	Observed Mean Response	Variance Of Observed Mean	Predicted Response Under Additivity	P value	95% Prediction Intervals Under Additivity
0.0014X	107.3	5.8	96.6	<0.001*	[91.1, 102.1]¥
0.004X	97.0	19.1	96.3	0.879	[87.3, 105.4]
0.0123X	96.2	23.9	95.4	0.879	[85.5, 105.4]
0.037X	77.8	9.3	92.7	<0.001*	[86.3, 99.1]**
0.111X	63.1	3.1	83.4	<0.001*	[78.6, 88.2]**
0.333X	37.3	9.4	48.8	0.004*	[41.0, 56.7]**
1X	16.4	1.4	13.0	0.213	[7.71, 18.3]

D. NHEK

Mixture Dilution	Observed Mean Response	Variance Of Observed Mean	Predicted Response Under Additivity	P value	95% Prediction Intervals Under Additivity
0.0014X	116.6	35.0	100.9	0.013*	[88.5, 113.3]¥
0.004X	95.7	12.1	100.7	0.217	[92.8, 108.7]
0.0123X	96.0	24.0	100.2	0.431	[89.8, 110.5]
0.037X	76.5	10.2	98.4	<0.001*	[91.3, 105.4]**
0.111X	64.3	1.6	91.8	<0.001*	[87.0, 96.7]**
0.333X	50.1	29.1	60.8	0.102	[47.9, 73.6]
1X	31.1	23.0	8.8	<0.001*	[0, 19.5]#

The sample size analyzed in each mixture dilution was 9 for each of the four keratinocyte cell strains. An * indicates significant departure from additivity using Hochberg's correction using an overall 5 % level of significance. A ¥ indicates a hormesis effect; a ** indicates a greater than additive or synergistic relationship; a # indicates a less than addivitive or antagonistic relationship. 1X = concentration of each metal leading to 50 % death in individual metal assays.

not jointly significant (p value >0.05) and were removed from the final model. This indicates that the single chemical data do not support the occurrence of hormesis at the concentrations tested and growth stimulation was, thus, a function of binary or higher metal combinations. It is interesting to consider a hormesis effect of a mixture, but not the individual components. Higher concentrations (e.g., 0.037X through 0.333X dilutions) of the mixtures in the NM1 and NHEK cell strains were associated with significant departure from additivity (Tables 2.2C, D). The observed responses were synergistic or more extreme (i.e., further down the concentration effect curve) than that predicted under additivity. In NHEK, the measured cytotoxicity at the highest mixture concentration (1X) was less extreme than that predicted by the additivity model, i.e. was antagonistic. Moderate concentrations of the mixture in the HaCaT cell line (i.e., 0.0123X - 0.111X) were also associated with synergistic cytotoxicities (Table 2.2B). However, at the two highest concentrations (0.333X and 1X dilutions) tested in HaCaT, an antagonistic response was seen. In a similar trend, the 0.111X mixture dilution in the RHEK-1 cell line (0.111X) was associated with synergistic response, while the 0.333X dilution showed antagonistic responses. Only NM1 did not demonstrate a significant antagonistic response to the metal mixture at any concentration. Figures 2.3A-D show the predicted response curve under the hypothesis of additivity and the observed response at the seven mixture points in the four cell strains. The departures from additivity are clearly seen for each cell line in this figure.

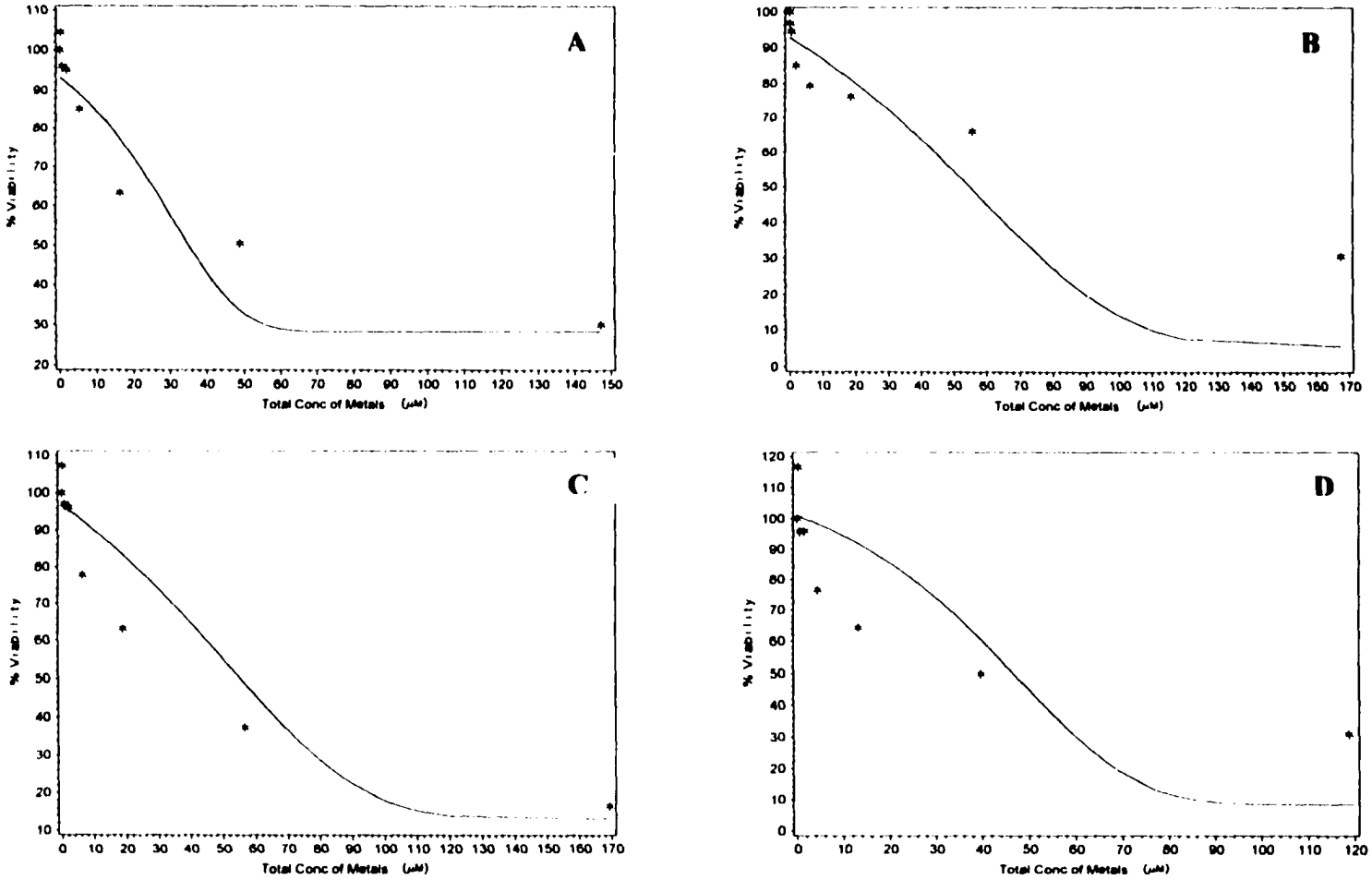

FIG. 2.3 Concentration effect curves along total concentration for the fixed ratio mixture ray. The solid line is the predicted response under the additivity model and the asterisks represent the observed sample mean responses at each of the mixture points in (A) RHEK-1, (B) HaCaT, (C) NM1, and (D) NHEK.

Potential role for reduced glutathione and metallothionein in the toxicological interactions of As, Cd, Cr, and Pb

As indicated above, the observed interactions among As, Cd, Cr, and Pb in RHEK-1, HaCaT, and NHEK switched from synergistic to antagonistic as the metal mixture increased from the 0.111X to 0.333X or 1X dilutions. We were interested in exploring potential mechanisms for this change and thus, analyzed levels of the important detoxifying molecules, GSH and hMT-I and hMT-II proteins in the keratinocyte strains treated with the metal mixture using a standard colorimetric assay and immunoblot analysis, respectively. Alterations in the levels of one or more of these molecules have been shown in other systems to modulate toxicity to metals. Table 2.3 shows the levels of GSH in RHEK-1, HaCaT, NM1 and NHEK cells treated with increasing concentrations of the four metal mixture for 24 hr. Interestingly, this analysis showed that in HaCaT and RHEK-1, the amount of intracellular GSH was fairly stable throughout the treatment range, except for at the 0.333X dilution, where the level increased approximately 2-fold over the control and preceding 0.111X treatment group. Only in RHEK-1 did the significant increase in GSH also occur in cells treated with the undiluted (1X) metal mixture; in HaCaT, GSH returned to control levels in cells treated with the 1X solution. In NM1 and NHEK, GSH was also elevated in response to treatment with the metal mixture; the highest level of GSH was measured in cells exposed to the 1X mixture concentration (4- and > 5-fold over untreated control cells for NM1 and NHEK, respectively). Levels of GSH were still 1.6-fold over control in NHEK cells treated with the 0.3X dilution and returned to control values at lower mixture concentrations. In contrast to the single peak in GSH in the other three keratinocyte cell strains, in NM1 two

TABLE 2.3

Levels of reduced glutathione in human keratinocytes treated with the four metal mixture

Treatment Group	Cell Line			
	RHEK-1	HaCaT	NM1	NHEK
control	1.00 ± 0.45	1.00 ± 0.31	1.00 ± 0.22	1.00 ± 0.23
0.0123X	1.07 ± 0.15	1.32 ± 0.35	2.25 ± 0.16	1.12 ± 0.11
0.037X	1.23 ± 0.12	1.34 ± 0.30	1.54 ± 0.33	0.99 ± 0.14
0.111X	0.90 ± 0.15	1.18 ± 0.09	0.75 ± 0.08	1.00 ± 0.09
0.333X	2.44 ± 0.16**	2.13 ± 0.25*	1.19 ± 0.52	1.60 ± 0.21
1X	1.60 ± 0.12**	1.12 ± 0.40	3.89 ± 1.04*	5.54 ± 1.17**

The human keratinocytes were treated for 24 hr with the 50X metal mixture stock or serial dilutions to have final metal mixture of 1X, 0.333X, 0.111X, 0.037X, and 0.0123X. GSH levels in cell lysates were determined as described in Materials and Methods. The relative GSH ratio of samples to control is expressed as mean ± SEM from the three independent experiments. **: a significant ($p < 0.001$) increase over control by Dunnett's test: *: $p < 0.05$.

peaks were consistently observed; approximately 2-fold elevations in GSH were also detected in cells treated with the lowest mixture concentration at 0.0123X. The differences in GSH were statistically significant as analyzed by Dunnett's multiple comparison analysis ($p < 0.05$) (Tamhane and Dunlop, 2000). In contrast to our results with GSH, where in most cases, there appeared to be a fairly high threshold for induction, total MT levels in RHEK-1, HaCaT, and NHEK cells increased in a dose-dependent manner with increasing concentration of the metal mixture. As shown in Fig. 2.4 and Table 2.4, the highest levels of induction in the three cell strains was observed at the 1X dilution point, 4.0-, 5.3-, and 4.0-fold for RHEK-1, HaCaT, and NHEK respectively. In contrast to these three cell strains, untreated NM1 showed only a very weak to undetectable signal corresponding to hMT-I/-II. In addition, there was no significant induction of the proteins upon treatment of the cells with the metal mixture at any concentration.

DISCUSSION

It is generally assumed that the concept of additivity is operative on low-level exposures to chemical mixtures (Svendsgaard and Hertzberg, 1994). Our studies are aimed at testing this hypothesis for environmentally-relevant metal mixtures. The basic approach of the analysis conducted on cytotoxicity data includes fitting an additivity model to the single metal data (Berenbaum, 1985, 1989; Gennings and Carter, 1995; Gennings *et al.*, 1997). Using this model, comparisons are then made between the observed responses at mixture points of interest as compared to the predicted response under the additivity model. If significant departure from additivity is found, then an

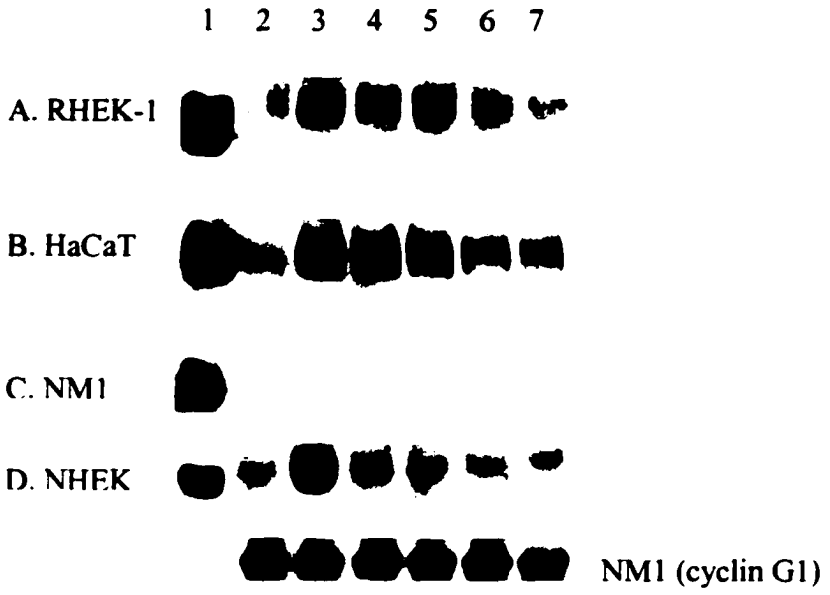

FIG. 2.4 Human metallothionein (MT) expression in keratinocytes exposed to a four-metal mixture. Total cellular protein (50 μg) from mixture treated and control RHEK-1 (A), HaCaT (B), NM1 (C), and NHEK (D) cells was analyzed by Western blotting for MT expression as described in Materials and Methods. Signal strength was quantified using NIH Image 1.55 b20. Equine renal MT-I was utilized as a positive control and runs at approximately 13 kDa (lane 1). The human MT isoforms migrate at a similar size range 13.5 kDa. Samples 2-7 are from cells exposed to: (2) water control; (3) 1X; (4) 0.333X; (5) 0.111X; (6) 0.037X; and (7) 0.0123X dilutions of the metal mixture. Constitutive expression of cyclin G1 in NM1 cells was shown to confirm the overall protein content and quality in cell lysates.

TABLE 2.4

Human metallothionein (hMT-I and -II) protein levels in human keratinocytes treated with the four metal mixture

Treatment Group	Cell Line			
	RHEK-1	HaCaT	NM1	NHEK
control	1.00 ± 0.37	1.00 ± 0.24	1.00 ± 0.15	1.00 ± 0.15
0.0123X	1.14 ± 0.18	1.49 ± 0.32	0.68 ± 0.24	0.56 ± 0.12
0.037X	1.97 ± 0.37	2.17 ± 0.46	1.31 ± 0.33	1.35 ± 0.23
0.111X	2.92 ± 0.57	3.42 ± 0.48**	1.52 ± 0.44	1.39 ± 0.26
0.333X	3.08 ± 0.76*	4.12 ± 0.62**	2.38 ± 0.63 [a]	2.30 ± 0.22**
1X	4.03 ± 0.80*	5.32 ± 0.89**	1.26 ± 0.27	4.02 ± 0.41**

Western blot analysis of human MT in cell lysates from four human keratinocyte strains was carried out as described in Materials and Methods. Chemiluminescent signals corresponding to the MT band at 13.5 kDa were quantified by NIH Image 1.55 b20. Mean relative MT signal (± SEM) is given in treated samples as compared to controls. Three independent experiments were carried out and data were pooled. **: a significant ($p < 0.0001$) increase over control by Dunnett's test; *: $p < 0.05$.

[a] In NM1 this apparent induction was not statistically significant; this is likely due to the low levels of MT and inconsistent expression detected.

interaction can be claimed at the mixture levels tested. In our studies, all three types of responses to the metal mixture were seen (*i.e.*, additivity, synergism, or antagonism), depending highly on both the keratinocyte cell line examined and the dose of the metal mixture. With some exceptions, the general trend of cytotoxicity by the four metal mixture appears to be hormesis to additivity to synergism and finally to antagonism as dose level increases. In that sense the additivity concept holds true for a narrow dose range.

In our studies three of the four lines, RHEK-1, NM1, and NHEK showed increased growth when exposed to very low concentrations (low ppb range) of the four metal mixture. One possible explanation for this observation is a hormesis effect. Much information has become available on the cellular and molecular basis of hormesis through studies on the biological effects of low levels of exposure to single chemicals or combinations of chemicals (Calabrese, 1997; Calabrese and Baldwin, 1997a, 1997b; Mehendale, 1994; Stebbing, 1982, 1997). Hormesis may be the cumulative consequence of transient and sustained "overcompensation" by homeostatic mechanisms in response to low levels of inhibitory challenge (Calabrese and Baldwin, 1999; Stebbing, 1997). There is precedent for a hormetic effect of As on keratinocytes. Germolec *et al.* (1996, 1997) demonstrated that very low levels (0.001-0.005 μM) of As induced proliferation in primary NHEK. Although in our studies, we did not see growth stimulation in the keratinocyte strains with any of the metals alone, the concentrations tested were in a higher range (0.3 to 300 μM) than in these previous studies. In contrast, in the mixture dilutions where the hormetic effect was apparent in our studies, the concentration of As was 0.010-0.013 μM, depending on the cell strain; our finding of growth stimulation in

these populations was, therefore, consistent with at least a partial effect of As. Whether or not the other three metals contributed is currently unknown. Of the four keratinocyte cell lines, only HaCaT did not show signs of hormesis at any concentration of the chemical mixture examined; it is possible that this keratinocyte strain displays differential induction of and/or sensitivity to growth regulatory molecules involved in the hormetic response as compared to RHEK-1, NM1, and NHEK.

Synergistic cytotoxicities of the four metal mixture were observed in all four cell types, albeit at different dose levels. Antagonistic responses were seen in RHEK-1, HaCaT and NHEK at high treatment concentrations. Particularly interesting was the abrupt switch in RHEK-1 and HaCaT from synergistic to antagonistic interactions among the metals at the highest mixture concentrations. There are many types of metal-metal interactions that may be responsible for the synergism or antagonism we observed. Among these would be alterations in detoxifying or metabolizing pathways. To address this issue, we have explored expression of multiple molecules potentially involved in detoxification of metals, hMT-I and –II and GSH, in the keratinocyte cell lines treated with the metal mixture. One of the primary mechanisms conferring resistance to Cd is overexpression of the members of the metallothionein (MT) gene family; these proteins may be involved in protection against metal-induced toxicity. The MT genes are differentially regulated in response to heavy metals, cytokines and reactive oxygen species (ROS). One possibility is that metals such as As or Cr increase expression of one or more of the MT genes indirectly through cytokine induction or generation of ROS, thus, having substantial impacts on Cd toxicity. The induction of MT expression by As, as well as this type of interactive effect, has been observed in numerous other studies

(Albores *et al.*, 1992; Hochadel and Waalkes, 1997; Kreppel *et al.*, 1993; Liu *et al.*, 2000a; Zhao *et al.*, 1997). In addition, in some instances (although not all) MT expression has been correlated with decreased sensitivity to the cytotoxic effects of chronic As exposure (Liu *et al.*, 2000b). As has also been shown to induce other genes such as those the encoding heat shock proteins (HSP), which may be involved in detoxification of As, itself, and Cd (Huot *et al.*, 1991; Li, 1983; Wu and Welsh, 1996). Increased expression of HSP27, in turn, correlates with increased total cellular GSH (Mehlen *et al.*, 1996). It has been demonstrated that the cellular levels of GSH and glutathione-S-transferase-pi (GST-pi) play important roles in resistance to As and other metals (Huang and Lee, 1996; Lee *et al.*, 1989; Rosen, 1995; Shimizu *et al.*, 1998; Wang and Lee, 1993). It is evident from these and other studies, that merely by alteration in expression levels of detoxifying molecules such as either MT or GSH, one metal may have substantial impact on the resultant toxicity of another when the two are present together in a mixture.

Several interesting findings resulted from our analysis of MT and GSH levels in the four keratinocyte strains. Somewhat contrary to our expectations, basal MT-IA levels in the four cell strains did not correlate with the differential sensitivity to Cd observed in our single metal cytotoxicity studies. However, these studies did suggest that either or both GSH or MT may play a role in the antagonistic interactions observed in cells treated with high mixture concentrations. The two-fold increase in GSH at just the point where synergistic interactions become antagonistic in RHEK-1 and HaCaT would be consistent with this hypothesis. Additionally, in NHEK, GSH levels were highly elevated at the mixture concentration (1X) where antagonistic interactions were observed. In contrast to

what we observed with GSH, MT proteins appear to be induced in a dose-dependent fashion with increasing mixture concentrations in three of the four cell strains. However, it may be that there is a critical intracellular level of MT required for detectable protection against the toxicity of one or more of the metals. Alternatively, both increased levels of GSH and MT may be required (Li *et al.*, 1994; Susanto *et al.*, 1998). Our inability to measure significant basal amounts or induction of hMT-I or –II in NM1 and to detect antagonistic interactions among the metals in the mixture at any concentration supports these hypotheses. It will be interesting to carry out these same types of studies on metal-metal interactions in the presence of the GSH-depleting agent, *L*-buthionine sulfoximine (BSO).

In summary, our studies are relevant and important to risk assessment of toxic metals in several regards. Our findings, via statistical analysis, that multiple heavy metals in a mixture do not necessarily act in an additive fashion at low doses as is commonly assumed is highly relevant in terms of developing accurate risk assessment strategies for these important environmental contaminants. The nature of the interaction between component metals in a mixture is extremely complicated, being both cell strain- and dose-dependent. Our single metal toxicity data supported these findings in that, for Cd and Pb, there are quite substantial differences in sensitivity among the same cell type isolated from different individuals. These findings suggest the involvement of a strong genetic component in susceptibility to the toxic effects of diverse chemicals. Under many conditions in each of the cell strains, we observed synergistic cytotoxicity of the mixture, clearly important findings for assessment of health effects in exposed populations. Given the complexity of chemical-biological interactions in the cells, these results again

emphasize the need for computer technology and biologically-based modeling in future risk assessment strategies of chemical mixtures.

ACKNOWLEDGMENTS

We thank to Drs. Chris Gennings, Walter H. Carter, Jr., and Ms. Susan Parker at the Department of Biostatistics, Virginia Commonwealth University, Richmond, VA for their statistical analyses on cell lines studied in this chapter. This study was supported by the Agency for Toxic Substances and Disease Registry (ATSDR) Cooperative Agreement U61/ATU881475, and the National Institute for Environmental Health Sciences (NIEHS) Superfund Basic Research Program Project P42 ES05949. The efforts of many colleagues at the Center for Environmental Toxicology & Technology at Colorado State University are gratefully acknowledged.

REFERENCES

Albores, A., Koropatnick, J., Cherian, M. G., and Zelazowski, A. J. (1992). Arsenic induces and enhances rat hepatic metallothionein production in vivo. *Chem. Biol. Interact.* **85**, 127-140.

Anderson, M. E. (1989). Enzymatic and chemical methods for determination of glutathione. In *Glutathione* (D. Dolphin, O. Avramovic, and R. Poulson, Eds.), pp. 339-365. John Wiley & Sons, New York.

ATSDR (1997). *1997 CERCLA Priority List of Hazardous Substances That Will be the Subjects of Toxicological Profiles & Support Document*, Agency for Toxic Substances and Disease Registry, U.S. Department of Health and Human Services, November.

Baden, H. P., Kubilius, J., Kredar, J. C., Steinberg, M. L., and Wolman, S. R. (1987). Isolation and characterization of a spontaneously arising long-lived line of human keratinocytes (NM1). *In Vitro Cell Develop. Biol.* **23**, 205-213.

Berenbaum, M. C. (1985). The expected effect of a combination of agents:the general solution. *J. Theor. Biol.* **114**, 413-431.

Berenbaum, M. C. (1989). What is synergy? *Pharmacol. Rev.* **41**, 93-141.

Boukamp, P., Petrusevska, R. T., Breitkreutz, D., Hornung, J., Markham, A., and Fusenig, N. E. (1988). Normal keratinization in a spontaneously immortalized aneuploid human keratinocyte cell line. *J. Cell Biol.* **106**, 761-771.

Calabrese, E. J. (1997). Hormesis revisited: new insights concerning the biological effects of low-dose exposures to toxins. *Environ. Law Report.* **27**, 10526-10532.

Calabrese, E. J. and Baldwin, L. A. (1997a). A quantitatively-based methodology for the evaluation of chemical hormesis. *Human Ecol. Risk Assess.* **3**, 545-554.

Calabrese, E. J. and Baldwin, L. A. (1997b). The dose determines the stimulation (and poison): Development of a chemical hormesis database. *Int. J. Toxicol.* **16**, 545-559.

Calabrese, E. J. and Baldwin, L. A. (1999). Chemical hormesis: its historical foundations as a biological hypothesis. *Toxicol. Pathol.* **27**, 195-216.

Cohen, M. D., Kargacin, C. B., Klein, C. B., and Costa, M. (1993). Mechanisms of chromium carcinogenicity and toxicology. *Crit. Rev. Toxicol.* **23**, 255-281.

DeRosa, C. T., Johnson, B. L., Fay, M., Hansen, H., and Mumtaz, M. M. (1996). Public health implications of hazardous waste sites: findings, assessment, and research. *Food Chem. Toxicol.* **34**, 1131-1138.

Fay, M. and Mumtaz, M. M. (1996). Development of a priority list of chemical mixtures occurring at 1188 hazardous waste sites using the HazDat database. *Food Chem. Toxicol.* **34**, 1163-1165.

Gennings, C. and Carter, Jr. W. H. (1995). Utilizing concentration-response data from individual components to detect statistically significant departures from additivity in chemical mixtures. *Biometrics* **51**, 1264-1277.

Gennings, C., Carter, Jr. W. H., Campain, J. A., Bae, D. S., and Yang, R. S. H. (2002). Statistical analysis of interactive cytotoxicity in human epidermal keratinocytes following exposure to a mixture of four metals. *J. Agric. Biol. Environ. Stat.* **7**, 58-73.

Gennings, C., Schwartz, P., Carter, Jr. W. H., and Simmons, J. E. (1997). Detection of departures from additivity in mixtures of many chemicals with a threshold model. *J. Agric. Biol. Environ. Stat.* **2**, 198-211.

Germolec, D. R., Spalding, J., Boorman, G. A., Wilmer, J. L., Yoshida, T., Simeonova, P. P., Bruccoleri, A., Kayama, F., Gaido, K., Tennant, R., Burleson, F., Dong, W., Lang, R. W., and Luster, M. I. (1997). Arsenic can mediate skin neoplasia by chronic stimulation of keratinocyte-derived growth factors. *Mut. Res.* **386**, 209-218.

Germolec, D. R., Yoshida, T., Gaido, K., Wilmer, J. L., Simeonova, P. P., Kayama, F., Burleson, F., Dong, W., Lang, R. W., and Luster, M. I. (1996). Arsenic induces

overexpression of growth factors in human keratinocytes. *Toxicol. Appl. Pharmacol.* **141**, 308-318.

Hochadel, J. F. and Waalkes, M. P. (1997). Sequence of exposure to cadmium and arsenic determines the extent of toxic effects in male Fischer rats. *Toxicology* **116**, 89-98.

Horne, M. C., Goolsby, G. L., Donaldson, K. L., Tran, D., Neubauer, M., and Wahl, A. F. (1996). Cyclin G1and cyclin G2 comprise a new family of cyclins with contrasting tissue-specific and cell cycle-regulated expression. *J. Biol. Chem.* **271**, 6050-6061.

Huang, R.-N. and Lee, T.-C. (1996). Arsenite efflux is inhibited by verapamil, cyclosporin A, and GSH-depleting agents in arsenite-resistant Chinese hamster ovary cells. *Toxicol. Appl. Pharmacol.* **141**, 17-22.

Huot, J., Roy, G., Lambert, H., Chretien, P., and Landry, J. (1991). Increased survival after treatments with anticancer agents of Chinese hamster cells expressing the human Mr 27,000 heat shock protein. *Cancer Res.* **51**, 5245-5252.

Kachinskas, D. J., Qin, Q., Phillips, M. A., and Rice, R. A. (1997). Arsenate suppression of human keratinocyte programming. *Mut. Res.* **386**, 253-261.

Kreppel, H., Bauman, J. W., Liu, J., McKim, J. M., Jr., and Klaassen, C. D. (1993). Induction of metallothionein by arsenicals in mice. *Fundam. Appl. Toxicol.* **20**, 184-189.

Laemmli, U. K. (1970). Cleavage of structural proteins during assembly of the head of bacteriophage T4. *Nature* **227**, 680-685.

Lee, T.-C., Wei, M. L., Chang, W. J., Ho, I. C., Lo, J. F., Jan, K. Y., and Huang, H. (1989). Elevation of glutathione levels and glutathione S-transferase activity in arsenic-resistant Chinese hamster ovary cells. *In Vitro Cell Develop. Biol.* **25**, 442-448.

Li, G. C. (1983). Induction of thermotolerance and enhanced heat shock protein synthesis in Chinese hamster fibroblasts by sodium arsenite and ethanol. *J. Cell Physiol.* **115**, 116-122.

Li, W., Kagan, H. M., and Chou, I. (1994). Alterations in cytoskeletal organization and homeostasis of cellular thiols in cadmium-resistant cells. *Toxicol. Appl. Pharmacol.* **126**, 114-123.

Liu, J., Liu, Y., Goyer, R. A., Achanzar, W., and Waalkes, M. P. (2000b). Metallothionein-I/II null mice are more sensitive than wild-type mice to the hepatotoxic and nephrotoxic effects of chronic oral or injected inorganic arsenicals. *Toxicol. Sci.* **55**, 460-467.

Liu, J., Liu, Y., Habeebu, S. M., Waalkes, M. P., and Klaassen, C. D. (2000a). Chronic combined exposure to cadmium and arsenic exacerbates nephrotoxicity, particularly in metallothionein-I/II mice. *Toxicology* **147**, 157-166.

Mehendale, H. M. (1994). Mechanisms of the interactive amplification of halomethane hepatotoxicity and lethality by other chemicals. In *Toxicology of Chemical Mixtures* (R.S.H.Yang, Ed.), pp. 299-334. Academic Press.

Mehlen, P., Kretz-Remy, C., Preville, X., and Arrigo, A. P. (1996). Human hsp27, drosophila hsp27 and human alphaB-crystalline expression-mediated increase in glutathione is essential for the protective activity of these proteins against TNFalpha-induced cell death. *EMBO J.* **15**, 2695-2706.

Mossman, T. (1983). Rapid colorimetric assay for cellular growth and survivals: Application to proliferation and cytotoxicity assays. *J. Immunol. Methods* **65**, 55-63.

Rheinwald, J. G. and Green, H. (1975). Serial cultivation of strains of human epidermal keratinocytes; the formation of keratinizing colonies from single cells. *Cell* **6**, 331-343.

Rheinwald, J. G. and Green, H. (1977). Epithelial growth factor and the multiplication of cultured human epidermal keratinocytes. *Nature* **265**, 421-424.

Rhim, J. S., Jay, G., Arnstein, P., Price, F. M., Sanford, K. K., and Aaronson, S. A. (1985). Neoplastic transformation of human epidermal keratinocytes by AD12-SV40 and Kirsten sarcoma viruses. *Science* **227**, 1250-1251.

Rosen, B. P. (1995). Resistance mechanisms to arsenicals and antimonials. *Basic Clin. Physiol. Pharmacol.* **6**, 251-263.

Shimizu, M., Hochadel, J. F., Fulmer, B. A., and Waalkes, M. P. (1998). Effect of glutathione depletion and metallothionein gene expression on arsenic-induced cytotoxicity and c-myc expression in vitro. *Toxicol. Sci.* **45**, 204-211.

Stebbing, A. R. D. (1982). Hormesis-the stimulation of growth by low levels of inhibitors. *Sci. Total Environ.* **22**, 213-234.

Stebbing, A. R. D. (1997). A theory for growth hormesis. *BELLE Newsletter* **6**, 1-11.

Susanto, I., Wright, S. E., Lawson, R. S., Williams, C. E., and DeRosa, C. T. (1998). Metallothionein, glutathione, and cystine transport in pulmonary artery endothelial cells and NIH3T3 cells. *Am. J. Physiol.* **274**, 296-300.

Svendsgaard,D.J. and Hertzberg,R.C. (1994). Statistical methods for the toxicological evaluation of the additivity assumption as used in the Environmental Protection Agency Chemical Mixture Risk Assessment Guidelines. In *Toxicology of Chemical Mixtures* (R.S.H.Yang, Ed.), pp. 599-642. Academic Press, San Diego.

Tamhane, A.C., and Dunlop, D.D. (2000) Multiple Comparisons of Means. In *Statistics and Data Analysis from Elementary to Intermediate*, pp. 475-476. Prentice-Hall, Inc., Upper Saddle River.

Wang, H. F. and Lee, T.-C. (1993). Glutathione S-transferase pi facilitates the excretion of arsenic from arsenic-resistant Chinese hamster ovary cells. *Biochem. Biophys. Res. Commun.* **192**, 1093-1099.

Wu, W. and Welsh, M. J. (1996). Expression of the 25-kDa heat shock protein (HSP27) correlates with resistance to the toxicity of cadmium chloride, mercuric chloride, cis-platinum(II)-diammine dichoride, or sodium arsenite in mouse embryonic stem cells transfected with sense or antisense HSP27 cDNA. *Toxicol. Appl. Pharmacol.* **141**, 330-339.

Yang, J. H., Thraves, P., Dritschilo, A., and Rhim, J. S. (1992). Neoplastic transformation of immortalized human keratinocytes by 2,3,7,8-tetrachlorodibenzo-p-dioxin. *Cancer Res.* **52**, 3478-3482.

Ye, J., Zhang, X., Young, H. A., Mao, Y., and Shi, X. (1995). Chromium(VI)-induced nuclear factor-kB activation in intact cells via free radical reactions. *Carcinogenesis* **16**, 2401-2405.

Yen, H.-T., Chiang, L.-C., Wen, K.-H., Chang, S.-F., Tsai, C.-C., Yu, C.-L., and Yu, H.-S. (1996). Arsenic induces interleukin-8 expression in cultured keratinocytes. *Arch. Dermatol. Res.* **288**, 716-717.

Zhao, C. Q., Young, M. R., Diwan, B. A., Coogan, T. P., and Waalkes, M. P. (1997). Association of arsenic-induced malignant transformation with DNA hypomethylation and aberrant gene expression. *Proc. Natl. Acad. Sci. USA* **94**, 10907-10912.

CHAPTER 3

Characterization of Gene Expression Changes Associated with MNNG, Arsenic, or Metal Mixture Treatment in Human Keratinocytes: Application of cDNA Microarray Technology

Dong-Soon Bae, William H. Hanneman, Raymond S. H. Yang, and Julie A. Campain

Abstract

The identification of molecular markers related to critical biological processes during carcinogenesis may aid in the evaluation of carcinogenic potentials of chemicals and chemical mixtures. Work from our laboratory demonstrated that a single treatment with MNNG enhanced spontaneous malignant transformation of the human keratinocyte cell line, RHEK-1. In contrast, chronic low level exposure of cells to arsenic alone or in a mixture containing arsenic, cadmium, chromium, and lead inhibited malignant conversion. To identify changes in gene expression that influence these different outcomes, cDNA microarray technology was utilized. Analysis of multiple human arrays in MNNG-transformed RHEK-1 cells, designated OM3, and those treated with arsenic or the arsenic-containing metal mixture showed unique patterns of gene expression. Genes that are overexpressed in OM3 include oncogenes, cell cycle regulators, and those involved in signal transduction, while genes for DNA repair enzymes and inhibitors of transformation and metastasis were suppressed. In arsenic-treated cells, multiple DNA repair proteins were overexpressed. Mixture-treated cells showed increased expression of

a variety of genes including metallothioneins and integrin β4. These cells showed decreased expression of oncogenes. DNA repair proteins. and genes involved in the MAP kinase pathway. For comparison. we are currently analyzing gene expression changes in RHEK-1 transformed by other means. The goal of these studies is to identify common batteries of genes affected by chemical modulators of the carcinogenic process. Mechanistic studies may allow us to correlate alterations in their expression with sequential stages in the carcinogenic process and may aid in the risk assessment of other xenobiotics.

Introduction

Epidemiological evidence suggests that some. if not all. environmentally relevant metals including arsenic (As). cadmium (Cd). chromium (Cr). and lead (Pb) are human carcinogens. Unfortunately. human exposures to such metals in both the occupational and environmental setting are common occurrences. In fact. due to high As (and other metal) concentrations in the drinking water supplies in many countries. chronic toxicity and development of neoplastic lesions have become health problems of global proportions (*1-2*). In the United States. As. Cd. Cr. and Pb. are the top four metals in site frequency count by the ATSDR Completed Exposure Pathway Site Count Report (*3*): three of these. As. Pb. and Cd are among the Superfund Top 10 Priority Hazardous Substances (*4*). In addition. these metals most often occur together: they are present in 8 of 10 and 5 of 10 of the Top 10 Binary Combinations of Contaminants in soil and water. respectively (*5*).

The mechanisms mediating metal-induced cytotoxicity and carcinogenicity are currently unclear. Many laboratories. using a variety of experimental systems. have

carried out detailed studies in attempts to address these issues. From this work, it has become apparent that metals affect multiple intracellular targets and exert a variety of diverse effects on cells *in vitro* (*6, 7*). Studies suggest that different metals have unique primary mechanisms of action that are cell- and/or tissue-specific (*6, 7*). Additionally, the activity of a metal in any given tissue is dependent on its speciation and metabolism (*6*). To further complicate the picture, metals have been shown to interact at multiple levels and, most likely, modify one another's cytotoxicity and/or carcinogenic potential (*8-11*). As a result, we are still a long way from a fundamental understanding of the actions of metals or metal mixtures at the cellular level, particularly as they relate to toxic endpoints. Accurate risk assessment of these highly relevant chemicals awaits our progress in this area.

The skin is one important target organ for As-mediated pathological effects, and is a useful model system for mechanistic studies in this area. Chronic exposure to As leads to skin disorders such as hyperkeratosis and, in many cases, carcinogenesis (*12, 13*). Both As and Cr, a well known skin sensitizer, have substantial effects on epidermal keratinocytes *in vitro* and/or *in vivo*; these metals have been shown to alter expression of numerous growth regulatory factors, to stimulate cell proliferation at low concentrations, and to inhibit the normal process of differentiation (*11, 14-19*). They have not, however, been shown to be directly transforming in this cell type. In transgenic Tg.AC mice, As acts as a co-promoter during skin carcinogenesis in standard two-stage models (*20*). These studies have suggested that TGF-α and GM-CSF may be useful biomarkers for As-associated carcinogenesis in keratinocytes; data from As-exposed human subjects support

this hypothesis (*20*). It is likely, however, that the picture is much more complex than this and the genes involved are more numerous.

New technologies in expression analysis at the RNA and protein levels have led to the development of the field of toxicogenomics, i.e. the use of genetic information to address issues, such as these, that are crucial in toxicology. As an approach to defining the mechanism(s) behind selective chemical toxicity, one may analyze gene expression changes in cells after exposure to the chemical(s) of interest. Methodologies such as microarray analysis allow one to gain a comprehensive view of the cellular pathways affected by the chemical(s) under scrutiny; comparison may then be made between multiple chemicals having the same or differing toxicities. Characterization of the relationship among chemical exposure, gene expression alterations, and development of acute or chronic toxicity should help in delineating important molecular events that are mechanistically linked to the different toxic endpoints. In addition, once gene expression changes induced by individual chemicals are identified and linked to functional endpoints, interactions in chemical mixtures will be substantially easier to understand and predict.

We have used human keratinocytes as an experimental model to define molecular events that may mediate the cytotoxicity and/or carcinogenicity of As alone and in environmentally relevant metal mixtures. We describe here an evaluation of the transforming potential of As alone and together with Cd, Cr, and Pb in previously immortalized human epidermal keratinocytes, as compared to the potent carcinogen, MNNG, and negative controls. Genetic alterations induced by the different chemical

treatments, and which may be involved in their selective toxicity and/or carcinogenicity, were analyzed by cDNA microarray technology.

Materials and Methods

Chemicals.

Sodium metaarsenite ($NaAsO_2$), cadmium chloride ($CdCl_2$), chromium oxide (CrO_3), chromium chloride ($CrCl_3$), lead acetate ($(C_2H_3O_2)_2Pb{\bullet}3H_2O$), and dimethyl sulphoxide (DMSO) were purchased from Sigma Chemical Co. (St. Louis, MO). *N*-methyl-*N'*-nitro-*N*-nitrosoguanidine (MNNG) was obtained from Aldrich (Milwaukee, WI).

Cell lines and culture reagents.

The AD12/SV40 immortalized human keratinocyte cell line (RHEK-1) was obtained from Dr. J. Rhim (Center for Prostate Disease Research, Rockville, MD) (*21,22*). RHEK-1 was cultured in Dulbecco's Modified Eagle's medium (DMEM) supplemented with 100 U/ml penicillin, 0.1 mg/ml streptomycin, 10 mM L-glutamine, and 10 % fetal bovine serum (FBS) (Summit Biotechnology, Ft. Collins, CO). Methlycellulose-based medium for determination of anchorage-independent growth was obtained as MethoCult™ from Stem Cell Technologies, Vancouver, Canada.

Establishment of keratinocyte cell lines following exposure to MNNG, As, or As-containing mixture.

RHEK-1 cells were plated at 2.5 x 10^5 cells per 75cm^2 flask. The conditions used for MNNG treatment were those described by Rhim *et al.* (*23*). Briefly, 24 hr after plating,

cultures were fed with medium containing the positive control MNNG at 0.01 or 0.1 μg/ml. or 0.5 % DMSO vehicle control. After 24 hour exposure (one treatment only). cells were washed with 1X phosphate buffered saline (PBS) and then refed with culture medium. Cells were subsequently subcultured weekly. RHEK-1 was also exposed to low doses (9. 11. and 14 ppb) of As^{3+}. the metal mixture. or water vehicle controls. continuously for approximately 6 months (or 25 passages). i.e. the test chemicals were added to the culture medium at each subculturing. The concentrations of As utilized corresponded to the $LD_{2.5}$. LD_5. and LD_{10}. as determined in our laboratory for this cell type (*11*). The low mixture treatment group was composed of 1. 10. 62. and 33 ppb of As. Cr. Cd. and Pb. respectively. In efforts to more closely mimic the actual exposure scenario with Cr. these chronic studies were carried out with a mixture of 1:1 Cr^{3+} and Cr^{6+}. The high mixture treatment group was exposed to 14. 104. 618. and 332 ppb of As. Cr. Cd. and Pb. respectively. The concentrations of the four metal mixture utilized corresponded to the LD_1 and LD_{10} of each individual metal in RHEK-1. The resulting cultures were designated: OM1 (DMSO-treated control cells): OM2 (0.01 μg/ml MNNG): OM3 (0.1 μg/ml MNNG): water control: As-Low (9 ppb As): As-Med (11 ppb As): As-High (14 ppb As): Mix-Low (LD_1 mixture): and Mix-High (LD_{10} mixture).

Methylcellulose (MC) cloning.

MC cloning as an index for anchorage independent growth was carried out every 2-3 passages for the As. metal mixture. and MNNG-treated cultures. For methylcellulose cloning. 1 x 10^4 cells/ml were plated in 35 mm gridded dishes in triplicate in 1.3 %

methylcellulose. The number of colonies was counted via manual inspection under phase contrast microscopy after 2 weeks and expressed as percent cloning efficiency.

Analysis of saturation density.

Saturation density was measured as the maximum number of cells obtained in cultures as a function of time. Cells (1×10^4 /cm^2) were plated in 25 cm^2 culture flasks in triplicate. Viable cells at 5, 8, 10, 12, 15, and 17 days after initial plating were counted by trypan blue exclusion on a hemocytometer. Culture medium was changed every 3 days. Unattached cells in the culture medium were pelleted by centrifugation and also counted.

Analysis of tumorigenicity in immunocompromised mice.

The tumorigenicity assay was carried out using a modification of Rhim *et al. (23)*. Briefly, cells from passage 16 and passage 25 (OM1 and OM3) or passage 25 (As-Low, As-High, Mix-Low, Mix-High, and the appropriate water controls) were collected by 0.05% trypsin treatment. Cells (2×10^6) in 0.1 ml of PBS were injected subcutaneously into the interscapular region of 4-8 week-old male Balb/c nu/nu mice. The mice were observed weekly for 3 months for tumor development and growth. The tumors were measured by caliper, excised, and fixed in 10 % formalin prior to sectioning and slide preparation. Tissue sections were stained with hematoxylin and eosin (H & E) and characterized by histopathological analysis.

RNA preparation.

Total RNA was isolated from cultures of control and chemically-treated RHEK-1 cells (at approximately 70 % confluence) at passage 25 using the RNAqueous kit (Ambion. Austin. TX) as per the manufacturer's directions. RNA purity and concentration were assessed by determination of absorption at 260 and 280 nm.

cDNA synthesis and radioactive labeling for the Clontech Atlas Human Cancer 1.2 Array.

Total RNA (2 μg per reaction) was reverse transcribed from each test sample with superscript in the presence of [α-^{32}P]dATP (Amersham. Piscataway. NJ) using the Atlas Pure Total RNA Labeling System (Clontech. Palo Alto. CA). Unincorporated isotope was removed by gel filtration in Chroma Spin-200 columns (Clontech). The Atlas Human Cancer 1.2 Array was supplied by the manufacturer on nylon membranes: 1185 genes were analyzed using this array. These membranes were prehybridized for 30 min at 68°C in ExpressHyb (Clontech) containing 0.1 mg/ml sheared salmon sperm DNA. They were then incubated with 2 x 10^6 cpm of radiolabeled cDNA probe (control OM1 or test sample OM3: water control or test samples As-High and Mix-High) per ml of ExpressHyb buffer overnight at 68°C. After high stringency washes in 2X standard saline citrate (SSC). 1% sodium dodecyl sulfate (SDS) at 68°C. the blots were exposed to storage phosphor screens (Molecular Dynamics. Sunnyvale. CA). Signals were scanned and captured using a Storm 860 Phosphorimager and ImageQuant software (Molecular Dynamics). Gene expression images were quantified using AtlasImage 1.0 program (Clontech) by the Atlas Technology Center. Relative changes in gene expression were

determined by normalizing the hybridization signals to the signals obtained from all the genes included in the array. Genes that demonstrated ≥2-fold changes in expression between control and treatment were reported.

cDNA synthesis and fluorescent labeling for NEN Arrays.

Two microarrays from New England Nuclear (Boston. MA) were utilized to analyze gene expression changes in OM3 versus OM1 and As-High and Mix-High versus the appropriate water controls. These were the NEN Human 2400 (2400 genes analyzed) and Oncogene/Tumor Suppressor (325 genes analyzed) arrays. In addition. gene expression in OM3 as compared to OM1 was analyzed by the NEN Kinase/Phosphatase array (275 genes analyzed): this latter analysis was not carried out on the metal-treated cultures. We do not. therefore. have data as to how the genes contained within this array are affected in the metal treated cells. Synthesis and labeling of cDNA were carried using the MICROMAX™ Direct cDNA Microarray System as per the manufacturer's directions. Briefly. 100 μg or 40 μg of total RNA for the Human 2400 or Oncogene/Tumor suppressor arrays. respectively. was reverse transcribed from each test sample with AMV Reverse Transcriptase in the presence of cyanine 3 (Cy3) (for OM1 and water controls) and cyanine 5 (Cy 5) (for OM3. As-High. and Mix-High) using the MICROMAX Direct cDNA Microarray System (NEN). For the NEN Kinase/Phosphatase array. 40 μg of RNA was used from OM1 and OM3. Labeled cDNAs from control and treated samples were purified by isopropyl alcohol precipitation. MICROMAX Microarray slides were utilized that contained the three different arrays. The entire reaction from the combined Cy3 and Cy5-labeled probes in Hybridization Buffer (NEN) were pipetted underneath

slide cover slips. Overnight hybridization was performed in a microarray hybridization cassette from Corning (Corning, NY) at 65°C. After three consecutive washes at room temperature in 0.5X SSC/0.01% SDS, 0.06X SSC/0.01% SDS, and 0.06X SSC, respectively, the glass slide was placed in a 50 mL polypropylene tube and centrifuged at 500 x g for 5 min to remove excess liquid prior to scanning. The slide was scanned in a BioChip Imager (Packard, Meriden, CT). Laser and photomultiplier tube (PMT) voltages were adjusted manually to maximize signal-to-noise. Cy3 and Cy5 signal intensities were standardized relative to one another by comparing the total signal intensities of all spots in each channel. The scanner output images were quantified using ScanAlyze (software developed by Michael Eisen, University of California at Berkeley).

Statistical analysis.

One-way ANOVA followed by Dunnett's test (*24*) was used to analyze differences between control and chemical-treated samples in saturation density, MC cloning, and tumorigenicity studies. P values < 0.05 were considered statistically significant.

Results

As and an As-containing metal mixture inhibit and MNNG enhances, malignant transformation in RHEK-1 human keratinocytes.

To analyze the effects of As, both alone and in metal mixtures, on malignant transformation we used the virally-immortalized human epidermal keratinocyte cell line, RHEK-1. To carry out this analysis, RHEK-1 cells were treated chronically with low levels of either As or a mixture of As, Cd, Cr, and Pb; this scenario was chosen to more closely reflect actual human exposures. For comparison, we also treated RHEK-1 with MNNG, a potent carcinogen that has previously been shown to malignantly transform this cell type.

With continued culture after chemical treatment, we were able to observe substantial changes in morphology in our RHEK-1 populations; however, these alterations were not the same in all cultures and were not consistently associated with malignant transformation. Solvent control RHEK-1 cells underwent substantial morphological changes with increasing time in culture, becoming very pleiomorphic with distinctive nests of cobblestone-like cells surrounded by spindlier, elongated layers of cells. It was noteworthy, however, that at approximately passage 13, RHEK-1 cells treated with both the low and high concentrations of MNNG began to develop foci of piled cells from which round cells were continually being released; these alterations were similar to those previously described by Rhim *et al.* (*21-23*) and were not present in the corresponding DMSO-treated OM1 cells. With continued subculturing, in populations treated with 0.1 μg/ml MNNG, these foci began to dominate the entire flask. By passage 16, these latter cultures consisted of substantially larger cells that were relatively

homogeneous in size and shape: this line was named OM3. Cultures treated with 0.01 μg/ml MNNG (OM2) also began to pile up in foci; however, the cells in these cultures remained small, similar to the control cells. The situation with the As- and metal mixture-treated populations was very different from that with MNNG. After undergoing chronic, long-term exposure to either As or the metal mixture, populations became increasingly uniform, both in size and morphology, as compared to the water control cultures. The cells in the As- and mixture-treated cultures were flat and had a regular polygonal epithelial appearance. This effect was dose-dependent for both As and the mixture. In addition, these cultures had no piling or rounded cells as seen with the MNNG treated populations.

At passage 4 after treatment, all cultures were analyzed biweekly for their ability to grow in semi-solid medium, that is, in an anchorage-independent manner. As early as passage 11, OM3 gained the AIG+ phenotype (Table 3.1). The cloning efficiency of OM3 at passage 11 averaged 0.34%, as compared to 0.02% in control OM1. While working with RHEK-1, we have observed that these cells spontaneously become less dependent on adherence for growth with increasing time in culture. After 25 passages, we noted an increase in the AIG of OM1; these cells formed colonies with an efficiency of 2.1% in MC. However, at this same passage 25, MC cloning ability in OM3 was approximately 19%. OM2 did not, at any time tested, exhibit a significantly higher cloning efficiency than OM1. In contrast to previous findings (*23*), treatment of RHEK-1 with the lower concentration of MNNG, 0.01 μg/ml, did not detectably affect the malignant behavior of the cells during the time course of our studies.

Table 3.1. Anchorage-independent growth of chemically treated human RHEK-1 keratinocytes.

Treatment Group	*Time in Culture*		
	p11	p16	p25
OM1 (DMSO Control)	0.02 ± 0.006	0.05 ± 0.04	2.1 ± 0.21
OM2 (0.01 μg/ml MNNG)	0.03 ± 0.006	0.06 ± 0.02	3.2 ± 0.67
OM3 (0.1 μg/ml MNNG)	0.34 ± 0.04*	1.60 ± 0.22*	18.9± 0.66*
As-Control (Water)	1.40 ± 0.05	1.46 ± 0.04	2.45 ± 0.03
As-Low (9 ppb)	1.41 ± 0.03	1.40 ± 0.05	2.11 ± 0.02*
As-Med (11 ppb)	0.73 ± 0.01*	1.17 ± 0.04*	ND
As-High (14 ppb)	0.95 ± 0.04*	0.77 ± 0.05*	2.39 ± 0.03
Mixture-Control (Water)	1.86 ± 0.006	2.63 ± 0.13	2.67 ± 0.10
Mix-Low (LD_1)	1.42 ± 0.04*	1.49 ± 0.05*	2.51 ± 0.08
Mix-High (LD_{10})	0.38 ± 0.03*	0.98 ± 0.06*	2.06 ± 0.04*

MC cloning assay was carried out as described in Materials and Methods. Values in MC colony formation study are expressed as % mean ± SE (n = 3). *: significantly different from control using One-way ANOVA followed by Dunnett's test, $p < 0.05$
ND: Not determined

In contrast to what was observed with MNNG-treated cells. As-High and Mix-High cultures did not exhibit increased AIG as compared to water controls at any passage or under any condition examined in our studies. However. spontaneous progression in water control RHEK-1 cells was quite rapid. even as compared to the progression observed in OM1: by passage 11. the As- and Mix-water controls exhibited AIG+ growth of 1.4-1.9%. By passage 16. these controls formed colonies in MC with efficiencies of 1.46 and 2.63%. respectively. Through passage 16. chronic treatment of RHEK-1 cells with As or the metal mixture acted in a dose-dependent manner to partially inhibit this spontaneous acquisition of AIG+ in RHEK-1. By passage 25. however. AIG+ in As-High and Mix-High were very similar to water control cultures. The results of this analysis are shown in Table 1.

Increased saturation density may be another characteristic of malignant transformation. Thus. we measured the saturation density of OM1. OM2. OM3. As-High. Mix-High. and the water controls (Table 3.2). Interestingly. and unexpectedly. when assayed at passage 16. OM3 showed decreased saturation density as compared to OM1: the maximum cell densities reached in these cultures were 5.7 and 3.2 x 10^5 cells per cm^2 for OM1 and OM3. respectively. OM2 did exhibit significantly increased saturation density as compared to both OM1 and OM3: this phenotypic change is likely related to the smaller size of OM2 cells (especially as compared to OM3) and not to malignant transformation. We also observed lower saturation density in RHEK-1 populations treated with the high concentrations of As and the metal-mixture as compared to controls: the ratios of the maximum cell density in these cultures was 4.2/6.2 and 2.9/4.0 for As-High and Mix-High versus the water controls. respectively.

Table 3.2. Saturation density of chemically treated RHEK-1 cultures.

Treatment Group	*Saturation density* (x 10^5/cm^2)
OM1 (DMSO Control)	5.7 ± 0.06
OM2 (0.01 µg/ml MNNG)	6.7 ± 0.06*
OM3 (0.1 µg/ml MNNG)	3.2 ± 0.09*
As-Control (Water)	6.2 ± 0.09
As-Low (9 ppb)	4.5 ± 0.08*
As-Med (11 ppb)	4.6 ± 0.15*
As-High (14 ppb)	4.2 ± 0.07*
Mixture-Control (Water)	4.0 ± 0.05
Mix-Low (LD_1)	3.1 ± 0.17*
Mix-High (LD_{10})	2.9 ± 0.06*

Experiments conducted with passage 16 cells. Saturation density analysis was carried out as described in Materials and Methods.
Values in saturation density are expressed as mean ± SE (n = 3).
*: significantly different from control using One-way ANOVA followed by Dunnett's test, $p < 0.05$

To test the tumorigenic potential of the chemically-treated RHEK-1 cells. Balb/c nu/nu mice were utilized. After subcutaneous injection of the control and treated cell populations into immunocompromised mice. several cultures rapidly (within three weeks) and consistently formed large dorsal tumors (Table 3.3). At passage 16. OM3 formed tumors in all injected mice in three weeks. Tumors formed in mice by passage 25 OM3 cells were significantly larger: the average sizes of the resulting tumors from these time points were 6.6 mm and 10.7 mm. respectively. At three weeks. in mice injected with passage 16 OM1 no tumors were observed: however when OM1 was cultured through 25 passages prior to being tested for tumorigenicity. the results were somewhat different. These passage 25 cells had progressed to the point where they formed small (2.4 mm average tumors in 3/10 mice) tumors by three weeks after injection. In both passage 16 and passage 25 OM1 by three months after injection. tumors of approximately 6-7 mm were observed in recipient mice. again supporting the hypothesis that RHEK-1 spontaneously progresses to a low level malignancy with continued time in culture. Observations from our studies on As and the metal mixture treated cultures were not highly surprising. given the MC cloning results described above. Neither As-High nor Mix-High cells were tumorigenic under these conditions. even at passage 25. where they had acquired the ability to grow in an anchorage-independent manner. In contrast. by three weeks. both water control cell populations formed tumors in a portion of injected mice: cells treated with the lower concentrations of As and the metal mixture also were tumorigenic (Table 3.3). Histopathological exam of excised tumors from each culture demonstrated that they were all poorly differentiated squamous cell carcinomas.

Table 3.3. Tumorigenicity of MNNG-, As-, and metal mixture-treated RHEK-1 cells.

Treatment group	*No. with tumors/ no. inoculated at week 3*	*Average tumor size of existing tumors at week 3* (mm)[a]
p16 OM1 (DMSO control)	0/10	0
p16 OM3 (0.1μg/ml MNNG)	10/10	6.6 ± 0.4*
p25 OM1 (DMSO control)	3/10	2.4 ± 0.3
p25 OM3 (0.1μg/ml MNNG)	10/10	10.7 ± 0.4 *
p25 As-Control (Water)	7/10	3.6 ± 0.4
p25 As-Low (9 ppb)	4/10	4.0 ± 0.4
p25 As-High (14 ppb)	1/10	1.3 ± 0.7
p25 Mixture-Control (Water)	9/10	5.2 ± 0.6
p25 Mix-Low (LD_1)	9/10	5.0 ± 0.6
p25 Mix-High (LD_{10})	2/10	2.2 ± 0.2*

The tumorigenicity assay was performed three times as described in Materials and Methods. Data were pooled and represented as mean number or size of all measurable tumors.

[a] Tumor size was expressed as mean ± SE (n = 10)

*: significantly different from corresponding control using One-way ANOVA followed by Dunnett's test, $p < 0.05$

Chromosome painting and karyotypic analysis confirmed that these tumors arose from the parental RHEK-1.

Analysis of changes in gene expression that arise during treatment of RHEK-1 with MNNG, As or the four-metal mixture.

We were interested in characterizing changes in gene expression that may be involved in mediating the different outcomes after treatment of RHEK-1 cells with MNNG, As, or the mixture of As, Cd, Cr, and Pb. To explore this issue, we have begun to use cDNA microarray technology to identify mRNA species that are over- or under-expressed in chemically-treated versus control cells. Our first observation from this analysis was that the patterns of gene expression in the treated cultures were unique, being distinct from both their respective controls and from cells that were exposed to different chemicals (Tables 3.4, 3.5, and 3.6). Among the three chemically-treated cell populations, OM3 showed the most numerous alterations in gene expression (Table 3.4). Not only did we use an additional array for studying OM1 and OM3, but this finding may also be attributed in part to the fact that MNNG is a very effective DNA damaging agent and mutagen, and likely has genome-wide effects. In all, 72 and 41 genes represented on the combined arrays were induced and suppressed, respectively in OM3 compared to OM1. In As-High, a total of 52 genes were altered in their expression as compared to the water-treated control; of these, 23 showed increased and 29 showed decreased expression (Table 3.5). Lastly, 13 genes were induced in the Mix-High populations and 51 were suppressed (Table 3.6). A comprehensive list of genes induced or suppressed under each

Table 3.4. Alterations in gene expression detected by microarray analysis of MNNG-treated RHEK-1 cells.

Induction (total 72)				
GenBank#	Name	Function	Array[a]	Fold[b]
M74088	Adenomatous polyposis coli protein (APC protein)	Tumor marker	1	4
S83171	BCL-2 binding athanogene-1 (BAG-1); glucocorticoid receptor-associated protein RAP46	Steroid receptor	1	>100
U43746	BRCA2	Zinc finger domain	1	3
X66141	Cardiac ventricular myosin light chain 2	Filament	1	>100
U28014	Caspase-4 precursor	Apoptosis	1	5
AF011792	Cell cycle progression 2 protein	Cell cycle regulation	1	3
X66364	Cell division protein kinase 5	Cell cycle regulation	1	3
L31951	C-jun N-termial kinase 2 (JNK2)	Transcription regulation	1	49
U43901	Colon carcinoma laminin-binding protein	Cancer marker	1	4
U11791	Cyclin H	Cell cycle regulation	1	5
J04164	Interferon-inducible protein 9-27	Cell growth regulation	1	61
AF019770	Macrophage inhibitory cytokine 1 (MIC1)	TGFβ superfamily	1	7
M28882	Melanoma-associated antigen A32; cell surface glycoprotein MUC 18	Tumor marker	1	12
J02958	Met proto-oncogene; hepatocyte growth factor receptor precursor	Protein tyrosine kinase	1	3
U39050	Mitogen-responsive phosphoprotein DOC2	Tumor suppressor from ovarian carcinoma cells	1	36
Y10313	Nerve growth factor (NGF)-inducible PC4 homolog	GF	1	6
U48296	PTPCAAX1 nuclear tyrosine phosphatase PRL-1	Nuclear phosphatase	1	4
X85134	RBQ-3	RB protein binding protein	1	36
X63679	TRAM protein	ER protein involved early in polypeptide translocation	1	4
X87852	Transmembrane protein sex precursor	Homology to cMET; a novel transmembrane protein	1	3
X56134	Vimentin	Intermediate filament	1	3
S65738	Actin depolymerizing factor	Actin depolymerization	2	4
U29344	Breast carcinoma fatty acid synthase	Involvement in breast carcinoma	2	3
M33011	(Clone GA733-2-2) carcinoma-associated antigen GA733-2	Cancer antigen from colorectal and pancreatic carcinoma	2	2
U66838	Cyclin A1	Cell cycle regulation	2	5
L37385	Homolog of mouse MAT-1 oncogene	Expression in breast cancer cells	2	3
J02854	Human 20-kDa myosin light chain (MLC) 2 mRNA	Smooth muscle and nonmuscle cell contractile activity	2	5
AF027205	Kunitz-type protease inhibitor	Protease inhibitor	2	3

(continued)

Table 3.4. continued

GenBank#	Name	Function	Array[a]	Fold[b]
X04741	mRNA for protein gene product 9.5	A novel cytoplasmic neuroendocrine marker protein	2	3
D78130	mRNA for squalene epoxidase	Metabolism	2	3
X56160	mRNA for tenascin	Extracellular matrix protein	2	3
X00699	mRNA fragment for class II histocompatibility antigen β-chain (pII-β-3)	Histocompatibility antigen	2	5
M13656	Plasma protease inhibitor	Protease inhibitor	2	2
U41303	Small nuclear ribonuleoprotein particle N	Pre-mRNA splicing	2	5
AF009615	ADAM10	Pro-tumor necrosis factor α processing enzyme	3	2
M32325	Adenocarcinoma-associated antigen (KSA)	Lung cell surface glycoprotein	3	3
X66087	A-myb mRNA	Nuclear protein, transcription factor (TF)	3	13
U74611	Apo-3	TNF receptor family	3	3
U14680	BRCA1	Zinc finger domain	3	3
X06182	C-kit proto-oncogene mRNA	A new cell surface receptor tyrosine kinase	3	6
M12783	C-sis platelet-derived growth factor 2 (SIS PDGF2)	Proto-oncogene	3	3
M14333	C-syn protooncogene	Protein tyrosine kinase family	3	2
X64229	Dek mRNA	Putative oncogene: gene translocation in acute myeloid leukemia	3	3
U77085	Epithelial membrane protein	Squamous cell associated gene	3	3
J04101	Erythroblastosis virus oncogene homolog 1 (ets-1)	Proto-oncogene: TF	3	3
S82592	Evi-1, Evi-1 protein	TF: overexpression in myeloid leukemia	3	4
M64240	Helix-loop-helix zipper protein (max)	TF: complex with myc	3	3
O04045	hMSH2	Human mismatch repair gene	3	3
U37547	IAP homolog B	Apoptosis inhibitory protein	3	4
U62962	Int-6	GF-like proto-oncogene	3	3
AF042857	Lung cancer antigen NY-LU-12 variant A	Nuclear zinc finger protein	3	3
Y18046	mRNA for FOP	FGFR1 oncogene partner	3	3
D63874	mRNA for HMG-1	Malignant transformation in gastrointestinal adenocarcinoma	3	2
X07876	mRNA for irp protein	GF-like proto-oncogene	3	3
Z36715	mRNA for Net transcription factor	A new ets TF that is activated by Ras	3	10
X03541	mRNA of trk oncogene	Tyrosine kinase: a transforming gene in a human colon carcinoma	3	3

(continued)

Table 3.4. continued				
GenBank#	Name	Function	Array[a]	Fold[b]
M92424	p53-associated mRNA	p53 associated gene in human sarcomas	3	2
K03199	p53 cellular tumor antigen	Tumor antigen from human vulva carcinoma cell line	3	2
L78132	Prostate carcinoma tumor antigen	Tumorigenesis and metastasis	3	2
Y00705	PstI mRNA for pancreatic secretory inhibitor (expressed in neoplastic tissue)	Trypsin inhibitor in cancer	3	5
L07868	Receptor tyrosine kinase (ERBB4) gene	EGF receptor family	3	3
U16296	T-lymphoma invasion and metastasis inducing TIAM1 protein	Found in virtually all analysed tumor cell lines of human origin	3	3
X15187	Tra1 mRNA forhomologue of murine tumor rejection antigen gp96	Cell surface glycoprotein	3	3
M76125	Tyrosine kinase receptor (axl)	A transforming gene	3	4
M18391	Tyrosine kinase receptor (eph)	Overexpression in several human carcinomas	3	3
M11730	Tyrosine kinase-type receptor (HER2)	Oncogene	3	3
V00572	mRNA encoding phosphoglycerate kinase	Kinase	4	2
AB011406	mRNA for alkalin phosphatase	Phosphatase	4	3
X04790	mRNA for A-raf-1 oncogene	Downstream signal molecule for Ras signal transduction	4	2
X75756	mRNA for protein kinase C (PKC) μ	Kinase	4	2
X52192	RNA for c-fes	Oncogene; protein tyrosine kinase	4	4
X59727	63 kDa protein kinase related to rat ERK3	MAP kinase signaling	4	9
Suppression (total 41)				
L22253	Arginine serine-rich splicing factor 7	mRNA splicing	1	3
U78095	Bikunin	Hepatocyte GF activator inhibitor 2	1	2
L34060	Cadherin 8	Cell differentiation	1	>100
M36067	DNA ligase I	DNA replication	1	3
X16707	Fos-related antigen (FRA1)	AP1	1	5
U34683	Glutathione synthase (GSH synthase)	Cell protection	1	2
L07515	Heterochromatin protein homolog 1	Chromatin stucture	1	13
X62534	High mobility group protein 2	Malignant transformation	1	4
X67081	Histone H4	Chromosome structure	1	4
U12255	IgG receptor FC large subunit P51 precursor	Immunoglobulin structure	1	3
X53587	Integrin β4	Cell differentiation	1	6
D21063	MCM2 DNA replication licensing factor	Nuclear protein	1	3
X74794	MCM4 DNA replication licensing factor	Nuclear protein	1	3
U77604	Microsomal glutathione S-transferase (GST) II	Cell protection	1	4
M15796	Proliferating cell nuclear antigen (PCNA)	Cell cycle regulation	1	3
J03040	Secreted protein acidic and rich in cysteine precursor	Secretory protein	1	4

(continued)

Table 3.4. continued				
GenBank#	Name	Function	Array[a]	Fold[b]
D21235	UV excision repair protein RAD23A	DNA repair	1	3
L47647	Creatine kinase B	Kinase	2	7
S78986	Id1 (Id1-a)	Inhibit transcription by forming inactive heterodimer	2	7
U68018	Mad protein homolog (hMAD-2)	Downstream molecule in TGF β receptor activation	2	3
X62570	mRNA for IFP53	IFN-inducible protein	2	9
X62571	mRNA for keratin-related protein	Cell differentiation	2	3
X71635	mRNA for neuropeptide Y-like receptor	G protein coupled receptor	2	5
AJ222700	mRNA for TSC-22 protein	TGF β-stimulated clone 22: apoptosis	2	4
U51478	Sodium/potassium-transporting ATPase β3 subunit	Ion transporter	2	5
AF007165	Suppressin	A novel suppressor of cell cycle entry	2	3
U49436	Translation initiation factor 5	Gene transcription translation	2	5
L25610	Cyclin-dependent kinase inhibitor: p21CIP1	Cdk-interacting protein	3	6
AF027964	MAD-related protein Smad2	Downstream molecule in TGF β receptor activation	3	4
D28124	mRNA for unknown product: putative neuroblastoma tumor suppressor gene	Putative tumor suppressor	3	2
U46691	Putative chromatin structure regulator	Transcriptional regulation	3	2
AF040704	Putative tumor suppressor protein 101F6	Putative tumor suppressor	3	2
AF060228	Retinoic acid receptor responder 3 (RARRES3)	Retinoid-induced class II tumor suppressor	3	7
X75208	HEK2 mRNA for protein tyrosine kinase receptor	Protein tyrosine kinase receptor	4	3
AB006757	mRNA for PCDH7	Metastasis inhibitor	4	5
U48959	MLC kinase	Kinase	4	4
M34668	Protein tyrosine phosphatase (PTPase-α) mRNA	Phosphatase	4	2
U40317	Protein tyrosine phosphatase (PTPase-σ)	Phosphatase	4	2
X62055	PTP1C mRNA for protein-tyrosine phosphatase 1C	Phosphatase	4	2
L09247	Receptor-type protein tyrosine phosphatase γ	Phosphatase	4	2
AF099989	Ste-20 related kinase SPAK	Kinase	4	2

Table 3.5. Alterations in gene expression detected by microarray analysis of As-treated RHEK-1 cells.

Induction (total 23)				
GenBank#	Name	Function	Array[a]	Fold[b]
M63959	α-2-macroglobulin receptor-associated protein precursor (α-2-MRAP)	Human homologue of a Heymann nephritis antigen	1	2
D30751	Bone morphogenetic protein 4 (BMP4)	Production of skeletal structure during development: TGF β family	1	5
L27211	Cyclin-dependent kinase 4 inhibitor (CDK4I): multiple tumor suppressor 1 (MTS1): p16-INK4	Cell cycle regulation	1	2
U07418	DNA mismatch repair protein MLH1: COCA2	DNA repair	1	4
M36089	DNA-repair protein XRCC1	DNA repair	1	4
X52541	Early growth response protein 1 (hEGR1)	TF	1	2
X79067	EGF response factor 1	Early response gene	1	6
U79718	Endonuclease III homolog 1 (HNTH1)	DNA repair	1	2
X16707	FRA1	AP1	1	3
M29039	Jun-B	AP1	1	3
M15796	PCNA	Cell cycle regulation	1	3
D21235	UV excision repair protein RAD23A	DNA repair	1	6
S79639	EXT1, putative tumor suppressor hereditary multiple exostoses candidate gene	Putative tumor suppressor	2	3
M96803	General β-spectrin	Membrane skeleton protein	2	3
U40992	Heat shock protein (hsp) 40 homolog	Cell protection	2	3
X95425	mRNA for EHK-1 receptor tyrosine kinase	Receptor tyrosine kinase: formation of neuronal pathway	2	4
AB000220	mRNA for semaphorin E	Non-MDR drug resistance gene	2	5
U14394	Tissue inhibitor of metalloproteinases-3 (TIMP-3)	Metalloprotease inhibitor	2	9
M19154	Transforming growth factor β2	TGFβ superfamily	2	3
M95787	22kDa smooth muscle protein	Structural protein	2	3
L04288	Cyclophilin-related protein	Function of natural killer cells	3	3
M98833	ERGB transcription factor: FLI-1 homolog	A new ETS TF	3	6
AF061836	Putative tumor suppressor protein RDA32	Putative tumor suppressor	3	6
Suppression (total 29)				
U78095	Bikunin	HGF activator inhibitor	1	7
M34225	Cytokeratin 8 (K8)	Cell differentiation	1	3
M26326	Cytokeratin 18 (K18)	Cell differentiation	1	3
K00065	Cytosolic superoxide dismutase 1 (SOD1)	Cell protection	1	4
U34683	GSH synthase	Cell protection	1	7
U90313	GST homolog	Cell protection	1	3
AF019770	MIC1	TGF β superfamily	1	35

(continued)

Table 3.5. continued				
GenBank#	Name	Function	Array[a]	Fold[b]
L33930	CD24 signal transducer and 3' region	A potential early tumor marker in human hepatocellular carcinoma	2	18
M77830	Desmoplakin I	Cell surface attachment site for cytoplasmic intermediate filaments	2	8
M20681	Glucose transporter-like protein-III (GLUT3)	Expression in fetal skeletal muscle	2	3
AB000712	hCPE-R mRNA for CPE-receptor	Clostridium perfringens enterotoxin receptor	2	6
X58072	hGATA3 mRNA for trans-acting T-cell specific transcription factor	TF	2	6
L42611	Keratin 6 isoform (K6e)	Cell differentiation	2	3
M26512	Keratin 8 mRNA, 5' end	Cell differentiation	2	4
M21389	Keratin type II (58 kD)	Cell differentiation	2	3
X52426	mRNA for cytokeratin 13	Cell differentiation	2	5
X00497	mRNA for HLA-DR antigens associated invariant chain p33	Transmembrane polarity	2	10
X06990	mRNA for intercellular adhesion molecule (ICAM)-1	Cell adhesion molecule	2	2
X69549	mRNA for rho GDP-dissociation inhibitor 2	Inhibit GTP binding; disruption of actin cytoskeleton	2	3
L41351	Prostasin	Prostate-specific marker	2	5
L33404	Stratum corneum chymotryptic enzyme	Serine protease	2	15
M73554	Bcl-1	Anti-apoptosis	3	3
U66894	Epithelium-restricted Ets protein ESX	Oncogene; TF	3	4
X51602	Flt mRNA for receptor-related tyrosine kinase	Fms-related tyrosine kinase	3	6
M32325	KSA	Lung cell surface glycoprotein	3	4
Z13009	mRNA for E-cadherin	Invasion suppressor; Ca dependent cell adhesion molecule	3	6
AF060228	RARRES3	Retinoid-induced class II tumor suppressor	3	4
AF070675	TNF-inducible protein CG12-1	Vascular endothelial gene	3	4
M90657	Tumor antigen L6	Tumor-associated cell surface antigen	3	3

Table 3.6. Alterations in gene expression detected by microarray analysis of mixture-treated RHEK-1 cells.

GenBank#	Name	Function	Array[a]	Fold[b]
Induction (total 13)				
M63959	α-2-MRAP	Human homologue of a Heymann nephritis antigen	1	3
D30751	BMP 4	TGF β family	1	4
U60519	Caspase-10 precursor	Apoptosis	1	4
M34570	Collagen 6 α 2 subunit	Structural protein	1	5
U79718	HNTH1	DNA repair	1	2
X16707	FRA1	AP1	1	4
D13365	Growth inhibitory factor: metallothionein-III (MT-III)	Cell growth regulation	1	3
X53587	Integrin β4	Cell differentiation	1	2
M29039	Jun-B	AP1	1	2
L27211	MTS1: CDK4I: p16-INK4	Cell cycle regulation	1	3
U90551	Histone 2A-like protein	Nuclear protein	2	3
X76717	MT-II mRNA	Cell protection	2	3
L31881	Nuclear factor I-X	Interference with transcriptional activation	2	3
Suppression (total 51)				
S83171	BAG-1	Steroid receptor	1	8
U09579	Cyclin-dependent kinase inhibitor 1: WAF1 CIP1	Cell cycle regulation	1	6
X52221	DNA excision repair protein ERCC2	DNA repair	1	11
L20046	DNA excision repair protein ERCC5	DNA repair	1	2
U04045	DNA mismatch repair protein MSH2	DNA repair	1	4
U39657	Dual-specificity mitogen-activated protein kinase kinase 6 (MAPKK 6)	MAP kinase signaling	1	23
U51166	G/T mismatch-specific thymine DNA glycosylase (TDG)	DNA repair	1	2
L31951	JNK2	Transcription regulation	1	3
AF019770	MIC1	TGF β superfamily	1	7
U53446	Mitogen-responsive phosphoprotein DOC2	Tumor suppressor from ovarian carcinoma cells	1	4
U48296	PTPCAAX1 nuclear tyrosine phosphatase PRL-1	Nuclear phosphatase	1	8
K00065	SOD1	Cell protection	1	3
X85960	Trk-T3 oncoprotein	Oncogene: tyrosine kinase	1	6
X56134	Vimentin	Intermediate filament	1	4
AF047347	Adaptor protein X11α	Slows cellular amyloid precursor protein processing and reduces Aβ40 and Aβ42 secretion	2	4
M22489	BMP-2A	TGF β family	2	6
L47647	Creatine kinase B	Kinase	2	5
M14780	Creatine kinase M	Kinase	2	5
M81635	Erythrocyte membrane protein	Cation transporter inhibitor	2	4

(continued)

Table 3.6. continued				
GenBank#	Name	Function	Array[a]	Fold[b]
M20681	GLUT3	Expression in fetal skeletal muscle	2	19
M97796	Helix-loop-helix protein Id-2	Nuclear protein: expression in early development	2	3
X77278	HYL tyrosine kinase mRNA	Nonreceptor protein tyrosine kinase	2	3
S78986	Id1; Id1-a	transcription regulator: helix-loop-helix protein	2	6
X04076	Kidney mRNA for catalase	Cell protection	2	4
X95425	mRNA for EHK-1 receptor tyrosine kinase	Formation of neuronal pathway	2	3
D87811	mRNA for GATA-6	TF	2	4
X71635	mRNA for neuropeptide Y-like receptor	G protein coupled receptor	2	9
Y10032	mRNA for putative serine/threonine protein kinase	Kinase	2	4
X92494	mRNA for STM-7 protein	A novel phosphatidyl inosine-4-phosphate-5-kinase	2	5
S75725	Prostacyclin-stimulating factor	PGI2 stimulating factor from fibroblast cells	2	6
X59727	63 kDa protein kinase related to rat ERK3	MAP kinase signaling	2	4
U49857	Transcriptional activator	Nuclear protein	2	3
M19154	Transforming growth factor β2	TGF β superfamily	2	4
M90657	Tumor antigen L6	Tumor associated cell surface antigen	2	15
U57059	Apo-2 ligand	TNF receptor family	3	7
K01884	Blym-1 transforming gene	Transforming gene	3	6
M62397	Colorectal mutant cancer protein.	Cancer marker	3	5
J03639	DBL oncogene encoding a transforming protein	Transforming oncogene	3	28
M34309	Epidermal growth factor receptor	GF receptor	3	3
Y00664	Germ line n-myc gene	TF	3	8
M16591	Hemopoietic cell protein-tyrosine kinase gene (HCK), clone λ-a2/1a	Protein tyrosine kinase	3	5
X03072	Int-1 mammary oncogene	GF-like proto-oncogene	3	5
X07384	mRNA for GLI protein	Oncogene: zinc finger protein	3	5
X87241	mRNA for hFat protein	Cadherin superfamily	3	4
X07876	mRNA for irp protein	GF-like proto-oncogene	3	4
Y00705	PstI mRNA for pancreatic secretory inhibitor	Trypsin inhibitor in cancer	3	4
AF069072	Putative lung tumor suppressor DAL1	Putative tumor suppressor	3	10
AF060228	RARRES 3	Retinoid-induced class II tumor suppressor	3	6
M57464	Ret proto-oncogene	Oncogene: tyrosine kinase	3	7
AF016028	Sarcospan-2	25kDa transmembrane component of Dystrophin glycoprotein complex	3	3
M55994	Tumor necrosis factor receptor II (TNFrII)	TNF receptor family	3	8

Table legends for Tables 3.4, 3.5, and 3.6

Microarray analysis was carried out using the Clontech Cancer 1.2. NEN Human 2400. and NEN Oncogene/Tumor Suppressor arrays for all samples as described in Materials and Methods. NEN Kinase/Phosphatase array was analyzed for MNNG-treated cells only.

[a] 1. Clontech Cancer 1.2: 2. NEN Human 2400: 3. NEN Oncogene/Tumor Suppressor: 4. NEN Kinase/Phosphatase array

[b] Values are represented as mean from 2 experiments for Array 2. 3. and 4 in chemically-treated cell population.

exposure scenario, along with their assigned (putative) function is shown in Tables 3.4-3.6.

Among the genes showing increased expression in OM3 as compared to the control population, OM1, were many that could potentially have impacts on cell proliferation, including: 1) cell cycle regulators (RBQ-3, cyclins H and A1, and CDK5); 2) growth factors (int-6, irp and PDGF2); and 3) oncogenes, several of which are involved in the MAP kinase signaling pathways including an Erk-3-related protein, JNK-2, PKCμ, A-raf-1, and Net (Table 3.4). Additionally, genes encoding proteins that modulate cell-cell or cell-matrix interactions were also induced; among these genes were macrophage inhibitory cytokine-MIC1, nerve growth factor-inducible PC4 homolog, and several protease inhibitors. Increased expression of several tumor associated markers such as melanoma (A32)- and prostate carcinoma-associated antigens and the APC protein was consistent with the malignant phenotype of OM3. Lastly, several proteins involved in DNA damage response and/or apoptosis, including p53-associated protein and caspase 4 were expressed at higher levels in the transformed line.

There were substantially fewer genes with decreased expression in OM3 as compared to OM1 (Table 3.4). Among these genes were representatives from several functional categories. Particularly striking were repressions in: 1) multiple protein tyrosine phosphatases, including PTP1C, PTPα, PTPσ, and receptor-type protein tyrosine phosphatase γ; 2) cell protective mechanisms such as the UV excision repair protein, RAD23A, glutathione synthase, and glutathione-S-transferase; and 3) integrin β4, cadherin 8, and a keratin-related protein. Additionally, several putative inhibitors of

transformation and metastasis such as RARRES3. suppressin. tumor suppressor protein 101F6. and PCDH7 exhibited decreased expression in OM3.

In our studies. there were several noteworthy genes/gene families that were altered in their expression in As-treated cells (Table 3.5). In these populations. the most striking induction was seen in DNA damage response genes. including XRCC1. RAD23A. endonuclease III homolog 1 (HNTH1). DNA repair protein MLH1. and an hsp40 homolog. Among other representative inductions were genes involved in cell cycle regulation (jun-B. FRA-1. MTS1/p16-INK4. PCNA. early growth response protein 1): oncogenes (EHK-1 receptor tyrosine kinase): two putative tumor suppressor genes (EXT1 and RDA32): and proteins regulating invasion and/or cell-cell interactions. BMP4 and TIMP-3. Genes suppressed in As-treated populations included cytoprotective molecules (cytosolic SOD. glutathione synthetase. and glutathione-S-transferase). ICAM-1. stratum corneum chymotryptic enzyme. MIC1. and bikunin. In our studies. treatment with As also was observed to inhibit expression of a variety of cytokeratins. including 6E. 8. 13. 18 and an unidentified 58 kD type II protein.

The metal mixture treated populations had a somewhat different spectrum of gene alterations than did cells exposed to As alone (Table 3.6). Relatively few genes showed increased expression under this exposure scenario. Genes involved in cell cycle regulation that were induced included: jun-B. MTS1/p16-INK4. FRA1. and nuclear factor 1-X. DNA damage response/cytoprotective/apoptosis mechanisms induced included multiple metallothioneins. caspase 10. and HNTH1. Also induced under these conditions were integrin β4 and BMP4. In contrast. many genes were repressed by metal mixture treatment as compared to control. Cell cycle regulatory proteins and cytokines showing decreased

expression included WAF1/CIP1. MAPKK6. GATA6. JNK2. TGFβ2. and mitogen-responsive phosphoprotein DOC2. Many oncogenes were suppressed including int-1. Ret. Blym-1. n-myc. DBL. and the EHK-1 receptor tyrosine kinase. Among the DNA damage response/cytoprotective/apoptosis genes showing decreased expression were ERCC2. ERCC5. MSH2. TDG. cytosolic SOD. and catalase. Many additional kinases/phosphatases were altered in their expression. including an ERK3-related protein kinase. HCK. several creatine kinases. HYL and PRL-1.

Detailed analysis of data from OM3. As-High. and Mix-High demonstrated that. in addition to numerous chemical-specific gene changes. several genes were altered in a similar or opposite manner under the different exposure conditions (Table 3.7). There were no genes commonly induced by MNNG and As or the metal mixture. although RARRES3 (a retenoid-induced tumor suppressor) was suppressed under all three treatment conditions. As and metal mixture treatment did increase expression of a common group of genes including JunB. FRA1. MTS1. and a member of the TGFβ family. BMP4 (*25;26*). These two exposures also commonly suppressed expression of tumor antigen L6. SOD1. and MIC1. another member of the TGFβ family. Interestingly. the largest group of genes were those oppositely regulated by MNNG and the metal mixture. among which were JNK2. ERK3. nuclear phosphatase PRL-1. an unidentified Ser/Thr protein kinase. integrin β4. and vimentin.

Table 3.7. Genes altered in their expression by multiple chemical treatments.

Genes Commonly Induced by:			
As/Mix/MNNG	**As/MNNG**	**Mix/MNNG**	**As/Mix**
			JunB FRA1 MTS1 Endonuclease III homolog 1 (HNTH1) BMP4 α-2-MRAP
Genes Commonly Suppressed by:			
As/Mix/MNNG	**As/MNNG**	**Mix/MNNG**	**As/Mix**
RARRES3	GSH synthase Bikunin	Creatine kinase B Id1-a mRNA for neuropeptide Y-like receptor	Tumor antigen L6 SOD1 MIC1 GLUT3
Opposite Regulation by:			
As/Mix/MNNG	**As/MNNG**	**Mix/MNNG**	**As/Mix**
MIC1 (⇓⇓⇑) FRA1 (⇑⇑⇓)	KSA (⇓⇑) RAD23A (⇑⇓) PCNA (⇑⇓)	JNK2 (⇓⇑) ERK3 (⇓⇑) DOC2 (⇓⇑) Nuclear tyrosine phosphatase (PRL-1) (⇓⇑) mRNA for irp protein (⇓⇑) BAG-1 (⇓⇑) Vimentin (⇓⇑) Pancreatic secretory inhibitor (⇓⇑) Integrin β4 (⇑⇓)	TGFβ2 (⇑⇓) mRNA for EHK-1 receptor tyrosine kinase (⇑⇓)

Discussion

In order to develop more efficient methodologies for evaluating carcinogenic potentials for environmentally relevant chemicals such as As and other metals, we have attempted to identify molecular markers involved in the process of carcinogenesis in keratinocytes. In our studies, the Ad12/SV40 immortalized human epidermal keratinocyte cell line, RHEK-1, slowly and spontaneously progressed to a malignant phenotype with continued passage. Progression of RHEK-1 was enhanced greatly by treatment of the cells with the strong initiating agent, MNNG. In contrast, treatment of RHEK-1 with DMSO, As alone, or As in the presence of Cd, Cr, and Pb acted to inhibit this progression. Microarray analysis allowed us to catalogue wide-spread changes in gene expression in treated cells that may potentially correlate with these different toxicological endpoints.

Several investigators have taken advantage of the SV-40 virus in development of immortalized and/or "transformed" cell lines from normal primary tissues (*27-29*). These studies have described a variety of phenotypic changes frequently associated with expression of viral T antigens in infected cultures, including increased cloning efficiency and proliferative potential, unlimited life span in culture, and anchorage and/or growth factor-independent growth. In these studies, clones surviving "crisis" are highly variable in their growth properties initially and change fairly rapidly with increasing time in culture (*27;30*). Transformation by SV40 appears to be progressive over time, with acquisition of AIG+ and tumorigenicity occurring spontaneously in some cell lines. In our studies, RHEK-1 progressed to the AIG+ or tumorigenic phenotype at vastly different rates depending on the chemical treatment the cells received. While this phenomenon

may have been due to either genetic or epigenetic mechanisms, depending on the chemical, specific alterations in gene expression are, without doubt, involved.

In studies such as these, where large numbers of genes are identified and assignment of a mechanistic role to specific gene changes is the desired goal, it is the analysis and interpretation of data that becomes difficult. In our studies, not only do we need to compare each chemically-treated RHEK-1 line with its appropriate control, but gene expression changes in cells treated with transformation-enhancing (MNNG) versus transformation-inhibitory (As and the metal mixture) chemicals also must be compared. To further complicate the picture, it must be kept in mind that genes altered in their expression after treatment of cells with potentially carcinogenic agents likely fall into at least two categories. The first would be genes directly involved in or mediating some aspect of malignant transformation, i.e. genes whose function or lack thereof is necessary for neoplastic progression. The second group would be composed of genes that are altered as a result of cytotoxic stress on the cell and are not involved in the malignant phenotype at all. As a first approach, analysis of the known or putative functions of identified genes may yield some insight into their potential roles in the toxicological endpoint of interest, i.e. transformation or toxicity.

From the alterations in gene expression that we observed in our studies, one could formulate several interesting hypotheses concerning transformation-specific effects on RHEK-1. More rapid conversion of this keratinocyte cell line to the tumorigenic phenotype by MNNG could potentially be mediated by constitutively increased expression of growth factors and/or oncogenes such as PDGF, members of the MAP kinase signaling pathway, and/or the cyclins or cyclin-dependent kinases. Activation of

the MAP kinase pathway is the primary response to mitogenic stimuli in all cell types (*31*). Multiple genes involved in this pathway were selectively induced in MNNG-transformed cells as compared to As and Mix-treated populations. In Mix-High populations, which were non-tumorigenic, JNK2, the ERK3 homolog, and MAPKK6 demonstrated substantially decreased expression as compared to water treated controls; these findings are consistent with a role for activation of the MAP kinase pathway in progression of RHEK-1. One can also speculate that altered expression of a host of protein phosphatases in a cell, such as was observed in OM3, would have profound impacts on its proliferative potential and facilitate its ultimate transformation. Protein phosphatases are crucial players in regulation of the mitogenic cascade, among other functions, and changes in their expression have been strongly linked to carcinogenesis in many studies (*32*). As malignant transformation is a multistep, and very complex, process, it is likely that many of the alterations in gene expression that we detected (as well as others) are involved.

Rhim *et al.* and Yang *et al.* have been able to derive multiple malignant lines from RHEK-1 by treating the cells with chemicals such as MNNG, TCDD and 4NQO, exposing them to X-ray, and transfecting them with oncogenic viruses (*21-23*). In collaborative studies with these investigators, we will compare gene expression patterns in these various lines as compared to OM1 and OM3; the primary goal here would be to identify, if there is one, a common battery of genes altered during progressive transformation of RHEK-1 by multiple chemical and physical agents. Having several transformed lines with the same basic wild-type background of gene expression should greatly facilitate our identification of genes potentially involved in malignant progression

of this cell type. Our results from these studies could then be tested with other cell types transformed by various means.

Many types of studies, both epidemiological and in the laboratory, have demonstrated that most, if not all, of the metals used in our work are human carcinogens. However, in our hands, both As and the As-containing metal mixture were inhibitory to malignant progression of RHEK-1. This is not the first demonstration of an "anti-carcinogenic" effect of As; the metal has been shown to inhibit formation of GST-P positive hepatic foci in chemically-treated rats *in vivo* and is currently being used in chemotherapeutic regimens for acute promyelocytic leukemia (*33-36*). Although the mechanism of arsenic trioxide's clinical effects remain unclear, it has been shown to induce apoptosis in leukemic and lymphoid cell lines *in vitro* (*35;36*). The observed changes in gene expression following exposure to As alone were not inconsistent with an anti-carcinogenic effect and indicated that the metal generally stimulated DNA protective mechanisms in exposed cells. Particularly interesting was the strong induction of multiple DNA repair proteins, including XRCC1, HNTH1, RAD23A, and MLH1, in the As-High populations, which may be a function of the clastogenic and/or co-mutagenic effects of the metal (*37-44*). Induction by As of multiple regulators of the cell cycle (jun-B, c-fos/FRA-1, and EGR1) has also been seen in other studies where it is assumed the metal is acting to promote carcinogenesis (*45;46*). Obviously, given the complexity of the cell, it is highly likely that the carcinogenic or anti-carcinogenic effect of the metal in any one situation or cell type is dependent on batteries of genes working together, and not any single gene change. As the metal mixture also acted to inhibit transformation of RHEK-1

in our studies. common gene expression changes seen in both As-High and Mix-High cells may be important in the process and worthwhile exploring in more detail.

Alterations in gene expression that differ depending on whether As is alone or mixed with other metals are also highly interesting and may potentially help us to understand the dose-dependent metal-metal interactions we have observed in these cells in other short-term cytotoxicity studies in the lab (*11:47*). For example. in contrast to the situation in As-High. only one of the same DNA repair genes. HNTH1. was induced in cells treated with the As-containing metal mixture. despite the fact that the concentration of As was the same in both cultures. In fact. we identified four DNA repair proteins in this latter population that were suppressed. likely by one of the other metals in the mixture. In addition. two metallothionein genes showed increased expression in Mix-High. certainly a result of the presence of Cd in the mix: cells treated with As alone did not exhibit increased expression of these important cytoprotective molecules and. in fact. showed decreased GSH and GST levels. Certainly. these findings have implications for the cytotoxicity of the metals alone and together in simple or complex mixtures.

In conclusion. we have utilized DNA microarray analysis to identify changes in gene expression in the human keratinocyte cell line. RHEK-1. in response to treatment with chemicals that enhance or inhibit its spontaneous malignant transformation. Our studies have shown unique and intriguing gene expression patterns in cells treated with either As. an As-containing chemical mixture. or the potent mutagen. MNNG. Meticulous analysis of gene expression patterns in a variety of cell types. as described above. and time-wise comparison of defined changes with acquisition of transformation-associated characteristics such as AIG and tumorigenicity should allow us to identify

potential players in each step of the process of malignant conversion. In future studies, these "transformation-associated" molecular markers will be used in biologically-based dose response models to predict the carcinogenic potentials of other xenobiotics. Additionally, once we have a clear mechanistic understanding of how single carcinogenic agents work and have been able to model the process using computational techniques, chemical mixtures will be much more amenable to study. Linkage of models through common metabolic pathways and/or mechanisms of cytotoxicity will allow a more comprehensive view of the potential health/carcinogenic effects of complex chemical mixtures.

Acknowledgments

This study was supported by the Agency for Toxic Substances and Disease Registry (ATSDR) Cooperative Agreement U61/ATU881475, and the National Institute for Environmental Health Sciences (NIEHS) Superfund Basic Research Program Project P42 ES05949. We thank Ms. Maxine Hennessey at Colorado State University for her help in microarray analysis. The efforts of many colleagues at the Center for Environmental Toxicology & Technology at Colorado State University are gratefully acknowledged.

Abbreviations

AIG+: anchorage independent growth positive

As: arsenic (As^{3+})

As-Low: RHEK-1 cells chronically exposed to 9 ppb of As

As-Med: RHEK-1 cells chronically exposed to 11 ppb of As

As-High: RHEK-1 cells chronically exposed to 14 ppb of As

Cd: cadmium (Cd^{2+})

Cr: chromium (a mixture of 1:1 Cr^{3+} and Cr^{6+})

GM-CSF: granulocyte/macrophage-colony stimulating factor

MAP: mitogen activated pathway

Mix-High: RHEK-1 cells chronically exposed to concentration of LD_{10} for As. Cd. Cr. and Pb

Mix-Low: RHEK-1 cells chronically exposed to concentration of LD_1 for As. Cd. Cr. and Pb

MNNG: *N*-methyl-*N'*-nitro-*N*-nitrosoguanidine

OM1: DMSO-treated control RHEK-1 cells

OM2: 0.01 μg/ml MNNG-treated. not transformed RHEK-1 cells

OM3: 0.1 μg/ml MNNG-treated. transformed RHEK-1 cells

Pb: lead (Pb^{2+})

RHEK-1: immortalized human epithelial keratinocyte cell line

TGF-α: transforming growth factor-α

References

1. Chen C-J. Chen CW. Wu M-M. Kuo T-L. Cancer potential in liver. lung. bladder. and kidney due to ingested inorganic arsenic in drinking water. Br J Cancer 66:888-892 (1992).

2. Tseng WP. Effects and dose--response relationships of skin cancer and blackfoot disease with arsenic. Environ Health Perspect 19:109-119 (1977).

3. ATSDR. 1997 CERCLA Priority List of Hazardous Substances That Will be the Subjects of Toxicological Profiles & Support Document. Atlanta. GA:Agency for Toxic Substances and Disease Registry. U.S. Department of Health and Human Services. November 1997.

4. De Rosa CT. Johnson BL. Fay M. Hansen H. Mumtaz MM. Public health implications of hazardous waste sites: findings. assessment. and research. Food Chem Toxicol 34:1131-1138 (1996).

5. Fay M. Mumtaz MM. Development of a priority list of chemical mixtures occurring at 1188 hazardous waste sites using the HazDat database. Food Chem Toxicol 34:1163-1165. (1996).

6. Goyer RA. Toxic effects of metals. In: Casarett & Doull's Toxicology: The Basic Science of Poisons (Klaassen CD. ed). New York:The McGraw-Hill Companies. Inc.. 1996:691-736.

7. Snow ET. Metal carcinogenesis: mechanistic implications. Pharmacol Ther 53:31-65 (1992).

8. Diaz-Barriga F. Llamas E. Mejia JJ. Carrizales L. Santoyo ME. Vega-Vega L. Yanez L. Arsenic-cadmium interaction in rats. Toxicology 64:191-203 (1990).

9. Elsenhans B. Schmolke K. Kolb K. Stokes J. Forth W. Metal-metal interactions among dietary toxic and essential trace elements in the rat. Ecotoxicol Environ Saf 14:275-287 (1987).

10. Nordberg GF. Anderson O. Metal interactions in carcinogenesis: enhancement. inhibition. Environ Health Perspect 40:65-81 (1981).

11. Bae DS. Gennings C. Carter WH Jr. Yang RSH. Campain JA. Toxicological interactions among arsenic. cadmium. chromium. and lead in human keratinocytes. Toxicol Sci 63:132-142 (2001).

12. Chen C-J. Chuang Y-C. Lin T-M. Wu H-Y. Malignant neoplasms among residents of a blackfoot disease-endemic area in Taiwan: high-arsenic artesian well water and cancer. Cancer Res 45:5895-5899 (1985).

13. Nriagu JO. Arsenic in the Environment. Part II. Human Health and Ecosystem Effects. New York:Wiley.1994.

14. Cohen MD. Kargacin CB. Klein CB. Costa M. Mechanisms of chromium carcinogenicity and toxicology. Crit Rev Toxicol 23:255-281 (1993).

15. Germolec DR. Spalding J. Boorman GA. Wilmer JL. Yoshida T. Simeonova PP. Bruccoleri A. Kayama F. Gaido K. Tennant R. Burleson F. Dong W. Lang RW. Luster MI. Arsenic can mediate skin neoplasia by chronic stimulation of keratinocyte-derived growth factors. Mut Res 386:209-218 (1997).

16. Germolec DR. Yoshida T. Gaido K. Wilmer JL. Simeonova PP. Kayama F. Burleson F. Dong W. Lang RW. Luster MI. Arsenic induces overexpression of growth factors in human keratinocytes. Toxicol Appl Pharmacol 141:308-318 (1996).

17. Kachinskas DJ. Qin Q. Phillips MA. Rice RA. Arsenate suppression of human keratinocyte programming. Mut Res 386:253-261 (1997).

18. Ye J. Zhang X. Young HA. Mao Y. Shi X. Chromium(VI)-induced nuclear factor-kB activation in intact cells via free radical reactions. Carcinogenesis 16:2401-2405 (1995).

19. Yen H-T. Chiang L-C. Wen K-H. Chang S-F. Tsai C-C. Yu C-L. Yu H-S. Arsenic induces interleukin-8 expression in cultured keratinocytes. Arch Dermatol Res 288:716-717 (1996).

20. Germolec DR. Spalding J. Yu H-S. Chen GS. Simeonova PP. Humble MC. Bruccoleri A. Boorman GA. Foley JF. Yoshida T. Luster MI. Arsenic enhancement of skin neoplasia by chronic stimulation of growth factors. Am J Pathol 153:1775-1785 (1998).

21. Rhim JS. Jay G. Arnstein P. Price FM. Sanford KK. Aaronson SA. Neoplastic transformation of human epidermal keratinocytes by AD12-SV40 and Kirsten sarcoma viruses. Science 227:1250-1252 (1985).

22. Yang JH. Thraves P. Dritschilo A. Rhim JS. Neoplastic transformation of immortalized human keratinocytes by 2.3.7.8-tetrachlorodibenzo-p-dioxin. Cancer Res 52:3478-3482 (1992).

23. Rhim JS. Fujita J. Arnstein P. Aaronson SA. Neoplastic conversion of human keratinocytes by adenovirus 12-SV40 virus and chemical carcinogens. Science 232:385-388 (1986).

24. Tamhane AC. Dunlop DD. eds. Multiple comparisons of means. In: Statistics and Data Analysis from Elementary to Intermediate. Upper Saddle River:Prentiss-Hall. Inc.. 2000:475-476.

25 Glozak MA. Rogers MB. Specific induction of apoptosis in P19 embryonal carcinoma cells by retinoic acid and BMP2 or BMP4. Dev Biol 179:458-470 (1996).

26 Wozney JM. Rosen V. Celeste AJ. Mitsock LM. Whitters MJ. Kriz RW. Hewick RM. Wang EA. Novel regulators of bone formation: molecular clones and activities. Science 242:1528-1534 (1988).

27. Sack GH. Jr. Human cell transformation by simian virus 40. In Vitro 17:1-19 (1981).

28. Rhim JS. Development of human cell lines from multiple organs. Ann N Y Acad Sci 919:16-25 (2000).

29. Rundell K. Parakati R. The role of the SV40 ST antigen in cell growth promotion and transformation. Semin Cancer Biol 11:5-13 (2001).

30. Steinberg ML. Defendi V. Transformation and immortalization of human keratinocytes by SV40. J Invest Dermatol 81:131s-136s (1983).

31. Wilkinson MG. Millar JBA. Control of the eukaryotic cell cycle by MAP kinase signaling pathways. FASEB J 14:2147-2157 (2000).

32. Parsons R. Phosphatases and tumorigenesis. Curr Opin Oncol 10:88-91 (1998).

33. Pott WA. Benjamin SA. Yang RS. Antagonistic interactions of an arsenic-containing mixture in a multiple organ carcinogenicity bioassay. Cancer Lett 133:185-190 (1998).

34. Pott WA. Benjamin SA. Yang RSH. Arsenic. alone and in chemical mixtures. antagonizes the development of glutathione S-transferase π (GST-P) positive foci in the rat liver. The Toxicologist 54:135 (2000).

35. Soignet SL. Maslak P. Wang ZG. Jhanwar S. Calleja E. Dardashti LJ. Corso D. DeBlasio A. Gabrilove J. Scheinberg DA. Pandolfi PP. Warrell RP. JR. Complete remission after treatment of acute promyelocytic leukemia with arsenic trioxide [see comments]. N Engl J Med 339:1341-1348 (1998).

36. Zhang W. Ohnishi K. Shigeno K. Fujisawa S. Naito K. Nakamura S. Takeshita K. Takeshita A. Ohno R. The induction of apoptosis and cell cycle arrest by arsenic trioxide in lymphoid neoplasms. Leukemia 12:1383-1391 (1998).

37. Jan KY. Huang RY. Lee T-C. Different modes of action of sodium arsenite. 3-aminobenzamide and caffeine on the enhancement of ethyl methanesulfonate clastogenicity. Cytogenet Cell Genet 41:202-208 (1986).

38. Lee T-C. Huang RY. Jan KY. Sodium arsenite enhances the cytotoxicity. clastogenicity. and 6-thioguanine resistant mutagenicity of ultraviolet light in Chinese hamster ovary cells. Mutat Res 148:83-89 (1985).

39. Lee T-C. Wang-Wuu S. Huang RY. Lee KCC. Jan KY. Differential effects of pre- and posttreatment of sodium arsenite on the genotoxicity of methyl methanesulfonate in Chinese hamster ovary cells. Cancer Res 46:1854-1857 (1986).

40. Li JH. Rossman TG. Mechanism of comutagenesis of sodium arsenite with n-methyl-n-nitrosourea. Biol Trace Elem Res 21:381 (1989).

41. Li JH. Rossman TG. Comutagenesis of sodium arsenite with ultraviolet radiation in Chinese hamster V79 cells. Biol Metals 4:197-200 (1991).

42. Okui T. Fujiwara Y. Inhibition of human excision repair by inorganic arsenic and the co-mutagenic effect in V79 Chinese hamster cells. Mut Res 172:69-76 (1986).

43. Wiencke JK. Yager JW. Specificity of arsenite in potentiating cytogenetic damage induced by the DNA crosslinking agent diepoxybutane. Environ Mol Mutagen 19:195-200 (1992).

44. Wiencke JK. Yager JW. Varkonyi A. Hultner M. Lutze LH. Study of arsenic mutagenesis using the plasmid shuttle vector pZ189 propagated in DNA repair proficient human cells. Mutat Res 38:335-344 (1993).

45. Simeonova PP. Wang S. Kashon ML. Kommineni C. Crecelius E. Luster MI. Quantitative relationship between arsenic exposure and AP-1 activity in mouse urinary bladder epithelium. Toxicol Sci 60:279-284 (2001).

46. Simeonova PP. Wang S. Toriuma W. Kommineni V. Matheson J. Unimye N. Kayama F. Harki D. Ding M. Vallyathan V. Luster MI. Arsenic mediates cell proliferation and gene expression in the bladder epithelium: association with activating protein-1 transactivation. Cancer Res 60:3445-3453 (2000).

47. Gennings C. Carter WH Jr. Campain JA. Bae DS. Yang RSH. Statistical analysis of interactive cytotoxicity in human epidermal keratinocytes following exposure to a mixture of four metals. J Agric Biol Environ Statistics 7:58-73 (2002).

CHAPTER 4

Gene Expression Patterns as Potential Molecular Biomarkers for Malignant Cellular Transformation in Human Keratinocytes Treated with MNNG, Arsenic, or Metal Mixture

Dong-Soon Bae. Robert J. Handa. Raymond S.H. Yang. and Julie A. Campain

ABSTRACT

To evaluate the carcinogenic potentials for As and other metals. we have identified molecular markers potentially involved in the transformation process in keratinocytes. Treatment with MNNG enhanced malignant transformation of the RHEK-1 cells. In contrast. As alone or in a mixture of As. Cd. Cr. and Pb inhibited this process. Microarray analysis showed unique gene expression patterns in RHEK-1 for each of MNNG. As. metal mixture treatments. From the analyses on Cancer 1.2 arrays. we have selected a suite of 16 genes involved in the enhancement or inhibition of malignant conversion. These 16 genes. 9 (IFN inducible protein 9-27. MAA A32. CCLB protein. integrin β4. XRCC1. K8. K18. MT3. MAPKK6) altered in a chemical-specific manner and 7 (MIC1. bikunin. MTS1. BMP4. RAD23A. DOC2. vimentin) commonly affected by the MNNG and As/mixture treatments. were examined for expression in detail by Real Time RT-PCR. From a qualitative standpoint. both microarray and Real Time PCR analyses gave comparable results for 9 chemical-specific genes (genes were consistently induced or suppressed under the different treatment regimens when measured by either

technique). Of the 7 commonly altered genes in their expression by multiple chemical treatments. 5 (MIC1. bikunin. MTS1. BMP4. RAD23A) showed expression patterns consistent with a role in the transformation process. i.e. they were oppositely regulated in MNNG-transformed RHEK-1 cells (designated as OM3) as compared to the non-malignant As- and mixture-exposed cells. We also identified two markers (MAA A32 and DOC2) that correlate with acquisition of measurable transformation-associated phenotypic characteristics in OM3 cells. We are currently analyzing gene expression changes in RHEK-1 transformed by other agents such as TCDD or NQO. Identification of a common battery of genes altered during progressive transformation of RHEK-1 should aid in a mechanistic understanding of this process. as well as strengthening the utility of these genes as biomarkers.

ABBREVIATIONS

As: arsenic: MNNG: 1-methyl-3-nitro-1-nitrosoguanidine: RHEK: immortal human epithelial keratinocyte: Cd: cadmium: Cr: chromium: Pb: lead: IFN: interferon: MAA: melanoma associated antigen: CCLB: colon carcinoma laminin binding: XRCC: DNA repair protein: K: keratin: MT: metallothionein: MAPKK: mitogen activated protein kinase kinase: MIC: macrophage inhibitory cytokine: MTS: multiple tumor suppressor: BMP: bone morphogenetic protein: RAD: UV excision repair protein: DOC: mitogen responsive phosphoprotein: RT-PCR: Reverse Transcription Polymerase Chain Reaction: NQO: 4-nitroquinoline-1-oxide: TCDD:2.3.7.8-Tetrachlorodibenzo-*p*-dioxin: bp: base pair

INTRODUCTION

In previous work in our laboratory using the immortalized human epidermal keratinocyte cell line, RHEK-1, we analyzed the transforming potential of As alone and in the presence of Cd, Cr, and Pb (1). These metals frequently occur together in the environment as contaminants in hazardous waste sites. These studies demonstrated that, although As had substantial effects on keratinocyte growth and differentiation, it was not capable of malignantly transforming RHEK-1, either by itself or in the metal mixture. In contrast, chronic low-level exposure to As or the four-metal mixture inhibited the spontaneous progression of virally immortalized RHEK-1 cells in a dose-dependent manner. This was in direct contrast to MNNG, which greatly enhanced conversion of RHEK-1 to an anchorage-independent and tumorigenic phenotype. Microarray analysis of treated cultures, demonstrated many alterations in gene expression that were unique to the different chemicals (1). At least some of the genes identified in this manner are likely involved in the process of transformation in this cell type.

Although, based upon epidemiological evidence, As, Cd, and Cr are human carcinogens, the exact mechanisms involved in transformation by these agents are unclear. The primary target for As in exposed individuals is the skin. Human epidermal keratinocytes, therefore, are a relevant model system for studying the transforming potential of As alone and in mixtures with other chemicals, both metal and non-metal. Chemically-mediated transformation has been extensively studied in keratinocytes, both *in vivo* in the mouse skin system and *in vitro*. From these studies a variety of genes have been implicated in malignant conversion in this cell type, including TGFα, ras, and p53 (10-12). In recent studies with TCDD (13-14), Yang *et al.* (13) suggested that altered

expression of growth regulatory genes, such as plasminogen activator inhibitor 2 (PAI 2), $TGF\beta_1$, or tumor necrosis factor α (TNFα), may be associated with malignant transformation of human keratinocytes. Both As and Cr, a well known skin sensitizer have substantial effects on epidermal keratinocytes: these metals have been shown to alter expression of numerous growth regulatory factors, to stimulate cell proliferation at low concentrations, and to inhibit the normal process of differentiation (2-8). They have not, however, acted to directly transform this cell type *in vitro* (1). Previous studies have suggested that transforming growth factor α (TGFα) and granulocyte macrophage colony stimulating factor (GM-CSF) may be useful biomarkers for As-mediated carcinogenesis in keratinocytes *in vivo* (9). It is likely that some of the genes identified in the different studies are commonly associated with transformation in this cell type; others may be chemical-specific. Characterization of the relationship among chemical exposure, gene expression alterations, and transforming potential of the different chemical treatments should help in delineating important molecular events that are mechanistically linked to the carcinogenic process. Although conventional approaches used in these studies, such as Northern analysis or RT-PCR, have been useful in the past, new technologies are now available which enable one to gain a much wider and complete view of batteries of genes affected by chemical treatment.

New technologies in expression analysis at the RNA and protein levels have led to the development of the field of toxicogenomics, i.e. the use of genetic information to address issues that are crucial in toxicology. Microarray analysis provides the advantage of being able to investigate expression of thousands of genes simultaneously in chemically-treated versus control cells. Combined with cluster analysis, which arranges

genes according to similarity in pattern of gene expression (14). the qualitative effect of a chemical on multiple molecular pathways can be determined. One limitation to the microarray technology, however, is that it is less sensitive and less quantitative than the traditional technologies that it has replaced. Both RT-PCR and Northern analysis allow for the relative quantification of expression of individual genes. Therefore, studies of global gene expression using microarrays are best if used in conjunction with these other more highly quantitative technologies.

Advances in PCR instrumentation and use of fluorescent labels for detection of amplification products have facilitated several approaches to single-tube Real Time PCR quantification of input target copies. In particular, hot-start PCR methodology with the glass capillary format of the LightCycler has been used for amplification and quantitative detection of a single copy of bacterial DNA of *Chlamydia* spp. by SYBR Green fluorescence (15). Rajeevan *et al.* (16) demonstrated that Real Time RT-PCR based on LightCycler technology is well suited to validate DNA array results because it is quantitative, rapid, and requires 1,000-fold less RNA than conventional assays. Real Time RT-PCR has been used to quantitatively confirm the results of microarray analysis on global gene expression in a variety of systems (16-19).

We describe here an extension of a previous work comparing microarray analysis with Real Time RT-PCR on a defined subset of genes altered in their expression by different chemical treatments in human keratinocytes.

MATERIALS AND METHODS

Chemicals

Sodium metaarsenite ($NaAsO_2$), cadmium chloride ($CdCl_2$), chromium oxide (CrO_3), chromium chloride ($CrCl_3$), lead acetate ($(C_2H_3O_2)_2Pb{\bullet}3H_2O$), and dimethyl sulphoxide (DMSO) were purchased from Sigma Chemical Co. (St. Louis, MO). *N*-methyl-*N'*-nitro-*N*-nitrosoguanidine (MNNG) was obtained from Aldrich (Milwaukee, WI).

Cell culture

The AD12/SV40 immortalized keratinocyte cell line (RHEK-1) was obtained from Dr. J. Rhim (Center for Prostate Disease Research, Rockville, MD) (20). RHEK-1 cells were cultured in Dulbecco's Modified Eagle's medium (DMEM) supplemented with 100 U/ml penicillin, 0.1 mg/ml streptomycin, 10 mM *L*-glutamine, and 10 % fetal bovine serum (FBS) (Summit Biotechnology, Ft. Collins, CO).

Cell line establishment following exposure to MNNG, As, or As-containing mixture

The detailed protocol to obtain the RHEK-1 cell lines utilized in these studies is described in Bae *et al.* (1). The RHEK-1 cell lines were designated as follows: (1) OM1: control cell population treated with 0.5% DMSO for 24 hours. (2) OM3: cells treated with 0.1 μg/ml MNNG for 24 hours. (3) As-Con: control population treated with sterile distilled water for 6 months. (4) As-High: cells treated with 14 ppb As^{3-} for 6 months. (5) Mix-Con: control population treated with sterile distilled water for 6 months, and (6) Mix-High: cells treated with 14 ppb As^{3-}, 104 ppb $Cr^{3-\text{ and }6-}$ (1:1), 618 ppb Cd^{2-}, and 332

ppb Pb^{2+} for 6 months. These metal concentrations correspond to the LC_{10} for each metal as obtained by the MTT assay.

Atlas Human Cancer 1.2 cDNA microarray analysis of chemically-treated RHEK-1

The detailed protocol for microarray analysis is described in Bae *et al.* (1). Relative changes in gene expression among the cell populations were determined by normalizing gene-specific hybridization signals to the signals obtained from all 1185 genes included in the Cancer 1.2 Array. A list of the genes included on this array can be found on Clontech's web site (http://atlas.clontech.com/). Only genes that demonstrated ≥ 2-fold change in expression ratio between control and treatment populations were reported.

Real Time RT-PCR

The Real Time RT-PCR protocol was as adaptation of a previously published protocol (21). RNA was purified from all control and treated RHEK-1 populations as described in Bae *et al.*, (1). To insure consistency across RNA samples from the same cell populations and to eliminate the complicating factors of cell density and other culture conditions multiple flasks of cells from each control and treatment group were grown to approximately 70% confluency and were pooled prior to RNA preparation. For Real Time RT-PCR analysis, 2-3 separate reverse transcriptase reactions were carried out on each pooled RNA sample to produce 2-3 individual cDNA's for further amplification. The genes analyzed by Real Time RT-PCR and the primers utilized are shown in TABLE 4.1. The sequences for gene-specific primers corresponding to the PCR targets on the Atlas Human Cancer 1.2 Array were obtained from Clontech. Primers themselves were

TABLE 4.1 Sequences of primers used in the Real Time RT-PCR

Gene	*GenBank Accession#*	*Primers*	*Location*	*PCR Product* (bp)	*Sequence* 5' – 3'
IFN-inducible protein 9-27	J04164	forward	615-639	194	TCATCCTGTCACTGGTATTCGGCTC
		reverse	809-784		GTGGGTATAAACTGCTGTATCTAGGG
Integrin β4	X53587	forward	5357-5380	340	TTCGGGCCAGAGCGCGAGGGCAT
		reverse	5697-5674		GACGCCTAGTGGGACATGGCGGG
MAA A32	M28882	forward	1756-1779	424	GAAGGGCAAGGCTGCCGTGCAGG
		reverse	2180-2154		TGGGATGAGCTTCACTCAACGTGGAG
CCLB protein	U43901	forward	460-485	321	CTGCGCTATGTGGACATTGCCATCC
		reverse	781-757		CTGAATAGGCACAGAGGGCACCTG
DOC 2	U53446	forward	1639-1662	189	GTGGGTCTAGGTGGTGTAACTGTC
		reverse	1828-1805		CAAAGGGTGAAGGCTGGTTCCAAC
XRCC 1	M36089	forward	1226-1250	313	TCCAGTCTCCAGGGCCATAGGCAG
		reverse	1539-1513		GAAGCCACTCAGCACCACTACCACAC
RAD 23A	D21235	forward	355-379	277	CCCACCTCAGGCATGTCCCATCCC
		reverse	632-608		GCAGATACTCCACGGCTCGGTGGG
K 8	M34225	forward	1190-1215	284	ATCGACATCGCCACCTACAGGAAGC
		reverse	1474-1450		ACGTCAGAGGACTCAGACACCAGC
K 18	M26326	forward	706-731	265	GAGGAAGTAAAAGGCCTACAAGCCC
		reverse	971-946		CCAAGGACTGGACTGTACGTCTCAG
MT 3	D13365	forward	28-52	316	GTTGCTTGGAGAAGCCCGTTCACC
		reverse	344-320		ACACCAGCCACACTTCACACAGGC
BMP 4	D30751	forward	943-969	378	GCCGGAGGGCCAAGCGTAGCCCTAAG
		reverse	1321-1294		CTGCCTGATCTCAGCGGCACCCACATC
MAPKK 6	U39657	forward	1060-1088	329	TTGGAGTCTGGGCATCACGATGATTGAG
		reverse	1389-1363		CCACCAATCCACAGTAGGGTCAACCG
MIC 1	AF019770	forward	713-736	211	ACGGGAGGTGCAAGTGACCATGTG
		reverse	924-899		TGGCTAACAAGTCATCATAGGTCTGG

(continued)

TABLE 4.1 continued

Gene	*GenBank Accession#*	*Primers*	*Location*	*PCR Product* (bp)	*Sequence* 5' – 3'
Bikunin	U78095	forward reverse	736-759 933-909	197	TTCCCACGCTGGTACTTTGACGTG GAGGATCAACACCATCACGAACAGC
MTS 1	L27211	forward reverse	482-506 836-808	354	GCGGAAGGTCCCTCAGACATCCCC CTCGCAAGAAATGCCCACATGAATGTGC
Vimentin	X56134	forward reverse	1164-1192 1604-1576	440	AGGAAATGGCTCGTCACCTTCGTGAATA GGAGTGTCGGTTGTTAAGAACTAGAGCT
SOD 1	K00065	forward reverse	198-226 496-468	298	AGTGCAGGGCATCATCAATTTCGAGCAG GATGCAATGGTCTCCTGAGAGTGAGATC
GSH synthase	U34683	forward reverse	1212-1235 1411-1388	199	AGAGGGCCTCCTACATCCTCATGG TGCATGCTCGATGGCTTTGGTTCG

synthesized and purified by Genset (La Jolla, CA). Total pooled RNA was treated with RNase-free DNase I (Boehringer-Mannheim, Indianapolis, IN) and reverse-transcribed to produce single-stranded cDNA using the SuperScript System (GibcoBRL, Rockville, MD). FastStart DNA Master SYBR Green I Mix (containing FastStart Taq DNA polymerase, dNTP, and SYBR Green I dye: Roche Molecular Biochemicals, Indianapolis, IN) was used in a 20 μl "Hot Start" PCR reaction with 4 mM $MgCl_2$, 0.3 μM of each primer, and diluted cDNA template. The amplification program consisted of 1 cycle of 95°C with 5-min hold ("hot start") followed by 30 - 40 cycles of 95°C with 2-second hold, gene primer-specific annealing temperature (range from 60 to 70°C) with 5-second hold, 72°C with gene product-specific hold (length of product [bp] / 25). Amplification was followed by melting curve analysis using the program run for one cycle at 95°C with 0-second hold, 65°C with 15-second hold, and 95°C with 0-second hold at the step acquisition mode. In the PCR methodology, the quantity of cDNA of interest in target cells accumulates according to the function, $Tn = To\ (E)^n$, where Tn is the amount of target sequence at cycle n, To is the initial amount of target, and E is the efficiency of amplification. In our experiments quantitative measurement of cDNA in chemically-treated and control cells was measured by LightCycler (Roche, Indianapolis, IN) as follows and as shown schematically for a representative DOC2 gene in FIG. 4.1. Briefly: (1) A standard curve for each primer pair was generated using a known amount of template gene. (2) From this standard curve, the parameters E and K (the number of copies of PCR product) were obtained. (3) The equation for the standard curve: $Cp = -(1/\log E) * \log To + (\log K/\log E)$, where Cp is the crossing point, was then utilized to calculate To in conjunction with the experimentally determined Cp for the unknown. (4)

A representative Real Time RT-PCR LightCycler reaction for the DOC2 gene is shown. RT-PCR was carried out as described in Materials and Methods using the DOC2 primer set and p25 OM1 RNA. The standard curve used to calculate the concentration of mRNA in the unknown test sample was generated using amounts of DOC2 DNA template between 0.069 and 69,000 fg. For quantitative analysis, the Fit Points Method with 2 fit points (designated with 2 upper +) was utilized to determine robust crossing points. Cp: crossing point; cycle number at which fluorescence intensity arises just above threshold/noise band (0.5 in this figure).

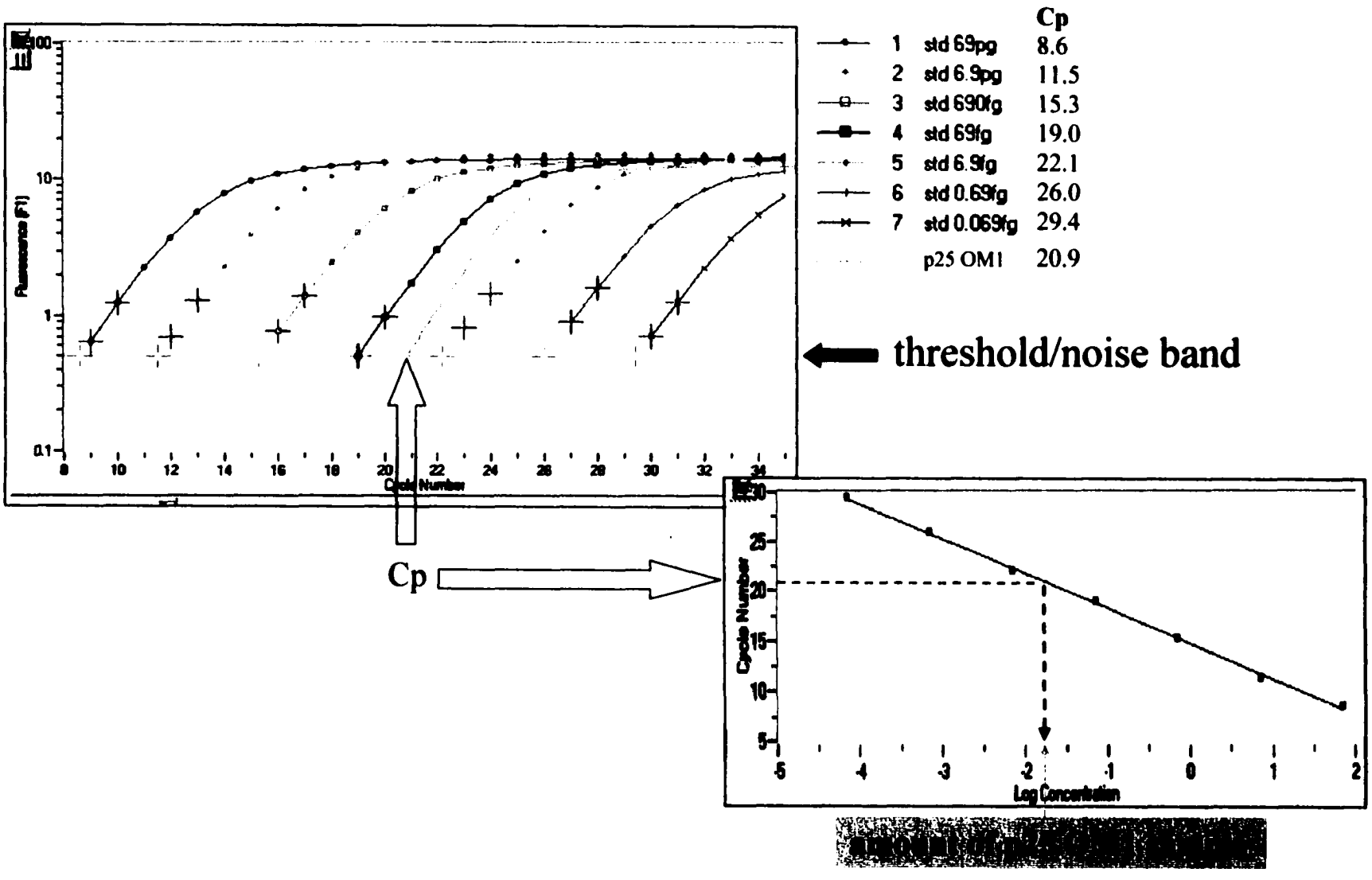

FIG. 4.1 Schematic representation of DOC2 mRNA quantification in an unknown sample using LightCycler technology

A subsequent melting curve analysis was carried out to confirm the specificity of PCR products. After the final amplification step, samples are gradually heated to reach a maximum temperature of 95°C. The degree of denaturation is calculated by LightCycler software as an intrinsic part of the Real Time PCR technology. As a negative control, template DNA was replaced with PCR-grade water. Two groups of genes were analyzed in these studies: (1) genes demonstrating substantial alterations in expression between cells treated with an individual chemical/mixture and the appropriate control; and (2) genes demonstrating alterations in expression in more than one chemical treatment group (i.e., MNNG + As / MNNG) as compared to controls.

Statistical analysis

One-way ANOVA followed by Dunnett's test was used to analyze differences between control and chemical-treated samples in Real Time RT-PCR studies. P values < 0.05 were considered statistically significant.

RESULTS

Analysis by Real Time RT-PCR of expression levels of selected genes altered in a chemical-specific manner in RHEK-1 cells

To confirm our findings with microarray analysis and to further explore these alterations in gene expression. we have performed Real Time RT-PCR on a selected subset of genes which were altered in their expression in RHEK-1 in a chemical-specific manner. The ten genes demonstrating the most substantial up- or down-regulation as measured by microarray analysis in response to treatment of RHEK-1 with MNNG-. As-. or the metal-mixture are listed in TABLE 4.2: from this list. several genes were selected for comparative Real Time RT-PCR studies from each of the individual chemical treatments. In MNNG-treated OM3. the genes selected were interferon (IFN) inducible protein 9-27. melanoma associated antigen A32 (MAA A32). and the colon carcinoma laminin binding (CCLB) protein genes (which were all induced ≥ 4-fold) and integrin β4 (which was down regulated) (TABLE 4.2A). No detectable changes in these 4 genes were observed in As- or mixture-treated RHEK-1 cells (data not shown). The genes chosen for further analysis from As-High. were DNA repair protein XRCC 1 (which was substantially up-regulated in treated versus control cells) and those encoding the simple epithelial keratins 8 and 18 (K8 and K18) (TABLE 4.2B): these latter two genes were representative of the many cytokeratins suppressed in As-High populations. There were no measurable changes in expression of these 3 genes in OM3 and mixture-exposed cells. As would be expected. RHEK-1 cells exposed to the four metal mixture (which included Cd) demonstrated increased mRNA levels for metallothionein 3 (MT 3). We chose this

TABLE 4.2 Chemical-specific changes in gene expression detected by microarray analysis in RHEK-1 cells exposed to MNNG, As, or the metal mixture.

(A) MNNG

Induced Gene	Fold*	Suppressed Gene	Fold*
IFN-inducible protein 9-27	+++	Cadherin 8	- - -
DOC 2	+++	***Integrin β4***	- -
MAA A32	+++	***BMP 4***	- -
c-Jun N-terminal kinase 2	+++	***Bikunin***	-
Cyclin H	++	Fibronectin precurser	-
MIC 1	++	High mobility group I and II	-
CCLB protein	+	DNA ligase I	-
Vimentin	+	***RAD 23A***	-
Adenomatous polyposis coli protein	+	***Glutathione (GSH) synthase***	-
Met protooncogene	+	Glutathione-s-transferase II (GST)	-

(B) As

Induced Gene	Fold*	Suppressed Gene	Fold*
RAD 23A	++	***MIC 1***	- - -
BMP 4	++	Metalloprotease	- - -
Epidermal growth factor response factor 1	++	Frizzled homolog	- - -
XRCC1	+	***Bikunin***	- -
MTS 1	+	Paxillin	- -
Endonuclease III homolog	+	***GSH synthase***	- -
DNA mismatch repair protein	+	***K 8***	-
Early growth response protein 1	+	***K 18***	-
Jun B	+	***Cytosolic superoxide dismutase 1 (SOD1)***	-
Fos-related antigen	+	GST homolog	-

(continued)

TABLE 4.2 continued

(C) metal mixture

Induced Gene	Fold*	Suppressed Gene	Fold*
Hemidesmosomal plague protein	++	***MAPKK 6***	- - -
Collagen 6 α 2	++	DNA excision repair protein ERCC 2	- - -
BMP 4	+	***MIC 1***	- -
MTS 1	+	WAF 1; melanoma differentiation associated protein 6	- -
MT 3	+	***Vimentin***	-
Jun B	+	***DOC 2***	-
Fos-related antigen	+	***SOD 1***	-
Caspase 10 precursor	+	DNA mismatch repair protein MSH 2	-
Low density lipoprotein receptor related protein	+	DNA excision repair protein ERCC 5	-
Cytovillin 2	+	DNA topoisomerase II β	-

Microarray analysis was carried out using the Clontech Atlas Human Cancer 1.2 Array as described previously (1) and in Materials and Methods. Representative genes induced or suppressed greater than 2-fold in RHEK-1 cells treated with MNNG, As, or the four-metal mixture as compared to controls are given. Relative expression ratios of 20 representative genes per chemical treatment group are shown as follows: * : +/- : 2.0 – 4.9 fold induction/suppression, ++/- - : 5.0 -10 fold induction/suppression, +++/- - - : > 10 fold induction/suppression.
The total number of genes altered greater than 2-fold in their expression using this array was: 63, 70, and 76, for OM3, As-High, and Mix-High, respectively. Genes in italic bold were further studied by quantitative Real Time RT-PCR.

gene for further analysis and the gene encoding the important mitogenic signal transduction protein, mitogen activated protein kinase kinase 6 (MAPKK 6) as a representative of repressed genes in this cell population (TABLE 4.2C).

In the LightCycler PCR reactions used in our studies, the absolute quantification method with SYBR Green I was utilized. In this case, target mRNA concentration was expressed as an absolute value (i.e., femtogram, copies) that was determined through utilization of a standard curve. In this quantification method, homologous standards and target samples were prepared in separate capillaries, then amplified during the same run. Five to seven serial standards with known amounts of target sequence were used to create a standard curve. As demonstrated in a representative curve, shown in FIG. 4.1, from our studies on the DOC2 gene, the estimated amount of the DOC2 gene in the p25 OM1 sample was 36.5 fg which corresponds to a crossing point (Cp) of 20.9, that is the cycle number at which the amplified products emit fluorescence above the threshold/noise band (i.e., located at 0.5 in FIG. 4.1) for the first time. The Cp value of the p25 OM1 sample was converted to a concentration as described in Materials and Methods. For optimized reactions, the dynamic range of this quantification method was up to 7 orders of magnitude. To verify the specificity and sensitivity of SYBR Green I detection, melting curve analysis was carried out after the amplification reaction. Melting curve analysis allowed differentiation between primer dimers and specific amplified product.

The pooled results from multiple Real Time RT-PCR analyses on the 9 genes selected from the chemical-specific gene expression profiles are shown in TABLE 4.3. Careful scrutiny of this data revealed that in approximately half of the cases gene-specific

TABLE 4.3 Comparison of gene expression changes in chemically-treated RHEK-1 as measured by microarray and Real Time RT-PCR: Selected genes altered in a chemical-specific manner

Gene	OM3		As-High		Mix-High	
	Array	PCR	Array	PCR	Array	PCR
IFN-inducible protein 9-27	61 ⇑	*16 ± 4.3 ⇑	-	-	-	-
MAA A32	12 ⇑	4.3 ±1.4 ⇑	-	-	-	-
CCLB protein	4 ⇑	1.4 ± 0.1⇑	-	-	-	-
Integrin β4	6 ⇓	*4.7 ± 0.8 ⇓	-	-	-	-
XRCC 1	-	-	4 ⇑	1.8 ± 2.1 ⇑	-	-
K 8	-	-	3.3 ⇓	*6.1 ± 0.7 ⇓	-	-
K 18	-	-	3.4 ⇓	*7.9 ± 0.6 ⇓	-	-
MT 3	-	-	-	-	3 ⇑	*9.4 ± 2.6 ⇑
MAPKK 6	-	-	-	-	23 ⇓	*9.4 ± 0.7 ⇓

- : not measured: *: statistically different from corresponding control at $p<0.05$
Microarray and Real Time RT-PCR analyses were carried out as described in Materials and Methods. Gene-specific primers used in the latter are shown in TABLE 1. Values in Real Time RT-PCR analysis are expressed as the average ratio ± SE of a chemically-treated sample as compared to its corresponding control. One microarray and 3 independent Real Time RT-PCR experiments were carried out.

comparative analysis between the three chemically-treated samples and their respective controls gave very consistent absolute values in all samples analyzed, with SE ≤ 20%. In the other instances, however, while a consistent induction or suppression was observed in all three replicates from a treatment condition, the absolute fold alteration in expression varied substantially. TABLE 4.3 also demonstrates for comparison the alterations in expression of these genes in the three chemically-treated RHEK-1 populations as measured initially by microarray analysis. From a qualitative standpoint, both types of analysis gave comparable results for these specific genes, that is, genes were consistently induced or suppressed under the different treatment regimens when measured by either technique. The absolute level of change in expression measured by microarray versus Real Time RT-PCR varied in our hands by a maximum of approximately 4-fold, with, in most cases, the values of induction or suppression being larger by microarray analysis.

Real Time RT-PCR on selected genes altered by multiple chemical treatments in RHEK-1 cells

We were interested in identifying genes that were altered in response to more than one of our tested chemical treatments. As MNNG acted to enhance and both metal treatments inhibited spontaneous transformation in RHEK-1, correlations made between these different outcomes and specific gene expression changes may provide mechanistic clues to the cancer process in this cell type. Seven genes in this category from TABLE 4.2(A-C), were more closely analyzed by Real Time RT-PCR. TABLE 4.4 demonstrates the mean induction/suppression (±SE) of these genes as measured by Real Time RT-PCR in multiple samples from each of the individual chemical treatment groups as compared

TABLE 4.4 Comparison of gene expression changes in chemically-treated RHEK-1 as measured by microarray and Real Time RT-PCR analyses: Genes altered by multiple chemical treatments

Gene	OM3		As-High		Mix-High	
	Array	PCR	Array	PCR	Array	PCR
MIC 1	7 ⇑	*7.5 ± 1.9 ⇑	35 ⇓	11.5 ± 7.3 ⇓	7 ⇓	10.2 ± 3.8 ⇓
Bikunin	2 ⇓	*1.4 ± 0.1 ⇓	--	*1.8 ± 0.3 ⇑	-	*7.7 ± 1.2 ⇑
MTS 1	--	*2.7 ± 0.5 ⇓	2 ⇑	2.5 ± 0.6 ⇑	3 ⇑	2.8 ± 1.5 ⇑
BMP 4	10 ⇓	3.1 ± 1.3 ⇓	5 ⇑	*10.4 ± 1.9 ⇑	4 ⇑	2.3 ± 0.6 ⇑
RAD 23A	3 ⇓	2.6 ± 0.8 ⇓	6 ⇑	1.6 ± 0.2 ⇑	--	*1.9 ± 0.2 ⇑
DOC 2	36 ⇑	*3.5 ± 0.2 ⇑	-	*3.8 ± 0.4 ⇑	4 ⇓	*2.5 ± 0.5 ⇓
Vimentin	3 ⇑	*10.4 ± 2.1 ⇑	--	8.6 ± 3.1 ⇑	4 ⇓	1.5 ± 0.2 ⇓

- : not detected

--: Expression detected in the array was too low to quantitate accurately. *: statistically different from corresponding control at $p<0.05$

The bikunin gene was initially chosen for further Real Time RT-PCR analysis as preliminary microarray analysis indicated it was repressed in As-treated cultures. The discrepancy in our microarray and Real Time RT-PCR results may be due to very low microarray signal intensity for this gene (As-Con/ As-High = 28/4). Microarray and Real Time RT-PCR analyses were carried out as described in Materials and Methods. Gene-specific primers used in the latter are shown in TABLE 1. Values in Real Time RT-PCR analysis are expressed as the average ratio ± SE of a chemically-treated sample as compared to its corresponding control. One microarray and 3 independent Real Time RT-PCR experiments were carried out.

to its respective control. As discussed above for the genes induced in a chemical-specific fashion, the variability in triplicates for these multiple samples ranged from 6% to as high as 63%; approximately half of the samples varied by less than 20%. All 7 genes were, however, consistent in their pattern of induction or suppression among the triplicates; this data also agreed well with the microarray analysis for 6 of the 7 genes. The bikunin gene was the exception to this in that the original microarray data showed repression in both OM3 and the As-High samples. Once a more sensitive and quantitative analysis of expression of this gene was carried out by Real Time RT-PCR, we were able to demonstrate that the bikunin gene is repressed in OM3 and, in contrast, is induced by approximately 30-50% in both the As-High and Mix-High cells. Of the 7 genes analyzed in this manner, 5 showed expression patterns consistent with a role in the transformation process, i.e. they were oppositely regulated in OM3 as compared to the non-malignant As-High and Mix-High cells. These genes were macrophage inhibitory cytokine 1 (MIC1), bikunin, multiple tumor suppressor 1 (MTS1), bone morphogenetic protein 4 (BMP4) and UV excision repair protein RAD23A. MIC1 was induced by MNNG and suppressed by both As and the metal mixture. Two tumor suppressor genes, bikunin and MTS1, and another TGFβ-like protein, BMP4, showed opposite regulation, being suppressed in OM3 and overexpressed in the lines derived from As- and metal-mixture treatment. RAD23A also showed this latter pattern. The remaining two genes, vimentin and DOC2 were substantially upregulated in RHEK-1 exposed to both MNNG and As, and showed decreased expression in the mixture treated cells.

Time-course studies on MNNG-associated genes by Real Time RT-PCR

We are interested in identifying molecular markers that correlate with acquisition of measurable transformation-associated phenotypic characteristics in our MNNG-transformed keratinocytes. To address this issue, we generated time course expression data on the IFN inducible protein, integrin β4, MAA A32, CCLB, and DOC2 genes in OM3, along with its control OM1, with continued passage in culture from the initial chemical treatment to acquisition of a fully malignant phenotype. Gene expression patterns were measured at p2, p7, p13, p16, and p25 by Real Time RT-PCR in OM3 as compared to OM1 and are summarized in TABLE 4.5. These passages in OM3 correspond to: (i) cells immediately following chemical treatment and with no discernible phenotypic changes, (ii) the first passage of cells demonstrating subtle morphological alterations, (iii) morphologically distinct cells that had acquired the ability to grow in an anchorage-independent manner (AIG+), (iv) a moderately tumorigenic population in immunocompromised mice, and (v) an extremely malignant population, generating tumors greater than 1 cm in three weeks or less and exhibiting a colony forming efficiency in methylcellulose (MC) of approximately 20% (FIG. 4.2). It should be noted that during continual passage, OM1 also underwent transformation-associated changes, albeit at a much slower rate than that observed in OM3. This phenomenon is likely due to the Ad12/SV40 viral infection used to immortalize the cells. In contrast to OM3, the p11, p13 and p16 OM1 cells were anchorage-dependent. By p25, however, OM1 began to demonstrate phenotypic changes that were consistent with partial transformation; among these changes was acquisition of anchorage-independent growth. Approximately 30% of mice injected with OM1 cells at p25 developed small, slowly growing squamous cell

TABLE 4.5 Time-dependent alterations in gene expression in OM1 and OM3 cells as determined by Real Time RT-PCR

Gene	Cell line	Time p2	p7	p13	p16	p25
IFN inducible protein 9-27	OM1	61 ± 6.3	42 ± 8.2	21 ± 4.6*	0.3 ± 0.01*	4 ± 0.5*
	OM3	65 ± 3.6	26 ± 1.3	33 ± 5.6	54 ± 5.4	77 ± 17
Integrin β4	OM1	174 ± 13	584 ± 24*	392 ± 74	753 ± 124*	3343 ± 37*
	OM3	407 ± 76	260 ± 1	193 ± 12*	76 ± 3*	581 ± 50
MAA A32	OM1	5 ± 1.1	14 ± 3.6	20 ± 4.9	14 ± 2.3	113 ± 41*
	OM3	18 ± 0.6	54 ± 7.2	53 ± 2.8	137 ± 8.5*	427 ± 16*
CCLB protein	OM1	1 ± 0.1	4 ± 0.7	6 ± 0.6	7 ± 0.6*	75 ± 1.3*
	OM3	3 ± 0.9	4 ± 0.2	4 ± 0.8	6 ± 0.7	109 ± 10*
DOC 2	OM1	19 ± 0.4	12 ± 1.7	16 ± 1.9	6 ± 0.2*	37 ± 1.5*
	OM3	14 ± 4.9	15 ± 0.1	18 ± 2.4	82 ± 3.1*	116 ± 20*

Real Time RT-PCR analysis was carried out as described in Materials and Methods. Gene-specific primers used are shown in TABLE 1. Cell populations analyzed were from various subcultures (up to passage (p) 25) after parental RHEK-1 cells were treated with 0.1 μg/ml MNNG or DMSO control. The amount (in femtogram) of selected cDNA's (representing mRNA) is given in OM3 as compared to OM1 at various time points. Mean value ± SE is shown from the duplicate experiments.

*: statistically different from p2 cells at $p<0.05$

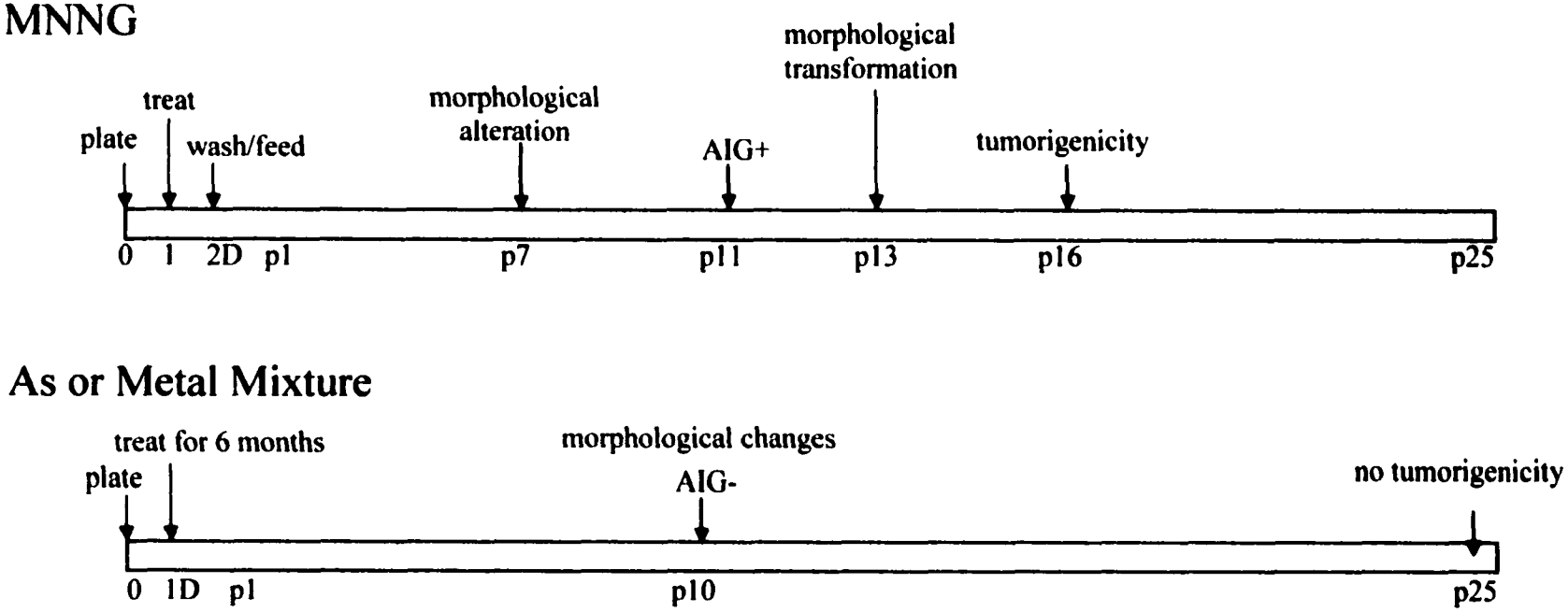

FIG. 4.2 Schematic of chemical transformation studies in RHEK-1 human keratinocytes
RHEK-1 cells were treated with MNNG, As or the metal mixture as described previously (1) and as summarized in Materials and Methods. Functional endpoints that have previously been associated with malignant transformation in this cell type (20) were assayed in treated and control cultures approximately every other passage. Passages at which cells underwent detectable alterations in morphology and/or acquired a more transformed phenotype are indicated. AIG: anchorage-independent growth; D:day

carcinomas. The phenotypic changes are described in detail in a previous publication (1). In summary, p11 to p16 in OM3 and p25 in OM1 appeared to be important time points for analysis of gene expression alterations that correlated with malignant conversion in these cell lines.

As demonstrated in TABLE 4.5, our time-course analysis revealed the following: (1) mRNA levels for the IFN-inducible protein gene changed with time in both OM1 and OM3; expression of the gene decreased sequentially in OM1, showing a maximum inhibition at passage 16 of 203-fold as compared to p2. In OM3, however, expression of IFN inducible protein initially decreased at p7, but then proceeded to rise again until reaching a level slightly higher than basal at p25; none of the changes in expression of the IFN inducible gene observed in OM3 were, however, statistically significant as compared to the p2 control. (2) The gene for integrin β4 also showed a unique pattern of expression throughout the time course. In OM1, mRNA for integrin β4 increased in a time-dependent fashion, reaching maximum levels of expression at p25, which was a 19-fold increase over basal levels at p2. In OM3, however, expression of the gene decreased in a linear fashion up until p16, after which it rose to levels slightly higher than basal at p25. (3) mRNA levels for the MAA A32, CCLB protein, and DOC2 genes increased with increasing time in culture in both OM1 and OM3; see FIG. 4.3 for a graphical representation of time-dependent changes in expression levels of the MAA A32 and DOC2 genes. Expression levels of all three genes peaked at p25 in both cell lines. (4) Maximum expression of the MAA A32 and DOC2 genes was approximately 3- to 4-fold higher in OM3. (5) The CCLB protein gene was expressed at very low levels in both OM1 and OM3 through p16; when measured in p25 cells, however, expression was

Real Time RT-PCR was carried out as described in Materials and Methods using the appropriate primer sets as shown in TABLE 1. Cell populations analyzed were from various subcultures (up to passage 25) after parental RHEK-1 cells were treated with 0.1 μg/ml MNNG or DMSO control. The amount (in femtogram) of (A) DOC2 or (B) MAA A32 cDNA (representing mRNA) is given in OM3 as compared to OM1 at various time points. Mean value was shown with SE from the duplicate experiments. *: statistically different from p2 cells at $p<0.05$. The number of 1, 2, and 3 indicates the RHEK-1 cell populations tested in tumorigenicity assay (1). The tumor formation potential of cells at 1 (OM3 at p25), 2 (OM3 at p16), and 3 (OM1 at p25) was very high, high, and very poor, respectively.

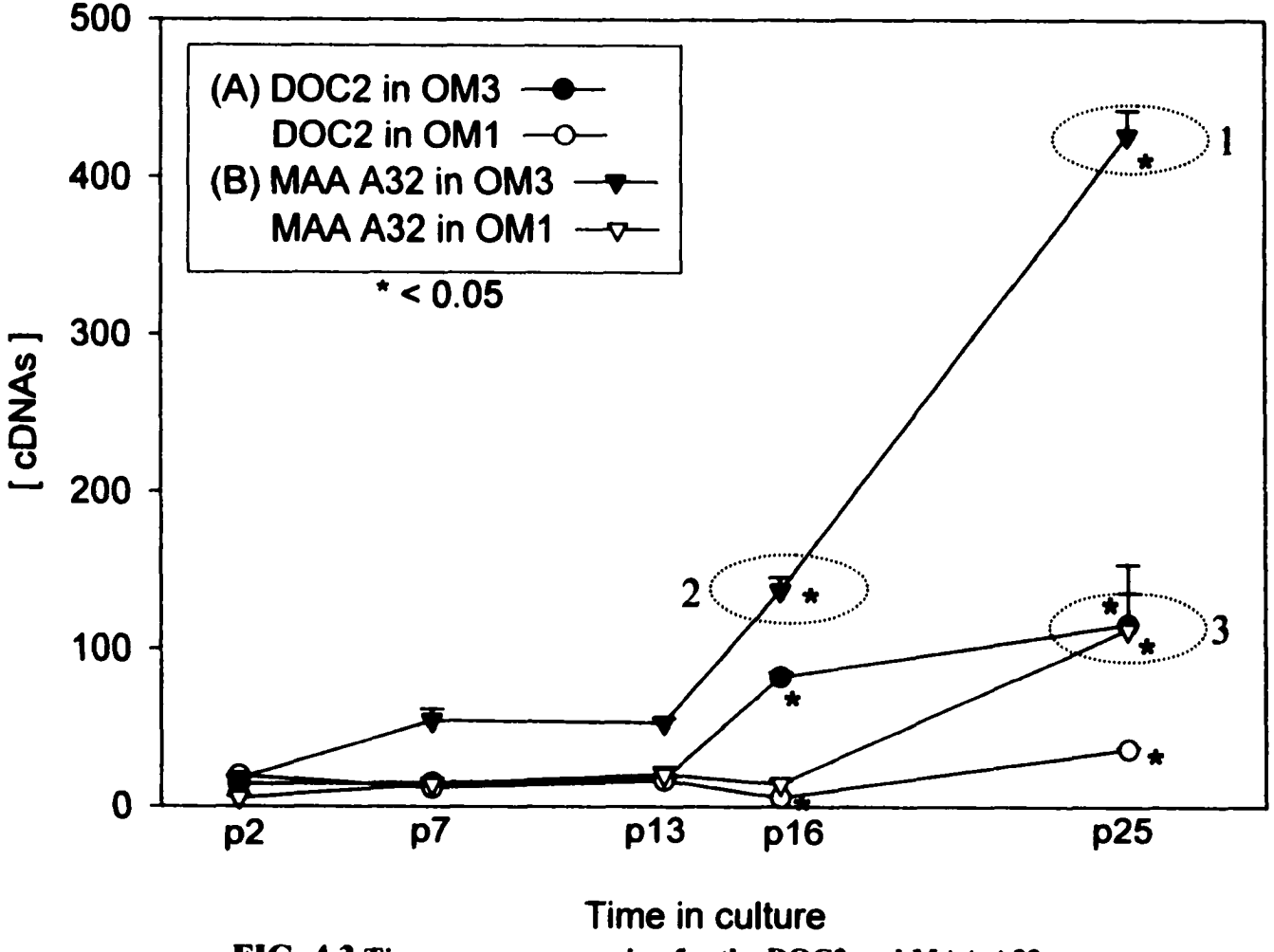

FIG. 4.3 Time-course expression for the DOC2 and MAA A32 genes

substantially induced, 75- and 36-fold as compared to basal p2, respectively for OM1 and OM3. (6) The MAA A32 and DOC2 protein genes exhibited very similar kinetics in both the control and MNNG-treated cells, increasing expression of these genes occurred earlier (at or before p16) in OM3 and continued to rise through p25. In contrast, in OM1, MAA A32 and DOC2 levels were very low at p16 and did not begin to rise substantially until p25.

DISCUSSION

Recently, there has been an explosion in refinements in the microarray technology itself, as well as its application in exploring a number of biological processes, including cancer development (22-36). So far, microarrays have been utilized to achieve differential gene expression profiling in many types of transformed cells including those from melanoma (24), tumors of the cervix (30), colon (22,23,35), lung (25), ovary (31,32,34), breast (28,33,36), bladder (27), pancreas (35), and alveolar rhabdomyosarcomas (26). These studies have compared gene expression in tumor cells as compared to their normal counterparts and to one another with the goals of identifying cancer-associated genes or providing molecular phenotyping that identifies distinct tumor classifications. This technology has allowed simultaneous analysis of multiple molecular events and offered much promise in providing insight into the complex network of cellular regulatory pathways and how they participate in carcinogenesis.

Previous studies in our laboratory using microarray gene expression profiling of three keratinocyte cell lines established following exposure to As, an As-containing

chemical mixture, or MNNG demonstrated unique patterns in response to each chemical treatment (1). These studies identified two groups of genes that were targeted for further study, genes uniquely regulated in a chemical-specific fashion and genes that were oppositely or similarly regulated by at least two of the three different chemical treatments. In our highly malignant MNNG-transformed cell line, OM3, several members of the MAP kinase signaling pathway were overexpressed, as were oncogenes. Genes for multiple cell surface proteins implicated in the process of transformation, multiple protein phosphatases, and those involved in the stress response also showed altered expression in OM3. These changes in gene expression were not observed in As- and the metal mixture-treated cells. In the As-treated cells, which possessed very poor tumorigenic potential as compared to both OM3 and the water-treated control populations, the most noteworthy changes in expression were observed in DNA repair proteins, which were highly induced, and in cytokeratins, many of which showed substantially decreased expression. We were very interested in the fact that these same changes were not observed in cells treated with the four metals together; despite the fact that the concentration of As was the same under both treatment conditions. Rather this Mix-High population demonstrated its own unique changes in mRNA abundance. Genes that were modulated by multiple chemical treatments included cytokines and other cell cycle regulatory proteins, tumor antigens, and DNA repair proteins.

The studies described herein utilized Real Time RT-PCR to more accurately quantify expression levels of a defined subset of genes representing those showing a chemical-specific expression pattern and those altered in more than one treatment group in our RHEK-1 cell lines. From a technological standpoint, both microarray and Real

Time RT-PCR generally gave qualitatively similar results in the current study. Similar to earlier work by Rajeevan *et al.* (16), the exceptions to this were the bikunin, superoxide dismutase 1, and GSH synthase genes, cases where the hybridization signal obtained from the initial microarray and/or the fold difference in expression between the samples analyzed was low (≤ 2 to 3-fold). During the last few years, there have been several studies comparing gene expression changes measured by microarray versus by more quantitative techniques such as Northern analysis and RT-PCR (16-19, 23, 25, 27). Data from these studies demonstrated that qualitative agreement among the different techniques is highly dependent on the quality of the data obtained and relative expression levels of the gene of interest (17-19,32,34). It has been suggested that genes with strong hybridization intensity in microarrays and at least twofold difference in expression between samples are most likely to be validated by PCR technologies (16). In studies by Backert *et al.*, 60% of genes identified consistently by microarray as having altered expression in cell lines derived from colonic carcinomas versus normal colon tissue were verified by Northern blotting or Real Time RT-PCR (23). Another issue when comparing the different techniques is the measured magnitude of change in expression of specific genes; two explanations have been suggested for the lack of consensus in this area between gene arrays and Real Time RT-PCR methods (19). Those were differences in target gene sequence and other differences intrinsic to the methodologies, including normalization procedures. In support of the latter, despite the fact that in our studies, the target sequence for the genes analyzed was the same for both techniques, substantial differences in the magnitude of expression of some genes were still observed. Given the state of art of the different technologies, microarrays best serve as a screening tool for

identifying potential genes and/or gene pathways in neoplastic transformation, while Real Time RT-PCR serves as a more quantitative verification tool for the candidate genes.

In OM3, we further examined expression of the IFN inducible protein, integrin β4, MAA A32, CCLB, and the DOC2 genes in both p25, when the cells were fully transformed, and in earlier passages in our time course study. Although the genes for IFN inducible protein and integrin β4 were altered in both OM1 and OM3 in a time-dependent fashion, it is difficult to tell from the patterns of expression of these genes, at just what stage (if any) they may be involved in malignant progression. At p25, OM1 expressed approximately 6-fold more integrin β4 than did its highly malignant counterpart OM3. This is consistent with previous studies in that changes in integrin-mediated cell adhesive interactions and cytoskeletal organization have been implicated in processes such as tumor cell growth and metastasis (37). Decreased expression of integrin β4 is fairly common in malignant cells (25, 30). It is not clear, however, why expression of this gene continues to increase in OM1 with time in culture, while the cells are spontaneously gaining more characteristics of the malignant phenotype during this same time period. Likewise, in OM3, as would be expected, substantial suppression of the integrin β4 gene occurs between p2 and p16; at p25, however, when the cells are their most tumorigenic, expression of the gene returns to basal.

On the other hand, the MAA A32, CCLB protein, and DOC2 genes were regulated in a manner more consistent with a role in acquisition of the phenotypic characteristics of transformation. The more rapid induction of these genes in OM3 as compared to OM1 and/or the higher levels of expression in the more malignant cells at p25 suggest that the products of these genes may be markers of the malignant process.

These findings are consistent with previous work on the MAA A32 and CCLB protein genes. The MAA A32, also designated as MUC18 cell surface glycoprotein, is a marker of tumor progression in human melanoma (38). The expression of this antigen by melanoma cells may contribute to their interaction with elements of the vascular system, an essential step in metastatic dissemination. The CCLB protein is a mitotic phosphoprotein that is upregulated in cancer cells in correlation with their invasive and metastatic phenotype (39,40). Interestingly, the time-dependent changes in expression of the DOC2 gene in OM1 and OM3 suggest that it might be involved in acquisition of malignant characteristics that support tumor formation in immunocompromised mice. Increased expression of the DOC2 gene is a late event in the malignant conversion of OM3, occurring several weeks after the cells gain the ability to grow in methylcellulose. However, the fact that this gene is also overexpressed in the non-malignant As-High as compared to its control makes the issue more complicated. Previous studies by Mok *et al.* (41) demonstrated that the DOC2 gene was expressed in normal ovarian surface epithelial cells, but was silent in every ovarian cancer cell line analyzed. Despite the fact that a previous study linked the DOC2 gene to the cell cycle and demonstrated that its expression rapidly increases following mitotic stimulation, the exact biological function of the DOC2 gene remains unclear (42).

Genes further analyzed in As and the metal-mixture treated RHEK-1 populations were XRCC1, K8, and K18 for As-High and MT3 and MAPKK6 for Mix-high cells. The human XRCC1 gene product has been reported to correct defective DNA strand break repair and sister chromatid exchange (43); induction of this gene in cells treated chronically with As may well be the normal response to the clastogenic activities of the

metal through oxidative stress or other types of DNA-damage. The two simple epithelial cytokeratins, K8 and K18, have been shown to be highly expressed in several epithelial cancers, including ovarian carcinoma (44). These genes are only expressed in keratinocytes under abnormal, i.e. during malignant progression, conditions. Their suppression in As-treated RHEK-1 cells is consistent with the inhibition of spontaneous cell transformation in this cell type. Induction of MT3 expression in Mix-High populations was not surprising due to the presence of As and Cd in the metal mixture; the role of MT3 in this case is likely a detoxification response as the protein acts to sequester various metals in cells and is highly inducible by Cd (45). MAPKK6 is activated by the treatment of cells with agents such as TNF and is involved in phosphorylation and activation of the p38 MAP kinase signal transduction pathway (46,47). Repression of MAPKK6 in Mix-High cells correlates with the poor tumorigenic potential of this cell population, as compared to the moderately tumorigenic Mix-Con cells.

We were highly interested in genes that were altered, either in an opposite or similar manner, in RHEK-1 by more than one chemical treatment. These genes, if expressed in a manner consistent with a role in transformation, i.e. oppositely regulated by MNNG and the As/Mixture treatments, may potentially provide us with candidate molecular markers for malignant conversion in this cell type. In our microarray studies, genes that fell into this category included MIC1, bikunin, MTS1, BMP4, and RAD23A.The MIC1 gene, which is expressed at high levels in OM3 and repressed in As-High and Mix-High populations, encodes a novel macrophage inhibitory cytokine, and is thought to limit the later phases of macrophage activation. To date, functional significance of this gene during cellular transformation has not been documented.

However, MIC1 is a divergent member of the TGFβ superfamily, some members of which are highly active in keratinocytes (48). Overexpression of this gene could potentially be involved in altered growth regulation and/or altered invasive ability in the malignant OM3 cells. Loss of sensitivity to TGFβ1 is a late, but consistent, event in the process of malignant transformation of virtually all cells of epithelial or hematopoietic origin *in vitro* (49). Many transformed cells express TGFβ; production of the cytokine by resistant tumor cells could potentially give them a substantial growth advantage over sensitive, surrounding normal cells. The remaining four genes bikunin, MTS1, BMP4, and RAD23A were all significantly repressed in OM3 and induced in the non-malignant populations derived from chronic As or metal mixture treatment. Evidence would support a potential roles for any/or each these genes in the carcinogenic process in keratinocytes. The bikunin (hepatocyte growth factor activator inhibitor) gene has been implicated in the inhibition of invasion in human chondrosarcoma and glioblastoma cells (50, 51). Reduced expression of bikunin may well be involved in the progression of those two human cancers. MTS1 (p16-INK4) is a potent inhibitor of cyclin/cycin-dependent kinase complexes and thus acts as an important tumor suppressor in many tissues (52). Abnormalities in this gene, which controls the G_1 checkpoint, can lead to both escape from senescence and cancer formation. MTS1 gene is deleted or mutated with high frequency in human melanoma cell lines and familial melanoma patients (52). The TGFβ-like BMP4 gene was originally identified by their bone-inducing activity (53). The roles of BMP4 in carcinogenesis are not documented yet. One functional role suggested by Glozak and Rogers (54) is that it may induce apoptosis in some cells (i.e., embryonal carcinoma cells). A human homologue of yeast RAD23A, HHR23A, is a nucleotide

excision repair complex involving the xeroderma pigmentosum group C protein. The normal function of this gene product is important for prevention of skin cancer (55). Like XRCC1, one strong possibility is that induction of RAD23A in As and metal mixture treated cells is a stress response to oxidative or DNA damage.

The vimentin gene, along with the DOC2 gene as discussed above, was induced in OM3 and As-High populations, but repressed in cells treated with the metal mixture. Overexpression of the vimentin gene, an intermediate filament protein, has been associated previously with the cancer phenotype. In human breast carcinomas, vimentin is frequently observed in cancer cells and correlates with increased malignancy (56). In addition, Moch *et al.*, demonstrated overexpression of vimentin in the two most common subtypes (clear cell and papillary) of renal cell carcinoma (57) as compared to normal kidney tissue. There are several possible explanations for the expression pattern we observe with the DOC2 and vimentin genes: One possibility is that the genes are completely unrelated to the process of transformation in RHEK-1 and are merely indirect results of a bevy of gene expression alterations in chemically-treated cells. Additionally, expression of the gene(s) may be associated with, but not sufficient for malignant conversion and in As-High cells, other gene products interfere in the process.

The overall goal of our studies is to identify potential target genes involved in chronic toxicity and carcinogenic activity of environmentally relevant chemicals and chemical mixtures in human epidermal keratinocytes. To this end, we have utilized cDNA microarray analysis and Real Time RT-PCR validation to correlate gene expression changes in chemically-treated RHEK-1 cells with time-sensitive acquisition of transformation-associated characteristics. Once candidate genes have been identified,

more mechanistic studies will be used to confirm the role of these genes in carcinogenic conversion of RHEK-1. This work should aid us greatly in our pursuit of reliable toxicity markers for use in computational risk assessment approaches.

ACKNOWLEDGEMENT

This study was supported by the Agency for Toxic Substances and Disease Registry (ATSDR) Cooperative Agreement U61/ATU881475, and the National Institute for Environmental Health Sciences (NIEHS) Superfund Basic Research Program Project P42 ES05949.

REFERENCES

1. Bae, D.S., Hanneman, W.H., Yang, R.S.H. and Campain, J.A. (2002) Characterization of gene expression changes associated with MNNG, arsenic, or metal mixture treatment in human keratinocytes: Application of cDNA microarray technology. *Environ. Health Perspect. Suppl.* (In Press)

2. Bae, D.S., Gennings, C., Carter, Jr., W.H., Yang, R.S.H., and Campain, J.A. (2001). Toxicological interactions among arsenic, cadmium, chromium, and lead in human keratinocytes. *Toxicol. Sci.* **63**, 132-142.

3. Cohen, M. D., Kargacin, C. B., Klein, C. B., and Costa, M. (1993). Mechanisms of chromium carcinogenicity and toxicology. *Crit. Rev. Toxicol.* **23**, 255-281.

4. Germolec, D. R., Spalding, J., Boorman, G. A., Wilmer, J. L., Yoshida, T., Simeonova, P. P., Bruccoleri, A., Kayama, F., Gaido, K., Tennant, R., Burleson, F., Dong, W., Lang, R. W., and Luster, M. I. (1997). Arsenic can mediate skin neoplasia by chronic stimulation of keratinocyte-derived growth factors. *Mut. Res.* **386**, 209-218.

5. Germolec, D. R., Yoshida, T., Gaido, K., Wilmer, J. L., Simeonova, P. P., Kayama, F., Burleson, F., Dong, W., Lang, R. W., and Luster, M. I. (1996). Arsenic induces overexpression of growth factors in human keratinocytes. *Toxicol. Appl. Pharmacol.* **141**, 308-318.

6. Kachinskas, D. J., Qin, Q., Phillips, M. A., and Rice, R. A. (1997). Arsenate suppression of human keratinocyte programming. *Mut. Res.* **386**, 253-261.

7. Ye, J., Zhang, X., Young, H. A., Mao, Y., and Shi, X. (1995). Chromium(VI)-induced nuclear factor-kB activation in intact cells via free radical reactions. *Carcinogenesis* **16**, 2401-2405.

8. Yen, H.-T., Chiang, L.-C., Wen, K.-H., Chang, S.-F., Tsai, C.-C., Yu, C.-L., and Yu, H.-S. (1996). Arsenic induces interleukin-8 expression in cultured keratinocytes. *Arch. Dermatol. Res.* **288**, 716-717.

9. Germolec, D. R., Spalding, J., Yu, H.-S., Chen, G. S., Simeonova, P. P., Humble, M. C., Bruccoleri, A., Boorman, G. A., Foley, J. F., Yoshida, T., and Luster, M. I. (1998). Arsenic enhancement of skin neoplasia by chronic stimulation of growth factors. *Am.J.Pathol.* **153**, 1775-1785.

10. Glick, A. B., Sporn, M. B., and Yuspa, S. H. (1991). Altered regulation of TGF-beta 1 and TGF-alpha in primary keratinocytes and papillomas expressing v-Ha-ras. *Mol.Carcinog.* **4**, 210-219.

11. Harper, J. R., Reynolds, S. H., Greenhalgh, D. A., Strickland, J. E., Lacal, J. C., and Yuspa, S. H. (1987). Analysis of the rasH oncogene and its p21 product in chemically induced skin tumors and tumor-derived cell lines. *Carcinogenesis* **8**, 1821-1825.

12. Lehman, T. A., Modali, R., Boukamp, P., Stanek, J., Bennett, W. P., Welsh, J. A., Metcalf, R. A., Stampfer, M. R., Fusenig, N., Rogan, E. M., and . (1993). p53 mutations in human immortalized epithelial cell lines. *Carcinogenesis* **14**, 833-839.

13. Yang, J. H., Vogel, C., and Abel, J. (1999). A malignant transformation of human cells by 2,3,7,8-tetrachlorodibenzo- p-dioxin exhibits altered expressions of growth regulatory factors. *Carcinogenesis* **20**, 13-18.

14. Eisen, M. B., Spellman, P. T., Brown, P. O., and Botstein, D. (1998). Cluster analysis and display of genome-wide expression patterns. *Proc.Natl.Acad.Sci. U.S.A* **95**, 14863-14868.

15. Huang, J., DeGraves, F.J., Gao, D., Feng, P., Schlapp, T., and Kaltenboeck, B. (2001) Quantitative detection of *Chlamydia spp.* by fluorescent PCR in the LightCycler. *BioTechniques* **30**, 150-157.

16. Rajeevan, M. S., Vernon, S. D., Taysavang, N., and Unger, E. R. (2001). Validation of array-based gene expression profiles by real-time (kinetic) RT-PCR. *J Mol.Diagn.* **3**, 26-31.

17. Waters, K. M., Safe, S., and Gaido, K. W. (2001). Differential gene expression in response to methoxychlor and estradiol through ERalpha, ERbeta, and AR in reproductive tissues of female mice. *Toxicol.Sci* **63**, 47-56.

18. Shultz, V. D., Phillips, S., Sar, M., Foster, P. M., and Gaido, K. W. (2001). Altered gene profiles in fetal rat testes after in utero exposure to di(n-butyl) phthalate. *Toxicol.Sci* **64**, 233-242.

19. Huang, Q., Dunn, R. T., Jayadev, S., DiSorbo, O., Pack, F. D., Farr, S. B., Stoll, R. E., and Blanchard, K. T. (2001). Assessment of cisplatin-induced nephrotoxicity by microarray technology. *Toxicol.Sci* **63**, 196-207.

20. Rhim, J.S., Jay, G., Arnstein, P., Price, F.M., Sanford, K.K., and Aaronson, S.A. (1985) Neoplastic transformation of human epidermal keratinocytes by AD12-SV40 and Kirsten Sarcoma Viruses. *Science* **277**, 1250-1252.

21. Solum,D.T. and Handa,R.J. (2002) Estrogen regulates the development of brain-derived neurotrophic factor mRNA and protein in the rat hippocampus. *J Neurosci.* **22**, 2650-2659.

22. Alon, U., Barkai, N., Notterman, D. A., Gish, K., Ybarra, S., Mack, D., and Levine, A. J. (1999). Broad patterns of gene expression revealed by clustering analysis of tumor and normal colon tissues probed by oligonucleotide arrays. *Proc.Natl.Acad Sci U.S.A* **96**, 6745-6750.

23. Backert, S., Gelos, M., Kobalz, U., Hanski, M. L., Bohm, C., Mann, B., Lovin, N., Gratchev, A., Mansmann, U., Moyer, M. P., Riecken, E. O., and Hanski, C. (1999). Differential gene expression in colon carcinoma cells and tissues detected with a cDNA array. *Int.J Cancer* **82**, 868-874.

24. DeRisi, J., Penland, L., Brown, P. O., Bittner, M. L., Meltzer, P. S., Ray, M., Chen, Y., Su, Y. A., and Trent, J. M. (1996). Use of a cDNA microarray to analyse gene expression patterns in human cancer. *Nat.Genet.* **14**, 457-460.

25. Hellmann, G. M., Fields, W. R., and Doolittle, D. J. (2001). Gene expression profiling of cultured human bronchial epithelial and lung carcinoma cells. *Toxicol.Sci* **61**, 154-163.

26. Khan, J., Simon, R., Bittner, M., Chen, Y., Leighton, S. B., Pohida, T., Smith, P. D., Jiang, Y., Gooden, G. C., Trent, J. M., and Meltzer, P. S. (1998). Gene expression profiling of alveolar rhabdomyosarcoma with cDNA microarrays. *Cancer Res.* **58**, 5009-5013.

27. Maxwell, S. A. and Davis, G. E. (2000). Differential gene expression in p53-mediated apoptosis-resistant vs. apoptosis-sensitive tumor cell lines. *Proc.Natl.Acad.Sci.U.S.A* **97**, 13009-13014.

28. Perou, C. M., Jeffrey, S. S., van de, R. M., Rees, C. A., Eisen, M. B., Ross, D. T., Pergamenschikov, A., Williams, C. F., Zhu, S. X., Lee, J. C., Lashkari, D., Shalon, D., Brown, P. O., and Botstein, D. (1999). Distinctive gene expression patterns in human mammary epithelial cells and breast cancers. *Proc.Natl.Acad Sci U.S.A* **96**, 9212-9217.

29. Scherf, U., Ross, D. T., Waltham, M., Smith, L. H., Lee, J. K., Tanabe, L., Kohn, K. W., Reinhold, W. C., Myers, T. G., Andrews, D. T., Scudiero, D. A., Eisen, M. B., Sausville, E. A., Pommier, Y., Botstein, D., Brown, P. O., and Weinstein, J. N. (2000). A gene expression database for the molecular pharmacology of cancer. *Nat.Genet.* **24**, 236-244.

30. Shim, C., Zhang, W., Rhee, C. H., and Lee, J. H. (1998). Profiling of differentially expressed genes in human primary cervical cancer by complementary DNA expression array. *Clin.Cancer Res* **4**, 3045-3050.

31. Wang, K., Gan, L., Jeffery, E., Gayle, M., Gown, A. M., Skelly, M., Nelson, P. S., Ng, W. V., Schummer, M., Hood, L., and Mulligan, J. (1999). Monitoring gene expression profile changes in ovarian carcinomas using cDNA microarray. *Gene* **229**, 101-108.

32. Welsh, J. B., Zarrinkar, P. P., Sapinoso, L. M., Kern, S. G., Behling, C. A., Monk, B. J., Lockhart, D. J., Burger, R. A., and Hampton, G. M. (2001). Analysis of gene expression profiles in normal and neoplastic ovarian tissue samples identifies candidate molecular markers of epithelial ovarian cancer. *Proc.Natl. Acad Sci U.S.A* **98**, 1176-1181.

33. West, M., Blanchette, C., Dressman, H., Huang, E., Ishida, S., Spang, R., Zuzan, H., Olson, J. A., Jr., Marks, J. R., and Nevins, J. R. (2001). Predicting the clinical status of human breast cancer by using gene expression profiles. *Proc.Natl.Acad Sci U.S.A* **98**, 11462-11467.

34. Wong, K. K., Cheng, R. S., and Mok, S. C. (2001). Identification of differentially expressed genes from ovarian cancer cells by MICROMAX cDNA microarray system. *Biotechniques* **30**, 670-675.

35. Zhang, L., Zhou, W., Velculescu, V. E., Kern, S. E., Hruban, R. H., Hamilton, S. R., Vogelstein, B., and Kinzler, K. W. (1997). Gene expression profiles in normal and cancer cells. *Science* **276**, 1268-1272.

36. Zhang, M., Martin, K. J., Sheng, S., and Sager, R. (1998). Expression genetics: a different approach to cancer diagnosis and prognosis. *Trends Biotechnol.* **16**, 66-71.

37. Gille, J. and Swerlick, R. A. (1996). Integrins: role in cell adhesion and communication. *Ann N.Y.Acad Sci* **797**, 93-106.

38. Lehmann, J. M., Riethmuller, G., and Johnson, J. P. (1989). MUC18, a marker of tumor progression in human melanoma, shows sequence similarity to the neural cell adhesion molecules of the immunoglobulin superfamily. *Proc.Natl.Acad Sci U.S.A* **86**, 9891-9895.

39. Jackers, P. (1996) Isolation from a multigene family of the active human gene of metastasis-associated multifunctional protein 37LRP/p40 at chromosome 3p21.3. *Oncogene* **13**, 495-503.

40. Clausse, N., van den, B. F., Delvenne, P., Jacobs, N., Franzen-Detrooz, E., Jackers, P., and Castronovo, V. (1998). TNF-alpha and IFN-gamma down-regulate the expression of the metastasis- associated bi-functional 37LRP/p40 gene and protein in transformed keratinocytes. *Biochem.Biophys.Res Commun.* **251**, 564-569.

41. Mok, S. C., Wong, K. K., Chan, R. K., Lau, C. C., Tsao, S. W., Knapp, R. C., and Berkowitz, R. S. (1994). Molecular cloning of differentially expressed genes in human epithelial ovarian cancer. *Gynecol.Oncol.* **52**, 247-252.

42. Xu, X. X., Yang, W., Jackowski, S., and Rock, C. O. (1995). Cloning of a novel phosphoprotein regulated by colony-stimulating factor 1 shares a domain with the Drosophila disabled gene product. *J Biol.Chem.* **270**, 14184-14191.

43. Thompson, L. H., Brookman, K. W., Jones, N. J., Allen, S. A., and Carrano, A. V. (1990). Molecular cloning of the human XRCC1 gene, which corrects defective DNA strand break repair and sister chromatid exchange. *Mol.Cell Biol.* **10**, 6160-6171.

44. Trask, D. K., Band, V., Zajchowski, D. A., Yaswen, P., Suh, T., and Sager, R. (1990). Keratins as markers that distinguish normal and tumor-derived mammary epithelial cells. *Proc.Natl.Acad Sci U.S.A* **87**, 2319-2323.

45. Hellemans, G., Soumillion, A., Proost, P., Van Damme, J., Van Poppel, H., Baert, L., and De Ley, M. (1999). Metallothioneins in human kidneys and associated tumors. *Nephron* **83**, 331-340.

46. Raingeaud, J., Whitmarsh, A. J., Barrett, T., Derijard, B., and Davis, R. J. (1996). MKK3- and MKK6-regulated gene expression is mediated by the p38 mitogen-activated protein kinase signal transduction pathway. *Mol.Cell Biol.* **16**, 1247-1255.

47. Chiariello, M., Marinissen, M. J., and Gutkind, J. S. (2000). Multiple mitogen-activated protein kinase signaling pathways connect the cot oncoprotein to the c-jun promoter and to cellular transformation. *Mol.Cell Biol.* **20**, 1747-1758.

48. Bootcov, M. R., Bauskin, A. R., Valenzuela, S. M., Moore, A. G., Bansal, M., He, X. Y., Zhang, H. P., Donnellan, M., Mahler, S., Pryor, K., Walsh, B. J., Nicholson, R. C., Fairlie, W. D., Por, S. B., Robbins, J. M., and Breit, S. N. (1997). MIC-1, a novel macrophage inhibitory cytokine, is a divergent member of the TGF-beta superfamily. *Proc.Natl.Acad Sci U.S.A* **94**, 11514-11519.

49. Fynan, T. M. and Reiss, M. (1993). Resistance to inhibition of cell growth by transforming growth factor-beta and its role in oncogenesis. *Crit Rev.Oncog.* **4**, 493-540.

50. Suzuki, M., Kobayashi, H., Fujie, M., Nishida, T., Takigawa, M., Kanayama, N., and Terao, T. (2002). Kunitz-type protease inhibitor bikunin disrupts phorbol ester-induced oligomerization of CD44 variant isoforms containing epitope v9 and subsequently suppresses expression of urokinase-type plasminogen activator in human chondrosarcoma cells. *J Biol.Chem.* **277**, 8022-8032.

51. Hamasuna, R., Kataoka, H., Meng, J. Y., Itoh, H., Moriyama, T., Wakisaka, S., and Koono, M. (2001). Reduced expression of hepatocyte growth factor activator inhibitor type- 2/placental bikunin (HAI-2/PB) in human glioblastomas: implication for anti-invasive role of HAI-2/PB in glioblastoma cells. *Int.J Cancer* **93**, 339-345.

52. Luca, M., Xie, S., Gutman, M., Huang, S., and Bar-Eli, M. (1995). Abnormalities in the CDKN2 (p16INK4/MTS-1) gene in human melanoma cells: relevance to tumor growth and metastasis. *Oncogene* **11**, 1399-1402.

53. Wozney, J. M., Rosen, V., Celeste, A. J., Mitsock, L. M., Whitters, M. J., Kriz, R. W., Hewick, R. M., and Wang, E. A. (1988). Novel regulators of bone formation: molecular clones and activities. *Science* **242**, 1528-1534.

54. Glozak, M. A. and Rogers, M. B. (1996). Specific induction of apoptosis in P19 embryonal carcinoma cells by retinoic acid and BMP2 or BMP4. *Dev.Biol.* **179**, 458-470.

55. Masutani, C., Sugasawa, K., Yanagisawa, J., Sonoyama, T., Ui, M., Enomoto, T., Takio, K., Tanaka, K., van der Spek, P. J., Bootsma, D., Hoeijmakers, J.H. and Hanaoka, F. (1994). Purification and cloning of a nucleotide excision repair complex involving the xeroderma pigmentosum group C protein and a human homologue of yeast RAD23. *EMBO J* **13**, 1831-1843.

56. Dandachi, N., Hauser-Kronberger, C., More, E., Wiesener, B., Hacker, G. W., Dietze, O., and Wirl, G. (2001). Co-expression of tenascin-C and vimentin in human breast cancer cells indicates phenotypic transdifferentiation during tumour progression: correlation with histopathological parameters, hormone receptors, and oncoproteins. *J Pathol.* **193**, 181-189.

57. Moch, H., Schraml, P., Bubendorf, L., Mirlacher, M., Kononen, J., Gasser, T., Mihatsch, M. J., Kallioniemi, O. P., and Sauter, G. (1999). High-throughput tissue microarray analysis to evaluate genes uncovered by cDNA microarray screening in renal cell carcinoma. *Am.J.Pathol.* **154**, 981-986

CHAPTER 5

Genomic Analyses on Four Chemically Transformed RHEK-1 Cell Lines

Dong-Soon Bae, Johng S. Rhim, Rusty S. Thomas, Raymond S.H. Yang, and Julie A. Campain

Abstract

We were interested in identifying genes commonly affected in the immortal RHEK-1 cells transformed by chemical agents, 1-methyl-3-nitro-1-nitrosoguanidine (MNNG), 4-nitroquinoline-1-oxide (NQO), and 2,3,7,8-tetrachlorodibenzo-*p*-dioxin (TCDD) using cDNA microarray methodology. To this end, Clontech Human 3.8 II DNA microarrays were analyzed in triplicate in chemically-transformed versus control RHEK-1 cell lines. Differentially expressed genes in the various cell populations were identified by calculating the expression ratio in tretaed versus control. The co-regulated genes among chemically-transformed cell lines were graphically visualized by performing two-dimensional hierarchical cluster analysis. The coefficient of variation among 3 replicates for all genes spotted on arrays ranged from 1.7 % to 13. 7 % in the five RHEK-1 cell lines, which included an universal vehicle-control cell line. After a rigorous data reduction process, a common suite of gene expression alterations were identified in RHEK-1 strains transformed by MNNG, NQO, TCDD; in addition, genes were identified that were altered in a chemical-specific manner. Several oncogenes, genes involved in

control of cell growth/cell motility, and one recombination signal binding protein gene were induced in all four malignant RHEK-1 cell lines. In contrast, genes implicated in functional categories for apoptosis, cell-cell interaction, and the immune surveillance system were commonly suppressed. The following chemical-specific changes were demonstrated: (1) in the two MNNG-transformed cells, two markers for malignancy, CD24 antigen and jumping translocation breakpoint, were highly induced; (2) for NQO-transformed cells, friend leukemia virus integration 1 oncogene and cystatin F, which is involved in metastasis, were up regulated; and (3) two genes, core-binding factor and internexin neuronal intermediate filament protein α, involved in human leukemia were induced, while a complement component 1 q subcomponent was suppressed in TCDD-transformed cells. In total, 34 molecular markers were identified that were commonly up or down regulated by chemicals examined in our studies. These genes may be useful for further characterization of the transforming/ carcinogenic potential of untested compounds. The unique battery of genes altered by the individual chemical carcinogens may aid in determining the mechanism of action. We are currently analyzing protein expression changes in the same RHEK-1 cell lines above utilizing proteomic technologies to correlate expression levels between mRNA and its corresponding protein.

Introduction

Recent advances in genomics and bioinformatics allow toxicologists to assess the toxicological effects of xenobiotics on global gene expression at thousands of endpoints simultaneously (Afshari *et al.*, 1999; Nuwaysir *et al.*, 1999). Applications of these technologies in toxicology have been demonstrated in toxicity/safety screening.

mechanistic studies, classification of chemicals, and risk assessment. The information obtained from global gene expression analysis will allow investigators to target selected genes and to generate mechanistic hypotheses based upon the results obtained. Also, gene expression studies on known toxicants provide useful "biosignatures" that will be particularly valuable biomarkers in characterizing new and novel chemicals. The development of a screen via gene expression profiling would allow prioritization of untested chemicals based upon their toxic potential and would have significant impact on how cost-effectively we evaluate chemicals of interest.

For the last few years there have been many publications in the field of toxicology successfully demonstrating the utility of microarray analysis. First, for predictive toxicology, gene expression profiling has been performed to classify relatively well-characterized chemicals based upon the distinct expression profile for each different mode of action (i.e., hepatotoxins, DNA-damaging agents, cytotoxic anti-inflammatory drugs, etc.) (Burczynskin *et al.*, 2000; Hamadeh *et al.*, 2002a and 2002b; Thomas *et al.*, 2001, Waring *et al.*, 2001a and 2001b). These studies supported the hypothesis that gene expression profiles that correspond to different chemicals can be distinguished and that chemicals that work through similar mechanism of action alter similar groups of genes. For example, Thomas and colleagues (2001) accurately classified 24 chemical treatments into the 5 toxicological classes (peroxisome proliferators, aryl hydrocarbon receptor agonists, noncoplanar polychlorinated biphenyls, inflammatory agents, and hypoxia-inducing agents) based upon a diagnostic set of 12 transcripts found from cDNA microarrays. Second, for mechanistic toxicology, microarray analysis has been utilized to measure global gene expression patterns and thus, identify batteries of genes/pathways

potentially involved in individual chemical (i.e., sodium arsenite, dioxin, cisplatin, etomoxir, or di(n-butyl) phthalate)-induced toxicity (Huang *et al.*, 2001; Merrill *et al.*, 2002; Puga *et al.*, 2000; Shultz *et al.*, 2001; Yih *et al.*, 2002). In a recent study by Merrill *et al.* (2002), a mechanism for etomoxir (antidiabetic agent) toxicity was suggested by detecting differential expression of genes involved in oxidative stress and mitochondrial energy metabolism using the Human Stress Toxicology cDNA Arrays. The implication from array data for a potential mechanism for etomoxir toxicity, induced oxidative stress and impaired mitochondrial energy metabolism, was further confirmed by biochemical assays such as measurements of levels for GSH/GSSG, mitochondrial membrane potential, ATP, and superoxides (Merrill *et al.*, 2002).

The purpose of the study described here in Chapter 5 was to measure mRNA expression in four previously established and chemically transformed RHEK-1 cell lines utilizing DNA microarrays to identify a common battery of genes associated with chemically-mediated neoplastic transformation. Also, we attempted to identify genes that specifically discriminate one chemical from another. The findings from gene expression profiling of malignant RHEK-1 cell lines are discussed.

Materials and Methods

RHEK-1 cell lines analyzed in these studies

A total of five established RHEK-1 cell lines were examined for global gene expression profiling in the current studies. Three RHEK-1 cell lines [(1) F-4980; FNR-325H 5/0.01; (2) F-5063; 129Nu1913 Su-1; and (3) F-8904; TCDD-3/RHEK-1] previously transformed by the treatment with 0.01μg/ml MNNG, 0.1μg/ml NQO, or 3nM TCDD,

respectively, were obtained from Dr. J. Rhim at CPDR (Rockville, MD) (Rhim *et al.*, 1986; Yang *et al.*, 1992). The detailed protocol to establish these 3 cell lines is described in Rhim *et al.* (1986) and Yang *et al.* (1992). Two RHEK-1 cell lines established in our laboratory at CETT were OM3 and OM1; these lines are a malignant RHEK-1 clone transformed by MNNG and its solvent control (0.5% DMSO), respectively. The protocol used to obtain the OM3 and OM1 cell lines was described in Bae *et al.*, (2002). The following designation was used to describe transformed RHEK-1 lines in Chapter 5: the cell line transformed by the treatment with 0.01, 0.1μg/ml MNNG, NQO, or TCDD was described as MNNG1, MNNG2, NQO, or TCDD, respectively. One vehicle-treated RHEK-1 cell population was designated as OM1 that serves as a passage-matched control in current studies. All four chemically transformed cell lines have the capability of growing in an anchorage independent manner and forming highly malignant tumors in nude mice. The passage matched control for the three cell lines from Dr. J. Rhim was not available, thus the OM1 cell line from our laboratory was utilized as a universal control to study differential gene expression in chemically-treated RHEK-1 populations.

RNA isolation

The protocol to isolate total RNA from cultures of control and the four chemically-transformed RHEK-1 cells at a different passage is described in Bae *et al.* (2002). Briefly, cryo-preserved frozen stocks of cells at p25, p6, and p21 for MNNG1, NQO, and TCDD-transformed cell lines, respectively, and both OM1 and MNNG2 cells at p25 were brought up and cultured in three T-75 cm^2 flasks per each cell line. The reasons for analyzing NQO and TCDD cell lines at p6 and p21, respectively, were that those

particular passage cells were the cells tested for positive in tumorigenicity assay and those passage cells were only available from Dr. J. Rhim. Cells from 3 flasks were pooled together for RNA isolation.

cDNA synthesis and fluorescent labeling for the Human 3.8 II array

Total RNA (5 μg per reaction) was reverse transcribed from each test sample with PowerScript™ reverse transcriptase and random primer mix in triplicate. Untranscribed RNAs were removed by the treatment with RNase H. The cDNAs were purified by filtration with QuickClean resin in a 0.22μm Spin Filter (Clontech, Palo Alto, CA) and collected by precipitation with 3M sodium acetate and 100% ethanol. The DNA pellet was air-dried, dissolved in fluorescent labeling buffer, and then coupled with fluorescent dye to amino-modified first-strand cDNA in the presence of cyanine 3 (Cy3) (for OM1 control) or Cy5 for 4 chemically-transformed cells. Both fluorescent dyes were obtained from Amersham Pharmacia Biotech. The sodium acetate and ethanol precipitation and the consecutive column chromatography via Qiaquick PCR purification Kit (Qiagen, CA) were carried out to purify cDNAs from excess uncoupled dye. Probe quality was assessed by measuring absorbance at 260, 280, 450, 550, and 650 nm for the Cy3-labeled samples or 260, 280, 520, 650, and 750 nm for the Cy5-labeled samples using UV/VIS spectrophotometry. The absolute amount of labeled probe was quantified by measuring Cy3 absorbance at 550nm and Cy5 absorbance at 650 nm. The A_{650} for Cy3 and A_{750} for Cy5 measurement provide a baseline adjustment. The labeled probe was added to the prewarmed (50°C) GlassHyb Hybridization Solution and then added to the array in the plastic hybridization chamber (Clontech). Overnight hybridization was performed at 50°C

in an upright position in a test tube rack. After four consecutive washes at room temperature in GlassHyb Wash Solution once, GlassHyb Wash Solution + 1X SSC twice, and 0.1X SSC once, the glass slide was placed in a dry Wash Container (Clontech) and centrifuged at 1,000 x g for 5 min to remove excess liquid prior to scanning. The slide was scanned in a BioChip Imager (Packard, Meriden, CT). Laser and photo multiplier (PMT) voltages were adjusted manually to maximize signal-to-noise ratio. Cy3 and Cy5 signal intensities were standardized relative to one another by comparing the total signal intensities of all spots in each channel. The scanner output images were quantified using ScanAlyze (Michael Eisen, University of California at Berkeley).

Cluster analysis and other statistical analysis

Before cluster analysis (Eisen *et al.*, 1998), the array data output from ScanAlyze analysis was adjusted to achieve median centering of genes for the current experimental design where we are looking at 4 RHEK-1 transformed cell lines compared to a common reference sample (OM1). For each gene, we have a series of ratio values that are relative to the expression level of that gene in OM1. This is achieved by adjusting the values of each gene to reflect their variation from some property of the series of observed values such as the median. This is what median centering of genes does. Centering the data for arrays can also be used to remove certain types of biases. The results of many two-color fluorescent hybridization experiments are not corrected for systematic biases in ratios that are the result of differences in RNA amounts, labeling efficiency and image acquisition parameters. Median centering the data has the effect of correcting this bias (Eisen, 1998).

The median polished data set was loaded into Cluster software and then filtered to remove genes that have negative (background is higher than spot intensity) ratio in any of

triplicate experiments. The Cluster software assembles a set of genes (or arrays) into a tree, where genes are joined by very short branches if they are very similar to each other, and by increasingly longer branches as their similarity decreases. The similarity metrics in current studies are based on Pearson correlation which is the most commonly used. Finally, 2 dimensional hierarchical clustering was performed via Cluster and visualized in TreeView software.

For calculation of correlation coefficient for assessing variability in triplicate array experiments, Microsoft Excel program was utilized. One-way ANOVA followed by Dunnett's test was performed to analyze differences between control and chemical-treated RHEK-1 cell lines in gene expression profiling studies.

Results

To identify commonly or uniquely regulated genes in tumorigenic RHEK-1 keratinocytes, the global gene expression analysis of 3,757 sequence-verified human genes on Clontech Human 3.8II Array was performed in 4 cell lines obtained by exposure to MNNG, NQO, or TCDD. Since studies conducted here were aimed at identifying potential markers for chemical carcinogenesis, one global array type with a high-density glass format was selected instead of a more focused array with a low-density of genes.

When we designed the *in vitro* gene expression profiling of RHEK-1 cell lines, there was no standardized method for calculating the number of experimental replicates to achieve statistical significance given an experimental protocol. Only one published article addressed the importance of replication at that time (Lee *et al.*, 2000). To greatly reduce misclassification (either false positive or false negative) and enhance reliability in array results, at least 3 replicates should be used in designing experiments using cDNA microarrays, particularly when gene expression data from single specimens are being analyzed (Lee *et al.*, 2000). According to recommendations, triplicate arrays were analyzed with 3 separate probe labelings and hybridizations; RNA was from a pooled sample from each cell line treated in an identical manner. In the current studies, there were chip replicates in the experimental design. However, there were not biological replicates; the reason for this is described in Materials and Methods in Chapter 4. The reproducibility within replicate experiments was assessed by plotting the signal intensity of all 3,757 genes for each set of replicates (i.e., replicate 1 vs. replicate 2, replicate 1 vs. replicate 3, and replicate 2 vs. replicate 3) in a scatter plot with a correlation coefficient. One representative scatter plot for the TCDD-transformed RHEK-1 cell line is shown in

Figure 5.1. For the five RHEK-1 cell lines (OM1, MNNG1, MNNG2, NQO, and TCDD) analyzed by DNA microarray technology, the TCDD cell line demonstrated the highest reproducibility in terms of gene expression among 3 replicates with a coefficient of variation, 1.73% (the tightest variation). The Pearson's correlation coefficient (R^2) was 0.9474, 0.9153, and 0.9322, for replicate 1 vs. replicate 2, replicate 1 vs. replicate 3, and replicate 2 vs. replicate 3, respectively. If the expression extent is the same in 3 experiments, all 3,757 genes should be located on a linear line. The coefficient of variation for NQO, MNNG2, MNNG1, and OM1 was 2.38%, 5.6%, 10.1%, and 13.7%, respectively.

The genes commonly and consistently up regulated or down regulated at ≥2-fold ratio in their expression in 4 chemically transformed cell populations over vehicle-treated one (OM1) are shown in Table 5.1 and Table 5.2, respectively. Two selection criteria for choosing these genes were applied: (1) genes consistently altered at ≥2-fold ratio in all triplicate arrays for 4 chemically transformed cell lines, and (2) genes that have a known or putative function based on sequence homology with a gene from a different biological system. The name and known (or putative) function and expression fold of 34 selected genes are listed in Tables 5.1 and 5.2. Several oncogenes, genes involved in control of cell growth/cell motility, and one recombination signal binding protein gene were commonly induced in the 4 chemically transformed RHEK-1 cell lines. In contrast, several functional categories for apoptosis, cell-cell interaction, and immunosurveillance system were commonly suppressed. These 34 genes commonly regulated by chemicals tested in our laboratory may serve as molecular markers for the identification of potential carcinogenic agents in the RHEK-1 model system.

Figure 5.1 Reproducibility testing within 3 replicates for TCDD-transformed RHEK-1 cell line

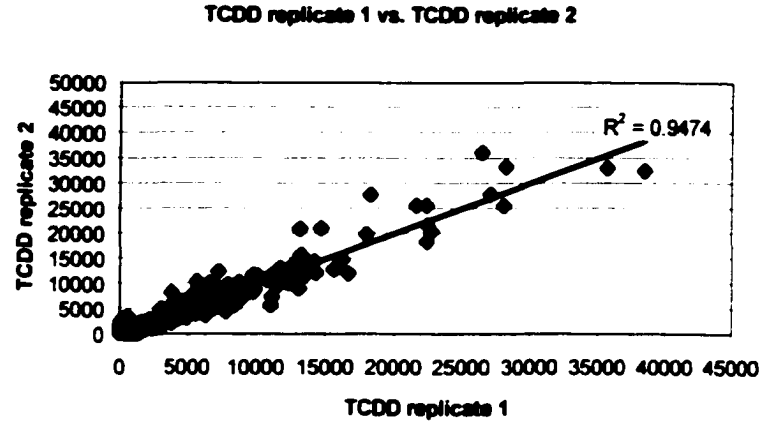

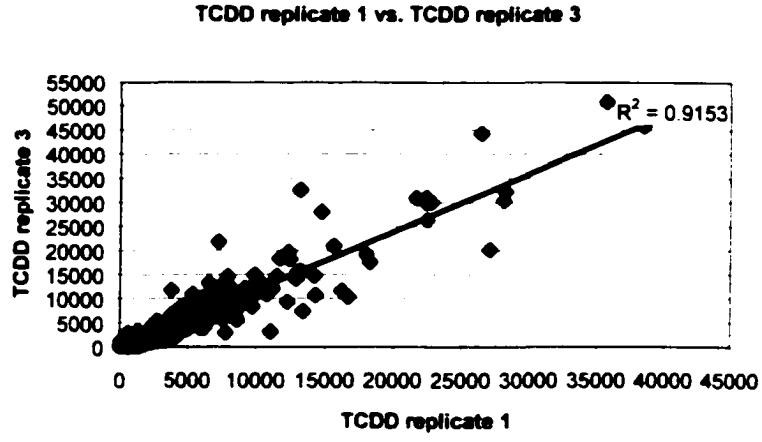

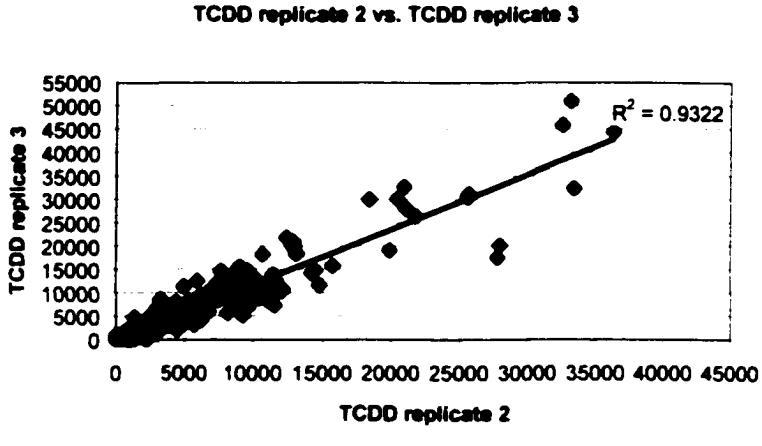

Table 5.1. Genes commonly upregulated by MNNG, NQO, and TCDD in RHEK-1 cells *: gene expression fold in MNNG2, MNNG1, NQO, and TCDD-transformed cell line compared to vehicle-treated cells (left to right)

Name	Fold*	Function(s)
Ca^{2+} activated chloride channel	2.3/2.5/2.3/2.2	Membrane channel
CGI-120 protein	2.6/2.1/2.6/2.8	A novel gene found with Caenorhabditis elegans template
COP9 subunit 6	6.3/5.1/11/2.7	RNA binding & macromolecule assembly; control of cell growth
Differentiation related protein difl3	3.4/8.9/14/2.3	Differentially expressed gene in leukemia cell line k562 differentiation; homology with oncodevelopmental soluble placental tissue protein 17
DNA-directed polymerase κ	9.1/6.1/2.9/3.3	A newly identified low fidelity polymerase
Flavin containing monooxygenase 1	2.6/9.6/2.6/3.1	Chemical metabolism
p21/cdc42/Rac1-activated kinase 1	4.4/4.4/11/2.6	Regulate actin organization/cell motility
Purine-rich element binding protein B	3.9/3.7/6.1/2.3	Histone family
Ras homolog gene family	3.1/8.2/3.4/2.0	Oncogene
Recombining binding protein suppressor of hairless (Drosophila)	3.8/5.1/11/3.5	Recombination signal binding protein gene
RNB6	6.1/25/4.6/3.3	Homology with a novel rat cDNA; control of cell motility through actin filament assembly

Table 5.2. Genes commonly downregulated by MNNG, NQO, and TCDD in RHEK-1 cells *: gene expression fold in MNNG2, MNNG1, NQO, and TCDD-transformed cell line compared to vehicle-treated cells (left to right)

Name	Fold*	Function(s)
Apoptosis-inducing ser/thr kinase 17b	4.4/8.1/4.2/3.4	Apoptosis
Aquaporin 4	3.8/6.2/6.2/3.6	Membrane transporter
Cadherin 12 type 2	4.1/5.7/5.0/3.6	Cell-cell interaction
CD164 antigen, sialomucin	5.3/8.1/5.3/8.6	An adhesive glycoprotein; a novel core protein in gastric carcinoma
CGI-68 protein	9/10/12/10	Leucine carboxyl methyltransferase for protein phosphatase 2A
Cold shock domain protein A	4.4/4.7/4.5/3.4	DNA binding protein
Cytokine receptor-like factor 1	4.1/4.5/3.8/3.2	A novel soluble protein: a possible regulatory role in the immune system
Ephrin A1 (human B61 mRNA)	4.6/18/11/5.7	A novel secreted protein
Fibroblast growth factor (acidic) intracellular binding protein	15/6.4/5.3/4.6	An intracellular protein
G protein-coupled receptor 64	6.0/3.6/3.8/5.3	A novel member of the 7 transmembrane domain receptor family
Homeo box A1 (HOX A1)	3.4/3.4/3.7/3.2	Transcription factor
Low density lipoprotein-related protein 1	3.8/5.9/6.5/4.4	Ca binding cell surface protein
Nebulin	3.0/3.0/3.9/5.5	A giant filamentous protein specific for vertebrate skeletal muscles
Phosphodiesterase 6A, cGMP-specific, rod, α	3.3/3.1/2.4/2.7	Photoreceptor signal transduction
Proprotein convertase subtilisin/kexin type 7	3.7/10/4.7/11	Ca-dependent serine protease prohormone convertase PC8
Rhodopsin kinase	5.1/14/7.0/3.4	β-adrenergic receptor kinase
Serine threonine protein kinase	7.3/6.8/8.4/4.5	Fas-mediated apoptosis
Solute carrier family 11 (proton-coupled divalent metal ion transporters), member 2	5.0/4.1/3.4/2.9	Membrane transporter
Solute carrier family 12 (potassium/chloride transporters), member 7	3.9/3.2/5.3/4.0	Membrane transporter
Solute carrier family 21 (organic anion transporter), member 6	3.1/2.7/3.6/3.0	Membrane transporter
Ubiquilin 2	15/3.9/33/20	Possible involvement in apoptosis
Ubiquitin specific protease 21	4.4/3.5/6.9/4.3	A novel USP23
U2 small nuclear ribonucleoprotein auxiliary factor (65kD)	9.6/8.1/3.4/5.7	An essential mammalian splicing factor

To explore the possibility of classifying chemicals based upon unique expression biosignatures, we attempted to identify chemical-specific gene expression in the 4 different cell lines utilized here. The distinct set of genes altered in their expression in the MNNG, NQO, or TCDD-transformed cell lines is listed in Table 5.3. Ten genes either up- or down-regulated substantially in their expression in each chemically transformed cell line are shown. Since there was less number of genes altered in a chemical-specific manner, less rigorous selection criterion (altered expression in 2 out of 3 replicates at least) was applied to identify the genes in Table 5.3. Few of the chemical-specific genes were well studied with respective to development of malignancy; the majority of genes listed are not yet functionally characterized.

For unique MNNG-regulated genes, two markers for malignant cells, CD24 antigen and jumping translocation breakpoint, were induced at 3.3- and 4.9-fold (average value of triplicate analyses). Another interesting gene associated with carcinogenesis was p53-induced protein. Two interesting genes were specifically expressed at high levels in the NQO-transformed cell line. Those are protein inhibitor cystatin F (30-fold induction) and an ETS oncogene, friend leukemia virus integration (3.7-fold induction). For the TCDD-transformed cell line, 2 genes (core-binding factor and internexin neuronal intermediate filament protein α) implicated in human leukemia were up-regulated at 9-fold and 5-fold, respectively. One gene encoding a complement component 1 q subcomponent involved in immune functions was down regulated at 3-fold in TCDD-transformed cell line. For the remaining 23 genes in Table 5.3, we do not yet have an understanding of the relationship between altered expression and tumorigenesis in RHEK-1 cells.

Table 5.3 Genes uniquely affected by MNNG, NQO, or TCDD in RHEK-1 cells

Chemical	Name	Fold*	Function(s)
MNNG	CD24 antigen	⇑ 3.3 (1.6,6.6,2.0,4.2,4.2,1.4)	Small cell lung & hepatocellular carcinoma antigen
	Hepatocyte nuclear factor 4, γ	⇑ 2.5 (2.6,2.2,2.2)	Transcription factor
	Homeo box A2	⇑ 4.5 (2.2,3.13.5.1)	Developmental regulation
	HSPC037 protein	⇓ 26 (91.45,1,1.4,6,11)	Undefined gene from CD34+ hematopoietic stem/progenitor cells
	Jumping translocation breakpoint	⇑ 4.9 (16,1.9,2.7,5.2,2.3,1.4)	A novel membrane protein: expressed in malignant cells
	Neutral sphingomyelinase	⇓ 14 (29,26,1,1.3,3,23)	Signal transduction
	Pancreas enriched phospholipase Cε	⇓ 4.5 (5.5,9,1,2.6,1.3,7.4)	Signal transduction
	p53-induced protein	⇑ 14 (2.6,2.1,72,2.4,2.6,1.3)	Apoptosis
	REV1 (yeast homolog)-like	⇑ 11 (13.0,1.1,2.47.3)	Required for mutagenesis induced by UV light
	SRY (sex determining region Y)-box 21	⇑ 3.5 (7,2,2,4,2,2)	Transcription factor
NQO	c-type lectin-like receptor 2	⇓ 4.8 (2.1,0,12.4)	Novel lectin-like receptor
	Cystatin F (leukocystatin)	⇑ 30 (84,0.7,6.4)	Liver metastasis: proteinase inhibitor
	Friend leukemia virus integration 1	⇑ 3.7 (3.2,4.8,3.1)	Ets oncogene family
	GS15	⇓ 5.6 (3.7,5.1,7.7)	Golgi SNARE GS15 sequence
	Hyaluronan-mediated motility receptor	⇓ 3.0 (0.3.8,5.1)[a]	Receptor
	ISL1 transcription factor	⇑ 4.1 (0.4.8,7.6)	Transcription factor
	KRAB-zinc finger protein SZF1-1	⇑ 4.6 (4.8,4.4,4.5)	Transcriptional repressor in stem/progenitor cell differentiation
	Protein kinase, AMP-activated, α1 catalytic subunit	⇑ 4 (4.3,3.6,4.2)	Kinase
	Spindle pole body protein	⇓ 4.7 (0.7.1,7.1)[a]	Associated with tubulin
	Usher syndrome 2A (autosomal recessive, mild)	⇑ 6 (7.7,8.0,1.4)	Laminin EGF and fibronectin type III motif: usherin protein

(continued)

Table 5.3 Continued

Chemical	Name	Fold*	Function(s)
TCDD	ANKHZN protein (a novel one)	⇑ 17 (2.4,44,4)	Ankyrin repeats hooked to a zinc finger motif
	Complement component 1, q subcomponent, β polypeptide	⇓ 3.1 (2.3,3.2,3.8)	Antibody-dependent and independent immune functions
	Core-binding factor, runt domain, a subunit 2, translocated to 2	⇑ 8.6 (22,2.4,1.6)	Implicated in human leukemia; positive association with transformation assay
	Fumarate hydratase	⇑ 48 (140,0.5,2.3)	Nuclear gene encoding mitochondrial protein
	Internexin neuronal intermediate filament protein α	⇑ 5.3 (6.2,8.4,1.2)	Pathogenesis of adult T cell leukemia and neurological disorders
	Myosin, heavy polypeptide 3, skeletal muscle, embryonic	⇑ 6.9 (16,2.3,2.4)	Component of skeletal muscle
	Neuromedin U	⇑ 5 (12,1.4,2)	uterine contractile effects; expression in GI tract; a potent agonist at the orphan G protein-coupled receptor FM3
	Semenogelin I	⇓ 4.5 (5.7,3.6,4.1)	Predominant protein in human semen
	Solute carrier family 25 (mitochondrial carrier; adenine nucleotide translocator), member 4	⇓ 2.9 (3.3,3.1,2.4)	Membrane transporter
	WD repeat domain 3	⇑ 5.9 (1.6,14,2.3)	A novel gene may play roles in hematopoietic differentiative progression and lineage commitment

*: Average gene expression fold in chemical-transformed cell line compared to vehicle-treated cells is followed by expression fold of 3 arrays in parenthesis. For MNNG, average fold is shown first in "Fold" column from MNNG1 and MNNG2 data.
#: Hybridization signal is very low.
SNARE: soluble N-ethyl maleimide sensitive factor attachment protein receptor

We were interested in identifying co-regulated gene clusters based on their similarity in expression patterns among 3,757 genes by performing global gene expression studies and subsequently performing cluster analysis in 4 malignantly transformed RHEK-1 cell lines. For each RHEK-1 transformed cell line, the ratio of the expression of each transcript to the expression of the transcript in the control OM1 sample is graphically represented by the color of the corresponding square cell. Green represents down-regulation of the transcript and red represents up-regulation of the transcript. Cells with ratios of 1.0 (genes unchanged) are colored black. Color saturation reflects the magnitude of the change. A dendrogram is shown to indicate the nature of the computed relationship among chemicals in Figure 5.2 (A). As expected MNNG1 and MNNG2 cell lines were clustered together. Interestingly, NQO and TCDD were clustered very closely. Similar clustering patterns were found by running another data analysis and visualization software package AtlasNavigator 1.0 from Clontech. The representative thumbnail image for TCDD and NQO co-regulation vs. MMMG2 and MNNG1 co-regulation is demonstrated in Figure 5.2 (B). This type of cluster was predominant in overall 2-dimentional clustering. The representative TCDD or NQO-specific gene cluster is shown in Figure 5.2 (C). Finally, a representative cluster common to chemical treatment is depicted in Figure 5.2 (D).

(A)

(B)

	Early growth response 2
	Solute carrier family 6
	Tumor protein p53-binding protein 2
	Nuclear factor of kappa light polypeptide gene enhancer in B cells
	Lung type-I cell membrane-associated glycoprotein
	Jumping translocation breakpoint
	Ras inhibitor
	HSPC037 protein

(C)

	ANKHZN protein (a novel one)
	Internexin neuronal intermediate filament protein α
	Cystatin F (leukocystatin)
	Friend leukemia virus integration 1

(D)

	COP9 subunit 6
	Differentiation related protein dif13
	p21/cdc42/Rac1-activated kinase 1
	Ras homolog gene family
	RNB6
	Apoptosis-inducing ser/thr kinase 17b
	Cadherin 12 type 2
	Cytokine receptor-like factor 1
	Serine threonine protein kinase
	Solute carrier family 12 (potassium/chloride transporters), member 7

Ratio Key

Fig. 5.2 A dendrogram (A) and the representative thumbnail for (B) TCDD, NQO vs. MNNG, (C) TCDD and NQO-specific pattern, and (D) commonly regulated genes from Cluster and TreeView Analyses in 4 malignant RHEK-1 cell lines

Discussion

The ultimate goal of the studies described here was to identify gene expression profiles that are reflective of the mechanism of toxicity of chemicals and to generate a reference database on known chemical carcinogens. This database will subsequently be used to determine the carcinogenic potential of unknown chemicals by comparative analysis. It may be feasible to identify a small number of genes to serve as predictive markers for early screening tests for potential carcinogenicity of chemicals. Measurement of mRNA expressions in four previously established and chemically transformed RHEK-1 cell lines utilizing DNA microarrays identified a common battery of genes potentially associated with chemically-mediated neoplastic transformation in RHEK-1 cells. Also, we demonstrated that different chemicals (i.e., MNNG, NQO, TCDD) induce specific gene expression signatures which discriminate one chemical from another.

Rigorous selection criteria were applied when we chose our genes from TreeView for further studies. First, only genes consistently altered at ≥2-fold in triplicate arrays were selected for identifying the commonly regulated set while genes changed at ≥2-fold in at least duplicate arrays were chosen for identifying chemical-specific expression pattern. Second, only genes that have either a known or putative function based on sequence homology with a gene from a different biological system were chosen. Considering the highly variable nature of microarray data, these selection criteria were necessary to minimize false positive signals and to focus in on a workable number of genes. For example, if we chose genes consistently down-regulated at ≥3-fold in all 3 arrays, 48 genes are on the candidate list. If we chose genes down-regulated in 2 out of 3 arrays at ≥3-fold in NQO sample, 68 additional genes will be added to the candidate list.

By being less rigorous in terms of consistency among replicates during the data reduction process, the number of candidate genes on a list exponentially increases. A similar trend was observed for up-regulated genes in the NQO sample. Also, keeping only substantially (in terms of ratio and/or signal intensity) regulated genes on a final list is very important to do more quantitative confirmation studies via Real Time RT-PCR in the future. As discussed in Chapter 4, genes with high expression ratio and high signal intensity from microarray analysis are more likely to be confirmed by Real Time RT-PCR analysis.

Two genes (ras homolog gene family and dif13) involved in oncogenesis (Shimizu *et al.*, 1997; Than *et al.*, 1999) were commonly up regulated in all 4 transformed RHEK-1 cells. Mutation and/or overexpression of c-ras has been strongly implicated in chemically-induced initiation of skin tumor development in the murine system (Balmain and Brown, 1985). In addition, the c-ras genes are mutated in approximately 10-30% of human tumors (Rodenhuis, 1992). The ras homolog gene family was induced at 4.2-fold average ratio (also at very high hybridization signal) across all samples. There are also 5 other members of the ras homolog gene family on Human 3.8 II arrays used in the current studies. Surprisingly, none of these other 5 members of the ras family was consistently induced. A ras inhibitor was consistently down-regulated in MNNG1, MNNG2, and NQO (data not shown). The second commonly up regulated gene in these cell lines was dif13 that is associated with the oncodevelopmental process. The differentiation related protein dif13 has shown homology with oncodevelopmental soluble placental tissue protein 17 (Than *et al.*, 1999).

Three genes mechanistically associated with regulation of cell growth or cell motility were highly induced in all MMMG1, MMNG2, NQO, and TCDD samples. The COP9 subunit 6 is involved in control of cell growth, as well as RNA binding and macromolecule assembly (Asano *et al.*, 1997). Both p21/cdc42/Rac1-activated kinase 1 and RNB6 genes have been reported to play a role in regulating actin filament organization and cell motility (Ohta *et al.*, 1997; Sells *et al.*, 1999).

There were 5 genes altered in all 4 malignant RHEK-1 cell lines that have been shown to have defined functions, but have not, to date, been associated with carcinogenesis. These 5 genes are Ca^{2+} activated chloride channel, DNA-directed polymerase κ, flavin containing monooxygenase 1 (FMO1), purine-rich element binding protein B, and recombining binding protein suppressor of hairless. The purine-rich element binding protein B originally identified from Epstein-Barr virus strain B95-8 transformed B lymphoblastoid cell line is one novel member of the histone family (unpublished). The recombining binding protein suppressor of hairless (Drosophila) is a recombination signal binding protein (Amakawa *et al.*, 1993). The Ca^{2+} activated chloride channel (CLCA) is a membrane channel (Agnel *et al.*, 1999). Some members (bovine CLCA2, mouse CLCA2, and human CLCA2) of CLCA serve as adhesion molecules for lung metastatic cancer cells. In contrast, expression of hCLCA2 in normal mammary epithelium implies that hCLCA2 acts as a tumor suppressor in breast cancer (Pauli *et al.*, 2000). DNA-directed polymerase κ is a newly identified low fidelity polymerase (Ohashi *et al.*, 2000). FMO1 gene plays a role during the xenobiotic biotransformation (Dolphin *et al.*, 1991).

The last common up regulated gene in Table 5.1 is CG1-120 protein that was found due to its sequence similarity with *Caenorhabditis elegans*. No known biological function is available for this novel gene.

Future mechanistic studies attempting to correlate induced expression of these genes with malignant transformation must be carried out. One way to accomplish this is through use of genetically altered cells that over- or under-express the gene of interest: alterations in the transformed phenotype of the altered cells would strongly support a role for a particular gene in malignant transformation process.

Evasion of apoptosis and escape from immune surveillance are two important functional categories of carcinogenesis (evasion of apoptosis is one of the "hallmarks of carcinogenesis" as defined by Hanahan and Weinberg (2000)). Several genes belonging to these categories were suppressed in the four malignant RHEK-1 cell lines. These genes were apoptosis-inducing serine/threonine kinase 17b, serine threonine protein kinase, ubiquilin 2, and cytokine receptor-like factor 1. The first 3 genes are involved in induction of apoptosis (Kaye *et al.*, 2000; Sanjo *et al.*, 1998; Tian *et al.*, 1995). The last one encodes a novel soluble protein with a possible regulatory role in the immune system (Elson *et al.*, 1998).

The second group of down regulated genes identified in malignant RHEK-1 cells is that of the membrane transporter family which encompasses aquaporin 4 (Yang *et al.*, 1995) and three solute carrier family members (i.e., family 11, 12, and 21) (Abe *et al.*, 1999; Kishi and Tabuchi, 1997; Mount *et al.*, 1999). No mechanistic association between decreased expression of membrane transporter and role(s) of this gene in cell transformation has been reported. One member of the cadherin family, cadherin 12 type 2

(Suzuki *et al.*, 1991; Tanihara *et al.*, 1994), was substantially suppressed in all malignant RHEK-1 cells. Another member of the cadherin family, cadherin 8, was also down regulated in the MNNG2 cell population analyzed by Clontech Cancer 1.2 array in Chapter 3. These findings support the idea of a decrease in cell differentiation and increase in cell motility during malignant transformation.

The remaining 14 genes on the list for commonly suppressed by MNNG, NQO, and TCDD in RHEK-1 cells are not mechanistically and clearly related with malignancy based on currently available literature information. For example, CD 164 antigen (sialomucin), which has been reported to be related to polymorphic epithelial mucin (PEM) and a novel core protein MGC-24 that has been implicated in gastric carcinoma and as negative regulator of hematopoiesis (Masuzawa *et al.*, 1992; Zannettino *et al.*, 1998), was consistently suppressed in our malignant RHEK-1 cells. The literature information on PEM and MGC-24 genes is unclear with regards to the role of these proteins in cancer. Depending on the type of tissue, malignant transformation leads to both increased and decreased expression of sialomucin.

Two mechanistically well-characterized genes were induced in an MNNG-specific manner as shown in Table 5.3. A CD24 antigen which is involved in small cell lung and hepatocellular carcinoma (Huang and Hsu, 1995; Jackson *et al.*, 1992) and jumping translocation breakpoint (generally overexpressed in malignant cells; Platica *et al.*, 2000) were induced at about 3- and 5-fold, respectively in both MNNG1 and MNNG2. A p53-induced protein implicated in apoptosis was also induced in the MNNG-transformed cell line. The remaining 7 genes have been shown to have their defined functions, but have not, to date, been associated with malignant conversion.

For NQO-specific alterations in gene expression, cystatin F which is associated with liver metastasis (Morita *et al.*, 1999) and one ETS oncogene, friend leukemia virus integration 1 (Hromas *et al.*, 1993), were identified as upregulated genes as shown in Table 5.3. Cystatin F was also characterized as a glycosylated human low molecular weight cysteine proteinase inhibitor expressed in metastasizing cancer (Koppel *et al.*, 1984; Ni *et al.*, 1998). The remaining 8 genes have been shown to have defined functions, but have not, to date, been associated with malignant conversion.

Two genes, core-binding factor and internexin neuronal intermediate filament protein α, implicated in human leukemia (Calabi and Cilli, 1998; Reddy *et al.*, 1998) were up-regulated at 9-fold and 5-fold, respectively. The study of chromosomal translocations in tumors has led to the identification of novel genes such as core-binding factor runt domain a subunit 2 translocated to 2 (CBFA2). CBFA2 is a human homologue of the *Drosophila melanogaster* segmentation gene *runt* and encodes a transcriptional regulator (Calabi and Cilli, 1998). The involvement of a human type IV internexin neuronal intermediate filament protein during the pathogenesis of adult T cell leukemia and neurorogical disorders was reported based upon the specific interaction of human T-cell leukemia virus protein and internexin neuronal intermediate filament protein α (Reddy *et al.*, 1998). One gene encoding a complement component 1 q (C1q) subcomponent involved in antibody-dependent and independent immune functions (Kishore and Reid, 2000) was down regulated at 3-fold in TCDD-transformed cell line. C1q plays a key role in the recognition of immune complexes, thereby initiating the classical complement pathway (Reid, 1983).

Since the output of microarray analysis relies on what are spotted on arrays, biologically well-characterized information on the particular gene is very critical to researchers to convert the lengthy list of genes into a network of genes in a physiologically reasonable manner. By creating this biological network, the relationship between the perturbation in gene expression by exposure to test agent and functional outcome in cells can be built on and a mechanistic understanding can be achieved. The scientific rationale to connect a battery of candidate genes requires continuous basic research on individual genes and the multiple genes involved in a pathway. For many of the genes listed on DNA microarrays studied here, information has been reported on the exact sequence of the gene, transcript, and corresponding protein and the location of the gene on the chromosome. However, many genes have not yet been characterized in terms of their biological function. The successful and useful application of DNA microarray technology in understanding the mechanism(s) of chemical carcinogenesis needs to wait on the complete functional annotation of the human genome project.

The genomic studies on 4 chemically-induced malignant RHEK-1 cell lines described here have identified a total of 55 genes that could potentially be involved in the neoplastic conversion of nontumorigenic RHEK-1 cells; current studies are, however, strictly correlative. Further mechanistic studies are needed to prove a causal relationship between these candidate genes and malignant phenotype in this cell type.

Acknowledgements

This study was supported by the Agency for Toxic Substances and Disease Registry (ATSDR) Cooperative Agreement U61/ATU881475. and the National Institute for Environmental Health Sciences (NIEHS) Superfund Basic Research Program Project P42 ES05949. The efforts of Ms. Christine Battaglia during cell harvest and freezing at the Center for Environmental Toxicology & Technology at Colorado State University are gratefully acknowledged.

References

Abe. T.. Kakyo. M.. Tokui. T.. Nakagomi. R.. Nishio. T.. Nakai. D.. Nomura. H.. Unno. M.. Suzuki. M.. Naitoh. T.. Matsuno. S.. and Yawo. H. Identification of a novel gene family encoding human liver-specific organic anion transporter LST-1. J Biol.Chem.. *274*: 17159-17163. 1999.

Afshari. C. A.. Nuwaysir. E. F.. and Barrett. J. C. Application of complementary DNA microarray technology to carcinogen identification. toxicology. and drug safety evaluation. Cancer Res.. *59*: 4759-4760. 1999.

Agnel. M.. Vermat. T.. and Culouscou. J. M. Identification of three novel members of the calcium-dependent chloride channel (CaCC) family predominantly expressed in the digestive tract and trachea. FEBS Lett.. *455*: 295-301. 1999.

Amakawa. R.. Jing. W.. Ozawa. K.. Matsunami. N.. Hamaguchi. Y.. Matsuda. F.. Kawaichi. M.. and Honjo. T. Human Jk recombination signal binding protein gene (IGKJRB): comparison with its mouse homologue. Genomics. *17*: 306-315. 1993.

Asano. K.. Vornlocher. H. P.. Richter-Cook. N. J.. Merrick. W. C.. Hinnebusch. A. G.. and Hershey. J. W. Structure of cDNAs encoding human eukaryotic initiation factor 3 subunits. Possible roles in RNA binding and macromolecular assembly. J Biol.Chem.. *272*: 27042-27052. 1997.

Bae. D. S.. Hanneman. W. H.. Yang. R. S. H.. and Campain. J. A. Characterization of gene expression changes associated with MNNG. arsenic. or metal mixture treatment in human keratinocytes: application of cDNA microarray technology. Environ.Health Perspect.. 2002. In Press.

Burczynski. M. E.. McMillian. M.. Ciervo. J.. Li. L.. Parker. J. B.. Dunn. R. T.. Hicken. S.. Farr. S.. and Johnson. M. D. Toxicogenomics-based discrimination of toxic mechanism in HepG2 human hepatoma cells. Toxicol.Sci.. *58*: 399-415. 2000.

Calabi, F. and Cilli, V. CBFA2T1, a gene rearranged in human leukemia, is a member of a multigene family. Genomics, *52*: 332-341, 1998.

Dolphin, C., Shephard, E. A., Povey, S., Palmer, C. N., Ziegler, D. M., Ayesh, R., Smith, R. L., and Phillips, I. R. Cloning, primary sequence, and chromosomal mapping of a human flavin- containing monooxygenase (FMO1). J Biol.Chem., *266*: 12379-12385, 1991.

Eisen, M. B. Manual for Cluster and TreeView. 1998.

Eisen, M. B., Spellman, P. T., Brown, P. O., and Botstein, D. Cluster analysis and display of genome-wide expression patterns. Proceedings of the National Academy of Sciences of the United States of America, *95*: 14863-14868, 1998.

Elson, G. C., Graber, P., Losberger, C., Herren, S., Gretener, D., Menoud, L. N., Wells, T. N., Kosco-Vilbois, M. H., and Gauchat, J. F. Cytokine-like factor-1, a novel soluble protein, shares homology with members of the cytokine type I receptor family. J Immunol, *161*: 1371-1379, 1998.

Hamadeh, H. K., Bushel, P. R., Jayadev, S., DiSorbo, O., Bennett, L., Li, L., Tennant, R., Stoll, R., Barrett, J. C., Paules, R. S., Blanchard, K., and Afshari, C. A. Prediction of compound signature using high density gene expression profiling. Toxicol.Sci, *67*: 232-240, 2002a.

Hamadeh, H. K., Bushel, P. R., Jayadev, S., Martin, K., DiSorbo, O., Sieber, S., Bennett, L., Tennant, R., Stoll, R., Barrett, J. C., Blanchard, K., Paules, R. S., and Afshari, C. A. Gene expression analysis reveals chemical-specific profiles. Toxicol.Sci, *67*: 219-231, 2002b.

Hanahan, D. and Weinberg, R. A. The hallmarks of cancer. Cell, *100*: 57-70, 2000.

Hromas, R., May, W., Denny, C., Raskind, W., Moore, J., Maki, R. A., Beck, E., and Klemsz, M. J. Human FLI-1 localizes to chromosome 11Q24 and has an aberrant transcript in neuroepithelioma. Biochim.Biophys.Acta, *1172*: 155-158, 1993.

Huang, Q., Dunn, R. T., Jayadev, S., DiSorbo, O., Pack, F. D., Farr, S. B., Stoll, R. E., and Blanchard, K. T. Assessment of cisplatin-induced nephrotoxicity by microarray technology. Toxicol.Sci, *63*: 196-207, 2001.

Huang, L. R. and Hsu, H. C. Cloning and expression of CD24 gene in human hepatocellular carcinoma: a potential early tumor marker gene correlates with p53 mutation and tumor differentiation. Cancer Res, *55*: 4717-4721, 1995.

Jackson, D., Waibel, R., Weber, E., Bell, J., and Stahel, R. A. CD24, a signal-transducing molecule expressed on human B cells, is a major surface antigen on small cell lung carcinomas. Cancer Res, *52*: 5264-5270, 1992.

Kaye, F. J., Modi, S., Ivanovska, I., Koonin, E. V., Thress, K., Kubo, A., Kornbluth, S., and Rose, M. D. A family of ubiquitin-like proteins binds the ATPase domain of Hsp70- like Stch. FEBS Lett., *467*: 348-355, 2000.

Kishi, F. and Tabuchi, M. Complete nucleotide sequence of human NRAMP2 cDNA. Mol.Immunol, *34*: 839-842, 1997.

Kishore, U. and Reid, K.B.M. C1q: structure, function, and receptors. Immunopharmacology, *49*: 159-170, 2000.

Koppel, P., Baici, A., Keist, R., Matzku, S., and Keller, R. Cathepsin B-like proteinase as a marker for metastatic tumor cell variants. Exp.Cell Biol., *52*: 293-299, 1984.

Koseki, T., Inohara, N., Chen, S., and Nunez, G. ARC, an inhibitor of apoptosis expressed in skeletal muscle and heart that interacts selectively with caspases. Proc.Natl.Acad Sci U.S.A, *95*: 5156-5160, 1998.

Lee, M. L., Kuo, F. C., Whitmore, G. A., and Sklar, J. Importance of replication in microarray gene expression studies: statistical methods and evidence from repetitive cDNA hybridizations. Proc.Natl.Acad.Sci.U.S.A, *97*: 9834-9839, 2000.

Masuzawa, Y., Miyauchi, T., Hamanoue, M., Ando, S., Yoshida, J., Takao, S., Shimazu, H., Adachi, M., and Muramatsu, T. A novel core protein as well as polymorphic epithelial mucin carry peanut agglutinin binding sites in human gastric carcinoma cells: sequence analysis and examination of gene expression. J Biochem.(Tokyo), *112*: 609-615, 1992.

Merrill, C. L., Ni, H., Yoon, L. W., Tirmenstein, M. A., Narayanan, P., Benavides, G. R., Easton, M. J., Creech, D. R., Hu, C. X., McFarland, D. C., Hahn, L. M., Thomas, H. C., and Morgan, K. T. Etomoxir-induced oxidative stress in HepG2 cells detected by differential gene expression is confirmed biochemically. Toxicol.Sci, *68*: 93-101, 2002.

Morita, M., Yoshiuchi, N., Arakawa, H., and Nishimura, S. CMAP: a novel cystatin-like gene involved in liver metastasis. Cancer Res, *59*: 151-158, 1999.

Mount, D. B., Mercado, A., Song, L., Xu, J., George, A. L., Jr., Delpire, E., and Gamba, G. Cloning and characterization of KCC3 and KCC4, new members of the cation-chloride cotransporter gene family. J Biol.Chem., *274*: 16355-16362, 1999.

Ni, J., Fernandez, M. A., Danielsson, L., Chillakuru, R. A., Zhang, J., Grubb, A., Su, J., Gentz, R., and Abrahamson, M. Cystatin F is a glycosylated human low molecular weight cysteine proteinase inhibitor. J Biol.Chem., *273*: 24797-24804, 1998.

Nuwaysir, E. F., Bittner, M., Trent, J., Barrett, J. C., and Afshari, C. A. Microarrays and toxicology: the advent of toxicogenomics. Mol.Carcinog, *24*: 153-159, 1999.

Ohashi, E., Ogi, T., Kusumoto, R., Iwai, S., Masutani, C., Hanaoka, F., and Ohmori, H. Error-prone bypass of certain DNA lesions by the human DNA polymerase kappa. Genes Dev., *14*: 1589-1594, 2000.

Ohta, S., Mineta, T., Kimoto, M., and Tabuchi, K. Differential display cloning of a novel rat cDNA (RNB6) that shows high expression in the neonatal brain revealed a member of Ena/VASP family. Biochem.Biophys.Res Commun., *237*: 307-312, 1997.

Pauli, B. U., Abdel-Ghany, M., Cheng, H. C., Gruber, A. D., Archibald, H. A., and Elble, R. C. Molecular characteristics and functional diversity of CLCA family members. Clin.Exp.Pharmacol.Physiol, *27*: 901-905, 2000.

Platica, O., Chen, S., Ivan, E., Lopingco, M. C., Holland, J. F., and Platica, M. PAR, a novel androgen regulated gene, ubiquitously expressed in normal and malignant cells. Int.J Oncol., *16*: 1055-1061, 2000.

Puga, A., Maier, A., and Medvedovic, M. The transcriptional signature of dioxin in human hepatoma HepG2 cells. Biochem.Pharmacol., *60*: 1129-1142, 2000.

Reddy, T. R., Li, X., Jones, Y., Ellisman, M.H., Ching, G.Y., Liem, R.K.H., and Wong-Staal, F. Specific interaction of HTLV tax protein and a human type IV neuronal intermediate filament protein. Proc. Natl. Acad. Sci. USA, *95*: 702-707, 1998.

Reid, K.B.M. Proteins involved in the activation and control of the two pathways of human complement. Biochem. Soc. Trans., *11*: 1-12, 1983.

Rhim, J. S., Fujita, J., Arnstein, P., and Aaronson, S. A. Neoplastic conversion of human keratinocytes by adenovirus 12-SV40 virus and chemical carcinogens. Science, *232*: 385-388, 1986.

Sanjo, H., Kawai, T., and Akira, S. DRAKs, novel serine/threonine kinases related to death-associated protein kinase that trigger apoptosis. J Biol.Chem., *273*: 29066-29071, 1998.

Sells, M. A., Boyd, J. T., and Chernoff, J. p21-activated kinase 1 (Pak1) regulates cell motility in mammalian fibroblasts. J Cell Biol., *145*: 837-849, 1999.

Shimizu, F., Watanabe, T. K., Okuno, S., Omori, Y., Fujiwara, T., Takahashi, E., and Nakamura, Y. Isolation of a novel human cDNA (rhoHP1) homologous to rho genes. Biochim.Biophys.Acta, *1351*: 13-16, 1997.

Shultz, V. D., Phillips, S., Sar, M., Foster, P. M., and Gaido, K. W. Altered gene profiles in fetal rat testes after in utero exposure to di(n-butyl) phthalate. Toxicol.Sci, *64*: 233-242, 2001.

Suzuki, S., Sano, K., and Tanihara, H. Diversity of the cadherin family: evidence for eight new cadherins in nervous tissue. Cell Regul., *2*: 261-270, 1991.

Tanihara, H., Sano, K., Heimark, R. L., St John, T., and Suzuki, S. Cloning of five human cadherins clarifies characteristic features of cadherin extracellular domain and provides further evidence for two structurally different types of cadherin. Cell Adhes.Commun., *2*: 15-26, 1994.

Than, N. G., Sumegi, B., Than, G. N., Kispal, G., and Bohn, H. Cloning and sequencing of human oncodevelopmental soluble placental tissue protein 17 (PP17): homology with adipophilin and the mouse adipose differentiation-related protein. Tumour.Biol., *20*: 184-192, 1999.

Thomas, R. S., Rank, D. R., Penn, S. G., Zastrow, G. M., Hayes, K. R., Pande, K., Glover, E., Silander, T., Craven, M. W., Reddy, J. K., Jovanovich, S. B., and Bradfield, C. A. Identification of toxicologically predictive gene sets using cDNA microarrays. Mol.Pharmacol., *60*: 1189-1194, 2001.

Tian, Q., Taupin, J., Elledge, S., Robertson, M., and Anderson, P. Fas-activated serine/threonine kinase (FAST) phosphorylates TIA-1 during Fas-mediated apoptosis. J Exp.Med., *182*: 865-874, 1995.

Waring, J. F., Ciurlionis, R., Jolly, R. A., Heindel, M., and Ulrich, R. G. Microarray analysis of hepatotoxins in vitro reveals a correlation between gene expression profiles and mechanisms of toxicity. Toxicol.Lett., *120*: 359-368, 2001a.

Waring, J. F., Jolly, R. A., Ciurlionis, R., Lum, P. Y., Praestgaard, J. T., Morfitt, D. C., Buratto, B., Roberts, C., Schadt, E., and Ulrich, R. G. Clustering of hepatotoxins based on mechanism of toxicity using gene expression profiles. Toxicol.Appl.Pharmacol., *175*: 28-42, 2001b.

Yang, B., Ma, T., and Verkman, A. S. cDNA cloning, gene organization, and chromosomal localization of a human mercurial insensitive water channel. Evidence for distinct transcriptional units. J Biol.Chem., *270*: 22907-22913, 1995.

Yang, J. H., Thraves, P., Dritschilo, A., and Rhim, J. S. Neoplastic transformation of immortalized human keratinocytes by 2,3,7,8-tetrachlorodibenzo-p-dioxin. Cancer Res., *52*: 3478-3482, 1992.

Yih, L. H., Peck, K., and Lee, T. C. Changes in gene expression profiles of human fibroblasts in response to sodium arsenite treatment. Carcinogenesis, *23*: 867-876, 2002.

Zannettino, A. C., Buhring, H. J., Niutta, S., Watt, S. M., Benton, M. A., and Simmons, P. J. The sialomucin CD164 (MGC-24v) is an adhesive glycoprotein expressed by human hematopoietic progenitors and bone marrow stromal cells that serves as a potent negative regulator of hematopoiesis. Blood, *92*: 2613-2628, 1998.

CHAPTER 6
Summarizing Discussion

6.1 Additivity Model to Detect Interactions among Chemicals or Different Types of Agents

In several previous studies, a methodology based on the assumption of additivity has been applied to mixtures of chemicals or other types of agents to detect significant departure from additivity (Charles *et al.*, 2002a and 2002b; Chaudhry *et al.*, 2001; Gennings, 2000; Gennings *et al.*, 2002). For example, the nature of the interactions between the vitamin D3 analog (ILX-23-7553) and Adriamycin or irradiation was characterized by a rigorous statistical evaluation through use of an additivity model or response surface approach (Chaudhry *et al.*, 2001). More recently, the additivity model approach illustrated chemical interactions after treatment with 3 endocrine active ternary mixtures in an estrogen receptor α (ERα) reporter assay (Charles *et al.*, 2002b). Application of the additivity model to environmentally relevant mixtures will allow more accurate risk assessment by detecting adverse effects from chemical interactions in mixtures and thus, improve strategies for protecting the environment and public from exposure to potentially harmful combination(s) of agents.

6.2 Potential Mechanisms for Dose- and Cell Strain-Dependent Chemical-Chemical Interactions

For the design of mixtures studies, researchers need to carefully consider the importance of dose selection since dose-dependent interactive chemical effects have been reported in several recent studies (Bae *et al.*, 2001; Charles *et al.*, 2002b; Gennings *et al.*, 2002). In our studies, represented in detail in Chapter 2, we observed substantial difference in the nature of the cytotoxic interactions among the metals in the four-metal mixture depend on the chemical dose and keratinocyte cell strain being examined. In studies by Charles *et al.* (2002b), one (17β estradiol, genistein, DDT) of 3 ternary mixtures tested in ER reporter assay exhibited antagonistic chemical interactions ($p<0.001$) in terms of estrogenic responses at high concentrations, but not at low concentrations. None of the mixtures tested in these studies showed any evidence of synergy. The competition among 17β estradiol, genistein, and DDT at the ER was suggested as a potential mechanism for the antagonism observed at the highest concentration of mixture (Charles *et al.*, 2002b). There was also discussion by this investigator that an ER reporter assay (measures activation of ER transactivation by test chemicals) produces cell-line specific estrogen-mediated responses (Charles *et al.*, 2002b).

At the different dose levels that cause dissimilar types of interactions, a number of mechanisms of toxicity for individual metals may work in concert. One hypothesis tested in our studies (Bae *et al.*, 2001; Gennings *et al.*, 2002) and described in Chapter 2, to explain why dose-dependent and cell strain-dependent cytotoxic interactions occur in keratinocytes was the induction, at high metal mixture concentrations, of cell protective mechanisms (especially, GSH and MT). In support of this hypothesis, the NM-1 cell line

was the only keratinocye line that did not show an antagonistic cytotoxic interactions and statistically significant induction of MTs at high mixture concentrations among 4 cell strains studied.

What other areas of interactions might be happening to modulate the cytotoxicity of the metal mixture in different types of keratinocyte strains? Several interesting areas for further studies would be absorption/excretion kinetics of metal mixture as well as individual metals, identifying common cellular/biological target (i.e., DNAs or proteins), and measuring expression changes in genes involved in downstream pathways following exposure to metal/metal mixture.

To further understand the exact cellular mechanisms other than alterations in levels of GSH and MT behind the observed metal interactions, a global DNA microarray analysis would be extremely useful. This analysis would help to dissect what additional pathways are involved mechanistically in three different types of cytotoxic interactions (synergistic, antagonistic, or hormesis) we observed in the four human keratinocyte strains. One of the major successful applications of array analysis is providing potential clues for mechanism of action(s) by which the chemical of interest acts in a biological system. Applying microarray technology to mixtures studies should, therefore, be highly productive and allow one to carefully characterize chemical interactions at the molecular level.

Finding, from these types of studies, that high dose levels of the chemicals in the mixtures exhibited different types of interactions than the same chemicals mixed together at low dose levels is extremely important, and should be taken into consideration during risk assessment on chemical mixtures. Simple linear extrapolation of high dose laboratory

observations to low dose human exposure to mixtures is not necessarily the most accurate or the most realistic and should be approached with skepticism.

6.3 Alternative Method to Assess Potential Carcinogenecity of Chemicals by RHEK-1 Transformation Assay

The *in vitro* RHEK-1 transformation assay was utilized as a model system to assess the potential carcinogenic effect of As and an As-containing metal mixture and to study the multi-stages of chemical carcinogenesis. There is a phrase that is often mentioned during the physiologically based pharmacokinetic/ pharmacodynamic (PBPK/PD) workshop at CSU, "No model is perfect, but some models are useful". The wisdom of this sentence is true for our keratinocyte model used here. In contrast to rodent systems recommended by IARC for detecting transforming potential of chemicals, a human immortal RHEK-1 cell line is very versatile in that it allows us to reproduce previous studies (Rhim *et al.*, 1986) and to establish and characterize cell lines that represent different stages of chemically-mediated neoplastic transformation. Some limitations in utilizing this culture system for identifying potential carcinogens are discussed below.

We have observed that RHEK-1 cells spontaneously progress to malignancy after approximately six months in culture as discussed in detail in Chapter 3. For one example, MNNG-induced malignant OM3 cells at p25 formed large squamous cell carcinomas in nude mice within 3 weeks. However, the vehicle-treated and passage-matched OM1 cells gave rise to tumors if allowed to go out to more > 3 months. Thus, the tumorigenicity end point in these cells needs to be expressed in terms of both tumor size and tumor latency, instead of just the number of tumors. Tumor latency becomes a more important criterion

than tumor incidence when chemicals with different levels of potential carcinogenicity have to be differentiated by a tumorigenicity end point. Thus, the absolute answer for whether test chemical is a potential carcinogen or not in the RHEK-1 transformation assay is harder to conclude than the relative answer that test chemical may have weaker or stronger potential for carcinogenicity compared to MNNG (a positive control for transformation). A carefully designed study that encompasses well-defined negative and positive controls for transformation is necessary to achieve easily interpretable results and conclusions if the RHEK-1 system is used for chemically- (or other agent) induced malignant transformation.

Although chemicals tested so far (MNNG, NQO, TCDD) in the RHEK-1 cell line does not require biotransformation to affect cellular and molecular targets in cells because the parent compound is the ultimate carcinogen. For chemicals that may need metabolism to produce the ultimate carcinogen(s), the presence of metabolic enzymes in the *in vitro* test system becomes a very critical issue to accurately assess potential carcinogenicity of the test chemical. The RHEK-1 cell line does not have certain metabolic capabilities (i.e., cytochrome P450), therefore, supplementation of metabolic components is necessary for test chemicals that require metabolic activation for generation of their ultimate carcinogenic forms. In other studies carried out at CETT, BaP has been shown to be substantially more toxic to RHEK-1 in the presence of S9 microsomal fraction from Sprague Dawley rat liver S9. This finding is in contrast to primary keratinocytes in that these cells have capability to metabolize BaP.

6.4 As and an As-Containing Metal Mixture Inhibit Spontaneous Progression of RHEK-1 Cells

Although the carcinogenic effect of As in humans is unequivocal, laboratory animal evidence for the carcinogenecity of As is uncertain. Although data from recent studies support the hypothesis that As or its metabolite, DMA, may act as a promoter, progressor, or cocarcinogen, findings from our laboratory and others suggest that As may exert an antagonistic or protective effect in some assay systems (Bae *et al.*, 2002, Pott *et al.*, 2001). The inability to reproduce the carcinogenicity of As in a human keratinocyte culture system may be the reflection of the dose of As, or metabolite, that is actually reaching the intracellular target. Differences in the cellular and molecular interactions of As and/or its metabolites in intact skin versus keratinocyte cultures may be also responsible for the disparities of As carcinogenic effects between epidemiological and *in vitro* studies.

The cell transforming effects of As have been shown in 3 rodent cell culture systems [Syrian hamster embryo (SHE) cells (Lee *et al.*, 1985), C3H/10T1/2 murine cell line (Landolph, 1990), and rat liver epithelial cell line (TRL 1215: Zhao *et al.*, 1997)]. Both As(III) and As(V) induced morphological transformation of SHE cells in a dose-dependent manner and induced chromosome damage (Lee *et al.*, 1985). Interestingly, both As(III) and As(V) compounds induced anchorage-independent (AI) growth of human diploid foreskin fibroblasts. However, these colonies were stable only for 8 passages, at which time the cells senesced, and never assumed the fully malignant phenotype (Biederman and Landolph, 1987). Only As(III) induced a low, reproducible level of morphological transformation in C3H/10T1/2 cells (Landolph, 1990). These transformed cells grew in soft agar, and formed fibrosarcomas in nude mice. The TRL

1215 cell line derived from the liver of 10-day old Fisher F344 rats was malignantly transformed following chronic (≥18 weeks) treatment with As(III) at 0.125, 0.25, and 0.5 μM (Zhao *et al.*, 1997). The As concentrations tested in our RHEK-1 cells for the 6-month chronic studies in Chapter 3 were 0.12, 0.14, and 0.18 μM. We chose these low As concentrations to more closely reflect the actual human exposure scenario.

Elucidation of the metabolic pathway for As has changed our understanding of the significance of methylation. The intermediate methylated and dimethylated As metabolites in the trivalent oxidation state are more cytotoxic and genotoxic than are inorganic arsenicals in the trivalent oxidation state. Interestingly, the capacity of TRL 1215 cells to methylate As was reported (Zhao *et al.*, 1997). We have not examined the As methylation activity in our RHEK-1 cells. Although, it has been shown that there was no apparent correlation between the capacity to methylate inorganic As and susceptibility of cells to As toxicity (Styblo *et al.*, 2000), it will be interesting to analyze the As methylation activity in RHEK-1 cells. There was a substantial difference in methylation capacity for inorganic As between primary rat hepatocytes and primary human keratinocytes (at least 200-fold slower rate in human keratinocytes). If there are increasing evidences that the metabolic methylation of As has to be considered an activation process during the overall biotransformation process for As, a difference in As methylation rate between rat liver TRL 1215 cells and human RHEK-1 keratinocytes may be a crucial factor for malignant cell transformation. Alternatively, a very unique characteristic of human cells, their chromosomal stability, may responsible for much more difficulty in human cell transformation than in rodent cells.

6.5 Considerations for Experimental Design of Array Analysis

The new technologies for gene analysis have been and will be quite helpful for the toxicology field of research, but one must always keep in mind that experimental design is the first and most important step in performing microarray analysis. If the appropriate controls and number of samples tested are not optimized, even the most brilliant geneticist and bioinformatician will be unable to define the significance of the vast array of data that will be generated. At present, there is no one standard guide or consensus for the design and conduct of an expression-profiling experiment as the study design is determined by the type of question the researcher is asking. Some common considerations for design of microarray experiments are presented in Table 6.1 (Afshari, 2002). By considering these critical parameters, more useful and interpretable data can be generated from gene expression experiments.

Table 6.1 Important considerations in the design of a microarray experiment
(Afshari, 2002)

Biological parameters
Sampling of appropriate number of replicates
Inclusion of other relevant samples: nonactive analogs, inhibitors, knockouts
Measurement of accompanying biological characteristics: physiology, pathology
Development of stringent treatment and harvest protocols
Technical parameters
Choice of chip, validation of identity of gene set
Hybridization of chip replicates, inclusion of dye swap
Choice of sample used as control in ratio analysis (universal, matched, other)
Scanning protocol that ensures proper laser power settings for optimal signals
Approach for validation of results
Data analysis parameters
Image analysis software, method of normalization and background subtraction
Data processing and long-term storage and backup
Data format, standardization, flexibility for import into multiple programs
Determination of appropriate visualization tools
Application of statistical approaches to determine gene significance
Gene annotation and ontology linkages

6.6. Challenges During Generation and Interpretation of Microarray Data

There have been some concerns in terms of the reproducibility of genome-wide transcriptional analysis with oligonucleotide or cDNA microarrays. This inconsistency is likely due, in part, to experimental variations from multi-step biochemical reactions and methods of data interpretation. Due to its high throughput nature, DNA microarray technology is vulnerable to variations introduced during experimental processes. Although a number of statistical algorithms have been developed to control experimental variations and to normalize data appropriately, high quality input images are still the prerequisite for obtaining significant new output. This requires reproducible procedures for labeling of cDNA targets, prehybridization, hybridization, and washing of slides to consistently generate high intensity and low background images (high signal-to-noise ratios). The types of considerations, concerns and some potential ways to overcome these issues during the processes of experimentation and data interpretation are discussed along with sequential steps involved in microarray analysis in the following subsections.

6.6.1. Importance of biological and hybridization replicates in generating reliable data

Lately, there have been many efforts to address the importance of biological and hybridization chip replicates in gene expression profiling via DNA arrays or chips. Two consecutive genome-wide transcriptional analyses on aerobic versus anaerobic cultures of yeast by the Affymetrix GeneChip clearly illustrated the need for experimental replication in DNA microarray studies (ter Linde *et al.*, 1999, Piper *et al.*, 2002). The finding from the first studies (ter Linde *et al.*, 1999) utilizing a single chip, 257 of the 818 "changed calls" (a call of increase or decrease in expression), was identified as false positive in the second studies that included sextuplicate chips (Piper *et al.*, 2002). That

means every one of three genes identified as altered during aerobic yeast culture in a single chip analysis was false positive under the experimental conditions examined. A recent study by Li and Johnson (2002) has shown the usefulness of a set of simple noise-filtering methods to evaluate and minimize the variance of microarray datasets (Li and Johnson, 2002). One of methods introduced was "rank analysis" which determine the acceptable number of independent samples necessary to eliminate false positives from the dataset. A dramatic reduction in the number of genes passing the rank analysis was achieved by using the second method, a 3 x 3 matrix comparison. Replicates are required to lower the expression noise and to display a low level of differential expression significantly.

6.6.2. Variation during probe generation

The direct incorporation of cyanine dye-conjugated nucleotides during cDNA labeling results in the different incorporation rates of cyanine (Cy) 3 and Cy 5 due to more bulky structure of Cy 5. In several papers that utilized direct labeling for differential gene expression studies, the investigator had to perform dye swap for circumventing the low incorporation rate of Cy 5 (Bartosiewicz *et al.*, 2000; Thomas *et al.*, 2001). A recent and alternative labeling method using the incorporation of aminoallyl nucleotides followed by conjugation to Cy-dye has been introduced (Schroeder *et al.*, 2002). This indirect labeling technique solves the issue addressed above and allows up to 10-fold more probe production and higher specific activity. The scheme for direct and indirect labeling methods for cDNAs is illustrated in Fig. 6.1 (redrawn from Yu *et al.*, 2002).

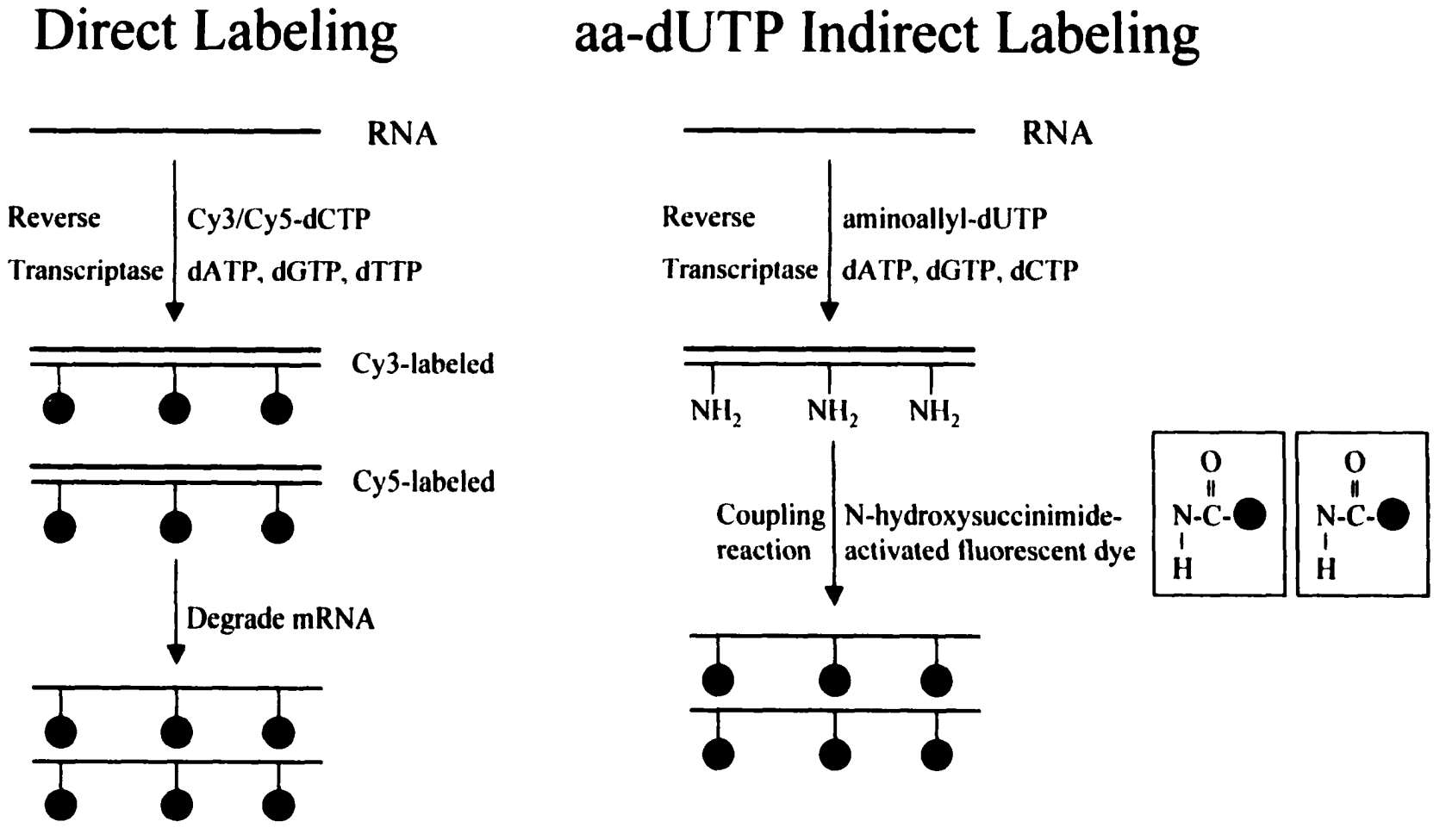

Figure 6.1 Schematic representations of experimental procedures for target labeling

6.6.3. Expression reproducibility

The reproducibility of microarray data is generally expressed by showing the coefficient of variation (standard deviation divided by the mean) for average difference change. The most critical parameter that influences the reproducibility and accuracy of ratio estimates of microarray experiments is the signal intensity. There have been many publications to assess and improve intra-laboratory reproducibility for last few years (Yang *et al.*, 2001). Using replicate experiments and simulated data, Yang *et al* (2001) explored a statistical method for flagging weak spots to improve normalization and ratio estimates in microarrays. This new method by normalizing data with "trimmed" mean of log ratios has preformed slightly better than the most popular method which uses global intensity and mean of ratios (Yang *et al.*, 2001).

As of today, there has been no report comparing gene expression patterns among different arrays. From our own gene expression data set in Chapters 3 and 5, we evaluated reproducibility in the ratio and direction of gene expression among different types of arrays since we found there are 34 overlapping genes among the spotted genes on these different arrays. The comparison was made on the data we collected from the MNNG-transformed RHEK-1 cell line, OM3. Nineteen out of 34 genes compared showed agreement in terms of direction of gene expression, not in terms of absolute expression fold (Table 6.2). The 56% agreement in the trend of expression between arrays which come from different commercial companies (NEN and Clontech), different types of probe (cDNA or oligonucleotide), and different types of labeling method (radioactive or fluorescent) suggests not a bad correlation, but is definitely not the ideal 100% agreement that researcher would expect from DNA microarray technology.

Table 6. 2 Reproducibility testing by comparing expression folds from different types of array on the same gene. Gene is highlighted in green if there is consistent agreement in terms of direction of expression between 2 arrays compared.

Gene Name(s)	GenBank #	Array Type*	Expression Fold#
Cell cycle progression 2 protein	AF011792	1	3 ⇑
cell cycle progression 2 protein	AF011792	5	1.4 ⇓
[redacted]			
Receptor-type protein tyrosine phosphatase g	L09247	3	2 ⇓
protein tyrosine phosphatase, receptor type, G	L09247	5	2.7 ⇑
[redacted]			
cadherin 8, type 2	L34060	5	3.8 ⇑
Cadherin 8	L34060	1	100 ⇓
v-erb-b2 avian erythroblastic leukemia viral oncogene homolog 2 (neuro/glioblastoma derived oncogene homolog)	M11730	5	1.3 ⇓
Tyrosine kinase-type receptor (HER2)	M11730	4	3 ⇑
[redacted]			
BCL2-associated athanogene	S83171	5	1.7 ⇓
BCL-2 binding athanogene-1 (BAG-1); glucocorticoid receptor-associated protein RAP46	S83171	1	100⇑
Cyclin H	U11791	1	5 ⇑
cyclin H	U11791	5	1.0

(continued)

Table 6. 2 Continued

Gene Name(s)	GenBank #	Array Type*	Expression Fold#
T-lymphoma invasion and metastasis inducing TIAM1 protein	U16296	4	3 ⇑
T-cell lymphoma invasion and metastasis 1	U16296	5	1.0
[redacted]			
Colon carcinoma laminin-binding protein	U43901	1	4 ⇑
laminin receptor 1 (67kD, ribosomal protein SA)	U43901	5	1.7 ⇓
Sodium/potassium-transporting ATPase b3 subunit	U51478	2	5 ⇑
ATPase, Na+/K+ transporting, beta 3 polypeptide	U51478	5	1.0
Cyclin A1	U66838	2	5 ⇑
cyclin A1	U66838	5	1.7 ⇓
microsomal glutathione S-transferase 2	U77604	5	1.6 ⇑
Microsomal glutathione S-transferase (GST) II	U77604	1	4 ⇓
v-kit Hardy-Zuckerman 4 feline sarcoma viral oncogene homolog	X06182	5	1.3 ⇓
C-kit proto-oncogene mRNA	X06182	4	6 ⇑
[redacted]			
mitogen-activated protein kinase 4	X59727	5	1.7 ⇓
63 kDa protein kinase related to rat ERK3	X59727	1	9 ⇑
[redacted]			
cyclin-dependent kinase 5	X66364	5	1.4 ⇓
Cell division protein kinase 5	X66364	1	3 ⇑
minichromosome maintenance deficient (S. cerevisiae) 4	X74794	5	3.2 ⇑
MCM4 DNA replication licensing factor	X74794	1	3 ⇓
[redacted]			

*: DNA array types utilized in current thesis studies; 1: Clontech Cancer 1.2; 2: NEN human 2400; 3: NEN kinase/phosphatase; 4: NEN oncogene/tumor suppressor; 5: Clontech Human 3.8II

#: Gene expression fold; For genes with higher expression in treated RHEK-1 cells, the expression fold was expressed by chemically-treated cells/control cells; For genes with higher expression in control RHEK-1 cells, the expression fold was expressed by control cells/chemically-treated cells.

Recently one published article reported a very interesting finding about inter-laboratory reproducibility (Piper *et al.*, 2002). The fold change data between the aerobic and unaerobic yeast cultures were generated from the Affymetrix GeneChip in triplicate and analyzed by a statistical analysis software package, "Significance Analysis of Microarrays (SAM)" indicated generally good agreement between laboratory A and B. The consistency of the fold change (in terms of expression direction) in the two laboratories was over 95% for genes with a fold change above 2.0 and over 97% for genes with a fold change above 3.0-fold. Not surprisingly, the agreement worsened at low fold change values (1.5-2-fold) with about 60% consistency probably due to high variation in signal intensity. This indicates that, at low fold changes, some laboratory bias may occur. Again this paper highlights the importance of signal intensity to influence data reproducibility and the caution with which such small fold changes should be treated (Piper *et al.*, 2002).

6.6.4. Numerically and graphically expressing gene expression profile

"Fold difference", i.e., the ratio of gene expression in a treated sample over the control sample is used as a quantitative measurement of differential gene expression. Genes regulated in a similar manner are then graphed together as a "cluster". These clusters can be arranged hierarchically or spatially to form self-organized maps. Expression clusters can be used to search common motifs of genetic regulation to find new regulatory mechanisms. Bioinformatics, with the use of algorithms, provides tools to trace out metabolic pathways, cellular interactions and to discern genetic networks (Gifford, 2001). However, before using these predicting algorithms, it is imperative to distinguish between significant fold difference values and false-positive results to avoid reporting

data that may actually not be physiologically relevant. For these reasons, it is important to confirm the presence of newly discovered expressed genes in a specific tissue by Northern blot, *in situ* hybridization or Real Time RT-PCR. Particularly, *in situ* hybridization is considered as the best approach for some cases, because it permits one not only to validate, but also to visualize the expression pattern in the type(s) of cells during a specific time.

6.6.5. Different conclusions from the same array data

One of the challenging issues for array data analysis is the inconsistency of multiple analysis methods/software packages (personal communication with Dr. Hanneman). The reproducibility of the data after statistical analysis on raw results obtained from DNA microarrays is very critical to increase reliability and sensitivity of data and to perform subsequent analysis (i.e., hierarchical cluster analysis) for classification of class of chemicals or diseases. A previous study by Kadota *et al.* (2001) has introduced a data processing method that very efficiently extracts reproducible data from the result of duplicate hybridization experiments. Processing adult mouse tissue expression profile data that contained 1,881,600 points of analysis using the method, preprocessing implementation for microarray (PRIM), showed the clustered results to be more highly consistent and sensitive than those obtained using previously reported filtering methods (Alizadeh *et al.*, 2000; Kadota *et al.*, 2001; Ross *et al.*, 2000; White *et al.*, 1999). This new PRIM methodology is a filtration program to process the raw array data automatically and consists of 3 steps as follows: (1) removal of the spots that were flagged during the visual inspection of the microarray images; (2) removal of the spots having a signal intensity lower than a threshold value; and (3) removal of the spots that

are beyond a threshold distance from the least-mean square line through a plot of the data obtained in one duplicate experiment against the data obtained in the other duplicate experiment. To set the thresholds in the second and third steps, the product of N (the ratio of the number of spots that passed the filtration program vs. the initial number of spots after step 1 above) and R (the correlation coefficient of the expression ratio between duplicate experiments) was utilized. By setting the thresholds by calculating the product of N and R instead of using one of them, the data set is kept with N as large as possible at a value of R that would give a proper result. Four different filtering methods (Alizadeh *et al.*, 2000; Ross *et al.*, 2000; White *et al.*, 1999), including PRIM, were compared in terms of R, N, and the number of branches in the dendrogram to assess the reproducibility of data interpretation. The PRIM method demonstrated the most consistent and highest number of final branches (a good index of the reproducibility for the replicate experiments) in the hierarchical clustering among 4 methods that are available (Kadota *et al.*, 2001).

6.6.6. Microarray data sharing

During the initial development of microarrays, much discussion revolved around the technology itself. Now the discussion has shifted to data analysis and data sharing. There is great interest in the sharing of cDNA microarray. Sharing of microarray data has many advantages such as improving analysis and confidence, and facilitating global comparisons between experiments (Becker, 2001; Geschwind, 2001). There are several issues related to format and quality of data and validation procedures will need to be addressed beforehand. One of the several issues that have to be resolved before sharing

array data is feasible common way of assignments to the same gene. The identification number (i.e., GenBank accession number, EST number, etc) of each gene on the array is usually different from one microarray brand to another one, it is very difficult to know a critical gene (i.e., designated with GenBank accession number) discovered from one array is the same with gene that designated as different type of identification number (i.e., EST number) when the same sample was analyzed in two arrays. This issue brings up the necessity of the usage of Unigene nomenclature to share and compare different platform microarray data (Becker, 2001; Geschwind, 2001).

6.6.7. Integration of available database

It is important to combine gene expression data with other data sources, such as the published literature and protein expression databases, to achieve biological interpretation of numerical array data. DNA microarrays are now standard tools in numerous laboratories. Future progress will certainly come from computational fields, particularly from algorithm improvement and also from the integration of all biological information databases (texts, genes, proteins, structure) after data standardization. In silico exploitation of this huge amount of information is a promising way to analyze powerfully an integrated atlas of both the transcriptome and proteome. Figure 6.2 illustrates how these approaches can be integrated for providing useful data from the gene to the physiological function (Soulet and Rivest, 2002).

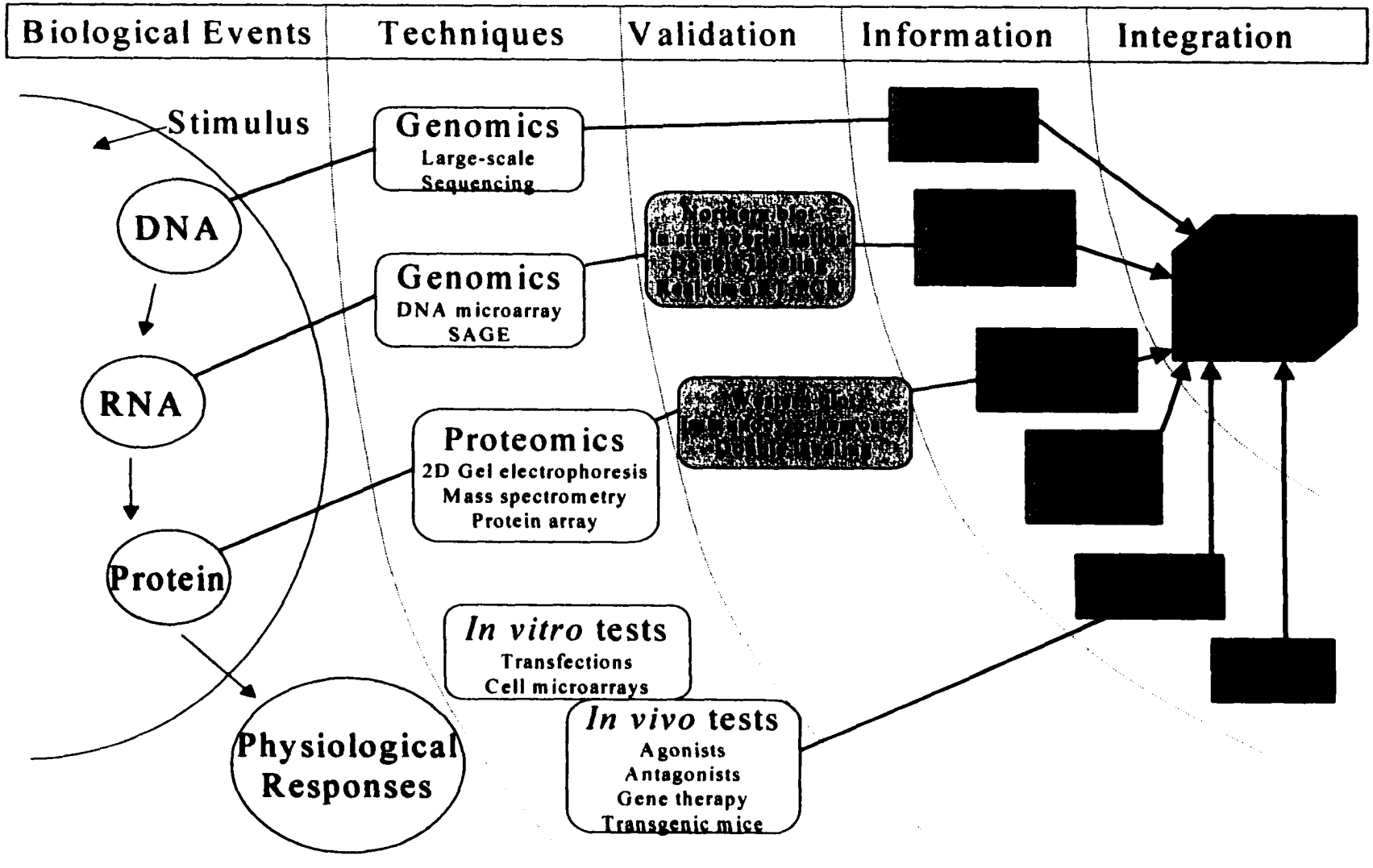

Figure 6.2 A scheme depicting DNA microarrays in a network of experimental tools and the resulting information
(Redrawn from Soulet and Rivest, 2002)

References

Afshari, C. A. Perspective: microarray technology, seeing more than spots. Endocrinology, *143*: 1983-1989, 2002.

Alizadeh, A. A. and Staudt, L. M. Genomic-scale gene expression profiling of normal and malignant immune cells. Current Opinion in Immunology, *12*: 219-225, 2000.

Bae, D. S., Gennings, C., Carter, W. H., Jr., Yang, R. S. H., and Campain, J. A. Toxicological interactions among arsenic, cadmium, chromium, and lead in human keratinocytes. Toxicol.Sci., *63*: 132-142, 2001.

Bae, D. S., Hanneman, W. H., Yang, R. S. H., and Campain, J. A. Characterization of gene expression changes associated with MNNG, arsenic, or metal mixture treatment in human keratinocytes: application of cDNA microarray technology. Environ.Health Perspect., 2002.

Bartosiewicz, M., Trounstine, M., Barker, D., Johnston, R., and Buckpitt, A. Development of a toxicological gene array and quantitative assessment of this technology. Arch.Biochem.Biophys., *376*: 66-73, 2000.

Becker, K. G. The sharing of cDNA microarray data. Nat.Rev.Neurosci., *2*: 438-440, 2001.

Biedermann, K. A. and Landolph, J. R. Induction of anchorage independence in human diploid foreskin fibroblasts by carcinogenic metal salts. Cancer Res, *47*: 3815-3823, 1987.

Charles, G. D., Gennings, C., Zacharewski, T. R., Gollapudi, B. B., and Carney, E. W. An Approach for Assessing Estrogen Receptor-Mediated Interactions in Mixtures of Three Chemicals: A Pilot Study. Toxicol Sci, *68*: 349-360, 2002a.

Charles, G. D., Gennings, C., Zacharewski, T. R., Gollapudi, B. B., and Carney, E. W. Assessment of interactions of diverse ternary mixtures in an estrogen receptor-alpha reporter assay. Toxicol Appl Pharmacol, *180*: 11-21, 2002b.

Chaudhry, M., Sundaram, S., Gennings, C., Carter, H., and Gewirtz, D. A. The vitamin D3 analog, ILX-23-7553, enhances the response to adriamycin and irradiation in MCF-7 breast tumor cells. Cancer Chemother.Pharmacol, *47*: 429-436, 2001.

Gennings, C. On testing for drug/chemical interactions: definitions and inference. J Biopharm.Stat., *10*: 457-467, 2000.

Gennings, C., Carter, W. H., Jr., Campain, J. A., Bae, D. S., and Yang, R. S. H. Statistical analysis of interactive cytotoxicity in human epidermal keratinocytes following exposure to a mixture of four metals. J Agricul Biol Environ Statistics, *7*: 58-73, 2002.

Geschwind, D. H. Sharing gene expression data: an array of options. Nat.Rev.Neurosci., *2*: 435-438, 2001.

Gifford, D. K. Blazing pathways through genetic mountains. Science, *293*: 2049-2051, 2001.

Kadota, K., Miki, R., Bono, H., Shimizu, K., Okazaki, Y., and Hayashizaki, Y. Preprocessing implementation for microarray (PRIM): an efficient method for processing cDNA microarray data. Physiol Genomics, *4*: 183-188, 2001.

Landolph, J. R. Neoplastic transformation of mammalian cells by carcinogenic metal compounds: cellular and molecular mechanisms. Biological Effects of Heavy Metals, pp. 1-18, 1990.

Lee, T. C., Oshimura, M., and Barrett, J. C. Comparison of arsenic-induced cell transformation, cytotoxicity, mutation and cytogenetic effects in Syrian hamster embryo cells in culture. Carcinogenesis, *6*: 1421-1426, 1985.

Li, J. and Johnson, J. A. Time-dependent changes in ARE-driven gene expression by use of a noise- filtering process for microarray data. Physiol Genomics, *9*: 137-144, 2002.

Piper, M. D., Daran-Lapujade, P., Bro, C., Regenberg, B., Knudsen, S., Nielsen, J., and Pronk, J. T. Reproducibility of oligonucleotide transcriptome analyses: an interlaboratory comparison using chemostat cultures of Saccharomyces cerevisiae. J Biol Chem., 2002.

Pott, W. A., Benjamin, S. A., and Yang, R. S. Pharmacokinetics, metabolism, and carcinogenicity of arsenic. Rev.Environ.Contam Toxicol., *169*: 165-214, 2001.

Rhim, J. S., Fujita, J., Arnstein, P., and Aaronson, S. A. Neoplastic conversion of human keratinocytes by adenovirus 12-SV40 virus and chemical carcinogens. Science, *232*: 385-388, 1986.

Ross, D. T., Scherf, U., Eisen, M. B., Perou, C. M., Rees, C., Spellman, P., Iyer, V., Jeffrey, S. S., van de, R. M., Waltham, M., Pergamenschikov, A., Lee, J. C., Lashkari, D., Shalon, D., Myers, T. G., Weinstein, J. N., Botstein, D., and Brown, P. O. Systematic variation in gene expression patterns in human cancer cell lines. Nat.Genet., *24*: 227-235, 2000.

Schroeder, B. G., Peterson, L. M., and Fleischmann, R. D. Improved quantitation and reproducibility in Mycobacterium tuberculosis DNA microarrays. J Mol.Microbiol.Biotechnol., *4*: 123-126, 2002.

Soulet, D. and Rivest, S. Perspective: how to make microarray, serial analysis of gene expression, and proteomic relevant to day-to-day endocrine problems and physiological systems. Endocrinology, *143*: 1995-2001, 2002.

ter Linde, J. J., Liang, H., Davis, R. W., Steensma, H. Y., van Dijken, J. P., and Pronk, J. T. Genome-wide transcriptional analysis of aerobic and anaerobic chemostat cultures of Saccharomyces cerevisiae. J Bacteriol., *181*: 7409-7413, 1999.

Thomas, R. S., Rank, D. R., Penn, S. G., Zastrow, G. M., Hayes, K. R., Pande, K., Glover, E., Silander, T., Craven, M. W., Reddy, J. K., Jovanovich, S. B., and Bradfield, C. A. Identification of toxicologically predictive gene sets using cDNA microarrays. Mol.Pharmacol., *60*: 1189-1194, 2001.

White, K. P., Rifkin, S. A., Hurban, P., and Hogness, D. S. Microarray analysis of Drosophila development during metamorphosis. Science, *286*: 2179-2184, 1999.

Yang, M. C., Ruan, Q. G., Yang, J. J., Eckenrode, S., Wu, S., McIndoe, R. A., and She, J. X. A statistical method for flagging weak spots improves normalization and ratio estimates in microarrays. Physiol Genomics, *7*: 45-53, 2001.

Yu, J., Othman, M. I., Farjo, R., Zareparsi, S., MacNee, S. P., Yoshida, S., and Swaroop, A. Evaluation and optimization of procedures for target labeling and hybridization of cDNA microarrays. Mol.Vis., *8*: 130-137, 2002.

Zhao, C. Q., Young, M. R., Diwan, B. A., Coogan, T. P., and Waalkes, M. P. Association of arsenic-induced malignant transformation with DNA hypomethylation and aberrant gene expression. Proc Natl Acad Sci USA *94*: 10907-10912, 1997.

CHAPTER 7

Future Directions

I. Research Expansion on Genomic Analyses

Our research to date has generated a substantial list of genes that may act as markers during malignant transformation of RHEK-1 cells. The next logical and scientific questions to be asked are "Are these genes truly altered in all 4 chemically transformed cell lines?", "Are these genes altered in different types of malignant cells?", "Are these candidate genes found to be altered in their expression in samples from cancer patients?", and "How are these candidate genes altered in their expression during acquisition of malignant characteristics such as AIG and tumorigenicity?" Due to the semi-quantitative nature of the microarray technology, findings from microarray analysis in Chapter 5 need to be confirmed by more quantitative gene expression methodology such as Real Time RT-PCR, Northern blot, or ribonuclease protection assay. It will be interesting to compare the involvement of candidate genes identified in Chapter 5 in keratinocytes with other malignant cell types (i.e., liver, bladder, lung, prostate, breast, *etc*) by means of the same type of DNA arrays. If the same set of genes is consistently altered in multiple cell types, the candidate genes from current dissertation studies may be tissue and/or cell type-independent and universal molecular markers for carcinogenesis in *in vitro* culture systems. Further genomic research on human cancer samples from a variety of tissue

origins will strengthen the critical involvement of a suite of genes we identified in Chapter 5. Since we only looked at gene expression patterns in four tumorigenic RHEK-1 cell lines at a very late stage of transformation, there is a possibility that the unique sets of candidate genes we identified may possibly be associated with neoplastic transformation phenomenologically, not casually. We began to address the time-course issue by measuring mRNA transcripts of 5 genes in OM3 and OM1 cells in our Real Time RT-PCR studies (Chapter 4). Very thorough time-course studies are needed to casually correlate progressive changes in the morphology or growth characteristics of the cells with changes in expression of a distinct subset of genes. A set of molecular markers at early stage of neoplastic transformation will be very useful to utilize those markers for exposure assessment during risk assessment of xenobiotics.

One interesting topic as an extension of the current genomic analysis for the future is characterization of the low dose MNNG-treated RHEK-1 cell population (OM2), since OM2 cells were very weakly anchorage-independent at late passage 25. Their tumorigenicity is also very weak compared to high dose MNNG-treated OM3 cells. As there is little understanding of the relationship between gene expression and dose-dependent induction of toxicity (especially carcinogenicity), genomic analysis on OM2 cells will be very informative. By analyzing gene expression profiles at multiple doses, it may be possible to distinguish a toxic response from physiologically adaptive responses that are not linked to toxicity.

II. Reaching toward Post-Genomic Era

The important question after genomic analyses in Chapter 5 is "Are the protein products of these candidate genes expressed and do they play critical roles in the process of neoplastic transformation in RHEK-1 cells?" Although a good correlation between transcript and protein expression levels is expected, mismatches can occur (Anderson and Seilhamer, 1997; Gygi *et al.*, 1999), as posttranscriptional mechanisms control the turnover and the posttranslational modifications of proteins. Moreover, alternative splicing can generate multiple transcripts that enhance the diversity of protein functions. Thus, it would be useful to obtain information about protein expression in the multiple RHEK-1 cell lines analyzed in Chapter 5 of this dissertation and correlate this information with expression levels of mRNA transcripts. Only genes that are induced or suppressed at both the mRNA and protein level should have functional consequences within the cell.

Like genomics, proteomics takes advantage of recent developments in technology to allow, as an initial goal, the mapping of all proteins expressed (the proteome) in different biological systems. Although we are still at the embryonic stage of the proteomic era, there is no doubt that protein analysis in normal cells and those exposed to xenobiotics will have a great impact in toxicology. The ultimate goal for examining the toxicity/safety of xenobiotics can be achieved if direct analyses of the tissue and cells in the *in vivo* animal or human are carried out. To this end, technologies such as Laser Capture Microdissection (LCM), are providing the opportunity to examine the purified cells of target tissue (i.e., liver) for mechanistic understanding of compound toxicity.

III. Exploring the Possibility for Chemical Classification and Carcinogen Identification by Custom Microarray Approach

Based on the data collected from genomic analyses on 4 chemically transformed cell lines in Chapter 5, an alternative and predictive methods can be developed for chemical classification and carcinogen identification. One approach would be by creating a custom "Chemical Carcinogen" array that detects potential chemical carcinogens (Figure 7.1).

One approach for predicting carcinogenic potential is to classify chemicals based upon their capacity to alter transcriptional programs in a manner that is similar to known toxicants (Nuwaysir *et al.*, 1999). Test chemicals that induce transcriptional responses in a manner similar to those induced by a known carcinogen could then be classified as harboring carcinogenic potential and examined carefully by more thorough toxicological tests. This approach has two underlying assumptions: (1) that we have enough scientific information to allow proper classification of prototype/reference toxicants and (2) that most if not all toxic chemical exposures will alter gene expression at some level (Thomas *et al.*, 2001). In support of this second assumption, signal transduction pathways that culminate in a transcriptional response mediate the toxicity of many chemicals. In addition, toxicity is commonly manifested as inflammation, proliferation, apoptosis, necrosis, and/or cellular differentiation. All of these toxic endpoints are intimately linked to specific alterations in gene expression (Thomas *et al.*, 2001).

There is a close relationship between tumor development resulting from exposure to a potentially toxic chemical and the deregulation of normal cellular, molecular, and biochemical capabilities in cancerous cells. These phenotypic outcomes reflect a

succession of genotypic changes, each conferring one or another type of growth advantage that lead to the progressive conversion of normal human cells into cancer cells (Nowell, 1976). Furthermore, the carcinogenic potential of a chemical may be related to its induction or suppression of a defined suite of genes that may be associated with the multiple stages of carcinogenesis directly or indirectly. For example, carcinogenic potential may be correlated with the extent of expression of critical growth regulatory genes for the proliferation and differentiation of cells. The prediction of carcinogenicity for a test chemical can be qualitatively described by comparing it to known carcinogenic chemicals, 1-methyl-3-nitro-1-nitrosoguanidine (MNNG), 4-nitroquinoline-1-oxide (NQO), and 2,3,7,8-tetrachlorodibenzo-*p*-dioxin (TCDD). The similarities among gene expression signatures will indicate shared mechanisms of action among the chemicals being compared (Fig. 7.1).

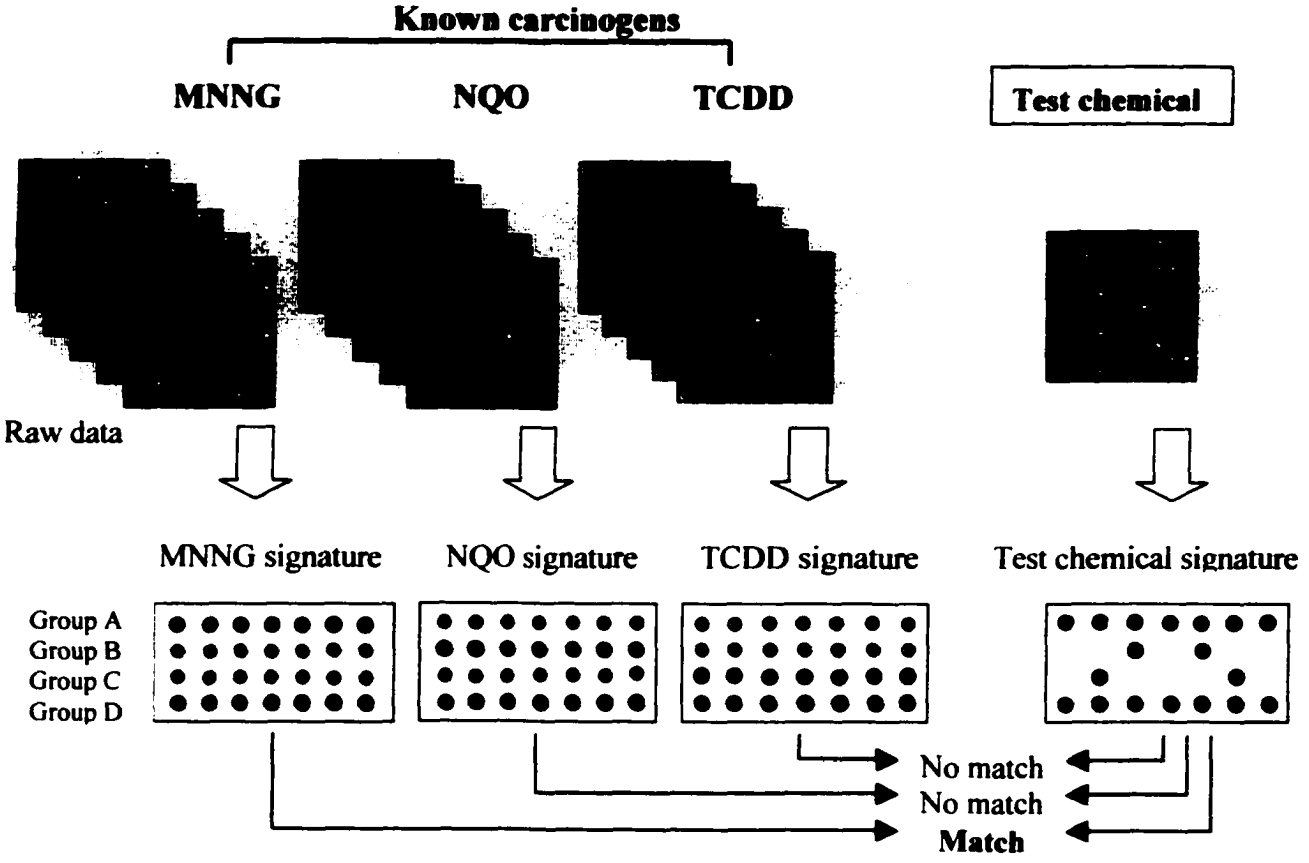

Fig. 7.1 An illustration of prediction for carcinogenicity of test chemical by gene expression signature using a small hypothetical custom array.
Genes in Group A represent 7 unique genes involved in MNNG-mediated transformation. Seven genes in Groups B and C represent loci specifically altered by NQO and TCDD, respectively. In contrast, 7 genes in Group D represent a common suite of genes altered in their expression regardless of chemical type. These last 7 genes are universally associated with chemical-induced malignant transformation in RHEK-1 cells directly or indirectly. As long as genes in Group D are regulated by test chemical as same as by MNNG, NQO, and TCDD, we can predict that test chemical may be a potential carcinogen. The test chemical signature in Group A genes is similar to one in MMNG-treated cells, it may be concluded that test chemical acts in mode of action like MNNG does in RHEK-1 cells.

The red color on arrays indicates higher expression in chemically-treated cells compared to control while the green color represents higher expression in control cells compared to chemically-treated ones. The yellow color denotes no significant change while the gray color indicates no measurable signal.

III. Modeling Multiple Stages of RHEK-1 Transformation

The cellular and molecular markers we identified from the results of Chapters 3, 4, and 5 will be utilized in the future to develop a multistage transformation model for RHEK-1 keratinocytes as demonstrated in Fig. 7.2. The critical cell lines/phenotypes would be immortal line, anchorage-independent growth (AIG) line, and tumorigenic line. The detail description about these RHEK-1 cell lines established after exposure to MNNG can be found in Fig. 4.2. The crucial parameters for this model would be: (1) growth and death rates of immortal, AIG, and tumorigenic RHEK-1 cells, (2) % cloning efficiency (CE) on semi-solid medium, and (3) molecular markers represent for conversion of one cell type to the next stage cell in Fig. 7.2. At this moment, we have quantitative data for % CE by AIG assay for each representative passage of RHEK-1 cells. Also, limited time-course information on 5 genes that were initially selected from analyzing very late stage (passage 25) MNNG-transformed OM3 cells as well as passage-matched vehicle control OM1 cells is available for modeling as discussed in Chapter 4. More systemic and global approach such as general DNA microarray analysis on each stage defined in Fig. 7.2 is needed to identify a subset of genes that is directly or indirectly associated with acquired capability for positive AIG on methyl cellulose medium or positive tumorigenicity in nude mice. Highly quantitative expression data could be generated for these genes through use of Real Time RT-PCR. Lastly, the growth and death rates for immortal, AIG, and tumorigenic RHEK-1 cells can be very quantitatively measured by the use of flow cytometry (Liao, 2001).

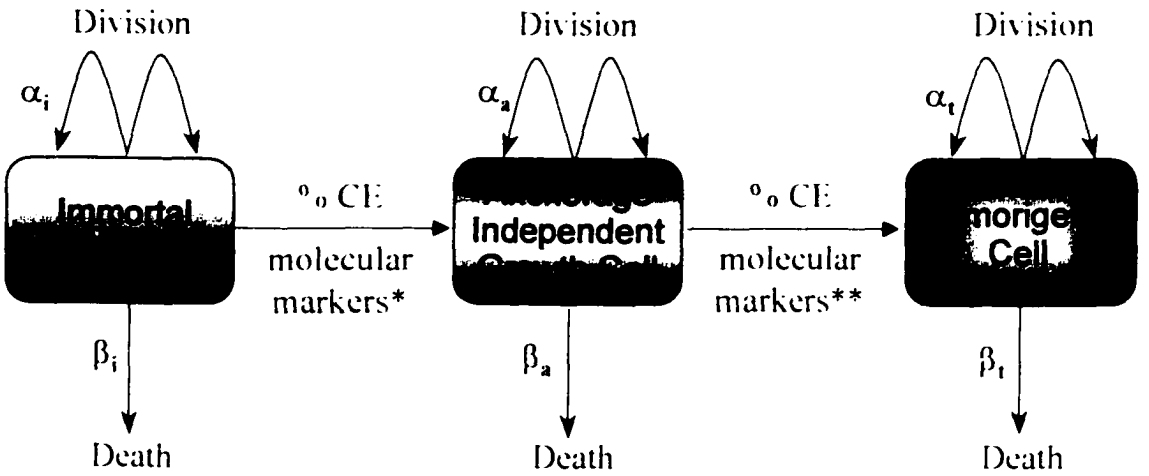

Fig. 7.2 A multistage transformation model for RHEK-1 cells
α_i, α_a, and α_t is growth rate for immortal, anchorage-independent, and tumorigenic RHEK-1 cells, respectively. β_i, β_a, and β_t is death rate for immortal, anchorage-independent, and tumorigenic RHEK-1 cells, respectively. CE: cloning efficiency from AIG assay. *: a subset of genes at p10-11 of OM3 cells; **: a subset of genes at p15-16 of OM3 cells from microarray and Real Time RT-PCR methodologies.

References

Anderson, L. and Seilhamer, J. A comparison of selected mRNA and protein abundances in human liver. Electrophoresis, *18*: 533-537, 1997.

Gygi, S. P., Rochon, Y., Franza, B. R., and Aebersold, R. Correlation between protein and mRNA abundance in yeast. Mol.Cell Biol., *19*: 1720-1730, 1999.

Liao, K. H., Gustafson, D. L., Fox, M. H., Chubb, L. S., Reardon, K. F., and Yang, R. S. A biologically based model of growth and senescence of Syrian hamster embryo (SHE) cells after exposure to arsenic. Environ.Health Perspect., *109*: 1207-1213, 2001.

Nowell, R.C. The clonal evolution of tumor cell populations. Science, *194*, 23-28, 1976.

Nuwaysir, E. F., Bittner, M., Trent, J., Barrett, J. C., and Afshari, C. A. Microarrays and toxicology: the advent of toxicogenomics. Mol.Carcinog. *24*: 153-159, 1999.

Thomas, R. S., Rank, D. R., Penn, S. G., Zastrow, G. M., Hayes, K. R., Pande, K., Glover, E., Silander, T., Craven, M. W., Reddy, J. K., Jovanovich, S. B., and Bradfield, C. A. Identification of toxicologically predictive gene sets using cDNA microarrays. Mol.Pharmacol., *60*: 1189-1194, 2001.